Synthesis of Small Molecule and Polymeric Systems for the Controlled Release of Sulfur Signaling Molecules

Chadwick R. Powell

Dissertation submitted to the faculty of the Virginia Polytechnic Institute and State University in partial fulfillment of the requirements for the degree of

Doctor of Philosophy
In
Chemistry

John B. Matson, Chair
Webster L. Santos
Harry W. Gibson
Judy S. Riffle

April 25th, 2019
Blacksburg, VA

Keywords: hydrogen sulfide (H_2S), carbonyl sulfide (COS), persulfide, 1,6-benzyl elimination, ring-opening

Copyright 2019

Synthesis of Small Molecule and Polymeric Systems for the Controlled Release of Sulfur Signaling Molecules

Chadwick R. Powell

ABSTRACT

Hydrogen sulfide (H_2S) was recognized as a critical signaling molecule in mammals nearly two decades ago. Since this discovery biologists and chemists have worked in concert to demonstrate the physiological roles of H_2S as well as the therapeutic benefit of exogenous H_2S delivery. As the understanding of H_2S physiology has increased, the role(s) of other sulfur-containing molecules as potential players in cellular signaling and redox homeostasis has begun to emerge. This creates new and exciting challenges for chemists to synthesize compounds that release a signaling compound in response to specific, biologically relevant stimuli. Preparation of these signaling compound donor molecules will facilitate further elucidation of the complex chemical interplay within mammalian cells.

To this end we report on two systems for the sustained release of H_2S, as well as other sulfur signaling molecules. The first system discussed is based on the *N*-thiocarboxyanhydride (NTA) motif. NTAs were demonstrated to release carbonyl sulfide (COS), a potential sulfur signaling molecule, in response to biologically available nucleophiles. The released COS is shown to be rapidly converted to H_2S in the presence of the ubiquitous enzyme carbonic anhydrase (CA). A synthetic route that affords NTAs with reactive functionalities was devised and the functional "parent" NTAs were successfully conjugated to a variety of substrates, ranging from small molecules to polymers. These functional NTAs provide a platform from which a library of NTA-based COS/H_2S may be

readily prepared convergently in an effort to move towards H_2S-releasing drug and polymer conjugates. Additionally, preliminary *in vitro* cytotoxicity studies indicate that NTAs are noncytotoxic at concentrations above 100 μM.

The second system discussed in this dissertation leverages the 1,6-benzyl elimination reaction (or self-immolative reaction) to facilitate the release of a persulfide (R–SSH) from a small molecule prodrug platform as well as a separate system that releases COS/H_2S from a polymer. The self-immolative persulfide prodrug was designed to be responsive to reactive oxygen species (ROS) and demonstrates efficacy as an antioxidant *in vitro*. Furthermore, the polymeric COS/H_2S self-immolative system was designed to respond to reducing agents, including H_2S itself, and shows promise as a H_2S signal amplification platform.

Synthesis of Small Molecule and Polymeric Systems for the Controlled Release of Sulfur Signaling Molecules

Chadwick R. Powell

GENERAL AUDIENCE ABSTRACT

Hydrogen sulfide (H_2S) has long been recognized as a malodorous and toxic byproduct of industrial chemical processes. However, the discovery of H_2S as a key signaling molecule in mammals has drastically shifted the paradigm of H_2S research over the last two decades. Research into the production and roles of H_2S in the body is ongoing, but has pointed to the implication of changes in H_2S production to the onset of a variety of disease states, including cardiovascular disease and Alzheimer's. As alterations in the body's production of H_2S have been correlated to certain disease states, collaborative research efforts among biologists and chemists have demonstrated the utility of H_2S-based therapeutics in helping to alleviate these disease states.

Our understanding of the roles of H_2S in the body, and potential benefits derived from H_2S-releasing drugs, can only continue to advance with the development and improvement of H_2S releasing compounds. The first portion of this dissertation focuses on the synthesis of a new class of H_2S-releasing compounds, termed *N*-thiocarboxyanhydrides (NTAs). NTAs release H_2S through an intermediate sulfur-containing molecule, carbonyl sulfide (COS), which may have signaling properties independent of H_2S. The COS that is released from the NTAs is rapidly converted to H_2S by the action of the ubiquitous enzyme carbonic anhydrase. A variety of functional NTAs were synthesized, which in turn were used to prepare a small library of NTA-based COS/H_2S releasing compounds. This work informs the preparation of H_2S-drug or H_2S-polymer conjugates.

The second portion of this dissertation examines a class of compounds broadly termed self-immolative prodrugs. The self-immolative prodrug platform was leveraged to release H_2S, or persulfides (R–SSH), another class of sulfur-containing molecules of biological interest. The self-immolative persulfide prodrug system was designed to be responsive to reactive oxygen species (ROS), a harmful cellular byproduct. The persulfide donor was successful in mitigating the harmful effects of ROS in heart cells. Independently, a polymeric self-immolative H_2S releasing system was designed to depolymerize in the presence of H_2S, resulting in the generation of 6-8-fold excess of H_2S upon depolymerization. We envision the self-immolative H_2S-releasing polymer will show promise in biological applications where a vast excess of H_2S is needed rapidly.

Dedication

This dissertation is dedicated to my parents, Thomas and Julia Powell.

Acknowledgements

I would like to begin by thanking my Ph.D. advisor, Prof. John Matson. Prof. Matson agreed to take me on as an undergraduate REU student in the summer of 2013. That summer was a critical point in my development as a chemist. I enjoyed my time in Prof. Matson's lab so much that summer that I had made my decision about attending graduate school at Virginia Tech before I returned for my senior year of undergraduate studies. That decision has paid handsomely for me as Prof. Matson has provided an environment that has allowed me to grow as a chemist and as a person. Thank you, John, for allowing me to take full ownership of my research, make mistakes, and learn from them.

I would also like to thank the members of my Ph.D. committee– Prof. Webster Santos, Prof. Harry Gibson, and Prof. Judy Riffle. I have had the privilege of learning from each of my committee members in the classroom as well as through their invaluable guidance during my graduate studies. Prof. Santos' knowledge and understanding of organic chemistry has been an excellent resource throughout my graduate career. Prof. Riffle taught me a great deal about polymer synthesis, particularly ring-opening polymerization and high-performance polymers. Prof. Gibson, who taught me key concepts in radical polymerization techniques and supramolecular chemistry, also mentored me as a teaching assistant in the Synthetic Techniques lab. I'm sure watching me lecture was not always easy, but I appreciate your patience and support. Being supported by a group of knowledgeable and accomplished chemists has been, and will continue to be, an inspiration as I move forward in my career.

Prof. Rhett Smith, my undergraduate research advisor at Clemson University deserves acknowledgement for giving me my first experiences in a chemistry lab. Prof. Smith took an early interest in my career and is the reason I applied for the REU program at Virginia Tech. He also provided insight and help in making my decisions on what type of research I wanted to do and where I wanted to do it.

To my family, thank you for your unwavering love and support. Both of my parents have been integral parts of my life and this document is as much theirs as it is mine. My Mom is always the first person I talk to when something big happens in my life, good or bad. There is no greater comfort in the world than the reassuring voice of your mother on the phone; I owe my sanity to that. I would like to thank my late father for believing in me and always compelling me to work hard and put my best foot forward. I wish you were here to read this. To my sister, thank you for your constant support, I have no doubt you are my biggest advocate.

I have had the privilege of working under two outstanding graduate mentors, both as an undergraduate at Clemson University and as an undergraduate and graduate student at Virginia Tech. Dr. Brynna Quarles was my first graduate mentor in Prof. Smith's lab at Clemson. Brynna expected a lot from her undergraduates and rising to meet her expectations improved my skills and work ethic. Brynna's knowledge, tenacity, and mentorship gave me a great example of what makes a successful chemist. My graduate mentor at Virginia Tech was Dr. Jeff Foster. Jeff was a beacon of productivity who always had feasible suggestions and helpful tips that proved invaluable to my research endeavors. Jeff also set the culture for the Matson lab, showing that it is possible to be highly productive and have fun while you're doing it. Jeff's work and ideas are ingrained in this

dissertation as well as many other dissertations from the Matson lab. I have no doubt that he will run a successful research program during his career.

Lastly, to my friends and fellow graduate students I have had the privilege to meet, work, and live with at Virginia Tech– you have made this process so much easier to get through. Christina Orsino, thank you for always being there and being supportive. Your kindness and understanding goes much further than you know. I am looking forward to seeing where life takes us. Kyle Arrington became a fast friend in the Matson lab. We bonded over chemistry and video games. Kyle is incredibly smart and is always ready and willing to help, his absence from the Matson lab after graduation was definitely felt.

Kearsley Dillon was my deskmate for the last three years of graduate school. When Kearsley wasn't trying to show me videos on YouTube, he was an excellent person to bounce research ideas off of. Kearsley is one of the smartest people I know and a joy to be around. The moment Kearsley joined the Matson lab it was evident that he was destined for success. Likewise, (Cryin') Ryan Carrazzone has been pleasure to work with since he joined the Matson lab and is well on his way to a successful and productive career in chemistry. Ryan is a great resource for questions concerning SEC, DLS, or fantasy football.

Kuljeet Kaur has been a great colleague in the Matson lab. Whenever I have an issue, research or otherwise, I know I can discuss it with Kuljeet and receive constructive feedback. Kuljeet provides excellent prospective that extends from chemistry, to geopolitics, to books and television shows. Scott Radzinski is a very talented polymer chemist who taught me a lot of synthetic polymer techniques early in my graduate career. Special shout out to Ryan Mondschein and Lindsey Anderson, who I spent four years watching football/playing games/traveling with. There are so many more people I could

list who have had an influence on me during my time here, but in the interest of space a blanket “thank you” will have to suffice.

I have had a couple of talented undergraduate researchers work under me during my time at Virginia Tech. Haley Young was an REU student during the summer of 2017. Haley was incredibly bright and motivated and one of my few regrets in graduate school is that I was not able to get her on a publication before she went off to graduate school. I also had the pleasure of working with Jake Viar, an undergraduate student at Virginia Tech, for two years. When Jake first joined the Matson lab he had no organic chemistry experience, but he learned quickly. Jake was masterful at taking things apart and putting them back together, a vital skillset in any chemistry lab.

Lastly, I would like to thank the support staff in the department of chemistry at Virginia Tech. Dr. Mehdi Ashraf-Khorassani displayed incredible patience and was very helpful in LCMS analysis of the persulfide work (Chapter 5). Without Mehdi that paper would still be on Prof. Matson’s desk. Geno Iannaccone and Ken Knott were great resources in regards to NMR. Without them the department would not function on a day-to-day basis.

Table of Contents

Attribution xiv

Chapter 1: A Review of Hydrogen Sulfide (H_2S) Donors: Chemistry and Potential Therapeutic Applications 1

1.1 Authors: 1

1.2 Abstract 1

1.3. Introduction 2

1.3.1. Physical and Chemical Properties of H_2S 3

1.3.2. Endogenous Production of H_2S 3

1.3.3. H_2S Signaling Mechanisms 6

1.4. Chemical Tools for Studying H_2S 7

1.5. Direct Delivery of H_2S 7

1.5.1. Inhalation 7

1.5.2. Sulfide Salts 8

1.6. Measuring H_2S Release Kinetics 10

1.7. Naturally Occurring Donors 12

1.8. Synthetic H_2S Donors 14

1.8.1. Considerations for Synthetic Donors 14

1.8.2. Hydrolysis Triggered Donors 15

1.8.3. Thiol-Triggered Donors 23

1.8.4. Light Triggered Donors 29

1.8.5. Enzyme-Triggered Donors 31

1.8.6. Dual Carbonyl Sulfide / H_2S Donors 33

1.9. Conclusions 39

1.10. Acknowledgements 40

1.11. References 40

Chapter 2: Therapeutic Delivery of H_2S via COS: Small Molecule and Polymeric Donors with Benign Byproducts 57

2.1. Authors 57

2.2. Abstract. 57

2.3. Introduction 58

2.4. Results and Discussion 60

2.5. Conclusions 66

2.6. References 67

2.7. Experimental 71

Chapter 3: Functional N-substituted *N*-Thiocarboxyanhydrides as Modular Tools for Constructing H_2S Donor Conjugates 96
3.1. Authors. 96
3.2. Abstract. 96
3.3. Introduction 96
3.4. Results and Discussion 99
3.5. Conclusions 108
3.6. Acknowledgements 108
3.7. References 108
3.8. Experimental 113
Chapter 4: Polycarbonates as Macromolecular Scaffolds for the Delivery of Hydrogen Sulfide 150
4.1. Authors. 150
4.2. Abstract 150
4.3. Introduction 150
4.4. Results and Discussion 152
4.5. Conclusions 158
4.6. Acknowledgements 159
4.7. References 159
4.8. Experimental 164
Chapter 5: A Reactive Oxygen Species (ROS)-Responsive Persulfide Donor: Insights into Reactivity and Therapeutic Potential 181
5.1. Authors 181
5.2. Abstract 181
5.3. Introduction 182
5.4. Results and Discussion 185
5.5. Conclusions 192
5.6. Acknowledgements 193
5.7. References 193
5.8. Experimental 199
Chapter 6: Self-Amplified Depolymerization of Oligo(thiourethanes) for the Release of COS/H_2S 230
6.1. Authors. 230
6.2. Abstract 230
6.3. Introduction 231

6.4. Results and Discussion. 233
6.5. Conclusions 240
6.6. Acknowledgements 241
6.7. References 241
6.7. Experimental 246
Chapter 7: Conclusions and Future Outlook 267

Attribution

This work was completed with the help of several colleagues. A brief description of the contributions from each person involved is included here.

Chapter 1: Chadwick R. Powell (graduate student, Department of Chemistry, Virginia Tech) performed the writing and editing of this chapter. Kearsley M. Dillon (graduate student, Department of Chemistry, Virginia Tech) performed the writing of select sections of this chapter. John B. Matson (Ph.D., Department of Chemistry, Virginia Tech) is the advisor and committee chair who provided guidance, writing, and editing of this chapter.

Chapter 2: Chadwick R. Powell (graduate student, Department of Chemistry, Virginia Tech) performed the most of the synthesis, compound characterization, H_2S releasing experimentation, and writing for this chapter. Jeffrey C. Foster (graduate student, Department of Chemistry, Virginia Tech) performed synthetic guidance and editing for this chapter. Benjamin Okyere (graduate student, Virginia-Maryland College of Veterinary Medicine) performed cell culture experiments for this chapter. Michelle Theus (Ph.D., Virginia-Maryland College of Veterinary Medicine) provided experimental guidance and editing of this chapter. John B. Matson (Ph.D., Department of Chemistry, Virginia Tech) is the advisor and committee chair who provided guidance, writing, and editing of this chapter.

Chapter 3: Chadwick R. Powell (graduate student, Department of Chemistry, Virginia Tech) performed the most of the synthesis, compound characterization, H_2S release experimentation, and writing for this chapter. Kuljeet Kaur (graduate student, Department of Chemistry, Virginia Tech) provided synthetic assistance and editing for this chapter. Mingjun Zhou (graduate student, Department of Chemistry, Virginia Tech) provided

MALDI-TOF analysis for this chapter. Mohammed Alaboalirat (graduate student, Macromolecular Science and Engineering, Virginia Tech) provided synthetic assistance for this chapter. John B. Matson (Ph.D., Department of Chemistry, Virginia Tech) is the advisor and committee chair who provided guidance, writing, and editing of this chapter.

Chapter 4: Chadwick R. Powell (graduate student, Department of Chemistry, Virginia Tech) performed the synthesis, compound characterization, H_2S releasing experimentation, and writing for this chapter. Haley Young (undergraduate student, Elizabethtown College) provided synthetic and experimental assistance for this chapter. Jake Viar (undergraduate student, Virginia Tech) provided synthetic assistance for this chapter. John B. Matson (Ph.D., Department of Chemistry, Virginia Tech) is the advisor and committee chair who provided guidance, writing, and editing of this chapter.

Chapter 5: Chadwick R. Powell (graduate student, Department of Chemistry, Virginia Tech) performed the synthesis, compound characterization, cell culture experiments, and writing for this chapter. Kearsley M. Dillon (graduate student, Department of Chemistry, Virginia Tech) provided synthetic guidance, compound characterization, and editing for this chapter. Yin Wang (Postdoctoral researcher, Department of Chemistry, Virginia Tech) provided assistance with cell culture experiments and editing for this chapter. Ryan J. Carrazzone (graduate student, Macromolecular Science and Engineering, Virginia Tech) performed NMR kinetic experiments for this chapter. John B. Matson (Ph.D., Department of Chemistry, Virginia Tech) is the advisor and committee chair who provided guidance, writing, and editing of this chapter.

Chapter 6: Chadwick R. Powell (graduate student, Department of Chemistry, Virginia Tech) performed the most of the synthesis, compound characterization, H_2S releasing

experimentation, and writing for this chapter. Jeffrey C. Foster (graduate student, Department of Chemistry, Virginia Tech) develop the project idea, initial synthesis of the monomer and polymer, and editing for this chapter. Sarah N. Swilley (graduate student, Department of Chemistry, Virginia Tech) provided experimental assistance with the NMR kinetic experiments for this chapter. Kuljeet Kaur (graduate student, Department of Chemistry, Virginia Tech) provided assistance with H_2S release experiments for this chapter. Samantha J. Scannelli (graduate student, Department of Chemistry, Virginia Tech) performed theoretical calculations. Diego Troya (Ph.D., Department of Chemistry, Virginia Tech) provided guidance on the theoretical calculations, writing, and editing for this chapter. John B. Matson (Ph.D., Department of Chemistry, Virginia Tech) is the advisor and committee chair who provided guidance, writing, and editing of this chapter.

Chapter 1: A Review of Hydrogen Sulfide (H_2S) Donors: Chemistry and Potential Therapeutic Applications

Reprinted with permission from: Powell, C. R., et al. (2018). "A Review of Hydrogen Sulfide (H_2S) Donors: Chemistry and Potential Therapeutic Applications." Biochemical Pharmacology **149**: 110-123. DOI: 10.1016/j.bcp.2017.11.014. Copyright 2017 Elsevier.

1.1 Authors:

Chadwick R. Powell, [§,†] Kearsley M. Dillon, [§,†] John B. Matson[§,†]

§Department of Chemistry, Virginia Tech, Blacksburg, Virginia 24061, United States
† Virginia Tech Center for Drug Discovery, Virginia Tech, Blacksburg, Virginia 24061, United States

1.2 Abstract

Hydrogen sulfide (H_2S) is a ubiquitous small gaseous signaling molecule, playing an important role in many physiological processes and joining nitric oxide and carbon monoxide in the group of signaling agents termed gasotransmitters. Endogenous concentrations of H_2S are generally low, making it difficult to discern precise biological functions. As such, probing the physiological roles of H_2S is aided by exogenous delivery of the gas in cell and animal studies. This need for an exogenous source of H_2S provides a unique challenge for chemists to develop chemical tools that facilitate the study of H_2S under biological conditions. Compounds that degrade in response to a specific trigger to release H_2S, termed H_2S donors, include a wide variety of functional groups and delivery systems, some of which mimic the tightly controlled endogenous production in response to specific, biologically relevant conditions. This review examines a variety of H_2S donor systems

classified by their H_2S-releasing trigger as well as their H_2S release profiles, byproducts, and potential therapeutic applications.

1.3. Introduction

Hydrogen sulfide (H_2S) has long been known as a foul smelling, toxic gas. Much of the early literature on H_2S focused on its removal from petroleum and pulp products, concerns due in large part to its noxious odor. The presence of H_2S in mammalian tissue has been known for decades, but it was not until the landmark paper by Abe and Kimura in 1996 that the endogenous production and signaling capacity of H_2S was elucidated.[1] Clarification of the cellular signaling mechanisms and biodistribution of its constitutive enzymes led to the induction of H_2S into a family of small signaling molecules known as gasotransmitters. The term gasotransmitter, coined by Wang in 2002, refers to the gaseous nature of these compounds at standard temperature and pressure in the bulk.[2] There are currently three accepted gasotransmitters: carbon monoxide (CO), nitric oxide (NO), and, most recently, H_2S. For a molecule to be considered a gasotransmitter, specific criteria must be met, including: regulated endogenous production, the ability to freely permeate cell membranes, and specific signaling function with specific cellular and molecular targets.[2] The acknowledgement of H_2S as a gasotransmitter has led to a renewed interest in this gas over the past two decades, with a focus on creating chemical tools to probe H_2S physiology, determining its signaling roles in various organs and systems across the plant and animal kingdoms, and exploiting its biological signaling capacity for therapeutic benefits.

1.3.1. Physical and Chemical Properties of H_2S

H_2S is a colorless, pungent gas with a boiling point of -60 °C.[3] A saturated aqueous solution of H_2S has a concentration of 0.11 M at room temperature and pH of ~4.0 owing to the acidic nature of H_2S (pK_{a1} = 6.98). In an unsaturated aqueous H_2S solution at body temperature (37 °C), the pK_{a1} is 6.76, meaning that roughly 40% of sulfide species in the body exist as H_2S with the remaining population as hydrosulfide anion (HS^-). A very small and likely negligible amount exists as S^{2-}. Unlike water, H_2S does not form hydrogen bonds and is lipophilic, allowing it to pass through biological membranes and act as a paracrine signaling molecule.[4] The hydrosulfide anion can undergo oxidation in the presence of O_2, forming oxidized sulfide species such as sulfite (SO_3^{2-}), sulfate (SO_4^{2-}), thiosulfate ($S_2O_3^{2-}$), polythionates ($S_nO_{n+2}^-$), and polysulfides (S_x^{2-}), as well as other oxidized polysulfide species.[5] It is unclear whether it is H_2S, HS^-, or both that contribute to observed biological activity.[6] To eliminate uncertainty and confusion, in any reference to H_2S hereafter we acknowledge the appreciable presence of both species in biologically relevant media.

1.3.2. Endogenous Production of H_2S

Endogenous production of H_2S is a result of direct enzymatic desulfhydration of cysteine, catalyzed by cystathionine-γ-lyase (CSE) and cystathionine-β-synthase (CBS), and indirect desulfhydration catalyzed by 3-mercapto-sulfurtransferase (3-MST) in the presence of reductants.[7] CBS is present mostly in the central nervous system and the liver, while CSE is primarily responsible for H_2S production in the cardiovascular system. 3-MST is located predominantly in the mitochondria and produces H_2S in concert with cysteine aminotransferase (CAT).[8-12] The pathways for endogenous production of H_2S are outlined in Figure 1.

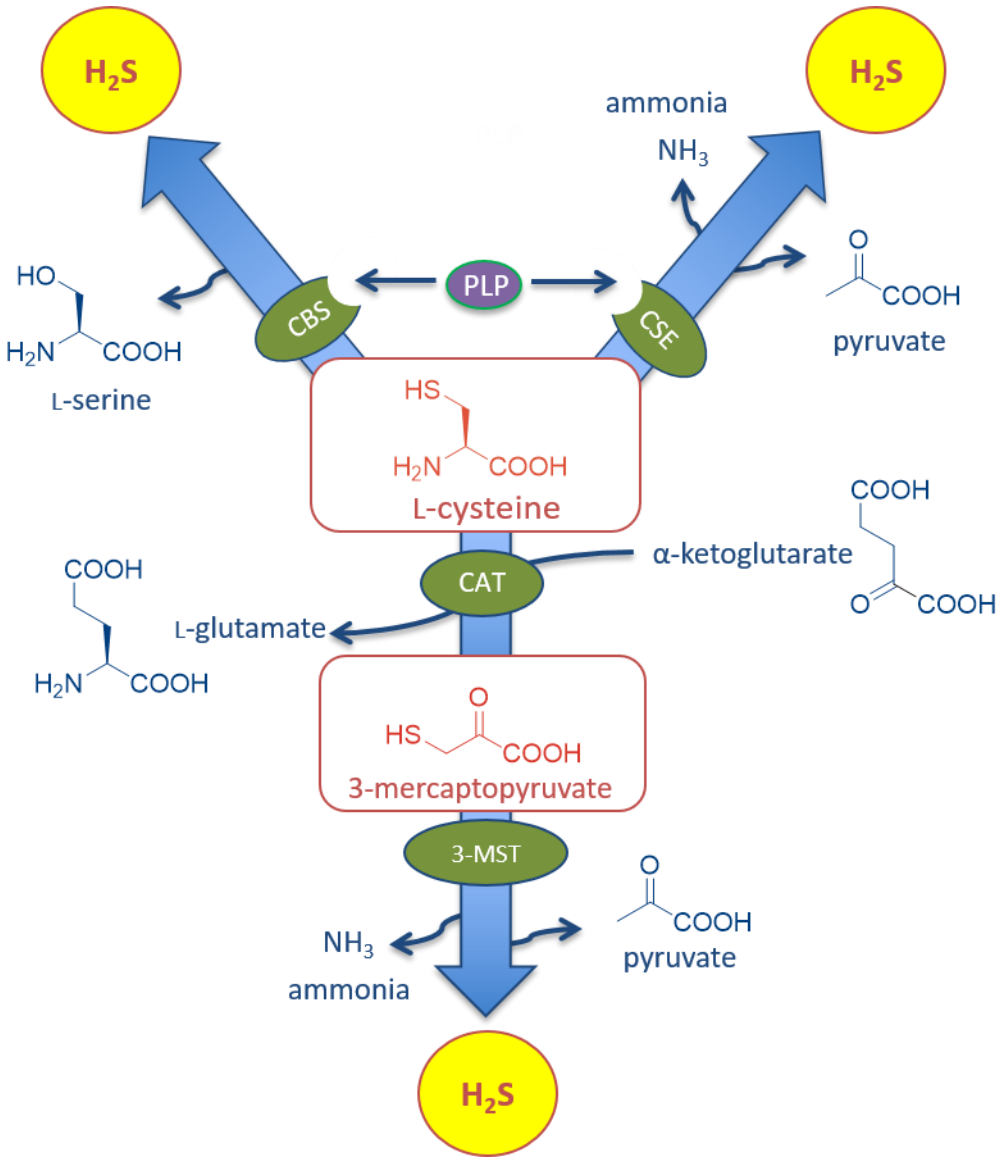

Figure 1. Graphical overview of endogenous H_2S production in mammalian cells.

1.3.2A. *CBS*

CBS typically catalyzes a pyridoxyl 5'-phosphate (PLP) dependent reaction in which L-homocysteine and L-serine are condensed to form L-cystathionine with the release of water.[10] In the presence of L-cysteine, CBS performs the same β-replacement reaction but releases H_2S

instead of water. CBS has very complex roles in the mammalian brain, acting as a powerful neuromodulator.[13-14] CBS-produced H_2S selectively enhances N-methyl-D-aspartate (NMDA) receptor responses and appears to alter long-term potentiation in the hippocampus.[15] CBS is regulated by testosterone, *S*-adenosyl-L-methionine, and calmodulin/Ca^{2+}-mediated pathways and may be a selective target for novel cancer therapies.

1.3.2B. *CSE*

CSE catalyzes the PLP-dependent reaction of cysteine and homocysteine to pyruvate and α-ketoglutarate, respectively, resulting in the release of ammonia (NH_3) and H_2S. CSE is located solely in the cytoplasm of cells and is sequestered mostly in the cardiovascular system. Thus, this enzyme is under scrutiny as a possible drug target to treat the millions affected by heart disease. Modulating CSE activity has a profound impact in treating animal models of atherosclerosis and other cardiovascular conditions.[16] Additionally, recent studies suggest that CSE-produced H_2S exerts numerous cytoprotective effects ranging from alleviating ischemia-reperfusion (I/R) injury and attenuating cardiac arrhythmia to reducing myocardial infarction.[17-19] In addition to activity in the cardiovascular system, CSE also contributes to cellular signaling and homeostasis in other organs. For example, Lefer showed that inhibition of CSE attenuated D-galactosamine- and lipopolysaccharide (LPS)-induced liver injury.[20] This attenuation results from increased cellular levels of thiosulfate and homocysteine, upregulation of NF-E2 p45 factor 2 (Nrf2) and antioxidant proteins, among other complex factors.

1.3.2C. *3-MST*

Of the three H_2S-generating enzymes, 3-MST has been the least studied thus far. 3-MST catalyzes the conversion of cysteine to pyruvate with the assistance of CAT in a two-step reaction. CAT first catalyzes a transamination reaction to convert L-cysteine and α-ketoglutarate into 3-

mercaptopyruvate and L-glutamate, respectively. 3-MST then converts 3-mercaptopyruvate into H_2S and pyruvate using L-cysteine or other biologically relevant thiols.[12] In addition to producing H_2S, 3-MST catalyzes formation of various sulfur oxides (SO_x) in perthiol redox cycles. 3-MST has complex, interconnecting roles with CBS in the brain.[21] Consequently, mutations in 3-MST causing reduced levels of H_2S and SO_x in the brain correlate to behavioral abnormalities and increased anxiety.[22]

1.3.3. *H_2S Signaling Mechanisms*

There are three main routes by which H_2S exerts its biological effects: metal center interactions,[23] reactive oxygen species (ROS)/reactive nitrogen species (RNS) scavenging,[24] and S-persulfidation.[8] Although the first two routes have significance, S-persulfidation is accepted as the key process by which H_2S acts in a signaling capacity. S-Persulfidation (more commonly but less accurately called S-sulfhydration) is the process in which a thiol (R–SH) is converted into a perthiol (R–SSH, also called a persulfide). S-Persulfidation modulates the biological activity of proteins due to the decrease in pK_a and increase in nucleophilicity of perthiols with respect to thiols.[25] For example, glyceraldehyde-3-phosphate dehydrogenase (GAPDH), an enzyme whose main functions are in the glycolysis and gluconeogenesis pathways, changes function upon S-persulfidation to inhibit cell apoptosis.[26] Similarly, S-persulfidation in K_{ATP} channels contributes to H_2S-induced vasodilation.[26] Due to the pronounced changes S-persulfidation enacts on proteins and small molecules, there is currently much investigation into the biological roles of perthiols and polysulfides.[27]

1.4. Chemical Tools for Studying H_2S

As interest in the physiological roles of H_2S has grown, the need for chemical tools used for studying H_2S has also increased. These tools include H_2S probes, which are molecules capable of responding to H_2S typically by changing their spectroscopic properties, CSE and CBS inhibitors, which reduce or eliminate endogenous H_2S production, and H_2S donors, which are molecules designed to release H_2S under specific conditions. For a review on compounds and methods used for detection of H_2S, we refer the reader to recent reviews on these topics.[28-30] We also refer the reader to reports on recent efforts to increase the selectivity and potency of CBS and CSE inhibitors.[31-32] Here we focus solely on H_2S donors. To study H_2S in a physiologically relevant manner, donors with variable release rates and triggers are needed. This review is not a comprehensive look at H_2S donors, but rather a critical examination of recent developments in H_2S donor chemistry, highlighting specific examples of donors and discussing important considerations in designing and choosing donors for biological studies.

1.5. Direct Delivery of H_2S

1.5.1. Inhalation

When considering exogenous delivery of gasotransmitters, the most conspicuous method of delivery is inhalation of the gas directly. Inhalation offers the possibility to tune total payload delivery by carefully modulating pressure over time, and it circumvents some of the issues with intravenous delivery such as oxidation and volatilization of dissolved H_2S. Despite the difficulties in working with toxic and flammable H_2S gas directly, this delivery mode has been tested. For example, exogenous systemic delivery of H_2S via inhalation at 80 ppm for 3 h or greater in mice showed a reversible decrease in motor activity and body temperature with a corresponding increase in blood sulfide concentration.[33-34] These studies led to the use of inhaled H_2S in hypothermic and

normothermic mice as a method of inhibiting pulmonary and systemic inflammatory responses during physiological stress.[35-36] However, H_2S inhalation has some inherent shortcomings due the toxicity and flammability of the gas, particularly gas storage, safe administration, and targeting. These technical difficulties limit the overall impact of inhalation as a viable method of H_2S delivery, and few researchers are currently actively examining this delivery strategy.

1.5.2. *Sulfide Salts*

The most common class of H_2S donors employed in biological studies are the sulfide salts, sodium hydrosulfide (NaSH) and sodium sulfide (Na_2S). Although commonly referred to as donors, sulfide salts are simply solid analogs of the gas, providing direct, instantaneous access to the biologically relevant forms of sulfide (H_2S and HS^-). Use of sulfide salts has been integral in the establishment of H_2S as a gasotransmitter, and these salts have been widely used to evaluate the therapeutic potential of exogenous H_2S delivery.

One of the early studies on exogenous H_2S delivery by Wang et al. employed aqueous NaSH solutions in evaluating rat aortic ring response in vitro.[37] NaSH delivery led to a 60% greater relaxation over controls, showing the vasorelaxant properties of H_2S. In a separate study by Du et al., delivery of NaSH solution via intravenous injection to rats with oleic acid-induced acute lung injury (ALI) alleviated the degree of ALI by decreasing IL-6 and IL-8 levels while simultaneously increasing IL-10 levels in the plasma and lung tissue.[38] This study also verified the hypothesis that down-regulation of endogenous H_2S levels in the cardiovascular system is involved in ALI pathogenesis.

Sulfide salts as H_2S donors have also exhibited efficacy in limiting cell damage from ROS in brain cells. Delivery of NaSH was tested as an antioxidant in an in vitro study where oxidative stress was induced in human nueroblastoma cells using hypochlorous acid (HOCl) to mimic HOCl

overproduction from myeloperoxidase in the brain of patients with Alzheimer's disease. Exogenous NaSH inhibited protein oxidation, lipid peroxidation, and overall cytotoxicity.[39] In a hepatic I/R injury model, delivery of Na_2S (up to 1.0 mg/kg) prior to reperfusion inhibited lipid peroxidation and preserved a healthy balance of reduced glutathione (GSH), overall providing protection against I/R injuries.[40] Aqueous solutions of sulfide salts have also demonstrated efficacy in promoting ulcer healing,[41-42] as well as quenching RNS.[43-44]

While sulfide salts are a popular choice amongst biologists interested in elucidating endogenous roles and therapeutic prospects of H_2S, there are drawbacks to these H_2S donors both as chemical tools for studying H_2S biology and as potential therapeutics. Sulfide salts hydrolyze immediately upon dissolution in water, instantaneously establishing the equilibrium between H_2S, HS^-, and S^{2-} species. Once this equilibrium is established, volatilization of H_2S occurs, lowering the overall concentration of sulfur species in solution. Additionally, air oxidation of HS^- catalyzed by trace metals in water further reduces the actual concentration of H_2S in solution.[6] These competing processes make it challenging to deliver a reproducible amount of H_2S via sulfide salts. In addition, sulfide salts lack targeting capabilities and thus are only of utility in systemic delivery. Finally, studies on H_2S biology using sulfide salts frequently require administration of high doses, causing H_2S blood and tissue concentrations to surge to supraphysiological levels and then drop rapidly. This delivery method lies in stark contrast to the endogenous production of H_2S, in which levels are tightly regulated. These shortcomings have led to the search for H_2S donors that give researchers the ability to control the dose, duration, timing, and location of release.

1.6. Measuring H_2S Release Kinetics

Aside from the direct sources of H_2S, all other donors must undergo some type of chemical reaction to release H_2S. Release may be triggered by water, light, a nucleophile such as a thiol, the action of an enzyme, or other stimuli. Measuring the kinetics of these reactions can be difficult and has been handled in several different ways by the community of researchers developing H_2S donors. Only in a few cases have rate constants been determined, making it difficult to compare release rates across different donor classes. Instead, most researchers compare different compounds within a specific class to assess structure-property relationships.

One common method of assessing release kinetics is to use an H_2S-selective electrochemical probe. These instruments provide a real-time analysis of H_2S concentration in solution, with release data taking the form of a curve approximating an inverted, extended U-shape. Most authors report both peaking time and peak concentration, marking the top of the inverted U-shape, or a peaking half-time, marking the time it takes to reach half of the peaking concentration. It is important to realize that this type of analysis does not enable calculation of a rate constant because the rates of H_2S loss due to volatilization, oxidation, and other reactions are unknown, and all of these reactions contribute to the shape of the curve. Additionally, peaking times and concentrations depend on the concentrations of the reactants. As a result, these types of peaking time/concentration data can only be used to compare across different donors that have been analyzed under the same conditions. These data may not reflect how donors would react in the bloodstream, where rapid dilution would alter their release profile.

Another strategy used to assess release kinetics is the methylene blue method, first reported by Fischer in 1883 and expounded upon by Siegel in 1965.[45-46] Reaction of sulfide species in an acidic aqueous solution of *N*,*N*-dimethylphenylenediamine and iron (III) chloride ($FeCl_3$) leads to

the formation of methylene blue. Siegel reported that methylene blue formation, monitored by readout of the absorbance at 650 nm, showed a linear relationship to concentration of Na_2S in solution from 0–80 μM. Methylene blue is a commonly employed assay in determining H_2S release from synthetic donors, allowing for the determination of release kinetics because cumulative release can be measured.

Close examination of the methylene blue method under the aforementioned conditions shows that methylene blue does not obey Beer's Law at concentrations greater than 1 μM due to the formation of dimer and trimer species.[6, 47] Additionally, formation of methylene blue occurs in the presence of a variety of sulfur species, including thiols, a common trigger of synthetic H_2S donors, further complicating analysis.[46] Therefore, control experiments must be conducted to properly account for methylene blue derived from the H_2S donor of interest compared with other potential sources. H_2S release half-lives determined by the methylene blue assay may not be comparable between various H_2S donor systems, but this method still has utility in direct comparisons between similar donors under identical experimental conditions.

H_2S-selective fluorescent probes are also routinely used in the detection and quantification of H_2S release kinetics. Many of these probes rely on the selective reduction of aryl or sulfonyl azides to amines by HS^- in a "turn on" fluorescence mechanism. One of the first examples of a probe based on the reduction of an aryl azide was from Chang and coworkers, who demonstrated the use of an aryl azide in imaging H_2S in cells.[48] Similarly, Wang and coworkers reported the synthesis of a reduction-based probe based on the prevalent dansyl fluorophore building block, a popular option amongst chemists for its relative ease of synthesis.[49] Probes that rely on the nucleophilicity of H_2S have also been reported in the literature and are typically used for quantification of sulfide in solution.[50-52] For a more comprehensive discussion on fluorometric

determination of sulfide in solution, the reader is referred to a recent review on the topic.[53] Lastly, researchers have derivatized various forms of sulfide in solution using monobromobimane, which appears to give a more accurate quantification of sulfide in solution compared to the previously discussed methods.[54]

1.7. Naturally Occurring Donors

Consumption of garlic and onions is recognized as beneficial for prevention or treatment of cardiovascular disease, hypertension, thrombosis, and diabetes.[55] While there is still debate over which ingredients in garlic contribute to the overall health benefits attributed to consumption, H_2S-releasing compounds from garlic extract appear to be important components. The isolated H_2S-releasing compounds from garlic are byproducts of the breakdown of thiosulfinates (R–SO_2–SR).[56] Allicin, the most common of the thiosulfinates, decomposes into diallyl disulfide (DADS), diallyl sulfide (DAS), and diallyl trisulfide (DATS).[57] Subsequent research by Kraus et al. on DADS, DAS, and DATS revealed that human red blood cells converted these compounds into H_2S in the presence of free thiols and that treatment of aortic rings with these compounds led to vasorelaxation, similar to experiments using sulfide salts.[58] Linear and cyclic di-, tri-, and higher order polysulfide species have also been isolated from a variety of other plants but have not been as extensively studied as the aforementioned garlic-derived donors.[59]

Many of the studies concerning the garlic-derived H_2S donors have focused on the mechanisms by which the donors release H_2S in the presence of thiols. Of the three allicin-derived H_2S donors, Kraus showed that DATS, the compound with the most sulfur atoms, led to substantial H_2S generation upon reaction with naturally occurring thiols, including GSH, cysteine, homocysteine, and *N*-acetylcysteine.[58] Little H_2S was released from DADS and DAS, consistent

with recent computational results indicating that DADS is a much poorer H_2S donor than DATS.[60] Of the thiols tested, treatment with GSH resulted in the greatest amount of H_2S release from all three allicin-derived species. Mechanistically, H_2S release may occur upon nucleophilic addition of a thiol to one of the alpha carbons of DATS, DADS, or DAS, as well as a sulfur atom within the polysulfide species, leading to the conclusion that the allyl substituent may influence rate of release. Treatment of rat aortic rings with the garlic-derived donors (100 μM) showed an increase in relaxation over addition of Na_2S (20 μM).

Naturally occurring H_2S donors may be attractive options for biologists carrying out in vivo studies with an eye toward clinical relevancy. This class of donors does not have some of the toxicity concerns that accompany many synthetic donors, and some natural H_2S donors are commercially available. The limitations to the use of DATS, DADS, and DAS are that they are not structurally amenable to chemical transformations, have poor water solubility, and generate various byproducts after H_2S release. Additionally, isolation of these compounds from the milieu of garlic may reduce the desired physiological effects upon administration. These drawbacks make it challenging to employ these compounds in vitro and in vivo to improve our understanding of the complicated interplay between H_2S and other signaling compounds. Synthetic donors that provide tunable H_2S release rates via structural modification with discrete byproducts allow for a more in-depth analysis of the physiological roles of H_2S and, optimistically, clinically relevant H_2S-releasing prodrugs.

1.8. Synthetic H_2S Donors

1.8.1. *Considerations for Synthetic Donors*

It is useful to consider important characteristics in H_2S donors for use both as biological tools and as potential therapeutics. Of course, there is not a single ideal donor; for example, there are situations where a fast donor may be required and others where slow release is best. Sometimes release immediately upon dissolution in water may be useful, while in other cases release in response to a specific external or internal stimulus would be ideal. Despite these variations, a few characteristics are broadly desirable. H_2S donors should be water-soluble, stable under storage conditions, and generate only innocuous (if any) byproducts. They should also have a specific and well-defined release mechanism (i.e., release only in response to a specific nucleophile, a specific wavelength of light, or a specific enzyme). Many of the H_2S donors in the literature achieve a portion of these criteria but are lacking in some aspect. Nevertheless, there are H_2S donors that have been, or are currently, under evaluation in clinical trials. A few notable examples include the naproxen-based H_2S donor ATB-346 (Antibe Therapeutics), which exhibits anti-inflammatory effects;[61] GIC-1001 (GIcare Pharma Inc.), an orally administered trimebutine maleate salt H_2S donor used as an alternative to sedatives in colonoscopies;[62] and SG-1002 (SulfaGENIX), which is >90 % α-sulfur with the remainder being oxidized sulfur species, and was evaluated in an investigation aimed at increasing circulating H_2S and NO levels after heart failure.

As the field of H_2S donor chemistry continues to grow, more opportunities will ultimately arise for clinical examination of these compounds in various disease indications. In the remainder of this review, we aim to critically examine the current literature of synthetic H_2S donors. At the beginning of this decade, this would have been a very short list, but this field has grown rapidly in

recent years. Here we discuss reported H_2S donors, categorized by their class of triggering mechanisms, as well as offer insight into potential future directions of the field.

1.8.2. *Hydrolysis Triggered Donors*

1.8.2A. *Lawesson's Reagent and Derivatives*

Lawesson's reagent (LR) is a popular reagent for the thionation of ketones, esters, amides, and alcohols to the corresponding sulfur analogs.[63] LR is commercially available, making it another popular choice for groups studying H_2S physiology. LR releases H_2S in aqueous media over a much longer period than sulfide salts, although reports on detailed release kinetics are sparse. In a study by Medeiros and coworkers, oral administration of LR prior to alendronate-induced gastric damage limited subsequent gastric impairment compared to controls.[64] The authors noted an increase in GSH levels in rats treated with LR, which they attributed to the relief of oxidative stress and inhibition of neutrophil infiltration. In another in vivo study employing LR as an H_2S donor, Cunha et al. demonstrated that exogenous H_2S delivery improved leukocyte adhesion and neutrophil migration to the site where sepsis was induced in mice, improving the overall survival probability of the infected mice.[65] The authors also noted that reducing endogenous H_2S production using a CSE inhibitor increased the mortality rate of the mice over the duration of the experiment. Despite these successes, LR has not been widely employed as an H_2S donor in large part due to its lack of water solubility. It also suffers from a release mechanism that is not well understood and an apparently very slow H_2S release rate.

GYY4137 is a water-soluble derivative of LR, which also releases H_2S via hydrolysis.[66] Originally prepared as a vulcanization agent for rubber in 1957 (U.S. Pat. No. 2,954,379, filed 1957), GYY4137 is readily accessed by stirring LR with morpholine at room temperature. In a direct amperometric comparison of H_2S release rates from GYY4137 and NaSH, GYY4137

released H_2S with a peaking time of ~10 min versus ~10 seconds for NaSH in phosphate buffer pH 7.4.[66] However, the peaking concentration for GYY4137 was ~40-fold lower than for NaSH even with a 10-fold higher concentration of GYY4137 used in this study. Incubation of GYY4137 in phosphate buffer (pH 7.4 or 8.5) showed a sustained release for over an hour as determined spectrophotometrically, with an increase in release rate at lower pH. Deng et al. later noted that GYY4137 maintained H_2S levels in cell culture above baseline for over 7 days,[67] but these results were obtained using the methylene blue assay, which cannot specifically provide evidence for H_2S over other sulfur-containing species and can provide spurious results in assays conducted in vitro and in vivo.[6] Based on these and other results, GYY4137 is generally regarded as a slow-releasing H_2S donor. Intravenous or intraperitoneal injection (ip) of aqueous solutions of GYY4137 (133 μmol/kg) in rats showed an increase in plasma sulfide levels after 30 min, which was sustained out to 2 h.[66] However, in this study sulfide levels were again measured by the methylene blue assay. GYY4137 (200 μM) treatment of isolated rat aortic rings showed a later onset, but more sustained relaxation of the aortic ring compared to NaSH (300 μM). Similarly, treatment of anesthetized rats with both GYY4137 and NaSH showed similar effects on blood pressure. However, GYY4137 caused a slower onset but a more prolonged decrease in blood pressure while treatment with NaSH elicited only a transient decrease.

Due to its commercial availability and ease of handling, GYY4137 is the most widely studied H_2S donor aside from sulfide itself. In addition to its cardiovascular effects, GYY4137 has also shown efficacy in killing several types of cancer cells (HeLa, HCT-116, Hep G2, MCF-7, U2OS) in vitro, with selectivity over normal (non-cancerous) cells.[67] However, very high doses (800 μM) were used in these studies, and a 5-day incubation period was used due to the slow-releasing nature of this donor. In the same cell lines, NaSH and a non-H_2S releasing GYY4137

control compound show diminished and no efficacy in cancer cell killing, respectively. The authors attribute the efficacy of GYY4137 over NaSH in inducing cancer cell death to the sustained H_2S release profile.

GYY4137 has proven to be a useful tool for biologists, particularly in investigating the importance of H_2S release rate on physiological outcomes. However, GYY4137 suffers from several drawbacks. First, it is often prepared and sold as a dichloromethane complex, which is residual from crystallization. Dichloromethane is metabolized to CO, another gasotransmitter with biological effects similar to H_2S.[68] Therefore, some of the effects attributed to GYY4137-derived H_2S may in fact come from CO. Additionally, few studies have used proper control compounds, such as "spent" GYY4137, which are needed to rule out the possibility of biological effects derived from byproducts after H_2S release. Finally, the slow hydrolysis rate makes it challenging to delineate observed effects from H_2S, intact GYY4137, and any byproducts after hydrolysis, complicating conclusiveness in studies comparing sulfide salts and GYY4137.

Xian and coworkers developed a GYY4137 analog via substitution of the P–C bond in GYY4137 with a P–O bond.[69] These *O*-substituted phosphorodithioates were synthesized in four steps, generating the *O*-aryl and alkyl substituted 1,8-diazabicyclo[5.4.0]undec-7-ene (DBU) salts. H_2S release kinetics, as measured by a dansyl azide "turn-on" fluorescent probe, showed comparable kinetics to GYY4137 for the *O*-aryl phosphorodithioates with less than 1 % of total H_2S released after 3 h, while the *O*-alkyl phosphorodithioates did not show any H_2S release within this time frame. Initial studies on H9c2 cardiomyocyte viability under H_2O_2-induced oxidative stress after incubation with the *O*-aryl phosphorodithioate donors (50 and 100 μM) showed enhanced viability compared to untreated controls, although the difference was not statistically significant over GYY4137. When tested on B16BL6 mouse melanoma cell lines, the *O*-aryl

phosphorodithioate donors showed decreased cell viability over untreated controls (~60 % relative to control) after 4 days. GYY4137 showed a >90 % killing of these cells relative to controls over the same time scale, indicating that the potency of GYY4137 may lie in the P–C bond that was removed in the *O*-aryl phosphorodithioates. These results provide evidence that factors beyond H_2S release may cause the biological effects attributed to GYY4137, perhaps stemming from some of the issues with GYY4137 discussed above.

Expounding upon the phosphorodithioate donor structure, Xian et al. more recently developed a series of phosphonamidothioates, denoted as JK donors.[70] These donors are substituted with amino acids via a phosphoroamide linkage through the amino acid N-terminus amine. In aqueous media at neutral and mildly basic pH, the JK donors showed low amounts of H_2S release. However, under mildly acidic conditions (pH $\leq$ 6.0), these compounds cyclized via nucleophilic addition of the carboxylic acid functionality of the amino acid, promoting H_2S release by breaking the relatively weak P–S bond. For the series of JK donors, lower pH accelerated release rates as measured by the methylene blue assay, while the GYY4137 control showed no release profile variability at various pHs. H_2S release profiles were also altered by the canonical R group substituent of the amino acid on the donor. The authors observed that any substitution at the amino acid R group (i.e., R $\neq$ H) promoted cyclization, and thus showed enhanced release profiles at neutral and basic pH over the unsubstituted donor. No other trends were observed when relating H_2S release to the amino acid R group of the JK donor. The proline JK derivative released a negligible amount of H_2S at all recorded pH values. The authors attributed the lack of H_2S release observed from the proline derivative to the particularly stable conformation adopted by the proline ring in the donor, which was corroborated by density functional theory calculations. The JK donors (25 and 50 μM) showed efficacy in reducing cellular damage resulting from anoxia/reoxygenation

(A/R) treatment with H_2O_2 in vitro. The donors were also successful in reducing infarct size per area-at-risk via intracardiac injection in mice in an I/R model. Further investigation of phosphorodithioate donors in vivo involved doping poly(caprolactone) (PCL) fibers with the small molecule donor and examining the effects on a cutaneous wound model in mice.[71] The doped PCL fibers showed an extended H_2S release profile over the small molecule in solution, which is expected for a hydrolysis-triggered donor, and showed enhanced wound healing times over the non-doped PCL fiber control. From an application standpoint, these donors may be useful in treating diseases such as cancer, where pH differences exist between healthy and diseased tissue.

1.8.2B. *Dithiolthiones*

1,2-Dithiole-3-thiones (DTTs) are a class of compounds also commonly considered to be in the family of hydrolysis-triggered H_2S donors. Made by the reaction of anethole with elemental sulfur, DTTs are easy to synthesize and can be readily attached to other molecules to make drug-DTT conjugates. However, this class of H_2S donors has two problems that must be considered when interpreting biological data. First, whether DTTs release significant amounts of H_2S under physiological conditions is unclear. Williams and coworkers showed that a substituted DTT hydrolyzed cleanly, with the thione species being converted into a carbonyl.[72] However, complete hydrolysis required 48 h at 120 °C in a DMSO/H_2O mixture. The authors noted that hydrolysis under physiological conditions was very slow and did not present any data at 37 °C. However, they did observe activity of several DTTs as COX-1 and COX-2 inhibitors, with less potency noted for the hydrolyzed DTTs against both targets. Second, it is also important to mention that anethole trithione (ADT), a DTT compound that is frequently derivatized and attached to other drugs to make H_2S-donating versions of these drugs, itself has biological activity. ADT is an FDA-approved bile secretion-stimulating drug that restores salivation and relieves dry mouth in

chemotherapy-induced xerostomia.[73] The mechanism of action is unknown. Several groups have studied ADT and other DTTs and observed potent biological activity that they attribute to the H_2S-donating ability of these drugs. For example, the phenol derivative of ADT, commonly denoted as ADT-OH, reduces cell viability via inhibition of histone deacetylase[74-75] and NF-κB activation.[76] Interestingly, a study by van der Vlies and coworkers demonstrated that conjugation of ADT-OH to poly(ethylene glycol) altered the cellular uptake mechanism and largely eliminated cytotoxicity at concentrations below 200 μM.[77] The reader is cautioned that in many papers reliable measurements of H_2S generation were not reported, and that often no control experiments were reported to rule out the possibility that the observed effects were due to the biological activity of DTTs themselves.

The DTT moiety has been appended to non-steroidal anti-inflammatory drugs (NSAIDs) and studied rather extensively. The first example of a DTT-NSAID was a diclofenac derivative published in 2007 by Moore and coworkers, termed *S*-diclofenac.[78] The DTT moiety in *S*-diclofenac was linked to the NSAID through an ester bond that released diclofenac and DTT upon esterase-catalyzed hydrolysis. Experiments in PBS buffer at room temperature showed no H_2S release, consistent with results noted above. Addition of rat liver homogenates showed a minimal amount of H_2S release from both ADT-OH itself and *S*-diclofenac, determined to about 5 % of the theoretical maximum H_2S release for both donors after 30 min, as measured by an electrochemical probe. When examining plasma H_2S concentrations in live rats 6 h after ip injection, *S*-diclofenac-treated animals had a higher plasma H_2S concentration than the sulfide salt control, measured to be ~35 μM. As this value is well beyond currently accepted ranges for plasma H_2S concentration (below 1 μM), it is likely that the method used here generated H_2S from many sources that were erroneously attributed to free H_2S in plasma. Although the amount of H_2S generated in vivo from

S-diclofenac is unclear, it is clear that it showed efficacy in several animal models, including models showing dose dependent responses towards inflammation[79-80] and ulcerative colitis.[81]

More recently, a DTT derivative with a mitochondria-targeting triphenylphosphonium bromide tail was reported and named AP-39.[82] H_2S release from AP-39 in mouse brain endothelial cells was monitored using an azide-based fluorescent H_2S probe, with increased probe fluorescence localized to the mitochondria. Very little if any increase in fluorescence was observed from ADT-OH alone. These results indicate that AP-39 does indeed target the mitochondria, resulting in an increase in H_2S production. Whether H_2S is generated directly from DTT itself or as a result of increased enzymatic H_2S production is unclear. Regardless of the mechanism of action, AP-39 exhibited antioxidative activity, helping to maintain cell homeostasis by suppressing the initiation of mitochondrial cell death pathways.

All of the DTT compounds noted above linked the DTT unit to the drug using an ester bond. Pluth and coworkers recently synthesized DTT-NSAID conjugates via an amide linkage, which is more stable to hydrolysis than the corresponding ester.[83] The authors demonstrated the enhanced hydrolytic stability of the amide linkage via HPLC and UV-vis spectroscopy; however, no studies have been completed in a biological context to date. The authors also did not report on H_2S release from these compounds. It is possible that the hydrolytically robust amide linkage would increase the stability of H_2S-donating NSAIDs in the acidic environment of the stomach.

A notable compound in the DTT-NSAID class of donors is "NOSH aspirin." NOSH aspirin is an aspirin derivative with a DTT moiety as well as a nitrate group capable of releasing NO.[84] Remarkably, NOSH aspirin showed >100,000 times the potency of aspirin alone after 48 h and approximately 250,000 times the potency of aspirin alone after 72 h in a human colon cancer cell line, with an IC_{50} value of 50 nM. Interestingly, when examining cell growth inhibition in the

presence of the three individual components of NOSH aspirin (ADT-OH, a small molecule NO donor, and aspirin), the cocktail had an IC_{50} of 450 μM, a 9,000-fold difference compared with intact NOSH-aspirin. These results indicate that cancer cell growth inhibition is influenced by more than simply delivering DTT and NO concurrently with aspirin, but the reasons for this synergy remain unknown. NOSH aspirin has also been studied in vivo, with a mean reduction of 85 % in tumor size after daily treatment for 18 days (100 mg/kg) compared to untreated controls. Additional in vitro studies on NOSH-aspirin in SH-SY5Y human neuroblastoma cells showed enhanced anti-inflammatory capabilities over both an H_2S-releasing aspirin derivative and an NO-releasing aspirin derivative, suggesting that NOSH-aspirin may be an effective treatment in brain injury.[85] NOSH-aspirin represents a promising area in conjugating NSAIDs to H_2S donor moieties in an effort to generate a concerted effect through combined delivery via clever chemistry.

Table 1. Hydrolysis triggered H_2S donors.

H_2S donor	General Structure	Bioactivity	References
Sulfide salts	NaHS, Na_2S	Anti-inflammation Cardioprotective effects Diabetes amelioration	38-45
Lawesson's reagent	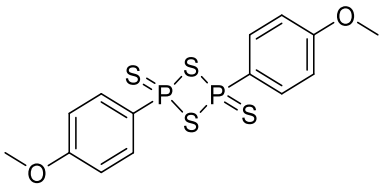	Anti-inflammation Vasodilation Anti-cancer	64-65
GYY4137	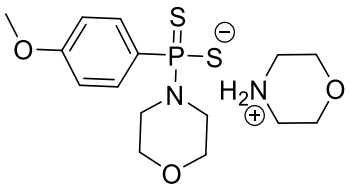	Ion channel modulation Anti-inflammation	66-68

Phosphorodithioates	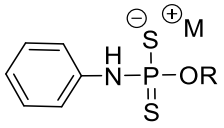	Anti-oxidant properties Anti-inflammation	69
Dithiolthiones	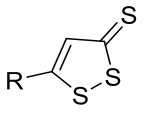	Anti-cancer proliferation Anti-inflammation	72-85

1.8.3. *Thiol-Triggered Donors*

1.8.3A. *N-Benzoylthiobenzamides*

Thiol-triggered H_2S donors were some of the first synthetic donors to be reported and are the most common class of non-hydrolysis-triggered synthetic donors. Thiol triggered donors are advantageous in that free thiols are relatively abundant nucleophiles in mammals and offer a platform from which thiol exchange can be used to accomplish H_2S release after nucleophilic addition. A series of *N*-(benzoylthio)benzamides reported by Xian et al. were among the first nucleophile-triggered H_2S donors.[86] Synthesized from substituted thiobenzoic acids, several *N*-benzoylthiobenzamides were evaluated for H_2S release, with a variety of release rates observed. The hypothesized thiol-triggered mechanism of release was confirmed with the formation of cystine, *N*-acetylcysteine, and benzamide in high yields. In cell studies, a selected *N*-(benzoylthio)benzamide protected human keratinocytes against methylglyoxal (MGO)-induced cell damage and dysfunction, a prevalent issue in diabetics.[87] These donors have also been evaluated in animal models of myocardial I/R injury, displaying a reduction in infarct size over controls in murine models, indicating a cardioprotective effect.[88]

In addition to small molecule applications, the therapeutic effects of these donors were also evaluated in polymer templates for tissue engineering applications. Wang et al. accomplished this by electrospinning PCL solutions containing various *N*-(benzoylthio)benzamide donors to make

fibrous polymeric scaffolds doped with the small molecule donor.[89] Donor-loaded PCL fibers led to increased expression of collagen type I and III in wound healing models in mice, demonstrating the potential for H_2S-releasing materials in treating chronic wounds.

1.8.3B. *Acyl Perthiols, Dithioperoxyanhydrides, and Polysulfides*

Another class of thiol-triggered donors, which ultimately require disulfide exchange to promote H_2S release, are the acyl perthiol donors. Acyl perthiol donors (RC(O)–S–SR') were first synthesized by Xian, where the R group is derived from penicillamine.[90] The donors were prepared from thiobenzoic acid derivatives and *N*-benzoyl cysteine methyl ester in two steps. These donors showed tunable release rates by varying the aromatic R substituent. H_2S release depended on both steric and electronic factors, with electron-withdrawing substituents accelerating release rates, and bulky substituents on the aromatic ring retarding release rates. These donors released H_2S over the course of minutes to hours under the conditions tested.

Analogous to Xian's acyl perthiol donors are the dithioperoxyanhydride class of donors (RC(O)–S–SC(O)R') reported by Galardon et al.[91] Both alkyl and aromatic dithioperoxyanhydride donors were readily prepared in one reaction step involving thiobenzoic acid and methoxycarbonylsulfenyl chloride ($CH_3OC(O)SCl$) with fair overall yields. The donors showed similar levels of H_2S released when triggered with both cysteine and GSH and slower release rates when treated with GSH, measured amperometrically. The compounds were non-cytotoxic at concentrations up to 200 μM in human fibroblasts and induced vasorelaxation in rat aortic ring models.

The final class of donors based on the breaking of an S–S bond are the tetrasulfide donors developed by Pluth et al.[92] This relatively simple design involves the treatment of a range of thiols with sulfur monochloride (S_2Cl_2) to generate the corresponding tetrasulfides (R–$(S)_4$–R). Aromatic

tetrasulfides released H_2S faster than their alkyl counterparts when triggered by GSH, likely as a result of the change in electrophilicity of the α/β sulfur. Interestingly, a trend in H_2S release rate was not observed when altering ring electronics, suggesting that other factors influence H_2S release from this system. Analogous to the observations of the amount of H_2S released for the natural donors DADS and DATS, the tetrasulfide donors released more H_2S than DATS, which was used in this study as a model donor.

1.8.3C. *Arylthioamides*

Arylthioamides ($ArC(S)–NH_2$) are a versatile class of donors that was first reported by Calderone and coworkers.[93] In this work, a series of twelve arylthioamides was synthesized either from substituted arylcyano compounds in two steps or via the direct thionation of select aryl amides using LR. All donors released H_2S in response to cysteine as measured amperometrically. Release studies were conducted at high concentrations of donor and thiol (1 mM and 4 mM, respectively), leading to rapid peak in release profile for all donors. The arylthioamides released only small amounts of H_2S, exhibiting maximum concentrations (C_{max}) between 3-21 μM. The fast rise to a steady state concentration for all the donors tested make these donors appear to be fast-releasing compounds; however, this quick rise to C_{max} in solution is misleading as the max H_2S concentration is a small fraction of the total available H_2S from the donors. The arylthioamides showed similar H_2S release profiles to DADS and GYY4137, two slow-releasing donors, when measured under the same experimental conditions. Interestingly, some of the donors released H_2S in the absence of a thiol trigger, indicating that they may also be hydrolysis-triggered. Alterations in ring electronics modulated release rates, but not in a predictable pattern. One donor, *p*-hydroxybenzothioamide, was evaluated in vitro in a rat aortic ring contraction study and completely abolished vasoconstriction at 1 mM in the presence of noradrenaline (NA) without the

addition of exogenous cysteine, suggesting that biologically relevant levels of cysteine triggered sufficient H_2S release, at least at this high donor concentration. This donor was also evaluated for its effect on hyperpolarization in human vascular smooth muscle cells (HASMCS), showing a similar ability to hyperpolarize HASMCs at 300 μM compared with 1 mM NaSH, suggesting that slow, sustained levels of H_2S from *p*-hydroxybenzothioamide may be more effective than high instantaneous concentrations of H_2S.

Due to the observed slow, sustained H_2S release profile of *p*-hydroxybenzothioamide and ease of conjugation to other compounds, other researchers have combined this donor with polymers and other drugs as conjugates.[61] For example, Bowden et al.[94] synthesized statistical copolymers containing L-lactide and a *p*-hydroxybenzothioamide lactide derivative and showed release of the donor in the timescale of days to weeks, although no studies of H_2S release were included in this report.[94] In another example, the development of a naproxen-hydroxybenzothioamide conjugate, ATB-346, was described.[61] In the initial report, its efficacy as an anticancer drug was investigated, revealing that it induced apoptosis in human melanoma cells in animal studies. ATB-346 has also shown efficacy in reducing gastrointestinal tract injury while maintaining utility as a chemopreventative agent against colorectal cancer when compared to naproxen.[95] Further studies on ATB-346 are underway by Antibe Therapeutics, where a phase II study was completed in 2016 for pain associated with osteoarthritis.

1.8.3D. *S-Aroylthiooximes*

S-Aroylthiooximes (SATOs) are a class of thiol-triggered donors developed by Matson and coworkers.[96] SATOs ($ArC(O)–S–N=CR_2$) are synthesized by condensation of an aryl aldehyde or ketone and an *S*-aroylthiohydroxylamine (SATHA, $ArC(O)–S–NH_2$) in the presence of catalytic acid, analogous to oxime formation. A variety of substituted small molecule SATOs were

synthesized, varying both the substituent on the SATHA component and the aldehyde or ketone. SATOs released H_2S in the presence of cysteine and other thiols but did not show release in the presence of amines or water alone. H_2S release was measured amperometrically as well as with the methylene blue method. A definitive electronics trend correlating the substituent on the SATHA ring with H_2S release was observed by fitting release half-lives as measured by methylene blue to a Hammett plot. Under the conditions tested, H_2S release half-lives ranged over an order of magnitude, from minutes to hours.

The modularity of the SATO formation reaction has allowed for SATOs to be extended to macromolecular systems.[97] Poly(SATOs) were synthesized via post-polymerization modification of functionalized polymethacrylates containing pendant aryl aldehydes with substituted SATHAs. H_2S release rates were slower in the polymer system than in analogous small molecules, and electronic effects were consistent with those observed in the initial small molecule SATO study. Extending the poly(SATO) system further, amphiphilic block copolymers containing SATO functional groups as the hydrophobic block were synthesized for studies on self-assembled polymer micelles for H_2S delivery.[98] The SATO micelles released H_2S over the course of several hours, approximately an order of magnitude slower than analogous small molecule SATOs under the same conditions. Treatment of HCT116 colon cancer cells with SATO micelles ([SATO] = 250 μM) reduced colon cancer cell viability to a greater degree than Na_2S, GYY4137, and a small molecule SATO at the same concentration, contributing further evidence suggesting that kinetics of H_2S release affects therapeutic potency.

In another example of the modularity of SATO chemistry, an amphiphilic peptide with the sequence IAVEEE was modified by appending an aryl aldehyde to the N-terminus.[99] The unsubstituted SATHA was conjugated to the modified peptide to form a SATO-based aromatic

peptide amphiphile. The SATO aromatic peptide amphiphiles self-assembled in aqueous media to form nanofibers that gelled in the presence of calcium to afford a hydrogel using just 1 wt.% peptide. These peptide-based H_2S donors exhibited sustained H_2S release in the gel state with a peaking time of ~120 min and detectable H_2S out to 15 h in PBS buffer in the presence of cysteine, as measured amperometrically. In vitro studies using mouse brain endothelial cells showed minimal toxicity of the gels, a promising result for future in vivo studies as these gels show great potential for localized H_2S delivery.

Table 2. Thiol-triggered H_2S donors.

H_2S Donor	General Structure	Bioactivity	References
N-Benzoylthiobenzamides	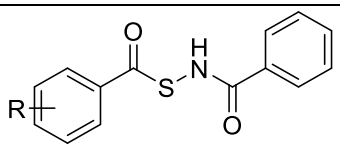	Cardioprotection	86-89
Acyl perthiols	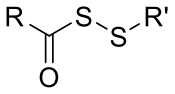	Cardioprotection	90
Dithioperoxyanhydrides	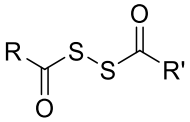	Vasodilation	91
Polysulfides	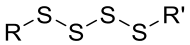	None reported	92
Arylthioamides	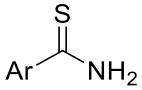	Vasodilation	61, 93-95
S-Aroylthiooximes	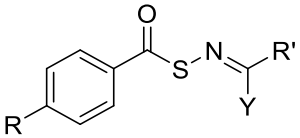	Anti-cancer proliferation	96-99

1.8.4. *Light Triggered Donors*

1.8.4A. *Geminal-dithiols*

Light-triggered prodrugs are useful tools for studies in vitro and hold promise as potential therapeutic candidates due to the bioorthogonality of visible light as a trigger. Light has an advantage over other triggers because it can affect H_2S release without perturbing any native biochemical processes, albeit only in areas of the body where sufficient light penetration is possible. Light-triggered prodrugs are ideal in applications where tissue-specific delivery is required. After prodrug administration, light of a particular wavelength can trigger release at the site of interest, minimizing off-target effects through direct spatial and temporal control over release.

One of the first examples of light-triggered H_2S donors was reported by Xian et al. in the form of geminal dithiols ($ArCH_2–S–C(CH_3)_2–S–CH_2Ar$). Gem-dithiols were prepared by treating *ortho*-nitrobenzylthiol or related derivatives with acetone and catalytic amounts of titanium(IV) chloride ($TiCl_4$) to bridge two thiols together via a thioacetal linkage.[100] The *ortho*-nitro group underwent cleavage when irradiated with UV light (365 nm), which has been demonstrated in a variety of systems,[101] to produce a geminal dithiol intermediate. This intermediate hydrolyzed to yield H_2S relatively rapidly. All of the donors released their full payload within ~30 min. Control experiments showed that no H_2S was released in the absence of UV light. Because hydrolysis of gem-dithiols is acid-catalyzed, H_2S release was accelerated at low pHs and retarded at higher pHs. A variety of other gem-dithiol derivatives were also prepared by varying the bridging group between thiols. In general, alkyl derivatives released H_2S with profiles similar to the model compound, but aryl variants exhibited much slower release by decreasing the rate of hydrolysis,

most likely due to changes in both sterics and electronics as a result of adding an aromatic ring to the bridging group.

1.8.4B. *Ketoprofenate Photocages*

Another example of a light-triggered H_2S prodrug is the ketoprofenate donor reported by Nakagawa et al.[102] Synthesis of this donor was accomplished in three synthetic steps. Upon irradiation by UV light, the donor released two equiv of 2-propenylbenzophenone and carbon dioxide (CO_2), along with one equiv of H_2S. To determine H_2S release behavior in a biological system, this donor was examined in a solution containing fetal bovine serum. No H_2S was detected without UV irradiation; however, 30 μM H_2S was detected from 500 μM donor after irradiation for 10 min, as measured by the methylene blue assay.

1.8.4C. *α-Thioetherketones*

In addition to small molecules, polymeric light-triggered H_2S donors have been reported. Connal and coworkers developed a prodrug that incorporated a UV-responsive α-thioetherketone linkage, which decomposed into a thioaldehyde species and benzophenone, a byproduct that has been approved as safe by the FDA.[103] In the presence of an amine, the thioaldehyde generated H_2S, and an imine byproduct. The authors incorporated this donor into polymeric systems using α-thioetherketone-modified styrene along with water-soluble comonomers. These polymers were then used to prepare hydrogels. Growth of 3T3 fibroblasts was observed on the hydrogels, and an H_2S-selective fluorescent probe was used to visualize H_2S in the fibroblasts after UV irradiation. The polymeric α-thioetherketone donors highlight promising potential applications for a variety of polymeric H_2S prodrug systems, particularly in applications that require localized delivery where gels and films may be advantageous.

Light-triggered H_2S donors provide feasible options for H_2S release under unique conditions, enabling a more specific triggering mechanism than nucleophiles typically offer. Using light as a trigger also provides the opportunity for spatiotemporal control of H_2S release. This donor class is most likely to find utility as chemical tools for studying H_2S biology in vitro due to the limited penetration depth of UV and visible light in mammalian tissue. However, the development of near-IR light-triggered donors may enable in vivo studies due to the ability of near-IR light to penetrate tissue at a greater depth than UV and visible light with little risk to surrounding tissue.

1.8.5. *Enzyme-Triggered Donors*

Utilizing enzymes as triggers for H_2S release offers several advantages over the other triggers mentioned. Enzymes are native to living organisms and often exhibit substrate and tissue specificity. Combined, these factors allow for specific drug targeting to a tissue of interest. Additionally, enzyme overexpression is a common cause of many diseases, offering potential targets to treat such diseases with the implementation of enzyme-triggered prodrugs. Although only a handful of enzyme-triggered H_2S donors have thus far been reported, these types of donors are poised to make a substantial impact in the coming years.

The first enzyme-triggered H_2S donors were a series of esterase-responsive compounds developed by Wang and coworkers.[104] These donors rely on a lactonization reaction popularly termed “trimethyl lock” (TML), which has been used to promote the release of a variety of drugs.[105] The TML system requires cleavage of a phenolic ester by an esterase, after which steric repulsion of three methyl groups triggers lactonization (via the Thorpe-Ingold effect), releasing a drug from a neighboring carbonyl group. In the case of the esterase-triggered H_2S donors, the

authors included a thioester, which reacts in the lactonization step to release H_2S. The authors prepared a number of derivatives in this study through variation of the phenolic ester moiety as well as addition or removal of the methyl substituents on the aromatic ring. Because specifically placed methyl groups are required to drive cyclization after ester cleavage, it was expected that removing them would offer an avenue of slowing H_2S release. Indeed, derivatives lacking aryl methyl groups exhibited longer times to reach 50 % of the peaking concentration, ranging from 45–99 min, whereas prodrug containing aryl methyl groups reached 50 % of peaking concentration in 13-29 min, as measured by an H_2S electrode probe. In addition, several NSAID-TML hybrids were synthesized and evaluated for their efficacy as anti-inflammatory agents, successfully inhibiting TNF-α secretion. Finally, one TML derivative in this study (BW-HP-102) reduced losses in myocardial tissue in a mouse I/R injury model.[106] The authors are currently investigating the pharmacokinetics, precise mechanism of action, and safety profile of BW-HP-102 in an effort to bring this compound to clinical trials.

In another example of enzyme-triggered H_2S donors, Chakrapani and coworkers merged the concepts of enzyme-specific cleavable functionalities with the protected geminal dithiol as an H_2S releasing moiety.[107] Rather than employing a photocleavable functionality, as seen in Xian's work, the authors used a *para*-nitro benzyl thioether as the geminal dithiol protecting group. The nitro group on the benzene ring underwent selective reduction to an amine in the presence of nitroreductase, an enzyme found in bacteria. Reduction by nitroreductase led to an unstable intermediate, which underwent self-immolation to release the deprotected geminal dithiol, which in turn decomposed to generate H_2S via hydrolysis. The donors (50 μM) showed sustained H_2S release out to 45 min using a fluorescent BODIPY probe, with peak instantaneous H_2S concentrations of 30 μM in the presence of nitroreductase. In vitro studies using *E. coli* strains

showed that the donor rescued the bacteria from oxidative stress resulting from treatment with common antibiotics, indicating that H_2S production in bacteria may be a mechanism leading to antibiotic resistance.

Table 3. Light and enzyme triggered H_2S donors.

H_2S Donor	General Structure	Bioactivity	References
Geminal-dithiols	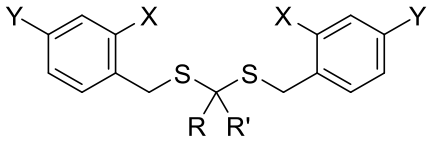	Restores AMR	100-101, 107
Ketoprofenate photocages	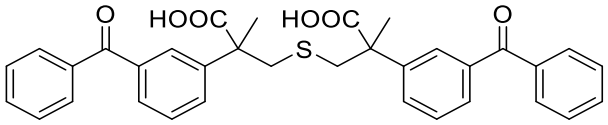	None reported	102
Trimethyl lock	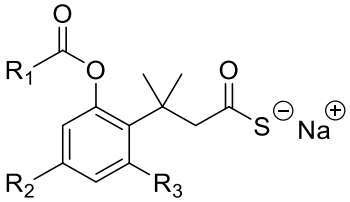	Anti-inflammation	104, 106-107

1.8.6. *Dual Carbonyl Sulfide / H_2S Donors*

A recent innovation in H_2S donor design is the synthesis of compounds that release carbonyl sulfide (COS), a compound that is an intermediate to H_2S generation and may itself be a gasotransmitter. Two studies in 1979 and 1980 first demonstrated that COS metabolism is linked to the generation of H_2S in vivo through the action of the ubiquitous enzyme carbonic anhydrase (CA).[108-109] Since these seminal papers on COS physiology, the literature had been quiet on the topic until recently. For a more detailed account of the potential roles of COS in mammalian biology the reader is referred to a recent review on the topic.[110] The link between COS and H_2S via CA opens a new avenue of H_2S research through the synthesis of compounds that release COS.

COS donors act as H_2S donors in the presence of CA, but also provide the opportunity to study COS as a potential gasotransmitter.

1.8.6A. *N-Thiocarboxyanhydrides*

N-Thiocarboxyanhydrides (NTAs) are a class of COS releasing compounds first reported in 1971 as monomers for the synthesis of polypeptides.[111] Matson and coworkers saw these molecules as a potential nucleophile-responsive COS/H_2S donor platform with the advantage of releasing only COS and innocuous peptide byproducts. The sarcosine NTA derivative (R=CH_3, NTA1) was synthesized in three steps from sarcosine (*N*-methyl glycine).[112] The generation of COS, triggered by opening of the NTA with glycine, and the resulting dipeptide byproduct were confirmed by GCMS and LCMS, respectively. In the presence of glycine and CA, the conversion of COS into H_2S was confirmed via the methylene blue assay. A polymeric NTA donor (polyNTA1) was also synthesized via conjugation of NTA1 to a norbornene moiety and subsequent polymerization by ring-opening metathesis polymerization (ROMP). Comparison of the H_2S release kinetics of the NTA1 and polyNTA1 using a fluorescent H_2S sensor showed a 4-fold increase in release half-life for the polymer compared with NTA1, with half-lives in the range of hours for both donor types under the testing conditions. In vitro studies with mouse brain endothelial cells showed an enhancement in endothelial cell proliferation after treatment with NTA1 (100 μM) over controls.

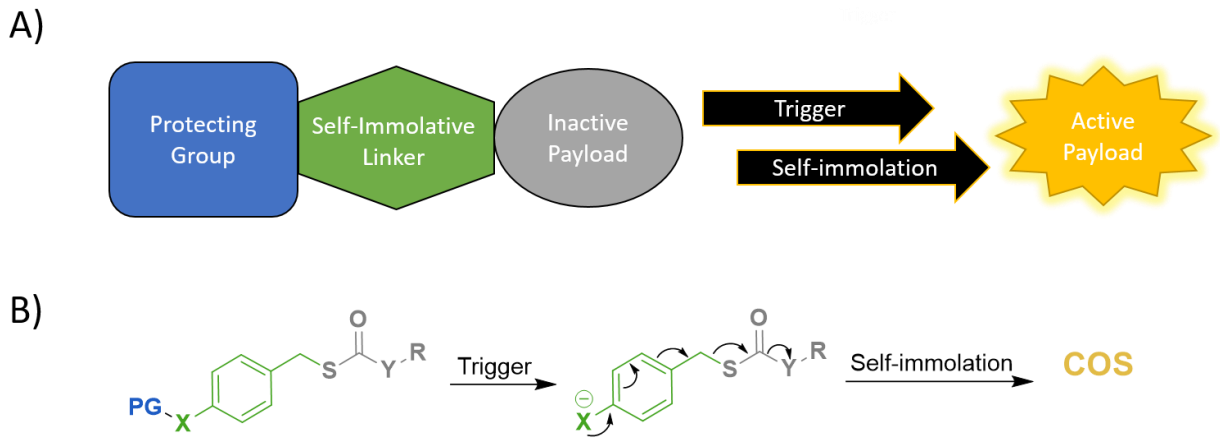

Figure 2. A) Schematic illustration depicting the concept of a self-immolative releasing its payload. B) An example mechanism depicting COS release from a generalized thiocarbamate.

1.8.6B. *Self-Immolative Thiocarbamates*

A separate class of COS releasing prodrugs is based on a self-immolative reaction mechanism whereby COS release is the result of the decomposition of a thiocarbamate-containing compound in the presence of a specific trigger (Figure 2). The first self-immolative COS/H_2S donors were reported by Pluth et al. in the form of analyte replacement probes.[113] These thiocarbamate-based donors were prepared by conjugation of an aryl azide to a pro-fluorophore via a thiocarbamate (R–O(S)–NHR) linkage. H_2S initiated self-immolation by reducing the aromatic azide to an amine, resulting in a cascade-like decomposition of the molecule to release COS, a quinone methide species, and the fluorophore. A 65-fold increase in fluorescence response to H_2S was observed over other reactive sulfur, nitrogen, and/or oxygen species (RSONS), demonstrating the trigger specificity of this self-reporting system.

Building off of their analyte replacement probes, Pluth and coworkers aimed to synthesize a similar class of self-immolative COS donors with RSONS-sensitive triggers.[114] These donors consist of an RSONS-active boron pinacol ester connected to *para*-substituted phenyl derivatives by way of the aforementioned thiocarbamate linkage. These donors were non-toxic and released H_2S in the presence of CA in response to H_2O_2, superoxide (O_2^-), and peroxynitrite ($ONOO^-$), with H_2O_2 resulting in the greatest amount of H_2S release, as measured amperometrically. Using the phorbol 12-myristate 13-acetate (PMA) assay, a well-established method to induce production of H_2O_2 in macrophages,[115] the authors demonstrated that endogenously produced ROS also triggered H_2S release in these donors. Additionally, these donors exhibited cytoprotective effects—the presence of the prodrug showed a significant dose-dependent increase in cell viability (10-50 μM) after treatment with H_2O_2 (100 μM) compared to controls. These data suggest that this prodrug was not only capable of quenching RSONS as a result of the rapid reaction between arylboronates and RSONS in vivo, but also of reducing cellular damage in an oxidative environment through H_2S release.

Pluth et al. have also reported on the synthesis of enzyme-triggered self-immolative COS prodrugs, with the same general thiocarbamate-based structure as those discussed previously.[116] These COS donors contain a *para*-pivaloyl group, which is preferentially cleaved in the presence of esterases. These donors were stable in aqueous media, exhibiting no H_2S release in the presence of physiologically relevant levels of CA in the absence of esterase. However, when the authors introduced porcine liver esterase a relatively rapid release of COS/H_2S resulted under the same conditions. Interestingly, these thiocarbamate donors exhibited higher levels of cytotoxicity than equivalent levels of Na_2S and GYY4137 in BEAS 2B human lung epithelial cells and in HeLa cells. The authors attribute the cytotoxicity to reduced cellular respiration and ATP synthesis,

which is in line with the well-known ability of H_2S to inhibit cytochrome c oxidase.[117] The authors suggest that COS itself may have physiological functions different from those of H_2S in certain biological environments, leading to these unexpected observations.

Another example of enzyme triggered self-immolative COS prodrugs was reported by Chakrapani et al.[118] In this work the authors examined the use of pivaloyloxymethyl carbonothioates ($ArCH_2S–C(O)–OR$) and carbamothioates ($ArCH_2S–C(O)–NHR$) as esterase-triggered COS donors. These prodrugs consist of a *para*-pivaloyloxymethyl linkage that blocked self-immolation until triggered. After cleavage of this linkage, a carbamothioate ($^{-}$S-C(O)-NHR) or carbonothioate ($^{-}$S-C(O)-OR) anion formed, allowing for self-immolation and tandem release of COS and either an ester or amine. H_2S release did not depend on ring electronics, and minimal differences in release profiles were observed between carbonothioate and carbamothioate donors. The authors concluded that rapid cleavage of the pivaloyloxymethyl group occurred, followed by self-immolation of a short lived intermediate to release COS and eventually H_2S in the presence of CA.

Another type of self-immolative H_2S prodrug comes in the form of "click-and-release" thiocarbamates.[119] This system utilized the inverse-electron demand Diels Alder reaction to click together tetrazine and thiocarbamate-containing *trans*-cyclooctene to selectively release COS. This strategy is different from other COS/H_2S donor systems because the triggering reaction is completely bio-orthogonal. In other words, release can theoretically be triggered by the researcher upon addition of tetrazine to cells or an animal. From this platform, Pluth and coworkers showed that H_2S release was dose-dependent on tetrazine, that the prodrug was non-toxic, and that CA was required to observe any measurable quantities of H_2S. However, the authors were unable to expand this strategy to a cellular environment due to incompatibility of the click-and-release reaction with

the fluorescent probes currently used to image H_2S. The authors attributed this limitation to the rapid scavenging of H_2S by tetrazine via a known reduction mechanism.

Bio-orthogonal, light-activated thiocarbamates have also been reported by Pluth et al.[120] This system utilized an *o*-nitrobenzyl functionality that underwent UV-triggered cleavage. UV light exclusively initiated the release of H_2S, as amino acid nucleophiles produced no response after incubation in PBS for 10 min. Additionally, this system exhibited tunable release, with 4,5-dimethoxy substituted derivatives reaching peak instantaneous H_2S concentrations twice as fast as the unsubstituted donor, likely a result of the increased light absorption of the dimethoxy derivative. These donors have yet to be evaluated in biological systems.

The advent of COS donors enables the study of COS itself, including the intriguing possibility that COS may enact biological effects that differ from H_2S. While complete inhibition of the ubiquitous enzyme CA may be difficult due to its many isoforms, clever methods to study COS will continue to be developed. With the persistent production of dual H_2S/COS donors by chemists, the physiological interactions of COS may eventually be fully elucidated, affording a greater understanding of how small sulfur species signal cells and interact in the body.

Table 4. Dual COS/H_2S donor systems.

H_2S Donor	General Structure	Bioactivity	References
N-Thiocarboxyanhydrides	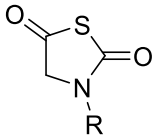	Angiogenesis	110
Arylboronate thiocarbamates	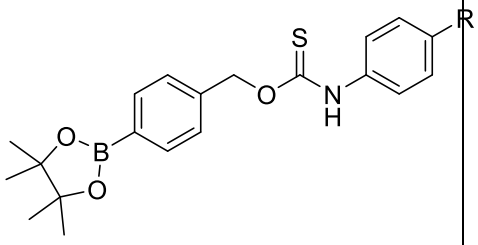	Cardioprotection	113
Esterase-triggered thiocarbamates	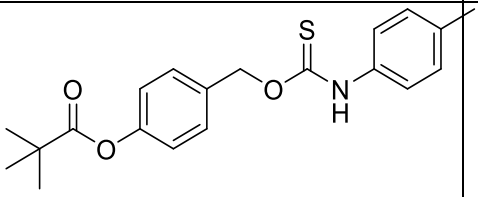	Reduction in cellular respiration	115-117
"Click and release" thiocarbamates	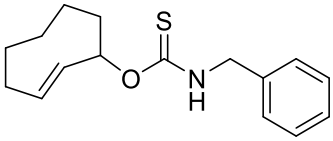	None reported	118
o-Nitrobenzyl thiocarbamates	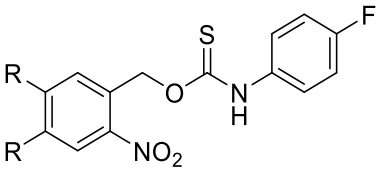	None reported	119

1.9. Conclusions

Remarkable progress has been made in the field of H_2S donor chemistry in the short amount of time since the therapeutic potential of H_2S was discovered. Continued innovation from synthetic chemists will be a major factor in driving H_2S research forward in the coming years, with an eye toward building H_2S donors that enable biological studies on the (patho)physiological roles of this

gas and have potential as clinically relevant H_2S-releasing therapeutics. Important questions remain unanswered in the H_2S field at large, which will require joint effort from chemists, pharmacologists, and biologists. One chief concern is determining the therapeutic window of H_2S for a given target as well as the active species giving the desired effect once the donor is delivered. An increased molecular and biological understanding of donor triggers and byproducts, species interchange, signaling mechanisms, and redox chemistry of H_2S donors will help elucidate biological activity and species involved. The chemistry of H_2S donors is often complicated by the release of reactive byproducts, including unidentified sulfur species, a topic that needs further attention. As the field of H_2S research continues to grow, it is imperative that these key issues be addressed so that the field as a whole can move forward. Persistent innovation in synthetic donors and increased understanding of H_2S physiology may eventually enable a pathway to the clinic for H_2S therapeutics.

1.10. Acknowledgements

We are grateful to the National Science Foundation (DMR-1454754) and the National Institutes of Health (R01GM123508) for support of our work in this area.

1.11. References

1. Abe, K.; Kimura, H., The Possible Role of hydrogen sulfide as an Endogenous Neuromodulator. *J. Neurosci.* **1996,** *16*, 1066-1071.

2. Wang, R., Two's Company, Three's a Crowd: Can H_2S Be the Third Endogenous Gaseous Transmitter? *FASEB J.* **2002,** *16*, 1792-8.

3. Ungerer, P.; Wender, A.; Demoulin, G.; Bourasseau, É.; Mougin, P., Application of Gibbs Ensemble and NPT Monte Carlo Simulation to the Development of Improved Processes for H_2S-rich Gases. *Mol. Simul.* **2004,** *30*, 631-648.

4. Cuevasanta, E.; Denicola, A.; Alvarez, B.; Möller, M. N., Solubility and Permeation of Hydrogen Sulfide in Lipid Membranes. *PLoS One* **2012,** *7*, e34562.

5. Chen, K. Y.; Morris, J. C., Kinetics of Oxidation of Aqueous Sulfide by Oxygen. *Environ. Sci. Technol.* **1972,** *6*, 529-537.

6. Hughes, M. N.; Centelles, M. N.; Moore, K. P., Making and Working with Hydrogen Sulfide. *Free Radic. Biol. Med.* **2009,** *47*, 1346-1353.

7. Kabil, O.; Banerjee, R., Redox Biochemistry of Hydrogen Sulfide. *J. Biol. Chem.* **2010,** *285*, 21903-7.

8. Li, L.; Rose, P.; Moore, P. K., Hydrogen Sulfide and Cell Signaling. *Annu. Rev. Pharmacool. Toxicol.* **2011,** *51*, 169-187.

9. Gadalla, M. M.; Snyder, S. H., Hydrogen Sulfide as a Gasotransmitter. *J. Neurochem.* **2010,** *113*, 14-26.

10. Miles, E. W.; Kraus, J. P., Cystathionine β-Synthase: Structure, Function, Regulation, and Location of Homocystinuria-causing Mutations. *J. Biol. Chem.* **2004,** *279*, 29871-29874.

11. Pan, L. L.; Liu, X. H.; Gong, Q. H.; Yang, H. B.; Zhu, Y. Z., Role of Cystathionine γ-Lyase/Hydrogen Sulfide Pathway in Cardiovascular Disease: A Novel Therapeutic Strategy? *Antioxid. Redox Signal.* **2011,** *17*, 106-118.

12. Shibuya, N.; Tanaka, M.; Yoshida, M.; Ogasawara, Y.; Togawa, T.; Ishii, K.; Kimura, H., 3-Mercaptopyruvate Sulfurtransferase Produces Hydrogen Sulfide and Bound Sulfane Sulfur in the Brain. *Antioxid. Redox Signal.* **2008,** *11*, 703-714.

13. Chen, X.; Jhee, K. H.; Kruger, W. D., Production of the Neuromodulator H_2S by Cystathionine Beta-synthase via the Condensation of Cysteine and Homocysteine. *J. Biol. Chem.* **2004,** *279*, 52082-6.

14. Niu, W.-N.; Yadav, P. K.; Adamec, J.; Banerjee, R., S-Glutathionylation Enhances Human Cystathionine β-Synthase Activity Under Oxidative Stress Conditions. *Antioxid. Redox Signal.* **2015,** *22*, 350-361.

15. Eto, K.; Kimura, H., The Production of Hydrogen Sulfide is Regulated by Testosterone and S-adenosyl-L-methionine in Mouse Brain. *J. Neurochem.* **2005,** *93*, 1633.

16. Mustafa, A. K.; Gadalla, M. M.; Sen, N.; Kim, S.; Mu, W.; Gazi, S. K.; Barrow, R. K.; Yang, G.; Wang, R.; Snyder, S. H., H_2S Signals Through Protein S-Sulfhydration. *Sci. Signal* **2009,** *2*, ra72-ra72.

17. Bos, E. M.; Wang, R.; Snijder, P. M.; Boersema, M.; Damman, J.; Fu, M.; Moser, J.; Hillebrands, J. L.; Ploeg, R. J.; Yang, G.; Leuvenink, H. G.; van Goor, H., Cystathionine γ-lyase Protects Against Renal Ischemia/Reperfusion by Modulating Oxidative Stress. *J. Am. Soc. Nephrol.* **2013,** *24*, 759-70.

18. Elrod, J. W.; Calvert, J. W.; Morrison, J.; Doeller, J. E.; Kraus, D. W.; Tao, L.; Jiao, X.; Scalia, R.; Kiss, L.; Szabo, C.; Kimura, H.; Chow, C.-W.; Lefer, D. J., Hydrogen sulfide Attenuates Myocardial Ischemia-Reperfusion Injury by Preservation of Mitochondrial Function. *Proc. Natl. Acad. Sci. U. S. A.* **2007,** *104*, 15560-15565.

19. Salloum, F. N., Hydrogen sulfide and Cardioprotection — Mechanistic Insights and Clinical Translatability. *Pharmacol. Ther.* **2015,** *152*, 11-17.

20. Shirozu, K.; Tokuda, K.; Marutani, E.; Lefer, D.; Wang, R.; Ichinose, F., Cystathionine γ-lyase Deficiency Protects Mice from Galactosamine/Lipopolysaccharide-induced Acute Liver Failure. *Antioxid. Redox Signal.* **2014,** *20*, 204-216.

21. Hartle, M. D.; Pluth, M. D., A Practical Guide to Working With H_2S at the Interface of Chemistry and Biology. *Chem. Soc. Rev.* **2016,** *45*, 6108-6117.

22. Nagahara, N.; Nagano, M.; Ito, T.; Shimamura, K.; Akimoto, T.; Suzuki, H., Antioxidant Enzyme, 3-Mercaptopyruvate Sulfurtransferase-Knockout Mice Exhibit Increased Anxiety-like Behaviors: A Model for Human Mercaptolactate-cysteine Disulfiduria. *Sci. Rep.* **2013,** *3*, 1986.

23. Pietri, R.; Román-Morales, E.; López-Garriga, J., Hydrogen Sulfide and Hemeproteins: Knowledge and Mysteries. *Antioxid. Redox Signal.* **2011,** *15*, 393-404.

24. Spassov, S. G.; Donus, R.; Ihle, P. M.; Engelstaedter, H.; Hoetzel, A.; Faller, S., Hydrogen Sulfide Prevents Formation of Reactive Oxygen Species through PI3K/Akt Signaling and Limits Ventilator-Induced Lung Injury. *Oxid. Med. Cell. Longev.* **2017,** *2017*, 1-14.

25. Ono, K.; Akaike, T.; Sawa, T.; Kumagai, Y.; Wink, D. A.; Tantillo, D. J.; Hobbs, A. J.; Nagy, P.; Xian, M.; Lin, J.; Fukuto, J. M., Redox Chemistry and Chemical Biology of H_2S, Hydropersulfides, and Derived Species: Implications of their Possible Biological Activity and Utility. *Free Radic. Biol. Med.* **2014,** *77*, 82-94.

26. Filipovic, M. R., Persulfidation (S-sulfhydration) and H_2S. *Handb. Exp. Pharmacol.* **2015,** *230*, 29-59.

27. Cuevasanta, E.; Möller, M. N.; Alvarez, B., Biological Chemistry of Hydrogen Sulfide and Persulfides. *Arch. Biochem. Biophys.* **2017,** *617*, 9-25.

28. Xuan, W.; Sheng, C.; Cao, Y.; He, W.; Wang, W., Fluorescent Probes for the Detection of Hydrogen Sulfide in Biological Systems. *Angew. Chem. Int. Ed.* **2012,** *51*, 2282-2284.

29. Pandey, S. K.; Kim, K.-H.; Tang, K.-T., A Review of Sensor-Based Methods for Monitoring Hydrogen Sulfide. *TrAC, Trends Anal. Chem.* **2012,** *32*, 87-99.

30. Lin, V. S.; Chen, W.; Xian, M.; Chang, C. J., Chemical Probes for Molecular Imaging and Detection of Hydrogen Sulfide and Reactive Sulfur Species in Biological Systems. *Chem. Soc. Rev.* **2015,** *44*, 4596-4618.

31. Asimakopoulou, A.; Panopoulos, P.; Chasapis, C. T.; Coletta, C.; Zhou, Z.; Cirino, G.; Giannis, A.; Szabo, C.; Spyroulias, G. A.; Papapetropoulos, A., Selectivity of Commonly Used Pharmacological Inhibitors for Cystathionine-β-synthase (CBS) and Cystathionine-γ-lyase (CSE). *Br. J. Pharmacol.* **2013,** *169*, 922-932.

32. Huang, C. W.; Moore, P. K., H_2S Synthesizing Enzymes: Biochemistry and Molecular Aspects. In *Chemistry, Biochemistry and Pharmacology of Hydrogen Sulfide*, Springer: 2015; pp 3-25.

33. Struve, M. F.; Brisbois, J. N.; James, R. A.; Marshall, M. W.; Dorman, D. C., Neurotoxicological Effects Associated With Short-term Exposure of Sprague-Dawley Rats to Hydrogen Sulfide. *Neurotoxicology* **2001,** *22*, 375-85.

34. Volpato, M. D. Gian P.; Searles, B. A. R.; Yu, P. D. B.; Scherrer-Crosbie, M. D. P. D. M.; Bloch, M. D. Kenneth D.; Ichinose, M. D. F.; Zapol, M. D. Warren M., Inhaled Hydrogen SulfideA Rapidly Reversible Inhibitor of Cardiac and Metabolic Function in the Mouse. *Anesthesiology* **2008,** *108*, 659-668.

35. Faller, S.; Ryter, S. W.; Choi, A. M. K.; Loop, T.; Schmidt, R.; Hoetzel, A., Inhaled Hydrogen Sulfide Protects Against Ventilator-Induced Lung Injury. *Anesthesiology* **2010,** *113*, 104-115.

36. Wagner, F.; Wagner, K.; Weber, S.; Stahl, B.; Knöferl, M. W.; Huber-Lang, M.; Seitz, D. H.; Asfar, P.; Calzia, E.; Senftleben, U.; Gebhard, F.; Georgieff, M.; Radermacher, P.; Hysa, V., Inflammatory Effects of Hypothermia and Inhaled H_2S During Resuscitated, Hyperdynamic Murine Septic Shock. *Shock* **2011,** *35*, 396-402.

37. Zhao, W.; Zhang, J.; Lu, Y.; Wang, R., The Vasorelaxant Effect of H_2S as a Novel Endogenous Gaseous K(ATP) Channel Opener. *EMBO J.* **2001,** *20*, 6008-6016.

38. Li, T.; Zhao, B.; Wang, C.; Wang, H.; Liu, Z.; Li, W.; Jin, H.; Tang, C.; Du, J., Regulatory Effects of Hydrogen Sulfide on IL-6, IL-8 and IL-10 Levels in the Plasma and Pulmonary Tissue of Rats with Acute Lung Injury. *Exp. Biol. Med.* **2008,** *233*, 1081-1087.

39. Whiteman, M.; Cheung, N. S.; Zhu, Y. Z.; Chu, S. H.; Siau, J. L.; Wong, B. S.; Armstrong, J. S.; Moore, P. K., Hydrogen Sulphide: A Novel Inhibitor of Hypochlorous Acid-Mediated Oxidative Damage in the Brain? *Biochem. Biophys. Res. Commun.* **2005,** *326*, 794-798.

40. Jha, S.; Calvert, J. W.; Duranski, M. R.; Ramachandran, A.; Lefer, D. J., Hydrogen Sulfide Attenuates Hepatic Ischemia-Reperfusion Injury: Role of Antioxidant and Antiapoptotic Signaling. *Am. J. Physiol. Heart Circ. Physiol.* **2008,** *295*, H801-6.

41. Wallace, J. L.; Vong, L.; McKnight, W.; Dicay, M.; Martin, G. R., Endogenous and Exogenous Hydrogen Sulfide Promotes Resolution of Colitis in Rats. *Gastroenterology* **2009,** *137*, 569-578.

42. Wallace, J. L.; Dicay, M.; McKnight, W.; Martin, G. R., Hydrogen Sulfide Enhances Ulcer Healing in Rats. *FASEB J.* **2007,** *21*, 4070-4076.

43. Whiteman, M.; Armstrong, J. S.; Chu, S. H.; Jia-Ling, S.; Wong, B. S.; Cheung, N. S.; Halliwell, B.; Moore, P. K., The Novel Neuromodulator Hydrogen Sulfide: An Endogenous Peroxynitrite 'Scavenger'? *J. Neurochem.* **2004,** *90*, 765-768.

44. Whiteman, M.; Li, L.; Kostetski, I.; Chu, S. H.; Siau, J. L.; Bhatia, M.; Moore, P. K., Evidence for the Formation of a Novel Nitrosothiol from the Gaseous Mediators Nitric Oxide and Hydrogen Sulphide. *Biochem. Biophys. Res. Commun.* **2006,** *343*, 303-310.

45. Fischer, E., Ueber das Triacetonalkamin. *Ber. Dtsch. Chem. Ges.* **1883,** *16*, 1604-1607.

46. Siegel, L. M., A Direct Microdetermination for Sulfide. *Anal. Biochem.* **1965,** *11*, 126-132.

47. Zhao, Z.; Malinowski, E. R., Window Factor Analysis of Methylene Blue in Water. *J. Chemometrics* **1999,** *13*, 83-94.

48. Lippert, A. R.; New, E. J.; Chang, C. J., Reaction-Based Fluorescent Probes for Selective Imaging of Hydrogen Sulfide in Living Cells. *J. Am. Chem. Soc.* **2011,** *133*, 10078-10080.

49. Peng, H.; Cheng, Y.; Dai, C.; King, A. L.; Predmore, B. L.; Lefer, D. J.; Wang, B., A Fluorescent Probe for Fast and Quantitative Detection of Hydrogen Sulfide in Blood. *Angew. Chem. Int. Ed.* **2011,** *50*, 9672-9675.

50. Liu, C.; Pan, J.; Li, S.; Zhao, Y.; Wu, L. Y.; Berkman, C. E.; Whorton, A. R.; Xian, M., Capture and Visualization of Hydrogen Sulfide by a Fluorescent Probe. *Angew. Che. Int. Ed.* **2011,** *50*, 10327-10329.

51. Montoya, L. A.; Pearce, T. F.; Hansen, R. J.; Zakharov, L. N.; Pluth, M. D., Development of Selective Colorimetric Probes for Hydrogen Sulfide Based on Nucleophilic Aromatic Substitution. *J. Org. Chem.* **2013,** *78*, 6550-6557.

52. Cao, X.; Lin, W.; Zheng, K.; He, L., A Near-Infrared Fluorescent Turn-On Probe for Fluorescence Imaging of Hydrogen Sulfide in Living Cells Based on Thiolysis of Dinitrophenyl Ether. *Chem. Commun.* **2012,** *48*, 10529-10531.

53. Lippert, A. R., Designing Reaction-Based Fluorescent Probes for Selective Hydrogen Sulfide Detection. *J. Inorg. Biochem.* **2014,** *133*, 136-142.

54. Shen, X.; Kolluru, G. K.; Yuan, S.; Kevil, C. G., Measurement of H_2S In Vivo and In Vitro by the Monobromobimane Method. *Methods Enzymol.* **2015,** *554*, 31-45.

55. Bayan, L.; Koulivand, P. H.; Gorji, A., Garlic: A Review of Potential Therapeutic Effects. *Avicenna J. Phytomed.* **2014,** *4*, 1-14.

56. Lawson, L. D.; Wood, S. G.; Hughes, B. G., HPLC Analysis of Allicin and Other Thiosulfinates in Garlic Clove Homogenates. *Planta Med.* **1991,** *57*, 263-70.

57. Brodnitz, M. H.; Pascale, J. V.; Van Derslice, L., Flavor Components of Garlic Extract. *J. Agric. Food Chem.* **1971,** *19*, 273-275.

58. Benavides, G. A.; Squadrito, G. L.; Mills, R. W.; Patel, H. D.; Isbell, T. S.; Patel, R. P.; Darley-Usmar, V. M.; Doeller, J. E.; Kraus, D. W., Hydrogen Sulfide Mediates the Vasoactivity of Garlic. *Proc. Natl. Acad. Sci. U. S. A.* **2007,** *104*, 17977-17982.

59. Pluth, M. D.; Bailey, T. S.; Hammers, M. D.; Hartle, M. D.; Henthorn, H. A.; Steiger, A. K., Natural Products Containing Hydrogen Sulfide Releasing Moieties. *Synlett* **2015,** *26*, 2633-2643.

60. Cai, Y.-R.; Hu, C.-H., Computational Study of H2S Release in Reactions of Diallyl Polysulfides with Thiols. *J. Phys. Chem. B* **2017,** *121*, 6359-6366.

61. De Cicco, P.; Panza, E.; Ercolano, G.; Armogida, C.; Sessa, G.; Pirozzi, G.; Cirino, G.; Wallace, J. L.; Ianaro, A., ATB-346, A Novel Hydrogen Sulfide-Releasing Anti-Inflammatory

Drug, Induces Apoptosis of Human Melanoma Cells and Inhibits Melanoma Development In Vivo. *Pharmacol. Res.* **2016,** *114*, 67-73.

62. Cenac, N.; Castro, M.; Desormeaux, C.; Colin, P.; Sie, M.; Ranger, M.; Vergnolle, N., A Novel Orally Administered Trimebutine Compound (GIC-1001) is Anti-Nociceptive and Features Peripheral Opioid Agonistic Activity and Hydrogen Sulphide-Releasing Capacity in Mice. *Eur. J. Pain* **2016,** *20*, 723-730.

63. Ozturk, T.; Ertas, E.; Mert, O., Use of Lawesson's Reagent in Organic Syntheses. *Chem. Rev.* **2007,** *107*, 5210-5278.

64. Nicolau, L. A. D.; Silva, R. O.; Damasceno, S. R. B.; Carvalho, N. S.; Costa, N. R. D.; Aragão, K. S.; Barbosa, A. L. R.; Soares, P. M. G.; Souza, M. H. L. P.; Medeiros, J. V. R., The Hydrogen Sulfide Donor, Lawesson's Reagent, Prevents Alendronate-Induced Gastric Damage in Rats. *Braz. J. Med. Biol. Res.* **2013,** *46*, 708-714.

65. Spiller, F.; Orrico, M. I. L.; Nascimento, D. C.; Czaikoski, P. G.; Souto, F. O.; Alves-Filho, J. C.; Freitas, A.; Carlos, D.; Montenegro, M. F.; Neto, A. F.; Ferreira, S. H.; Rossi, M. A.; Hothersall, J. S.; Assreuy, J.; Cunha, F. Q., Hydrogen Sulfide Improves Neutrophil Migration and Survival in Sepsis via K+ATP Channel Activation. *Am. J. Respir. Crit. Care Med.* **2010,** *182*, 360-368.

66. Li, L.; Whiteman, M.; Guan, Y. Y.; Neo, K. L.; Cheng, Y.; Lee, S. W.; Zhao, Y.; Baskar, R.; Tan, C.-H.; Moore, P. K., Characterization of a Novel, Water-Soluble Hydrogen Sulfide–Releasing Molecule (GYY4137). *Circulation* **2008,** *117*, 2351-2360.

67. Lee, Z. W.; Zhou, J.; Chen, C.-S.; Zhao, Y.; Tan, C.-H.; Li, L.; Moore, P. K.; Deng, L.-W., The Slow-Releasing Hydrogen Sulfide Donor, GYY4137, Exhibits Novel Anti-Cancer Effects In Vitro and In Vivo. *PLoS One* **2011,** *6*, e21077.

68. Moore, P. K.; Whiteman, M., *Chemistry, biochemistry and pharmacology of hydrogen sulfide*. Springer: 2015; Vol. 230.

69. Park, C.-M.; Zhao, Y.; Zhu, Z.; Pacheco, A.; Peng, B.; Devarie-Baez, N. O.; Bagdon, P.; Zhang, H.; Xian, M., Synthesis and Evaluation of Phosphorodithioate-Based Hydrogen Sulfide Donors. *Mol. Biosyst.* **2013,** *9*, 2430-2434.

70. Kang, J.; Li, Z.; Organ, C. L.; Park, C.-M.; Yang, C.-t.; Pacheco, A.; Wang, D.; Lefer, D. J.; Xian, M., pH-Controlled Hydrogen Sulfide Release for Myocardial Ischemia-Reperfusion Injury. *J. Am. Chem. Soc.* **2016,** *138*, 6336-6339.

71. Wu, J.; Li, Y.; He, C.; Kang, J.; Ye, J.; Xiao, Z.; Zhu, J.; Chen, A.; Feng, S.; Li, X.; Xiao, J.; Xian, M.; Wang, Q., Novel H2S Releasing Nanofibrous Coating for In Vivo Dermal Wound Regeneration. *ACS Appl. Mater. Interfaces* **2016,** *8*, 27474-27481.

72. Zanatta, S. D.; Jarrott, B.; Williams, S. J., Synthesis and Preliminary Pharmacological Evaluation of Aryl Dithiolethiones with Cyclooxygenase-2-Selective Inhibitory Activity and Hydrogen Sulfide-Releasing Properties. *Aust. J. Chem.* **2010,** *63*, 946-957.

73. Hamada, T.; Nakane, T.; Kimura, T.; Arisawa, K.; Yoneda, K.; Yamamoto, T.; Osaki, T., Treatment of Xerostomia with the Bile Secretion-Stimulating Drug Anethole Trithione: A Clinical Trial. *Am. J. Med. Sci.* **1999,** *318*, 146-51.

74. Perrino, E.; Cappelletti, G.; Tazzari, V.; Giavini, E.; Soldato, P. D.; Sparatore, A., New Sulfurated Derivatives of Valproic Acid with Enhanced Histone Deacetylase Inhibitory Activity. *Bioorg. Med. Chem. Lett.* **2008,** *18*, 1893-1897.

75. Tazzari, V.; Cappelletti, G.; Casagrande, M.; Perrino, E.; Renzi, L.; Del Soldato, P.; Sparatore, A., New Aryldithiolethione Derivatives as Potent Histone Deacetylase Inhibitors. *Bioorg. Med. Chem.* **2010,** *18*, 4187-94.

76. Sen, C. K.; Traber, K. E.; Packer, L., Inhibition of NF-κB Activation in Human T-Cell Lines by Anetholdithiolthione. *Biochem. Biophys. Res. Commun.* **1996,** *218*, 148-153.

77. Hasegawa, U.; van der Vlies, A. J., Design and Synthesis of Polymeric Hydrogen Sulfide Donors. *Bioconjugate Chem.* **2014,** *25*, 1290-1300.

78. Li, L.; Rossoni, G.; Sparatore, A.; Lee, L. C.; Del Soldato, P.; Moore, P. K., Anti-Inflammatory and Gastrointestinal Effects of a Novel Diclofenac Derivative. *Free Radic. Biol. Med.* **2007,** *42*, 706-719.

79. Sidhapuriwala, J.; Li, L.; Sparatore, A.; Bhatia, M.; Moore, P. K., Effect of S-Diclofenac, a Novel Hydrogen Sulfide Releasing Derivative, on Carrageenan-Induced Hindpaw Oedema Formation in the Rat. *Eur. J. Pharmacol.* **2007,** *569*, 149-54.

80. Baskar, R.; Sparatore, A.; Del Soldato, P.; Moore, P. K., Effect of S-Diclofenac, a Novel Hydrogen Sulfide Releasing Derivative Inhibit Rat Vascular Smooth Muscle Cell Proliferation. *Eur. J. Pharmacol.* **2008,** *594*, 1-8.

81. Fiorucci, S.; Orlandi, S.; Mencarelli, A.; Caliendo, G.; Santagada, V.; Distrutti, E.; Santucci, L.; Cirino, G.; Wallace, J. L., Enhanced Activity of a Hydrogen Sulphide-Releasing Derivative of Mesalamine (ATB-429) in a Mouse Model of Colitis. *Br. J. Pharmacol.* **2007,** *150*, 996-1002.

82. Szczesny, B.; Módis, K.; Yanagi, K.; Coletta, C.; Le Trionnaire, S.; Perry, A.; Wood, M. E.; Whiteman, M.; Szabo, C., AP39, A Novel Mitochondria-Targeted Hydrogen Sulfide Donor, Stimulates Cellular Bioenergetics, Exerts Cytoprotective Effects and Protects Against the Loss of Mitochondrial DNA Integrity in Oxidatively Stressed Endothelial Cells In Vitro. *Nitric Oxide* **2014,** *41*, 120-130.

83. Hammers, M. D.; Singh, L.; Montoya, L. A.; Moghaddam, A. D.; Pluth, M. D., Synthesis of Amino-ADT Provides Access to Hydrolytically Stable Amide-Coupled Hydrogen Sulfide Releasing Drug Targets. *Synlett* **2016,** *27*, 1349-1353.

84. Chattopadhyay, M.; Kodela, R.; Olson, K. R.; Kashfi, K., NOSH–Aspirin (NBS-1120), a Novel Nitric Oxide- and Hydrogen Sulfide-Releasing Hybrid is a Potent Inhibitor of Colon Cancer Cell Growth In Vitro and in a Xenograft Mouse Model. *Biochem. Biophys. Res. Commun.* **2012,** *419*, 523-528.

85. Lee, M.; McGeer, E.; Kodela, R.; Kashfi, K.; McGeer, P. L., NOSH-Aspirin (NBS-1120), a Novel Nitric Oxide and Hydrogen Sulfide Releasing Hybrid, Attenuates Neuroinflammation Induced by Microglial and Astrocytic Activation: A New Candidate for Treatment of Neurodegenerative Disorders. *Glia* **2013,** *61*, 1724-1734.

86. Zhao, Y.; Wang, H.; Xian, M., Cysteine-Activated Hydrogen Sulfide (H_2S) Donors. *J. Am. Chem. Soc.* **2011,** *133*, 15-17.

87. Yang, C. T.; Zhao, Y.; Xian, M.; Li, J. H.; Dong, Q.; Bai, H. B.; Xu, J. D.; Zhang, M. F., A Novel Controllable Hydrogen Sulfide-Releasing Molecule Protects Human Skin Keratinocytes Against Methylglyoxal-Induced Injury and Dysfunction. *Cell. Physiol. Biochem.* **2014,** *34*, 1304-17.

88. Zhao, Y.; Yang, C.; Organ, C.; Li, Z.; Bhushan, S.; Otsuka, H.; Pacheco, A.; Kang, J.; Aguilar, H. C.; Lefer, D. J.; Xian, M., Design, Synthesis, and Cardioprotective Effects of N-Mercapto-Based Hydrogen Sulfide Donors. *J. Med. Chem.* **2015,** *58*, 7501-7511.

89. Feng, S.; Zhao, Y.; Xian, M.; Wang, Q., Biological Thiols-Triggered Hydrogen Sulfide Releasing Microfibers for Tissue Engineering Applications. *Acta Biomater.* **2015,** *27*, 205-213.

90. Zhao, Y.; Bhushan, S.; Yang, C.; Otsuka, H.; Stein, J. D.; Pacheco, A.; Peng, B.; Devarie-Baez, N. O.; Aguilar, H. C.; Lefer, D. J.; Xian, M., Controllable Hydrogen Sulfide Donors and Their Activity against Myocardial Ischemia-Reperfusion Injury. *ACS Chem. Biol.* **2013,** *8*, 1283-1290.

91. Roger, T.; Raynaud, F.; Bouillaud, F.; Ransy, C.; Simonet, S.; Crespo, C.; Bourguignon, M.-P.; Villeneuve, N.; Vilaine, J.-P.; Artaud, I.; Galardon, E., New Biologically Active Hydrogen Sulfide Donors. *ChemBioChem* **2013,** *14*, 2268-2271.

92. Cerda, M. M.; Hammers, M. D.; Earp, M. S.; Zakharov, L. N.; Pluth, M. D., Applications of Synthetic Organic Tetrasulfides as H2S Donors. *Org. Lett.* **2017,** *19*, 2314-2317.

93. Martelli, A.; Testai, L.; Citi, V.; Marino, A.; Pugliesi, I.; Barresi, E.; Nesi, G.; Rapposelli, S.; Taliani, S.; Da Settimo, F.; Breschi, M. C.; Calderone, V., Arylthioamides as H_2S Donors: l-Cysteine-Activated Releasing Properties and Vascular Effects in Vitro and in Vivo. *ACS Med. Chem. Lett.* **2013,** *4*, 904-908.

94. Long, T. R.; Wongrakpanich, A.; Do, A.-V.; Salem, A. K.; Bowden, N. B., Long-Term Release of a Thiobenzamide from a Backbone Functionalized Poly(lactic acid). *Polym. Chem.* **2015,** *6*, 7188-7195.

95. Elsheikh, W.; Blackler, R. W.; Flannigan, K. L.; Wallace, J. L., Enhanced Chemopreventive Effects of a Hydrogen Sulfide-Releasing Anti-Inflammatory Drug (ATB-346) in Experimental Colorectal Cancer. *Nitric Oxide* **2014,** *41*, 131-137.

96. Foster, J. C.; Powell, C. R.; Radzinski, S. C.; Matson, J. B., S-Aroylthiooximes: A Facile Route to Hydrogen Sulfide Releasing Compounds with Structure-Dependent Release Kinetics. *Org. Lett.* **2014,** *16*, 1558-1561.

97. Foster, J. C.; Matson, J. B., Functionalization of Methacrylate Polymers with Thiooximes: A Robust Postpolymerization Modification Reaction and a Method for the Preparation of H_2S-Releasing Polymers. *Macromolecules* **2014,** *47*, 5089-5095.

98. Foster, J. C.; Radzinski, S. C.; Zou, X.; Finkielstein, C. V.; Matson, J. B., H_2S-Releasing Polymer Micelles for Studying Selective Cell Toxicity. *Mol. Pharm.* **2017,** *14*, 1300-1306.

99. Carter, J. M.; Qian, Y.; Foster, J. C.; Matson, J. B., Peptide-Based Hydrogen Sulphide-Releasing Gels. *Chem. Commun.* **2015,** *51*, 13131-13134.

100. Devarie-Baez, N. O.; Bagdon, P. E.; Peng, B.; Zhao, Y.; Park, C.-M.; Xian, M., Light-Induced Hydrogen Sulfide Release from "Caged" gem-Dithiols. *Org. Lett.* **2013,** *15*, 2786-2789.

101. Gaplovsky, M.; Il'ichev, Y. V.; Kamdzhilov, Y.; Kombarova, S. V.; Mac, M.; Schworer, M. A.; Wirz, J., Photochemical Reaction Mechanisms of 2-Nitrobenzyl Compounds: 2-Nitrobenzyl Alcohols Form 2-Nitroso Hydrates by Dual Proton Transfer. *Photochem. Photobiol. Sci.* **2005,** *4*, 33-42.

102. Fukushima, N.; Ieda, N.; Sasakura, K.; Nagano, T.; Hanaoka, K.; Suzuki, T.; Miyata, N.; Nakagawa, H., Synthesis of a Photocontrollable Hydrogen Sulfide Donor Using Ketoprofenate Photocages. *Chem. Commun.* **2014,** *50*, 587-589.

103. Xiao, Z.; Bonnard, T.; Shakouri-Motlagh, A.; Wylie, R. A. L.; Collins, J.; White, J.; Heath, D. E.; Hagemeyer, C. E.; Connal, L. A., Triggered and Tunable Hydrogen Sulfide Release from Photogenerated Thiobenzaldehydes. *Chem. Eur. J.* **2017,** *23*, 11294-11300.

104. Zheng, Y.; Yu, B.; Ji, K.; Pan, Z.; Chittavong, V.; Wang, B., Esterase-Sensitive Prodrugs with Tunable Release Rates and Direct Generation of Hydrogen Sulfide. *Angew. Chem. Int. Ed. Engl.* **2016,** *55*, 4514-8.

105. Borchardt, R. T.; Cohen, L. A., Stereopopulation control. III. Facilitation of intramolecular conjugate addition of the carboxyl group. *J. Am. Chem. Soc.* **1972,** *94,* 9175-9182.

106. Li, Z.; Organ, C. L.; Zheng, Y.; Wang, B.; Lefer, D. J., Abstract 17903: Novel Esterase-Activated Hydrogen Sulfide Donors Attenuate Myocardial Ischemia/Reperfusion Injury. *Circulation* **2016,** *134,* A17903-A17903.

107. Shukla, P.; Khodade, V. S.; SharathChandra, M.; Chauhan, P.; Mishra, S.; Siddaramappa, S.; Pradeep, B. E.; Singh, A.; Chakrapani, H., "On Demand" Redox Buffering by H_2S Contributes to Antibiotic Resistance Revealed by a Bacteria-Specific H_2S Donor. *Chemical Science* **2017,** *8,* 4967-4972.

108. Chengelis, C. P.; Neal, R. A., Studies of Carbonyl Sulfide Toxicity: Metabolism by Carbonic Anhydrase. *Toxicol. Appl. Pharmacol.* **1980,** *55,* 198-202.

109. Chengelis, C. P.; Neal, R. A., Hepatic Carbonyl Sulfide Metabolism. *Biochem. Biophys. Res. Commun.* **1979,** *90,* 993-999.

110. Steiger, A. K.; Zhao, Y.; Pluth, M. D., Emerging Roles of Carbonyl Sulfide in Chemical Biology: Sulfide Transporter or Gasotransmitter? *Antioxidants & Redox Signaling* **2017**, Ahead of print.

111. Hirschmann, R.; Dewey, R. S.; Schoenewaldt, E. F.; Joshua, H.; Paleveda, W. J.; Schwam, H.; Barkemeyer, H.; Arison, B. H.; Veber, D. F., Synthesis of Peptides in Aqueous Medium. VII. Preparation and use of 2,5-Thiazolidinediones in Peptide Synthesis. *J. Org. Chem.* **1971,** *36,* 49-59.

112. Powell, C. R.; Foster, J. C.; Okyere, B.; Theus, M. H.; Matson, J. B., Therapeutic Delivery of H_2S via COS: Small Molecule and Polymeric Donors with Benign Byproducts. *J. Am. Chem. Soc.* **2016,** *138*, 13477-13480.

113. Steiger, A. K.; Pardue, S.; Kevil, C. G.; Pluth, M. D., Self-Immolative Thiocarbamates Provide Access to Triggered H_2S Donors and Analyte Replacement Fluorescent Probes. *J. Am. Chem. Soc.* **2016,** *138*, 7256-7259.

114. Zhao, Y.; Pluth, M. D., Hydrogen Sulfide Donors Activated by Reactive Oxygen Species. *Angew. Chem. Int. Ed.* **2016,** *55*, 14638-14642.

115. Abbas, K.; Hardy, M.; Poulhès, F.; Karoui, H.; Tordo, P.; Ouari, O.; Peyrot, F., Free Radical Biology and Medicine Detection of Superoxide Production in Stimulated and Unstimulated Living Cells Using New Cyclic Nitrone Spin Traps. *Free Radic. Biol. Med.* **2014,** *71*, 281-290.

116. Steiger, A. K.; Marcatti, M.; Szabo, C.; Szczesny, B.; Pluth, M. D., Inhibition of Mitochondrial Bioenergetics by Esterase-Triggered COS/H_2S Donors. *ACS Chem. Biol.* **2017,** *12*, 2117-2123.

117. Szabo, C.; Ransy, C.; Modis, K.; Andriamihaja, M.; Murghes, B.; Coletta, C.; Olah, G.; Yanagi, K.; Bouillaud, F., Regulation of Mitochondrial Bioenergetic Function by Hydrogen Sulfide. Part I. Biochemical and Physiological Mechanisms. *Br. J. Pharmacol.* **2014,** *171*, 2099-122.

118. Chauhan, P.; Bora, P.; Ravikumar, G.; Jos, S.; Chakrapani, H., Esterase Activated Carbonyl Sulfide/Hydrogen Sulfide (H_2S) Donors. *Org. Lett.* **2017,** *19*, 62-65.

119. Steiger, A. K.; Yang, Y.; Royzen, M.; Pluth, M. D., Bio-Orthogonal “Click-and-Release” Donation of Caged Carbonyl Sulfide (COS) and Hydrogen Sulfide (H_2S). *Chem. Commun.* **2017,** *53*, 1378-1380.

120. Zhao, Y.; Bolton, S. G.; Pluth, M. D., Light-Activated COS/H_2S Donation from Photocaged Thiocarbamates. *Org. Lett.* **2017,** *19*, 2278-2281.

Chapter 2: Therapeutic Delivery of H_2S via COS: Small Molecule and Polymeric Donors with Benign Byproducts

Reprinted (adapted) with permission from: Powell, C. R., et al. (2016). "Therapeutic Delivery of H_2S via COS: Small Molecule and Polymeric Donors with Benign Byproducts." Journal of the American Chemical Society **138**: 13477-13480. Copyright 2016 American Chemical Society. https://pubs.acs.org/doi/abs/10.1021/jacs.6b07204

2.1. Authors.

Chadwick R. Powell,[§,†] Jeffrey C. Foster,[§,†] Benjamin Okyere,[‡] Michelle H. Theus,[‡] and John B. Matson*[§,†]

[§]Department of Chemistry, Virginia Tech, Blacksburg, Virginia 24061, United States

[†]Macromolecules Innovation Institute, Virginia Tech, Blacksburg, Virginia 24061, United States

[‡]Department of Biomedical Sciences and Pathobiology, Virginia–Maryland Regional College of Veterinary Medicine, Duck Pond Drive, Blacksburg, VA 24061, United States

2.2. Abstract.

Carbonyl sulfide (COS) is a gas that may play important roles in mammalian and bacterial biology, but its study is limited by a lack of suitable donor molecules. We report here the use of *N*-thiocarboxyanhydrides (NTAs) as COS donors that release the gas in a sustained manner under biologically relevant conditions with innocuous peptide by-products. Carbonic anhydrase converts COS into H_2S, allowing NTAs to serve as either COS or H_2S donors, depending on the availability of the enzyme. Analysis of the pseudo-first order H_2S release rate under biologically relevant conditions revealed a release half-life of 75 min for the small molecule NTA under investigation.

A polynorbornene bearing pendant NTAs made by ring-opening metathesis polymerization was also synthesized to generate a polymeric COS/H_2S donor. A half-life of 280 min was measured for the polymeric donor. Endothelial cell proliferation studies revealed an enhanced rate of proliferation for cells treated with the NTA over untreated controls.

2.3. Introduction

Since nitric oxide (NO) was first proposed to be an endothelium-derived relaxing factor in 1986,[1] an increasing number of scientists have been drawn to the field of signaling gases. These short-lived gaseous mediators, classified as gasotransmitters, exist in most tissues throughout the body and play a critical role in cellular signaling and homeostasis.[2] To meet the definition of a gasotransmitter, a gas must be enzymatically generated and regulated, have specific molecular targets and physiological functions, and be freely permeable to cellular membranes.[3] Three species are currently classified as gasotransmitters: NO, carbon monoxide (CO), and hydrogen sulfide (H_2S). However, evidence suggests that a variety of other gases may be involved in cellular processes. Gases currently under investigation include ammonia, methane, sulfur dioxide, and carbonyl sulfide (COS).[4-6] Of these, COS is perhaps the least studied in biological systems, in large part due to a lack of suitable donor molecules.

COS is the most abundant sulfur compound in the atmosphere (500 ppt), generated naturally from emissions from hot springs, trees, and volcanoes.[7] Despite its low overall atmospheric concentration, high concentrations near volcanoes may have enabled COS to serve as a condensing agent in prebiotic times for coupling amino acids.[8-9] Investigation into the role of COS in biology continues today, with COS-generating enzymes (thiocyanate hydrolases) identified in bacteria and COS generation and utilization hypothesized in mammals.[10] The study

of COS biology is complicated by its short half-life in vivo, primarily due to its fast hydrolysis by carbonic anhydrase (CA). CA is ubiquitous in plants and mammals and efficiently carries out its primary function of generating carbonic acid from water and carbon dioxide (CO_2). Due to its structural similarity to CO_2, COS is also a substrate for CA, which the enzyme rapidly converts into CO_2 and H_2S.[5] In fact, COS itself is relatively non-toxic—its toxicity is a result of this conversion into toxic levels of H_2S.[11]

Gasotransmitter donors have become vital tools for studying the biology of NO, CO, and H_2S. Donors are typically small molecules that release gasotransmitters under physiologically relevant conditions over a defined period of time.[3] Chemists strive to synthesize gasotransmitter donors that mimic the body's natural signaling through precise exogenous application. Today many small molecule donors are available that release NO, CO, or H_2S, all triggered by various stimuli with wide-ranging half-lives of release. For example, a variety of H_2S donors have been reported in recent years, with release triggers including water,[12-13] thiols,[14-16] light,[17-18] and enzymes[19]. Gasotransmitter donors can be covalently attached to drugs,[20-21] which extends the capacities of existing therapeutics, or to polymers, providing localized release. Multiple types of NO, CO, and H_2S-releasing polymers have been reported recently.[22-24] In contrast, COS donors have received little attention, which has impeded studies on COS biology or delivery of H_2S via COS release.

To address this gap, we set out to design a molecule that could readily generate COS in a controlled fashion, easily attach to a polymer scaffold, and conveniently decompose to yield biologically innocuous byproducts. We envisioned that this COS-releasing small molecule and the resulting polymer could serve as either COS donors (in the absence of CA) or as H_2S donors (in the presence of CA) to facilitate biological studies. There exist a handful of methods to generate

COS, including from potassium thiocyanate and sulfuric acid in the presence of water[7] and a recently published metal-catalyzed reaction of CO and elemental sulfur[25]. While useful for generating solutions of the gas, these methods are not capable of generating COS in a biological environment. In the lone example of COS use in a biological system, Pluth and coworkers recently reported on a class of turn-on fluorescent H_2S sensors that regenerate the detected H_2S through a decomposition reaction involving COS.[26] Considering our requirements for sustained release under biologically relevant conditions and non-toxic byproducts, we envisioned that *N*-thiocarboxyanhydrides (NTAs) might provide a suitable platform from which to build small molecule and polymeric COS donors.

2.4. Results and Discussion

NTAs were first reported in 1971 by Hirschmann et. al as an alternative to *N*-carboxyanhydrides (NCAs) for use in the solution-phase synthesis of oligopeptides.[27] More recently, NTAs have been synthesized from *N*-alkyl amino acids and polymerized to afford polypeptoids.[28] Because the ring-opening polymerization of NTAs occurs with loss of COS, we envisioned that NTAs could be suitable COS donors upon ring-opening by a biological nucleophile such as an amine. After COS release, conversion into the known gasotransmitter H_2S is expected to occur by one of two routes: 1) the rapid, enzymatic conversion by CA; or 2) hydrolysis, a relatively slower process.

In order to test our hypothesis that NTAs could be used as COS/H_2S donors, we began by synthesizing the NTA derivative of sarcosine (**NTA1**) through the route shown in Scheme 1. With modifications of literature procedures,[28] we were able to obtain **NTA1** in three steps with minimal purification. Although COS release from NTAs during ring-opening polymerization has been

hypothesized, direct detection of COS generation from ring-opening of NTAs has not been reported.

Scheme 1. Synthesis of NTA1.[a]

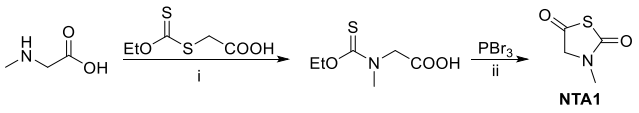

[a]Conditions: i) NaOH, H_2O, 98 % yield; ii) CH_2Cl_2, 0 °C, 53 % yield.

To identify COS evolution, **NTA1** was added to an aqueous solution of glycine in an air-tight vial. GC-MS analysis of samples taken of the vial headspace after 5 min revealed the presence of COS (m/z = 60). A small peak at m/z = 34 was also observed, which is consistent with slow hydrolysis of COS into H_2S (Figures S14-15).[29] Confirmation of the expected dipeptide byproduct upon nucleophilic attack by glycine was realized by LC-MS. (Figure S16). After confirming COS release, we next measured the H_2S release kinetics of **NTA1** both in the presence and absence of CA. Currently, there are no simple and reliable methods for measuring the rate of COS release in solution. However, the fast conversion of COS into H_2S in the presence of CA allows for indirect quantification of COS release kinetics using methods commonly employed to detect and quantify H_2S. To evaluate the rate of H_2S evolution, a colorimetric assay known commonly as the methylene blue assay was chosen.[30] In the presence of 300 nM CA and 1 mM glycine (biologically relevant values) in PBS buffer (pH = 7.4), the pseudo-first-order release half-life of H_2S for **NTA1** was measured to be 75 min (Figure S17). Further studies of H_2S release using an H_2S-selective electrochemical probe gave a peaking time of 45 min (Figure 1A). Additional release studies performed in complete endothelial cell media exhibited a faster release profile and a quicker return

to baseline (Figure S19). No measurable release was observed in the absence of CA. Although a half-life cannot be determined using this electrochemical method due to oxidation and volatilization of the gas, it is a reliable way to measure instantaneous H_2S concentration.

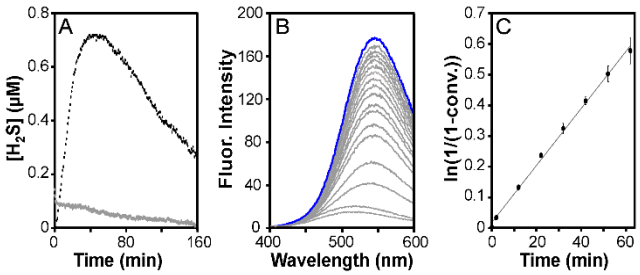

Figure 1. A) H_2S-selective electrochemical probe release curves for **NTA1** (10 μM) in the presence of glycine (1 mM) with 300 nM CA (black curve) or without CA (grey curve) in PBS buffer (pH = 7.4). B) Representative fluorescence spectra (λ_{ex} = 340 nm) exhibiting an increase in intensity over time as H_2S reduces the non-emissive Da-N_3 probe into fluorescent Da-NH_2. C) First-order kinetic plot of Da-NH_2 generation over time, as measured by the change in fluorescence emission intensity at 535 nm. Line represents the pseudo-first-order kinetic fit using the equation conv. = 1 – $e^{[-kt]}$.

Neither the colorimetric nor the electrochemical assay were suitable to quantify the H_2S release rate in the absence of CA because COS hydrolysis is sufficiently slow to limit the use of these methods. In order to make a comparison between the H_2S release rates with and without CA, additional analysis of the H_2S release profile of **NTA1** was performed using the azide derivative of dansyl sulfonamide developed by Wang et al.[31] The dansyl azide (Da-N_3) probe exhibits pronounced selectivity for the hydrosulfide anion (HS^-) over other anions and reactive species

commonly found in biological assays with a response time on the order of seconds. The probe acts through a turn-on fluorescence mechanism whereby HS^- reduces the non-fluorescent azide in solution to give the corresponding fluorescent amine (Da-NH_2). Although Da-NH_2 is a known CA inhibitor,[32] we used the initial rates of Da-N_3 reduction by **NTA1** to compare the rates of H_2S production in the presence and absence of CA.

Fluorescence assays were performed under similar conditions to those described above for the methylene blue and electrochemical probe experiments, monitoring the increase in emission intensity at 535 nm over 10 h (Figure 1B). Pseudo-first-order analysis of Da-NH_2 production in the first 60 min of the experiment in the presence of CA gave an H_2S release half-life of 120 min (Figure 1C). The discrepancy between the half-lives based on methylene blue and fluorescence is likely due to some inhibition of CA by Da-NH_2. Performing the assay in the absence of CA gave a release half-life of 990 min, in excellent agreement with previously measured COS hydrolysis rates in aqueous media of 796 min at pH 7.[29]

Next, we set about preparing an NTA-containing polymer for potential use in COS or H_2S-releasing films, hydrogels, nanoparticles, or other materials that could serve to localize gas delivery. A polymerization technique was needed that would be compatible with the reactive NTA moiety. Ring-opening metathesis polymerization (ROMP) is typically performed under mild conditions (room temperature, no potential nucleophiles or radical initiators), proceeds rapidly to high conversions, and is highly functional group tolerant.[33] Therefore, we designed a synthesis to couple a ROMP-active norbornene to a COS donor. ROMP monomer **NB-NTA** was prepared similarly to **NTA1** in three steps starting from iminodiacetic acid (Scheme 2A).

Polymerizations of **NB-NTA** were carried out in CH_2Cl_2 initiated by Grubbs' 3rd generation catalyst (H_2IMes)(pyr)$_2$(Cl)$_2$Ru=CHPh (**G3**). The resulting homopolymer was insoluble in water,

so a poly(ethylene glycol) (PEG) norbornene comonomer was introduced into the feed at a 9:1 ratio with respect to **NB-NTA** (Scheme 2B)**.** The polymerization yielded a water-soluble random copolymer (**polyNTA1**) with a number-average molecular weight (M_n) of 37 kDa and a dispersity of 1.06 (Figure S13).

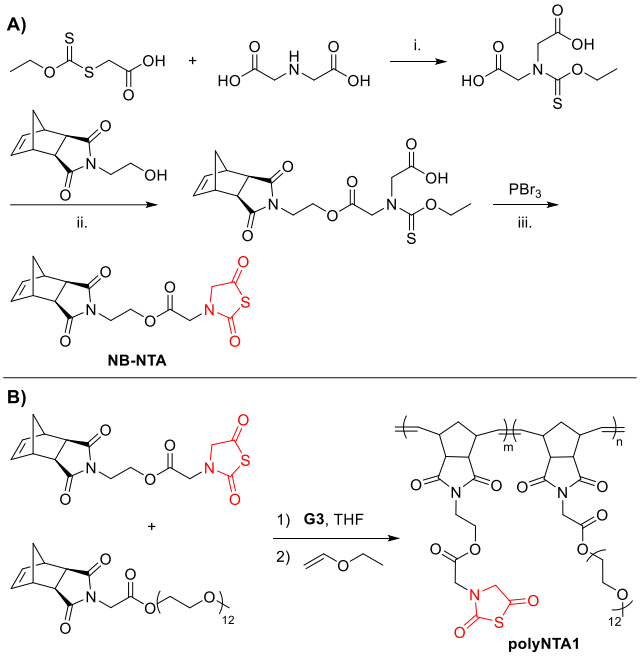

Scheme 2. Synthesis of norbornene-NTA monomer and copolymer polyNTA1.[a]

[a]Conditions: i) NaOH, H_2O, 52 % yield; ii) EDC, pyridine, CH_2Cl_2, 52 % yield; iii) CH_2Cl_2, 0 °C, 50 % yield.

H_2S release from copolymer **polyNTA1** was analyzed using the H_2S-selective electrochemical probe (Figure 2A). A rapid initial release was observed, followed by a plateau after approximately 2 h and sustained release out to at least 20 h. Additionally, the methylene blue assay (Figure 2B) revealed an H_2S release half-life of 280 min (Figure 2C), a three-fold increase over the small molecule **NTA1**. This result is consistent with similar gasotransmitter-releasing

copolymers in which the release of the polymeric donor is sustained over a longer period than the corresponding small molecules.[23] We speculate that this phenomenon may be due to the steric crowding imparted by the polymer backbone as well as the pendant PEG chains in **polyNTA1**.

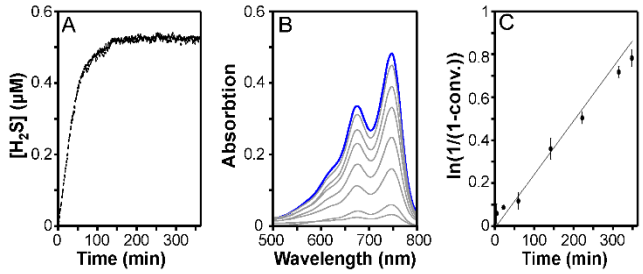

Figure 2. A) H_2S-selective electrochemical probe release curves for **polyNTA1** (1 μM) in the presence of glycine (100 μM) with 300 nM CA in PBS buffer (pH = 7.4). Release was sustained out to 20 h. (B) Absorbance spectra from the methylene blue assay. The increase in intensity over time corresponds to in situ generation of methylene blue from H_2S. C) First-order kinetic plot derived from the methylene blue data, measured by an increase in absorbance at 676 nm. Line represents the pseudo-first order kinetic fit using the equation conv = $1 - e^{[-kt]}$.

To test the ability of **NTA1** and **polyNTA1** to deliver H_2S in a biological system, we assessed their efficacy in promoting proliferation of brain-derived endothelial cells. Endothelial cell proliferation is an important first step in angiogenesis—the formation of new blood vessels from existing vessels—which is vital for several biological processes, most notably wound healing. H_2S promotes angiogenesis;[34] therefore, H_2S donors may be useful as wound healing agents.[35] Experiments were performed by treating endothelial cells with **NTA1**, Na_2S (an H_2S source used as a positive control), or the Sar-Gly dipeptide byproduct for 24 h, followed by measuring the percentage of BrdU positive cells in each treatment group. No CA enzyme was added to any of the treatment groups because the concentration of endogenous CA, which is widely

distributed in mammalian cells, is sufficient to quickly convert COS into H_2S.[11] A significant increase in endothelial cell proliferation was observed for both **NTA1** and Na_2S at 100 μM (Figure 3) compared with the untreated control group. No increase was observed for the Sar-Gly byproduct. Caspase activity was also measured for **NTA1** to assess apoptosis, revealing no significant activity up to 100 μM (Figure S20). We also evaluated the effect of **polyNTA1** on endothelial cell proliferation (Figure S21). No increase in proliferation was observed, which may be a result of the slower rate of H_2S generation from the polymeric donor.

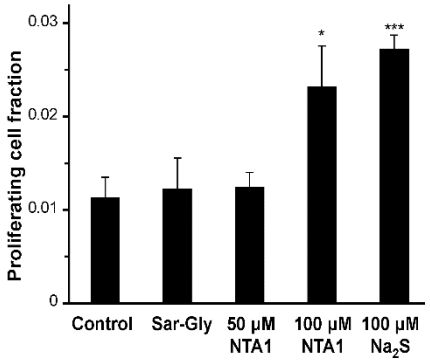

Figure 3. Endothelial cell proliferation data showing the ratio of proliferating cells in each treatment group. Cells were treated for 24 h in serum-free media, and quantification was performed by counting the number of $BrdU^+/Dapi^+$ cells (n = 7–8 for each treatment group). * indicates $p < 0.05$, *** indicates $p < 0.001$ relative to untreated control. Error bars represent standard error of the mean.

2.5. Conclusions

In summary, **NTA1** and **polyNTA1** were synthesized to afford donor compounds that released COS in a sustained manner; COS is then converted into H_2S in the presence of CA. In contrast to many H_2S donors that release potentially toxic byproducts, the products of release from

NTA1 are COS and an amino acid residue. Analysis of the H_2S release kinetics in the presence of CA gave release half-lives on the order of hours for both **NTA1** and **polyNTA1**. Treatment of endothelial cells with **NTA1** increased proliferation over relevant control groups. Taken together, these results demonstrate that NTAs offer a unique method to deliver H_2S in a therapeutic manner. Additionally, the polymeric delivery vehicles developed herein may enable localized, sustained H_2S delivery likely through intravenous or intraperitoneal injections for treatment of cardiovascular disease, cancer, and neurodegenerative disorders. We envision that NTAs will provide a chemical tool for studying COS in biological systems, facilitating a greater understanding of the roles that this gas plays in signaling biology.

2.6. References

1. Ignarro, L. J.; Buga, G. M.; Wood, K. S.; Byrns, R. E.; Chaudhuri, G., Endothelium-Derived Relaxing Factor Produced and Released From Artery and Vein is Nitric Oxide. *Proc. Natl. Acad. Sci. U. S. A.* **1987,** *84*, 9265-9269.

2. Mustafa, A. K.; Gadalla, M. M.; Sen, N.; Kim, S.; Mu, W.; Gazi, S. K.; Barrow, R. K.; Yang, G.; Wang, R.; Snyder, S. H., H_2S Signals Through Protein S-Sulfhydration. *Sci. Signal* **2009,** *2*, ra72-ra72.

3. Wang, R., Two's Company, Three's a Crowd: Can H_2S Be the Third Endogenous Gaseous Transmitter? *FASEB J.* **2002,** *16*, 1792-1798.

4. Wang, R., Gasotransmitters: Growing Pains and Joys. *Trends Biochem. Sci* **2014,** *39*, 227-232.

5. Olson, K. R., The Therapeutic Potential of Hydrogen Sulfide: Separating Hype From Hope. *Am. J. Physiol. Regul. Integr. Comp. Physiol.* **2011,** *301*, R297-R312.

6. Day, J. J.; Yang, Z.; Chen, W.; Pacheco, A.; Xian, M., Benzothiazole Sulfinate: a Water-Soluble and Slow-Releasing Sulfur Dioxide Donor. *ACS Chem. Biol.* **2016,** *11*, 1647-1651.

7. Svoronos, P. D. N.; Bruno, T. J., Carbonyl Sulfide: A Review of Its Chemistry and Properties. *Ind. Eng. Chem. Res.* **2002,** *41*, 5321-5336.

8. Leman, L.; Orgel, L.; Ghadiri, M. R., Carbonyl Sulfide-Mediated Prebiotic Formation of Peptides. *Science* **2004,** *306*, 283-6.

9. Huber, C.; Wächtershäuser, G., Peptides by Activation of Amino Acids with CO on (Ni,Fe)S Surfaces: Implications for the Origin of Life. *Science* **1998,** *281*, 670-672.

10. Balazy, M.; Abu-Yousef, I. A.; Harpp, D. N.; Park, J., Identification of Carbonyl Sulfide and Sulfur Dioxide in Porcine Coronary Artery by Gas Chromatography/Mass Spectrometry, Possible Relevance to EDHF. *Biochem. Biophys. Res. Commun.* **2003,** *311*, 728-34.

11. Chengelis, C. P.; Neal, R. A., Studies of Carbonyl Sulfide Toxicity: Metabolism by Carbonic Anhydrase. *Toxicol. Appl. Pharmacol.* **1980,** *55*, 198-202.

12. Lee, Z. W.; Zhou, J.; Chen, C.-S.; Zhao, Y.; Tan, C.-H.; Li, L.; Moore, P. K.; Deng, L.-W., The Slow-Releasing Hydrogen Sulfide Donor, GYY4137, Exhibits Novel Anti-Cancer Effects In Vitro and In Vivo. *PLoS One* **2011,** *6*, e21077.

13. Spiller, F.; Orrico, M. I. L.; Nascimento, D. C.; Czaikoski, P. G.; Souto, F. O.; Alves-Filho, J. C.; Freitas, A.; Carlos, D.; Montenegro, M. F.; Neto, A. F.; Ferreira, S. H.; Rossi, M. A.; Hothersall, J. S.; Assreuy, J.; Cunha, F. Q., Hydrogen Sulfide Improves Neutrophil Migration and Survival in Sepsis via K+ATP Channel Activation. *Am. J. Respir. Crit. Care Med.* **2010,** *182*, 360-368.

14. Zhao, Y.; Wang, H.; Xian, M., Cysteine-Activated Hydrogen Sulfide (H_2S) Donors. *J. Am. Chem. Soc.* **2011,** *133*, 15-17.

15. Foster, J. C.; Powell, C. R.; Radzinski, S. C.; Matson, J. B., S-Aroylthiooximes: A Facile Route to Hydrogen Sulfide Releasing Compounds with Structure-Dependent Release Kinetics. *Org. Lett.* **2014,** *16*, 1558-1561.

16. Zhao, Y.; Kang, J.; Park, C.-M.; Bagdon, P. E.; Peng, B.; Xian, M., Thiol-Activated gem-Dithiols: A New Class of Controllable Hydrogen Sulfide Donors. *Org. Lett.* **2014,** *16*, 4536-4539.

17. Devarie-Baez, N. O.; Bagdon, P. E.; Peng, B.; Zhao, Y.; Park, C.-M.; Xian, M., Light-Induced Hydrogen Sulfide Release from "Caged" gem-Dithiols. *Org. Lett.* **2013,** *15*, 2786-2789.

18. Chen, W.; Chen, M.; Zang, Q.; Wang, L.; Tang, F.; Han, Y.; Yang, C.; Deng, L.; Liu, Y.-N., NIR Light Controlled Release of Caged Hydrogen Sulfide Based On Upconversion Nanoparticles. *Chem. Commun.* **2015,** *51*, 9193-9196.

19. Zheng, Y.; Yu, B.; Ji, K.; Pan, Z.; Chittavong, V.; Wang, B., Esterase-Sensitive Prodrugs with Tunable Release Rates and Direct Generation of Hydrogen Sulfide. *Angew. Chem. Int. Ed. Engl.* **2016,** *55*, 4514-8.

20. Kodela, R.; Chattopadhyay, M.; Kashfi, K., NOSH-Aspirin: A Novel Nitric Oxide–Hydrogen Sulfide-Releasing Hybrid: A New Class of Anti-inflammatory Pharmaceuticals. *ACS Med. Chem. Lett.* **2012,** *3*, 257-262.

21. Velázquez, C. A.; Praveen Rao, P. N.; Citro, M. L.; Keefer, L. K.; Knaus, E. E., O_2-Acetoxymethyl-Protected Diazeniumdiolate-Based NSAIDs (NONO–NSAIDs): Synthesis, Nitric Oxide Release, and Biological Evaluation Studies. *Biorg. Med. Chem.* **2007,** *15*, 4767-4774.

22. Smith, D. J.; Chakravarthy, D.; Pulfer, S.; Simmons, M. L.; Hrabie, J. A.; Citro, M. L.; Saavedra, J. E.; Davies, K. M.; Hutsell, T. C.; Mooradian, D. L.; Hanson, S. R.; Keefer, L. K., Nitric Oxide-Releasing Polymers Containing the $[N(O)NO]^-$ Group. *J. Med. Chem.* **1996,** *39*, 1148-1156.

23. Foster, J. C.; Matson, J. B., Functionalization of Methacrylate Polymers with Thiooximes: A Robust Postpolymerization Modification Reaction and a Method for the Preparation of H_2S-Releasing Polymers. *Macromolecules* **2014,** *47*, 5089-5095.

24. Jo, Y. S.; van der Vlies, A. J.; Gantz, J.; Thacher, T. N.; Antonijevic, S.; Cavadini, S.; Demurtas, D.; Stergiopulos, N.; Hubbell, J. A., Micelles for Delivery of Nitric Oxide. *J. Am. Chem. Soc.* **2009,** *131*, 14413-14418.

25. Farrell, W. S.; Zavalij, P. Y.; Sita, L. R., Metal-Catalyzed "On-Demand" Production of Carbonyl Sulfide from Carbon Monoxide and Elemental Sulfur. *Angew. Chem. Int. Ed.* **2015,** *54*, 4269-4273.

26. Steiger, A. K.; Pardue, S.; Kevil, C. G.; Pluth, M. D., Self-Immolative Thiocarbamates Provide Access to Triggered H_2S Donors and Analyte Replacement Fluorescent Probes. *J. Am. Chem. Soc.* **2016,** *138*, 7256-7259.

27. Hirschmann, R.; Dewey, R. S.; Schoenewaldt, E. F.; Joshua, H.; Paleveda, W. J.; Schwam, H.; Barkemeyer, H.; Arison, B. H.; Veber, D. F., Synthesis of Peptides In Aqueous Medium. VII. Preparation and Use of 2,5-Thiazolidinediones In Peptide Synthesis. *J. Org. Chem.* **1971,** *36*, 49-59.

28. Tao, X.; Deng, Y.; Shen, Z.; Ling, J., Controlled Polymerization of N-Substituted Glycine N-Thiocarboxyanhydrides Initiated by Rare Earth Borohydrides Toward Hydrophilic and Hydrophobic Polypeptoids. *Macromolecules (Washington, DC, U. S.)* **2014,** *47*, 6173-6180.

29. Elliott, S.; Lu, E.; Rowland, F. S., Rates and Mechanisms for the Hydrolysis of Carbonyl Sulfide In Natural Waters. *Environ. Sci. Technol.* **1989,** *23*, 458-461.

30. Siegel, L. M., A Direct Microdetermination for Sulfide. *Anal. Biochem.* **1965,** *11*, 126-132.

31. Peng, H.; Cheng, Y.; Dai, C.; King, A. L.; Predmore, B. L.; Lefer, D. J.; Wang, B., A Fluorescent Probe for Fast and Quantitative Detection of Hydrogen Sulfide in Blood. *Angew. Chem. Int. Ed.* **2011,** *50*, 9672-9675.

32. Morcos, E. F.; Kussrow, A.; Enders, C.; Bornhop, D., Free-Solution Interaction Assay of Carbonic Anhydrase to its Inhibitors Using Back-Scattering Interferometry. *Electrophoresis* **2010,** *31*, 3691-5.

33. Bielawski, C. W.; Grubbs, R. H., Living Ring-Opening Metathesis Polymerization. *Prog. Polym. Sci.* **2007,** *32*, 1-29.

34. Papapetropoulos, A.; Pyriochou, A.; Altaany, Z.; Yang, G.; Marazioti, A.; Zhou, Z.; Jeschke, M. G.; Branski, L. K.; Herndon, D. N.; Wang, R.; Szabó, C., Hydrogen Sulfide is an Endogenous Stimulator of Angiogenesis. *Proc. Natl. Acad. Sci. U. S. A.* **2009,** *106*, 21972-21977.

35. Szabo, C.; Papapetropoulos, A., Hydrogen Sulphide and Angiogenesis: Mechanisms and Applications. *Br. J. Pharmacol.* **2011,** *164*, 853-65.

2.7. Experimental

Materials and Methods

All reagents were obtained from commercial vendors and used as received unless otherwise stated. NMR spectra were measured on Agilent 400 MHz or Bruker 500 MHz spectrometers. ^{1}H and ^{13}C NMR chemical shifts are reported in ppm relative to internal solvent resonances. Yields refer to chromatographically and spectroscopically pure compounds unless otherwise stated. GC-MS experiments were performed on a Hewlett Packard 5890 Series II GC and a Hewlett Packard 5972 Series Mass Selective Detector, equipped with a Restek RTX 1 DB-5 capillary column (30 m, 1.25 mm diameter, 0.25 μm film thickness), 250 °C injection temperature, 250 °C transfer line,

1 mL/minute flow rate. Analytical LCMS was performed on an Agilent 1200 system with a Waters SQ Detector 2 quadrupole-time-of-flight mass spectrometer using an XBridge C18 column (5 μm particle size, 6 x 100 mm) eluting with a gradient of 0% ACN to 15% ACN in water, with each solvent containing 0.1% formic acid. UV absorbance was monitored at 220 nm with a Waters 2489 UV/Vis detector. UV-Vis absorbance spectra were recorded on a Spectramax M2 plate reader (Molecular Devices). Fluorescence spectra were recorded on a Cary Eclipse fluorescence spectrophotometer equipped with a PMT detector (600 V), excitation and emission slit widths of 5 nm. Size exclusion chromatography (SEC) was carried out in THF at 1 mL min^{-1} at 30 °C on two Agilent PLgel 10 μm MIXED-B columns connected in series with a Wyatt Dawn Heleos 2 light scattering detector and a Wyatt Optilab Rex refractive index detector. No calibration standards were used, and dn/dc values were obtained by assuming 100% mass elution from the columns. High-resolution mass spectra were taken on an Agilent Technologies 6230 TOF LC/MS mass spectrometer.

Scheme S1. Synthesis of NTA1

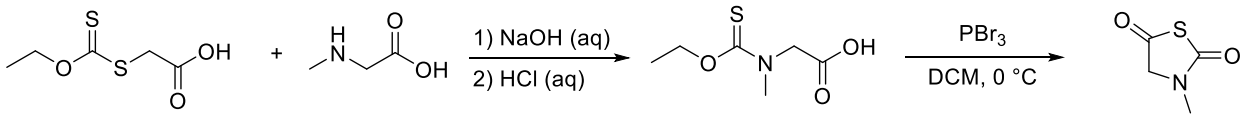

1 **2** **NTA1**

*2-[(Ethoxycarbonothioyl)thio]acetic acid (**1**)*

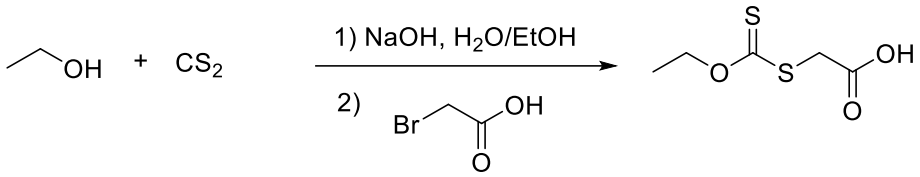

2-[(Ethoxycarbonothioyl)thio]acetic acid was synthesized according to literature procedures.[1,2] Briefly, a 2-necked round bottom flask was equipped with an N_2 inlet and a septum and then charged with ethanol (17 mL), NaOH (2.19 g, 54.7 mmol), water (42 mL), and a stir bar. Once the NaOH was completely dissolved, the solution was bubbled with N_2 for 15 min and the flask was cooled to 0 °C on an ice bath. Under N_2 flow, CS_2 (4.00 mL, 65.6 mmol) was added dropwise via syringe with vigorous stirring at 0 °C. After complete addition, the ice bath was removed and the reaction mixture was stirred for 2 h under N_2 and allowed to return to rt. In a separate flask, bromoacetic acid (7.60 g, 54.7 mmol) was dissolved in deionized water (20 mL) and added to the pale yellow reaction mixture via addition funnel. Immediately the reaction mixture turned dark orange. The reaction mixture was allowed to stir for 14 h at rt. The reaction mixture was acidified by slow addition of concentrated HCl (5 mL) and extracted with CH_2Cl_2 (3 x 50 mL). The organic layers were combined, washed once with brine (10 mL), dried over Na_2SO_4, and concentrated under vacuum. The resulting yellow solid was recrystallized from CH_2Cl_2/hexanes to afford the product as yellow crystals (7.41 g, 75 % yield) (m.p. = 44.4-50.6 °C). ^{1}H NMR ($CDCl_3$): δ 4.66 (q, *J* = 7 Hz, 2H), 3.98 (s, 2H), 1.43 (t, *J* = 7 Hz, 3H). ^{13}C NMR ($CDCl_3$): δ 212.2, 173.1, 71.1, 37.6, 13.8.

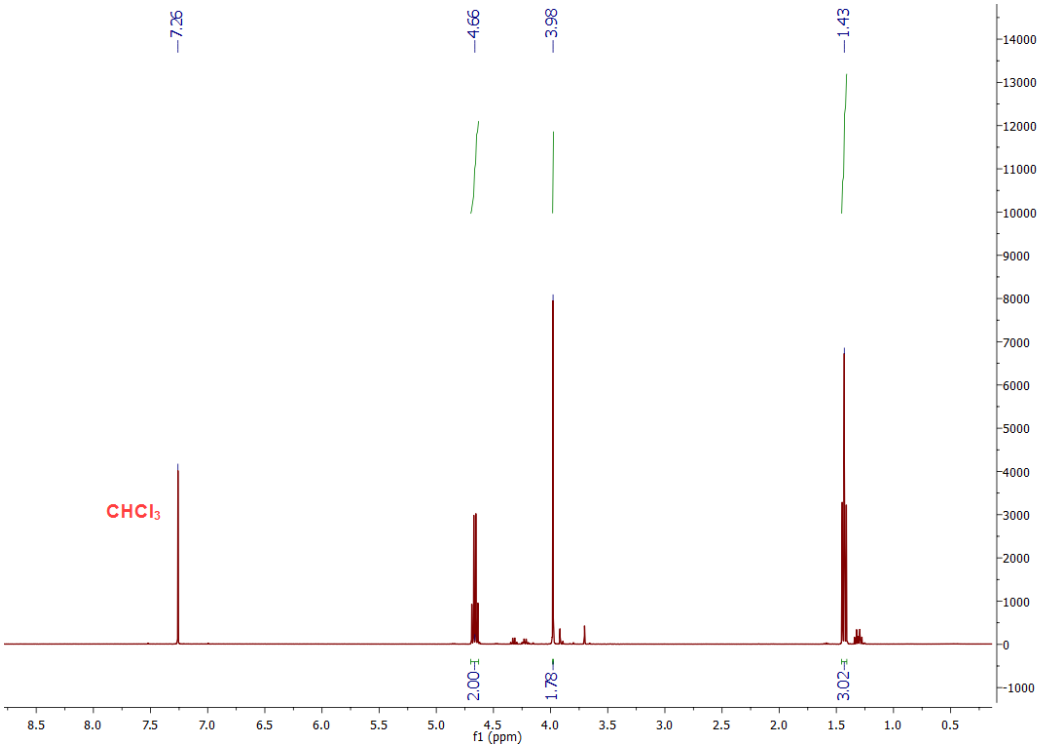

Figure S1. ^{1}H NMR spectrum ($CDCl_3$) of xanthate **1**.

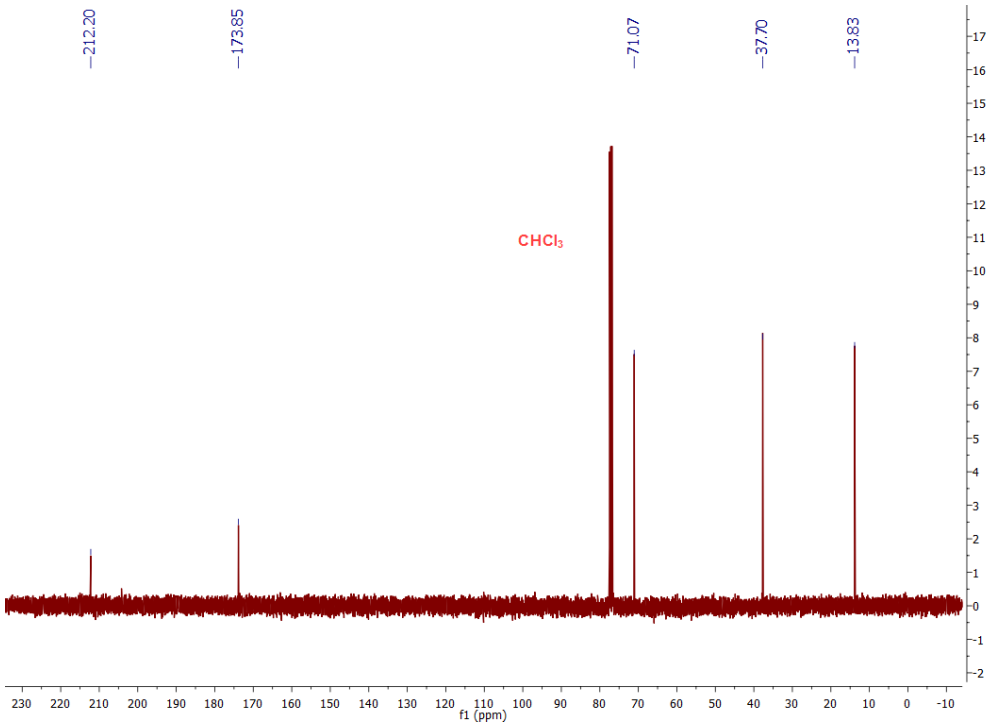

Figure S2. ^{13}C NMR spectrum ($CDCl_3$) of xanthate **1**.

*N-(Ethoxycarbonothioyl)-N-methylglycine (**2**)*

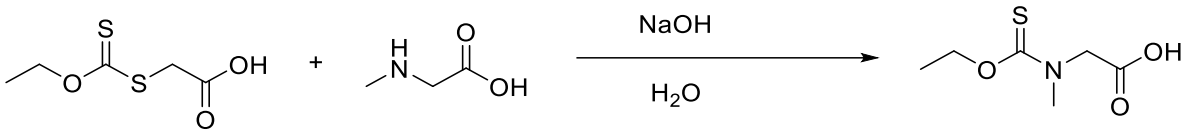

N-(Ethoxycarbonothioyl)-*N*-methylglycine was synthesized according to literature procedures.[1] A round bottom flask was charged with xanthate **1** (6.88 g, 38.1 mmol), sarcosine (3.40 g, 38.1 mmol), NaOH (3.05 g, 76.0 mmol), water (15 mL), and a stir bar to give a clear yellow solution. The reaction mixture was stirred at rt for 48 h and monitored by TLC eluting with 10 % MeOH in CH_2Cl_2 (UV visualization). Once the starting material had been completely consumed, the reaction mixture was acidified by dropwise addition of concentrated HCl, which immediately led to the formation of a white precipitate. HCl addition was continued until formation of the precipitate subsided (~ 10 mL HCl). The mixture was extracted with CH_2Cl_2 (3 x 30 mL). The organic layers were then combined and washed with 1 N HCl (2 x 15 mL) and brine (1 x 10 mL). The clear solution was then dried over Na_2SO_4 and concentrated under vacuum to afford the product as a white solid (6.62 g, 98 % yield). The thiocarbamate product was used directly in the next step without further purification.

*Sarcosine N-thiocarboxyanhydride (**NTA1**)*

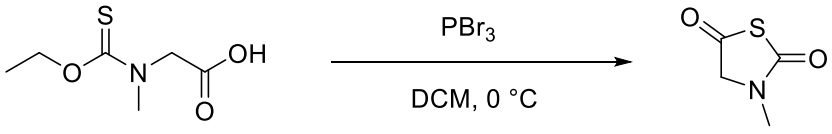

An oven-dried, 2-necked round bottom flask was equipped with an N_2 inlet, a septum, and a stirbar and then charged with thiocarbamate **2** (5.20 g, 29.3 mmol) and dry CH_2Cl_2 (37 mL) under N_2

flow. PBr_3 (2.80 mL, 29.3 mmol) was added dropwise via syringe at 0 °C to give a pale-yellow solution. The reaction mixture was allowed to stir at 0 °C for 15 min before removing the ice bath and allowing the reaction mixture to warm to rt as it stirred for an additional 1 h. The reaction mixture was transferred to a separatory funnel and washed carefully with saturated sodium bicarbonate solution (3 x 15 mL) followed by brine (1 x 15 mL). The organic solution was then dried over Na_2SO_4, and concentrated under vacuum to obtain the crude product as a yellow oil. The crude product was purified on a silica column, eluting with 1:1 hexanes/EtOAc to give the pure product as a light-yellow oil (2.04 g, 53 % yield). ^{1}H NMR ($CDCl_3$): δ 4.18 (s, 2H), 3.08 (s, 3H). ^{13}C NMR ($CDCl_3$): δ 193.9, 164.98, 61.7, 30.9; HRMS (ESI-TOF) calcd. for $C_4H_6NO_2S^+$ $[M+H]^+$ 132.0114, found 132.0114.

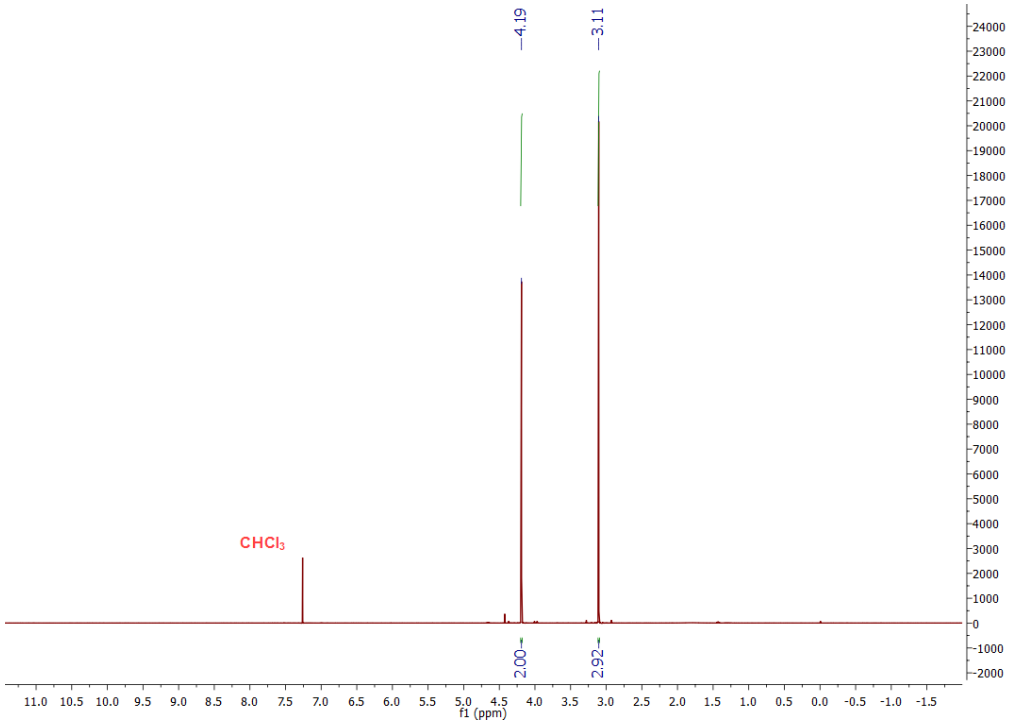

Figure S3. ^{1}H NMR spectrum ($CDCl_3$) of **NTA1**.

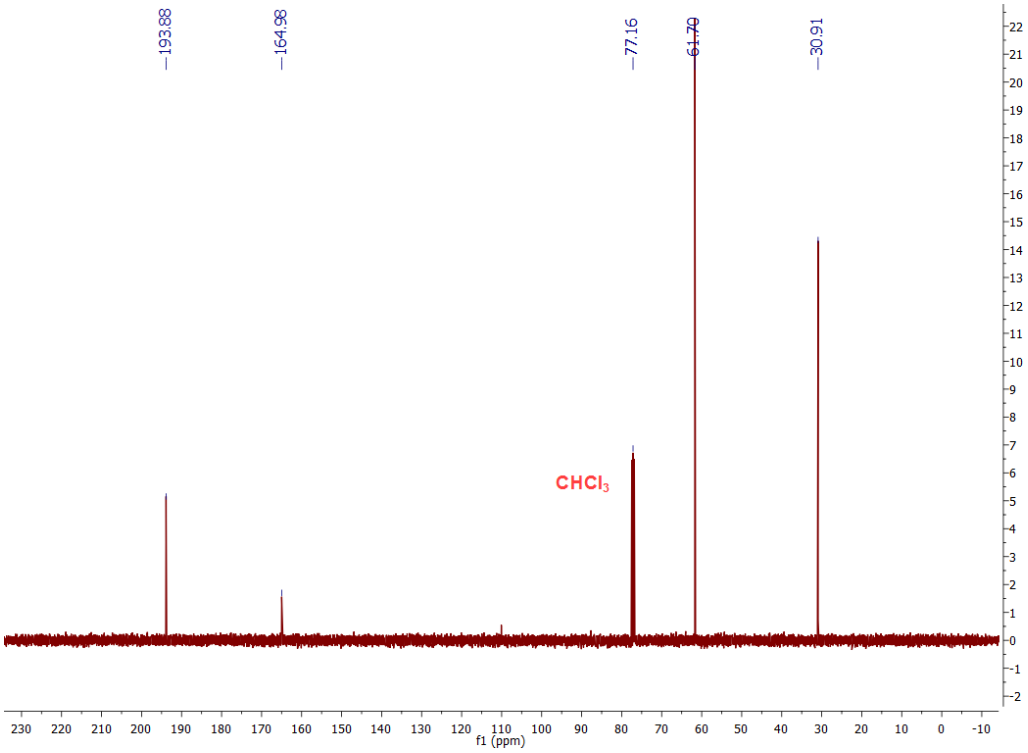

Figure S4. ^{13}C NMR spectrum ($CDCl_3$) of **NTA1**.

Scheme S2. NTA ROMP monomer Synthesis

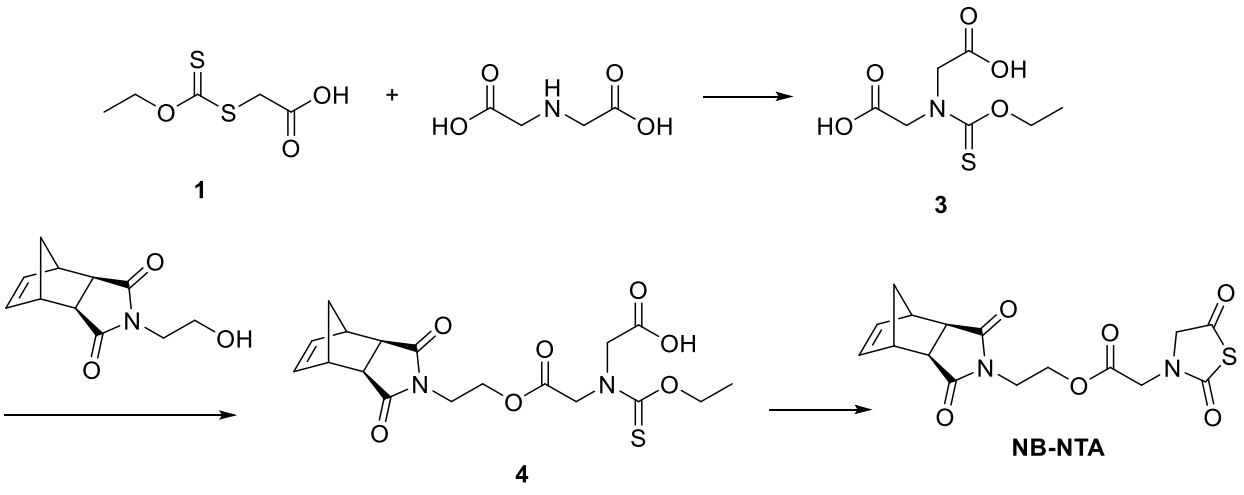

*2,2'-((ethoxycarbonothioyl)azanediyl)diacetic acid (**3**)*

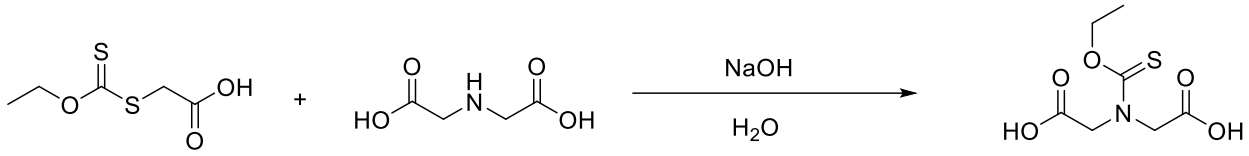

A round bottom flask was equipped with a stir bar and charged with **1** (2.20 g, 12.2 mmol), iminodiacetic acid (1.62 g, 12.20 mmol), NaOH (1.46 g, 36.6 mmol), and water (55 mL) to give a turbid solution. The slurry was stirred at rt for 14 h, at which point the reaction mixture had become a clear yellow solution. Reaction progress was monitored by TLC, eluting with 10 % MeOH in CH_2Cl_2. Once the reaction was complete, the reaction mixture was then acidified by dropwise addition of concentrated HCl (10 mL). The clear yellow solution was extracted with EtOAc (3 x 30 mL), and the organic layers were combined and washed with 1 N HCl (2 x 15 mL) and brine (1 x 10 mL). The organic solution was then dried over Na_2SO_4 and concentrated under vacuum to give the crude product as a white solid. The product was purified by recrystallization from hexanes/EtOAc to afford the product as a white solid (1.40 g, 6.33 mmol, 52 % yield) (m.p. = 131.2-132.7 °C). ^{1}H NMR (DMSO-d_6): δ 12.90 (s, 2H), 4.48 (s, 2H), 4.38 (q, J = 7 Hz, 2H), 4.22 (s, 2H), 1.22 (t, J = 7 Hz, 3H). ^{13}C NMR (DMSO-d_6): δ 189.1, 169.7, 169.6, 67.5, 54.8, 50.8, 13.9. HRMS (ESI-TOF) calcd. for $C_7H_{10}NO_5S^-$ $[M-H]^-$ 220.0273, found 220.0285.

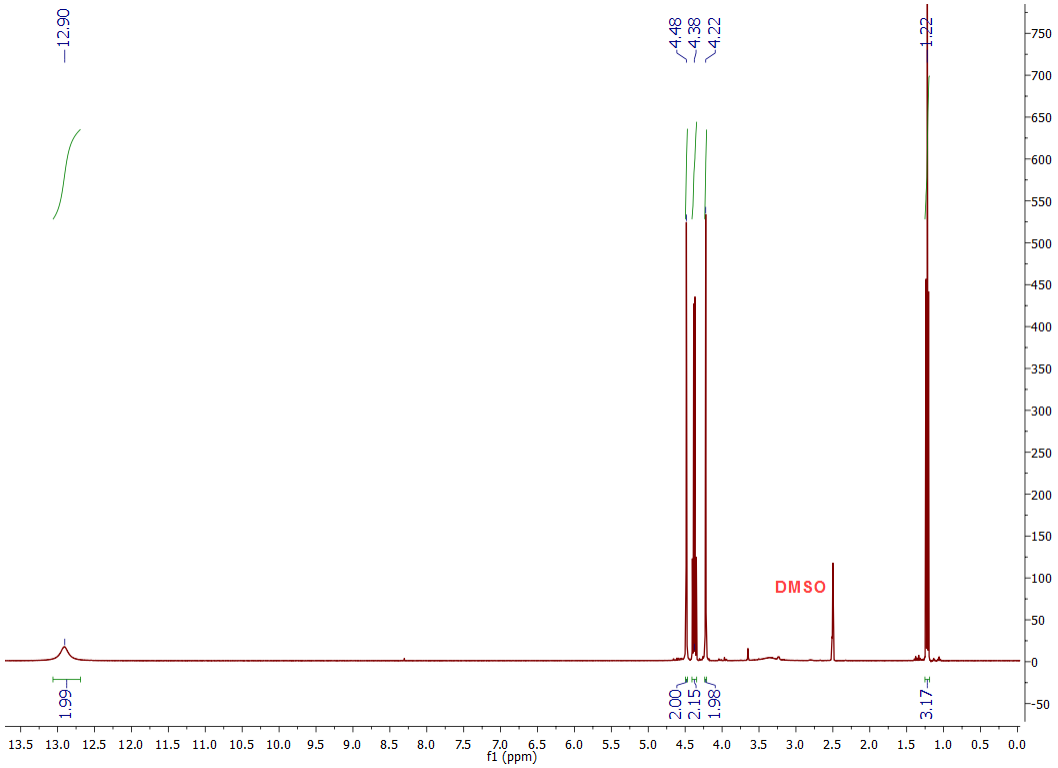

Figure S5. ^{1}H NMR spectrum (DMSO-d_6) of thiocarbmate diacetic acid **3**.

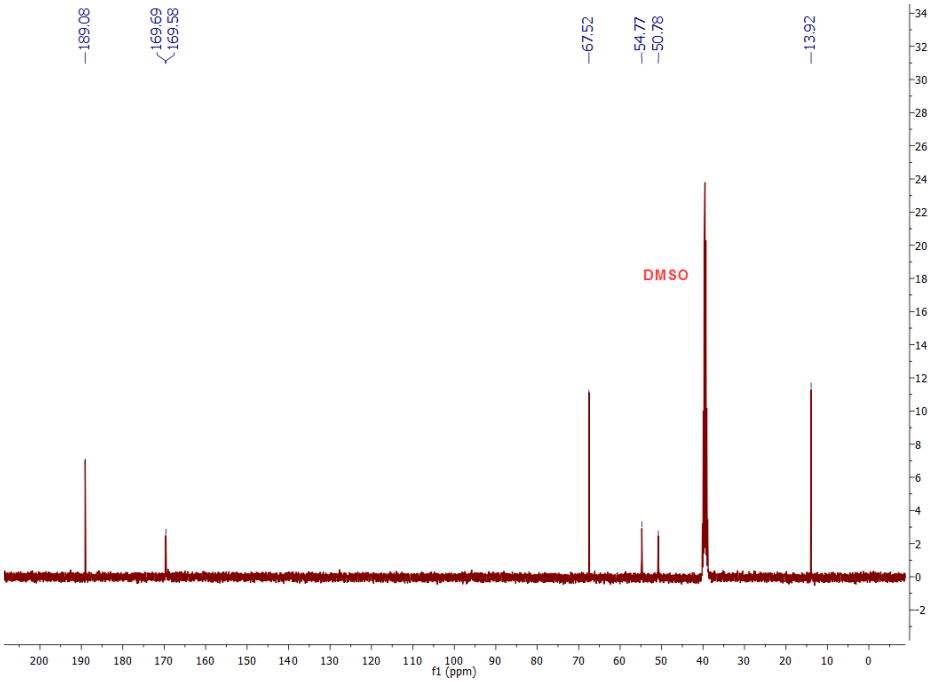

Figure S6. ^{13}C NMR spectrum (DMSO-d_6) of thiocarbamate diacetic acid **3**.

*Norbornene thiocarbamate acetic acid (**4**)*

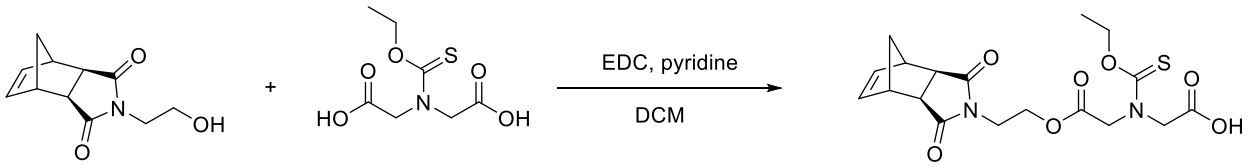

Exo-norbornene alcohol was synthesized according to literature procedures.[3] A round bottom flask was equipped with a stirbar and charged with dicarboxylic acid **3** (2.00 g, 9.04 mmol), pyridine (750 μL, 9.04 mmol) and CH_2Cl_2 (75 mL) giving a light yellow, slightly turbid solution. The flask was placed in an ice bath and a solution of EDC (1.73 g, 9.04 mmol) and *exo*-nobornene alcohol (9.37 g, 45.2 mmol) in CH_2Cl_2 (25 mL) was added dropwise via addition funnel. The reaction mixture was allowed to stir at rt for 14 h. Reaction progress was monitored by TLC, eluting with 5 % MeOH in CH_2Cl_2. The resulting clear yellow solution was washed with 1 N HCl (2 x 10 mL) and brine (1 x 10 mL). The organic solution was then dried over Na_2SO_4 and concentrated in vacuo to yield the crude product as a yellow oil. The product was purified on a silica column, eluting with 1-10 % MeOH in CH_2Cl_2 to give the pure product as a light-yellow oil (1.93 g, 4.70 mmol, 52 % yield). ^{1}H NMR ($CDCl_3$): δ 6.29 (m, 2H), 4.64 (m, 2H), 4.49 (m, 2H), 4.24-4.37 (m, 4H), 3.78 (m, 2H), 3.27 (s, 2H), 2.72 (m, 2H), 1.22-1.56 (m, 6H). ^{13}C NMR ($CDCl_3$): δ 190.44, 190.33, 178.38, 170.01, 168.47, 137.93, 69.10, 68.86, 62.66, 62.34, 55.16, 51.42, 50.58, 48.03, 45.38, 42.90, 42.85, 37.66, 37.53, 14.18, 14.10. HRMS (ESI-TOF) calcd. for $C_{18}H_{21}N_2O_7S^-$ $[M-H]^-$ 409.1036, found 409.1075.

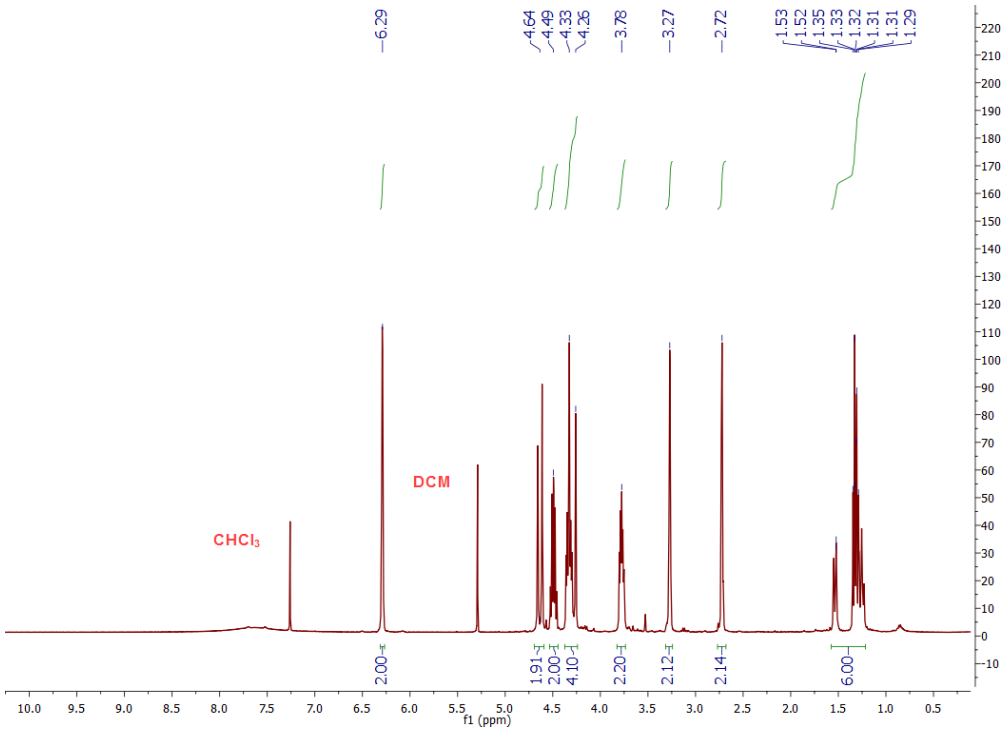

Figure S7. ^{1}H NMR spectrum ($CDCl_3$) of norbornene thiocarbmate acetic acid **4**.

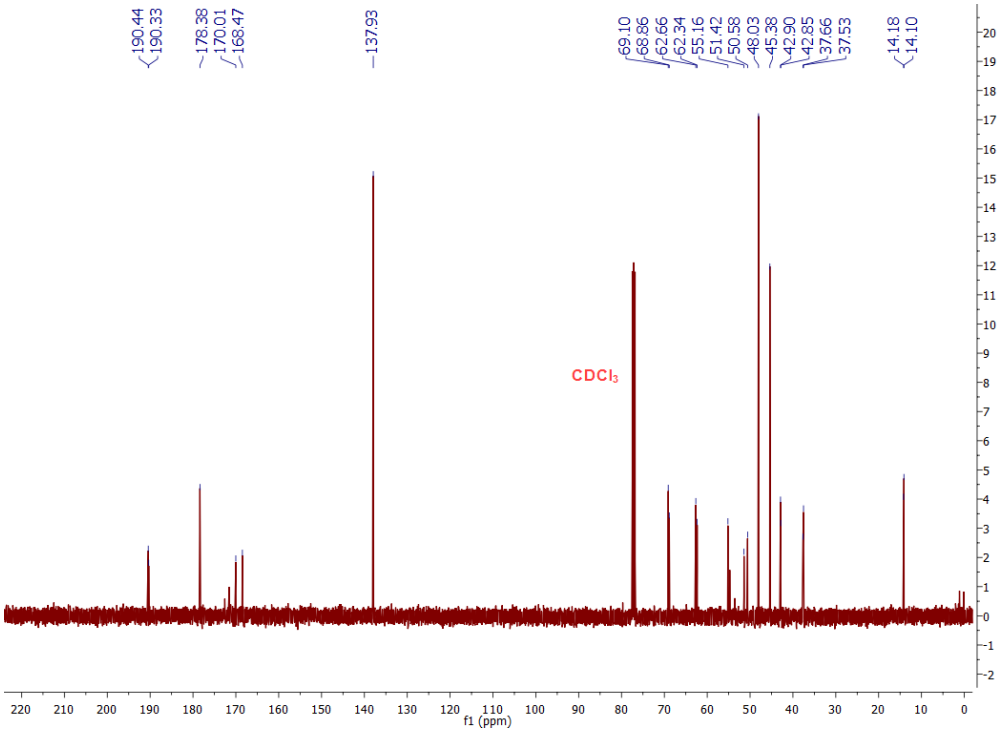

Figure S8. ^{13}C NMR spectrum ($CDCl_3$) of norbornene thiocarbamate acetic acid **4**.

Norbornene-NTA ROMP monomer **NB-NTA**

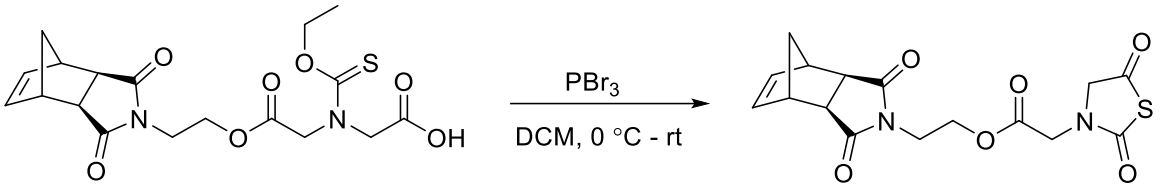

A flame-dried, two-necked round bottom flask was equipped with an N_2 inlet, a septum, and a stir bar. The flask was charged with **4** (0.302 g, 0.736 mmol) and dry CH_2Cl_2 (4 mL) under N_2 flow. The clear and colorless reaction mixture was then cooled to 0° C on an ice bath. Once cool, PBr_3 (0.09 mL, 1 mmol) was added dropwise to the reaction mixture via syringe. The reaction mixture was allowed to stir for 10 minutes at 0 °C. The ice bath was the removed, and the reaction mixture was allowed to warm to rt as it stirred for an additional 30 minutes. The reaction mixture was then transferred to a separatory funnel where it was washed with saturated bicarbonate solution added slowly (2 x, 2 mL) and brine (1 x, 2 mL). The organic solution was then dried over Na_2SO_4 and concentrated in vacuo to yield the crude product as a yellow oil. The crude product was purified on a silica column, eluting with CH_2Cl_2 to give the pure product as a light-yellow oil (0.135 g, 50 % yield). ^{1}H NMR ($CDCl_3$): δ 6.29 (t, *J* = 2 Hz, 2H), 4.36 (s, 2H), 4.32 (m, 2H), 4.22 (s, 2H), 3.77 (m, 2H), 3.27 (m, 2H), 2.70 (d, *J* = 1 Hz, 2H), 1.53 (m, 1H), 1.24 (m, 1H). ^{13}C NMR ($CDCl_3$): δ 193.3, 178.1, 167.4, 138.0, 62.9, 60.2, 48.1, 45.4, 44.5, 42.9, 37.5. HRMS (ESI-TOF) calcd. for $C_{16}H_{16}N_2O_6SNa^+$ $[M+Na]^+$ 387.0632, found 387.0621.

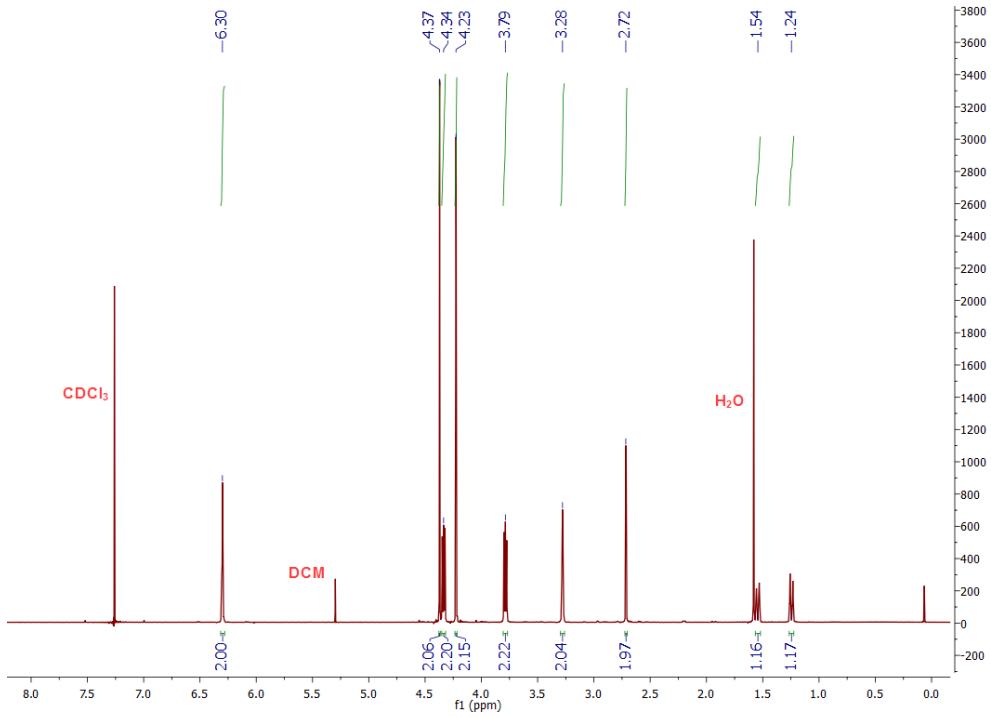

Figure S9. ^{1}H NMR spectrum ($CDCl_3$) of **NB-NTA**.

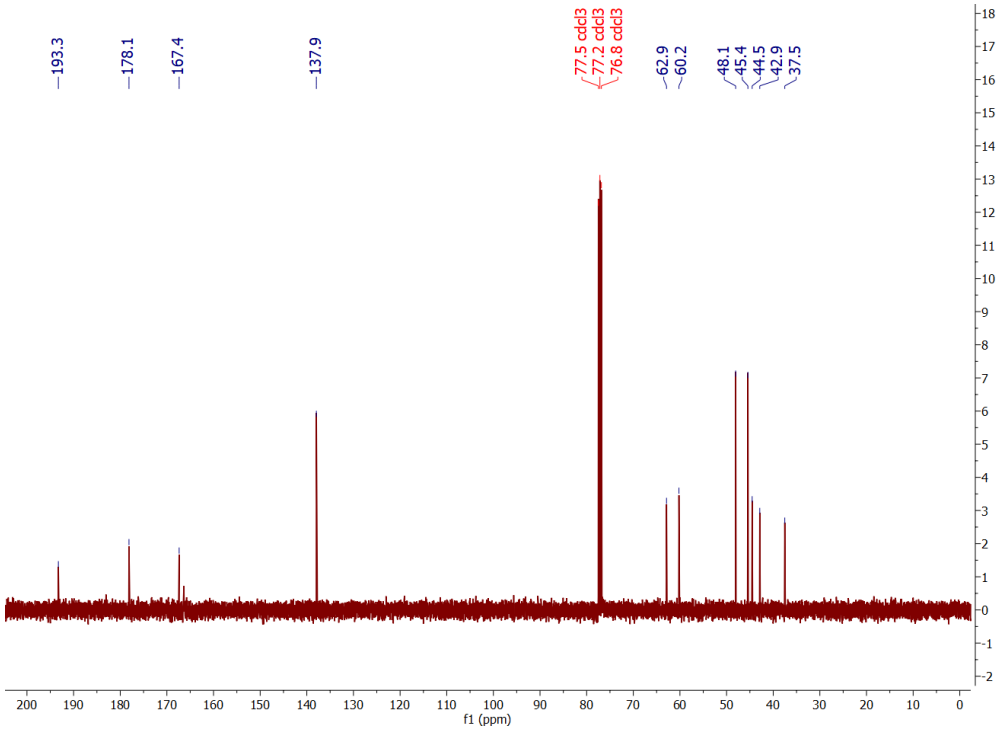

Figure S10. ^{13}C NMR spectrum ($CDCl_3$) of **NB-NTA**.

Synthesis of Norbornene-PEG$_{550}$ (**NB-PEG**)

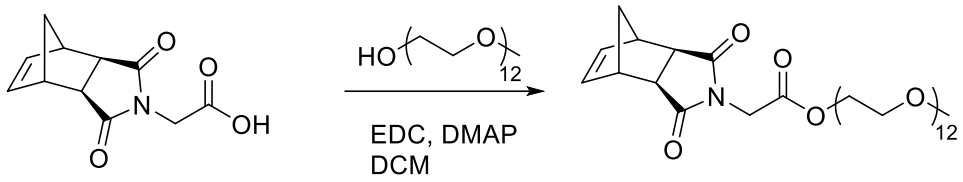

Exo-norbornene carboxylic acid was prepared by literature procedure.[4] A round bottom flask was equipped with a stirbar and charged with *exo*-norbornene carboxylic acid (2.021 g, 9.14 mmol), poly(ethylene glycol) monomethylether (M_n = 550 Da) (1.675 g, 3.05 mmol), and DMAP (0.112 g, 0.914 mmol). Dry CH_2Cl_2 (30 mL) was added, giving a clear yellow, slightly turbid solution. EDC (1.290 g, 9.14 mmol) was added in one portion, and the reaction mixture was allowed to stir at rt for 14 h. Reaction progress was monitored by TLC, eluting with 5 % MeOH in CH_2Cl_2. Once complete, the reaction mixture was transferred to a separatory funnel and washed with 1 N HCl (2 x, 15 mL) and brine (1 x, 15 mL). The organic layer was dried over Na_2SO_4 and concentrated under vacuum to yield the crude product as a light pink oil. The crude product was purified on a silica column, eluting with 5 % MeOH in CH_2Cl_2 to afford a clear, colorless oil (1.972 g, 2.56 mmol, 84 % yield).

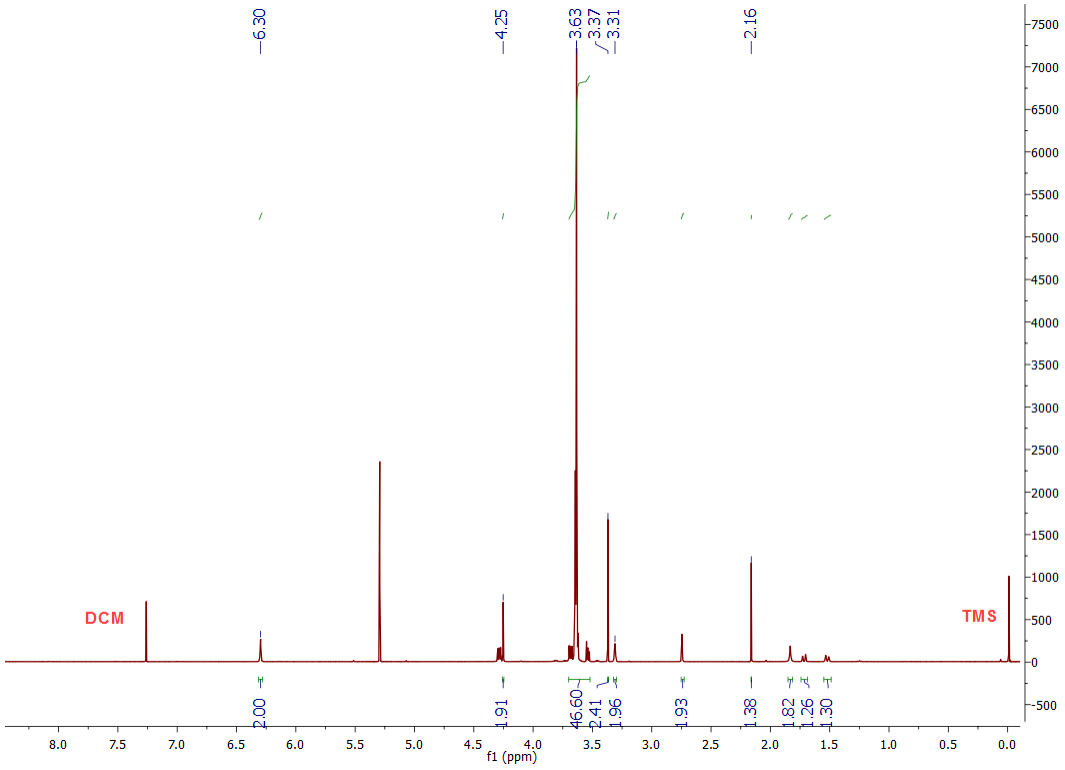

Figure S11. ^{1}H NMR of **NB-PEG** monomer.

*Synthesis of **polyNTA1** by ROMP*

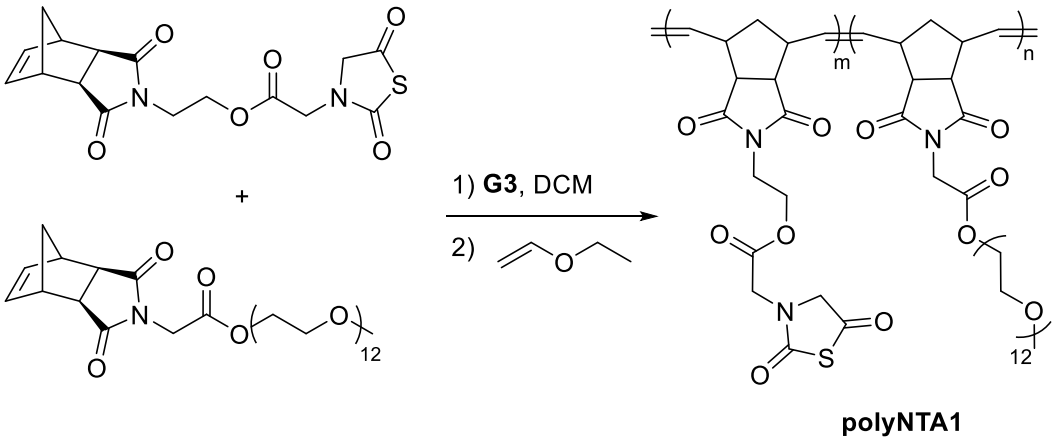

A 20 mL scintillation vial equipped with a screw-cap lid was charged with **NB-NTA** (10.5 mg, 29.0 μmol), **NB-PEG** (200 mg, 260 mmol), and dry CH_2Cl_2 (3.5 mL). **G3** catalyst, prepared according to a literature procedure,[5] was dissolved in dry CH_2Cl_2 in a second vial at a concentration

of 8.40 mg/mL. The **G3** solution (0.5 mL) was added rapidly by syringe to the monomer solution with vigorous stirring. The reaction mixture was stirred at rt for 1 h. A few drops of ethyl vinyl ether were then added to quench the polymerization, and then the reaction mixture was stirred for an additional 20 min. The polymer was isolated via precipitation from hexanes.

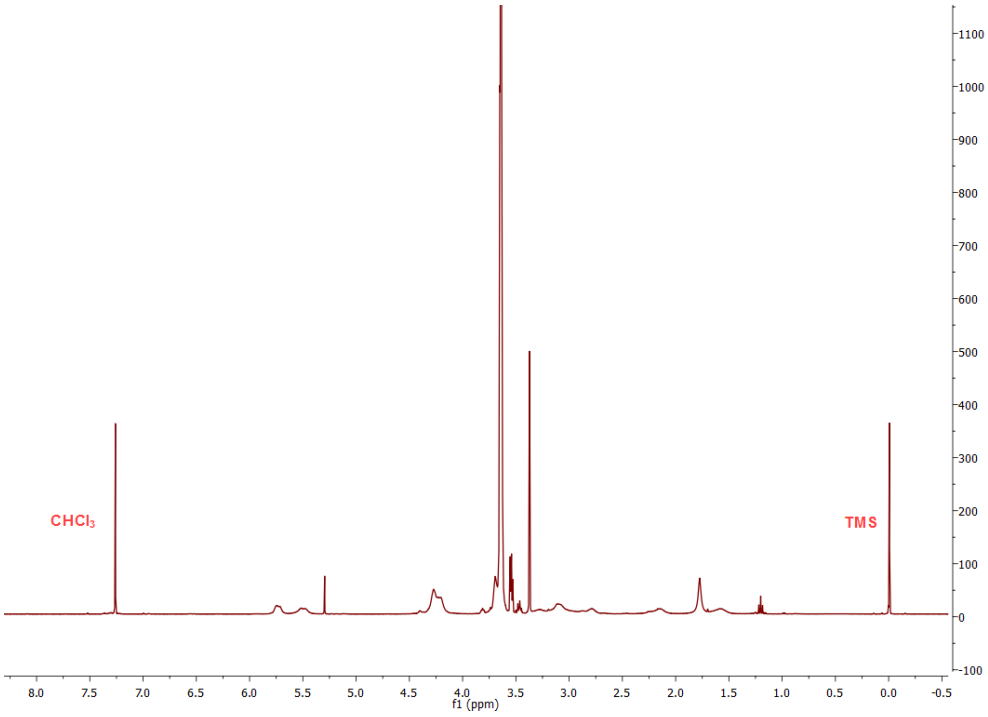

Figure S12. ^{1}H NMR of **polyNTA1**.

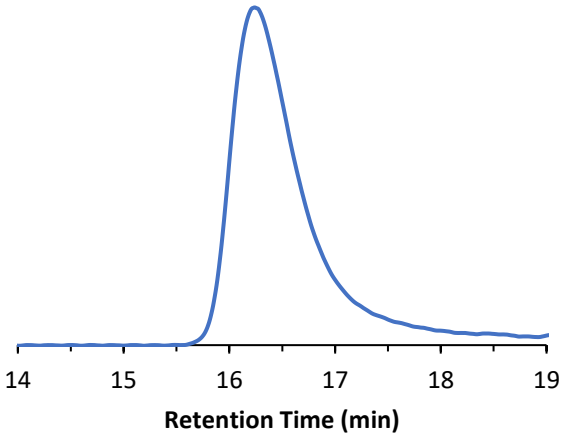

Figure S13. SEC analysis (RI trace) of **polyNTA1**.

Scheme S3. Proposed scheme for COS release from a generalized NTA structure

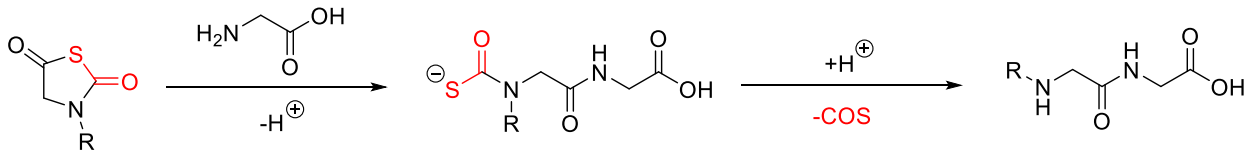

GC-MS detection of COS

A 1.5 mL vial was charged with 0.2 mL of a solution of **NTA1** (5 mM in DMSO), 0.8 mL glycine solution (12.5 mM in PBS buffer) and sealed with a screw cap lid with a rubber septum. The reaction mixture was allowed to sit at rt for 5 min, at which point an air-tight syringe was used to sample 100 µL of the vial headspace. This volume was injected into the GC-MS immediately. A control vial containing 0.8 mL glycine (12.5 mM in PBS buffer) and 0.2 mL DMSO was sampled using the same procedure at the 5-minute mark.

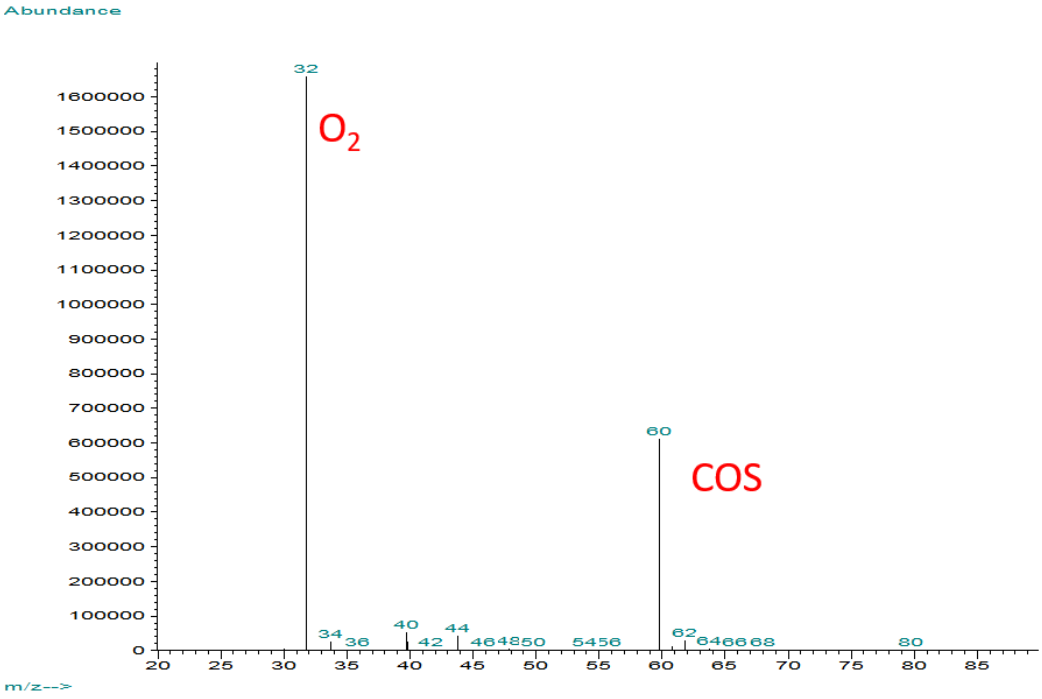

Figure S14. GC-MS mass chromatogram of **NTA1** reaction with glycine after 5 min.

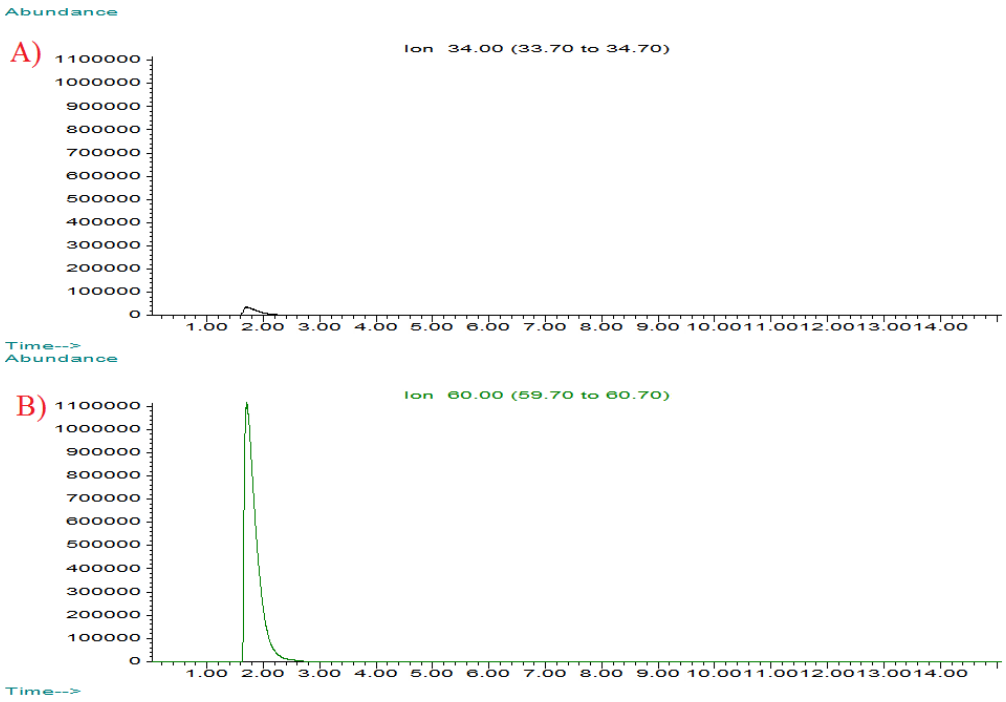

Figure S15. SIM mode monitoring of **NTA1** reaction with glycine after 5 min. A) H_2S abundance (m/z = 34.00) and B) COS abundance (m/z = 60.00).

Analysis of byproducts by LCMS

A one-dram vial was charged with **NTA1** (50.2 mg, 0.383 mmol) followed by addition of 1 mL glycine solution (0.46 M in 1X PBS) to give a colorless solution. After 8 h, 20 µL of the reaction mixture was injected onto the HPLC eluting 0 % ACN to 15 % ACN in water (0.1 % formic acid).

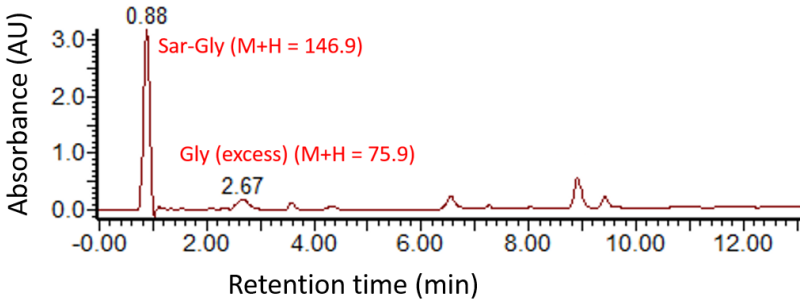

Figure S16. LCMS UV absorbance (λ = 220 nm) chromatogram of **NTA1** (0.38 M in phosphate buffered water) in the presence of glycine (0.42 M) after 8 h incubation.

Methylene blue H_2S release assay

Each assay described was run in triplicate in a one-dram vial containing 1.856 mL PBS buffer (pH = 7.4), 100 μL $Zn(OAc)_2$ solution (40 mM in H_2O), 20 μL **NTA1** or **poly(NTA1)** solution (10 mM in NTA functional group in DMSO), 20 μL CA solution (30 μM in PBS buffer), 4 μL glycine solution (500 mM in PBS buffer). Final concentrations were 100 μM **NTA1**, 2 mM $Zn(OAc)_2$, 1 mM glycine, and 300 nM CA. A control solution was run for each experiment containing all of the above components with the exception of **NTA1**. At predetermined timepoints, 100 μL was removed from each reaction vial and diluted with 100 μL $FeCl_3$ solution (30 mM in 1.2 M HCl) followed by 100 μL *N*,*N*-dimethyl-*p*-phenylenediamine solution (20 mM in 7.2 M HCl). Aliquots were stored until 90 minutes after the final aliquot had been taken to allow completion of methylene blue formation. The aliquots were transferred to a 96 well plate (250 μL/well) and their absorbance spectra were collected from 500 to 800 nm on a plate reader. Kinetic analysis was done

by subtracting the absorbance of the control experiment (no methylene blue formation) from the absorbance of each aliquot at that specific timepoint at 676 nm.

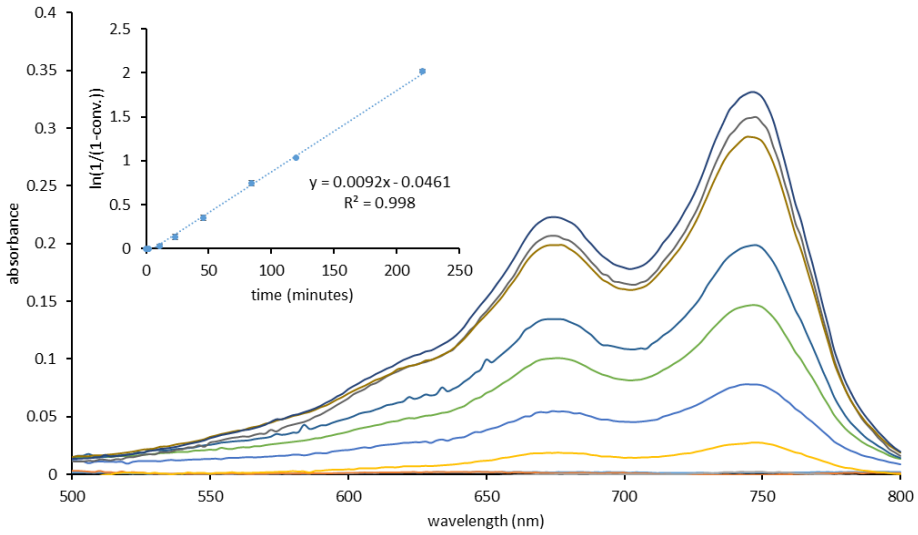

Figure S17. Representative absorbance spectra for the methylene blue spectrophotometric H_2S release assay with absorbance increasing over time. Inset shows the pseudo-first order kinetics plot derived from absorbances at 676 nm.

H_2S selective electrochemical probe calibration

A scintillation vial was charged with 1X PBS buffer (pH 7.4) (10 mL) and a small magnetic stir bar. The buffer solution was set to stir and the electrochemical probe was positioned in the vial. Once the probe current had equilibrated, a stock solution of NaSH (2 mM in H_2O) was added in 5 µL aliquots. Upon each addition of the NaSH stock solution to the vial, there was a spike in current which quickly stabilized. Upon current stabilization another addition was made until probe

response no longer appeared linear. The calibration curve was constructed by plotting the apparent concentration of H_2S in solution against the stabilized probe current.

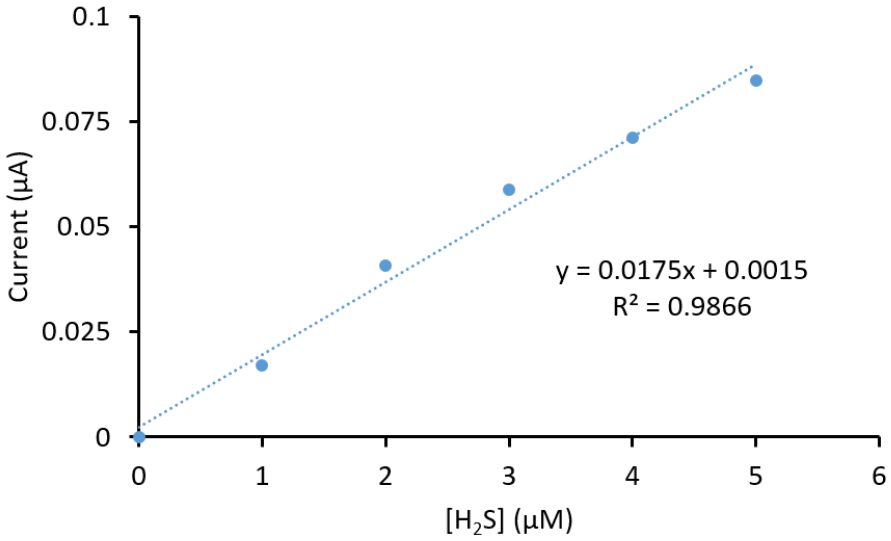

Figure S18. Calibration curve for H_2S release in 1X PBS buffer.

H_2S selective electrochemical probe release studies

A scintillation vial was charged with 9.73 mL of 1X PBS buffer (pH 7.4), 4 μL of a glycine solution (0.5 M in H_2O), 20 μL of a solution of **NTA1** (5 mM in DMSO), 250 μL of a solution of CA (6 μM in 1X PBS), and a small magnetic stir bar. Final concentrations were 10 μM **NTA1,** 100 μM glycine, and 300 nM CA. Once all of the reagents had been added, the probe was immediately inserted into the solution, and the probe current was recorded. The current initially spiked due to immersion in the solution, but stabilized quickly. This initial current spike is omitted from the reported data. Peaking time of H_2S in solution is measured at the point where the current readout is at a global maximum for the dataset.

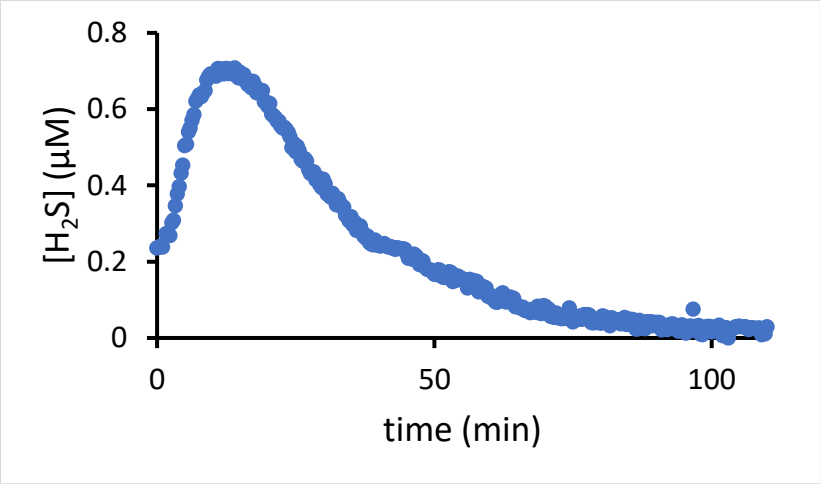

Figure S19. H_2S selective electrochemical probe release data for **NTA1** (10 µM) in complete endothelial cell media (10 mL). The faster peaking time is a result of a higher concentration of free amines available in complete cell media. The rapid return to baseline is likely a result of sulfhydration of the various proteins in the cell media by the H_2S released leading to a lower instantaneous concentration of sulfide.

Fluorescence H_2S release assay kinetics

Fluorescence assays were prepared in a 3 mL quartz cuvette with a threaded lid containing 1.80 mL 1X PBS buffer (pH 7.4), 0.1 mL glycine solution (30 mM in PBS buffer), 0.1 mL diethylenetriaminepentaacetic acid (DTPA) solution (2.5 mM in H_2O), 0.2 mL dansyl azide probe solution (3.76 mM in DMSO), and 0.020 mL CA solution (0.0375 mM in PBS). The fluorescence spectrum of this mixture was collected from 400 to 600 nm (λ_{ex} = 340 nm) as the t = 0 timepoint. To this solution was added 0.3 mL of **NTA1** solution (0.823 mM in DMSO). The cuvette was the capped, and Parafilm was wrapped around the cap to limit any potential volatilization of COS/H_2S. The cuvette was then placed in the fluorometer, and fluorescence spectra were collected every 10 min from 400 to 600 nm. Kinetic analysis was done by subtracting the zero-time point

fluorescence intensity from the fluorescence intensity at each time point at 540 nm. The pseudo-first-order half-life of H_2S release was determined by plotting time vs. ln(1/(1-% released), with $t_{1/2}$ = ln(2)/slope.

Brain-derived endothelial cell assays

Primary brain-derived endothelial cells (ECs) were plated in a 96-well plate containing serum-free media, pre-coated with 0.2% gelatin, at 20,000 cells/well. After 24 h incubation with the indicated treatments, cells were assessed for proliferation by adding 10 μM bromodeoxyuridine (BrdU; Sigma Aldrich, St. Louis, MO). Following 1 h incubation with BrdU, cells were fixed and stained with anti-BrdU (1:1000; ThermoFisher Scientific, Inc., Waltham, MA). ECs were counterstained with DAPI (1 mg/ml) and analyzed under TRITC/DAPI filters on an inverted IX-71 Olympus epi-fluorescence microscope equipped with a digital XM-10 camera and Cell Sense software package (Olympus, Valley, PA). For quantification of BrdU-positive ECs, four images per well were acquired and quantified as a ratio of BrdU/Dapi or proliferating cell fraction. For Casapase 3/7 assessment after 24 h incubation, cells were subjected to the Caspase-Glo 3/7 assay per manufactures instructions (Promega, Madison, WI). Data were graphed using GraphPad Prism, version 4 (GraphPad Software, Inc., San Diego, CA). Student's two-tailed t-test was used for comparison of two experimental groups. For three or more groups, multiple comparisons were done using one-way ANOVA followed by Tukey test for multiple pairwise examinations. Changes were identified as significant if p was less than 0.05. Mean values were reported together with the standard error of mean (SEM).

Mouse brain endothelial cell caspase assay

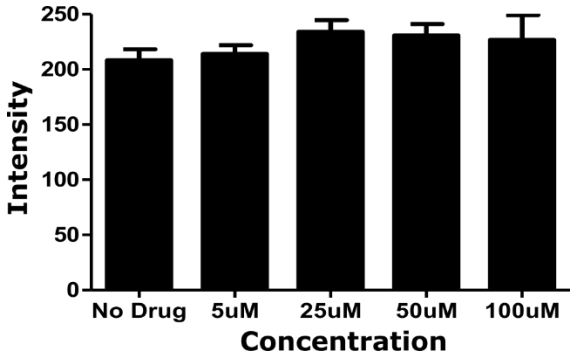

Figure S20. Caspase assay of brain-derived endothelial cells treated with 5-100 μM **NTA1**.

Mouse brain endothelial cell BrdU assay of PolyNTA1

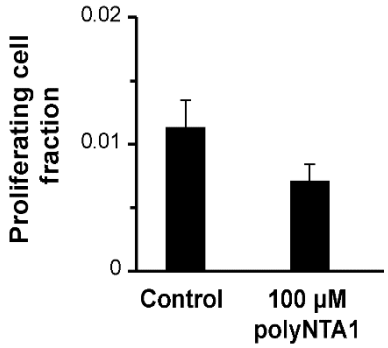

Figure S21. Endothelial cell proliferation data showing the ratio of proliferating cells in each treatment group. Cells were treated for 24 h in serum-free media, and quantification was performed by counting the number of $BrdU^+/Dapi^+$ cells (n = 6–8 for each treatment group). Error bars represent standard error of the mean. There was no statistically significant difference between these groups.

Experimental References:

1. Tao, X.; Deng, Y.; Shen, Z.; Ling, J., Controlled Polymerization of N-Substituted Glycine N-Thiocarboxyanhydrides Initiated by Rare Earth Borohydrides toward Hydrophilic and Hydrophobic Polypeptoids. *Macromolecules* **2014**, *47*, 6173.

2. Auty, S. E. R.; Andren, O.; Malkoch, M.; Rannard, S. P., The First Peripherally Masked Thiol Dendrimers: A Facile and Highly Efficient Functionalization Strategy of Polyester Dendrimers via One-Pot Xanthate Deprotection/Thiol-Acrylate Michael Addition Reactions. *Chem. Commun.* **2014**, *50*, 6574.

3. Qiao, Y.; Ping, J.; Tian, H.; Zhang, Q.; Zhou, S.; Shen, Z.; Zheng, S.; Fan, X., Synthesis and Phase Behavior of a Polynorbornene-Based Molecular Brush With Dual "Jacketing" Effects. *J. Polym. Sci., Part A: Polym. Chem.* **2015**, *53*, 2116.

4. Conrad, R. M.; Grubbs, R. H., Tunable, Temperature-Responsive Polynorbornenes with Side Chains Based on an Elastin Peptide Sequence. *Angew. Chem. Int. Ed.* **2009**, *48*, 8328.

5. Love, J. A.; Morgan, J. P.; Trnka, T. M.; Grubbs, R. H., A Practical and Highly Active Ruthenium-Based Catalyst that Effects the Cross Metathesis of Acrylonitrile. *Angew. Chem. Int. Ed.* **2002**, *41*, 4035

Chapter 3: Functional N-substituted *N*-Thiocarboxyanhydrides as Modular Tools for Constructing H_2S Donor Conjugates

This manuscript has been submitted for publication.

3.1. Authors.

Chadwick R. Powell,[§,†,‡] Kuljeet Kaur,[§,†,‡] Mingjun Zhou, [§,†,‡] Mohammed Alaboalirat, [§,†] and John B. Matson*[§,†,‡]

§Department of Chemistry, Virginia Tech, Blacksburg, Virginia 24061, United States
†Macromolecules Innovation Institute, Virginia Tech, Blacksburg, Virginia 24061, United States
‡Virginia Tech Center for Drug Discovery, Virginia Tech, Blacksburg, Virginia 24061, United States

3.2. Abstract.

We report a synthetic route toward a family of functional COS/H_2S-releasing N-substituted *N*-thiocarboxyanhydrides (NTAs) with functionalities to accommodate popular conjugation reactions, including olefin cross metathesis, thiol-ene, and copper-catalyzed azide-alkyne cycloaddition. The N-substituted NTAs were attached to small molecules, polymers, and a protein to synthesize novel H_2S donors convergently. All conjugates showed sustained H_2S release kinetics.

3.3. Introduction

Biology has benefitted immensely from the emergence of bioconjugation chemistry. The development of bioconjugates has led to key discoveries in measuring protein/ligand binding, developing effective MRI contrast agents, probing antibody–antigen interactions, and imaging biomolecules in vivo.[1] Expanding upon this work, many common bioconjugation reactions also

find use in other areas of chemistry, including surface modification[2] and polymer functionalization.[3] However, bioconjugation strategies have been applied only sparingly in the arena of gasotransmitter research,[4-6] which focuses on uncovering the biological roles and exploiting the therapeutic potential of endogenously produced signaling gases. We envisioned that popular bioconjugation reactions could be employed to synthesize a wide variety of gasotransmitter donor conjugates, specifically conjugates capable of delivering hydrogen sulfide (H_2S), from a small library of functionalized donors.

As first reported by Abe and Kimura in 1996, H_2S is a gasotransmitter.[7] Since this discovery, studies on the physiological roles of H_2S in the body have ensued.[8] More recent discoveries suggest that alterations in endogenous H_2S production contribute to a variety of disease states, including cardiovascular disease,[9] diabetes,[10] and Parkinson's disease,[11] among others.[12] These results also indicate that exogenous delivery of H_2S may be therapeutic in certain indications by promoting wound healing,[13] alleviating cardiovascular tissue damage in ischemia-reperfusion events,[14-15] and mitigating cellular damage in the central nervous system induced by reactive oxygen species (ROS).[16] However, compared with existing small molecule H_2S donors, donors appended to a variety of compounds and constructs, including established drugs, polymer scaffolds, and proteins, would likely increase the therapeutic viability of exogenous H_2S delivery moving forward.

Compared with H_2S "donor salts" NaSH and Na_2S, which lead to instantaneous release, synthetic H_2S donors can incorporate specific release triggers and extend the H_2S release half-life, better mimicking endogenous H_2S production.[17] These properties allow for greater sophistication in studying H_2S in biological settings and open avenues for targeted H_2S delivery. Over the past decade, various H_2S donors have been developed that respond to specific stimuli, including water,

nucleophiles, light, and enzymes, among others.[18-20] Additionally, current efforts focus on extending H_2S donors to polymeric drug delivery systems as well as modifying existing drugs with H_2S-releasing moieties.[21-25] However, nearly all synthetic H_2S donors lack reactive chemical "handles" for use in conjugation reactions, a necessity to develop a library of donors convergently. Based on previous work in our group on donors of carbonyl sulfide (COS), which is converted into H_2S *in vitro*, we aimed here to create a platform of dual COS/H_2S donors that could be readily conjugated to various scaffolds.

Previously, our lab reported on *N*-thiocarboxyanhydrides (NTAs) as a class of dual COS/H_2S donors with nontoxic, peptidic byproducts.[26] NTAs release COS in the presence of primary amines (e.g., glycine), and the ubiquitous enzyme carbonic anhydrase (CA) rapidly catalyzes hydrolysis of the released COS into H_2S (Scheme 1A). The initial version of NTAs as COS/H_2S donors was the NTA of sarcosine (**NTA1**) as it offered a straightforward synthesis from commercially available starting materials. However, **NTA1** lacks functional handles and is not conducive to conjugation reactions. Therefore, we sought a synthetic route to make NTAs that would tolerate the incorporation of functional groups used in common bioconjugation reactions. Functional NTAs would allow for the simple modification of existing small molecules, polymers, proteins, surfaces, or other platforms with COS/H_2S releasing NTAs, opening a range of novel H_2S donor systems. To this end, we devised a modular synthetic route to prepare NTAs with several functionalities via the same starting materials. Functional groups with high prevalence in the fields of bioconjugation and polymer chemistry such as alkynes, azides, alkenes, and norbornenes were targeted to allow access to popular conjugation reactions.

3.4. Results and Discussion

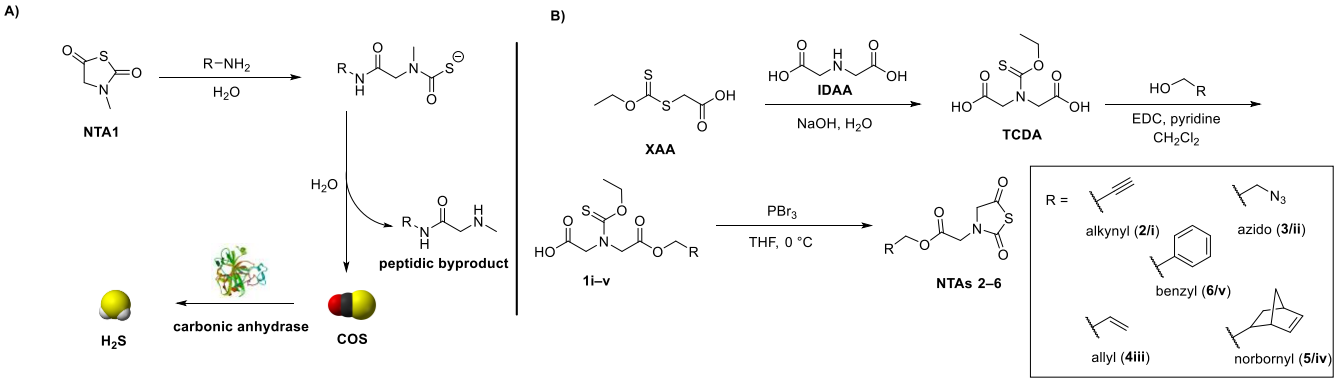

Scheme 1. A) Proposed mechanism of COS/H_2S release from donor **NTA1**, studied previously. B) Synthetic route to functional N-substituted NTAs.

N-Functional NTAs were prepared in three steps starting from commercially available 2-((ethoxycarbonothioyl)thio)acetic acid (XAA) and iminodiacetic acid (IDAA) (Scheme 1B), affording thiocarbamate diacetic acid (TCDA). This compound was subsequently monoesterified with commercially available functionalized alcohols to give compounds **1i-v** (see Appendix 3.6 for synthetic routes), followed by ring-closure with phosphorous tribromide (PBr_3) to give the corresponding NTAs, labelled **NTAs 2–6**. To show the versatility of this approach, five N-substituted NTAs were prepared as alkynyl, azido, allyl, norbornyl, and benzyl esters (Scheme 1B). We aimed specifically to synthesize alkynyl- and azido-NTAs (**NTA2** and **NTA3**) to accommodate the Huisgen [3+2] cycloaddition reaction (CuACC) between organo-azides and alkynes. Allyl-NTA (**NTA4**) was designed to facilitate olefin cross metathesis and thiol-ene reactions, owing to the prevalence of reactive thiol-ene substrates.[27] Lastly, benzyl-NTA (**NTA6**) was synthesized as a model compound to study H_2S release from NTAs under various conditions

(i.e., different pH and nucleophiles) in detail. All five NTAs are solids at room temperature and stable for months on the benchtop.

To assess whether NTAs decompose under common CuAAC reaction conditions, model reactions on small molecules were conducted. The CuAAC reaction was performed using alkynyl **NTA2** and 2-azidoethyl benzoate to form compound 7 (Table 1). The best conditions found for this reaction included a THF/H_2O solvent mixture (4:1 v/v) with sonication in lieu of magnetic stirring, as sonication best facilitated the dispersion of the precipitate formed upon addition of sodium ascorbate to copper sulfate pentahydrate ($CuSO_4 \cdot 5H_2O$). Under these conditions, we observed near quantitative conversion to the desired product by ^{1}H NMR spectroscopy in approximately 20 min at rt, with product isolation by flash chromatography (Table 1, compound 7).

To further highlight the robust nature of the CuAAC reaction with **NTA2**, we extended the scope of these conditions to conjugation of **NTA2** onto an azido-functionalized lysine (Fmoc–Lys(N_3)–OH) as well as a macromolecular substrate, azide-terminated poly(ethylene glycol) (PEG–N_3, molecular weight (MW) = 5.0 kg/mol). These two substrates were chosen as analogs to peptidic and polymeric drug delivery systems. Using the same reaction conditions outlined above, complete conversion to product was observed after approximately 60 min for reactions with both Fmoc–Lys(N_3)–OH (Table 1, compound 8) and PEG–N_3 (Table 1, compound 9). These reactions demonstrate that a single NTA can be used to functionalize a variety of systems from small molecules to polymers under similar reaction conditions.

In order to fully encompass the scope of the CuAAC click reactions for both alkyne and azide substrates, we synthesized an azide-functionalized NTA, **NTA3**. To evaluate the reactivity of **NTA3**, we performed CuAAC on a small molecule model compound, THP-protected propargyl

alcohol (Table 1, compound 10), and an alkyne-functionalized PEG (MW = 5.0 kg/mol) (Table 1, compound 11). Both reactions reached complete conversion within 75 min under the same CuAAC conditions described for **NTA2**.

We also investigated conjugation of NTAs using olefin cross metathesis (CM), a widely used tool in organic chemistry as a facile and mild means of forming carbon-carbon double bonds in bioconjugation,[28] drug development,[29] and polymer synthesis[30]. Grubbs and co-workers previously categorized terminal olefin CM substrates into four categories depending on their propensity to form homodimer CM products.[31] Ideal CM partners have mismatched reactivity (i.e., Type I + Type II or III), motivating the decision to choose methyl acrylate (Type III) as a model CM partner with allyl-NTA (**NTA4**) (Type I). CM reactions were conducted in the presence of Hoveyda-Grubbs second generation (HG2) catalyst with *p*-cresol as an additive, as reported by Tooze and coworkers.[32] In the presence of p-cresol and 2 equiv methyl acrylate, complete consumption of **NTA4** was observed in 2 h by TLC with 0.1 mol % catalyst loading. The desired NTA-methyl acrylate CM product (85:15 E/Z ratio (Figure S31)) was isolated by flash chromatography (Table 1, compound **12**).

The final class of reactions used for NTA conjugation was the radical thiol-ene reaction between thiols and electron-rich alkenes. Thiol-ene reactions can be initiated thermally or by UV light and do not require a metal catalyst, making them particularly attractive bioconjugation reactions. Thiols are commonly found in biological systems in the form of reduced cysteine or glutathione as well as cysteine residues on proteins. Additionally, polymers with thiol chain ends are readily prepared by reversible addition–fragmentation chain transfer (RAFT) polymerization followed by removal of the thio-carbonylthio species,[33] offering another mode for conjugation of NTAs to synthetic polymer systems.

For conjugation of NTAs to thiols via thiol-ene, (diphenylphosphorylmesityl)methanone (TPO) was used as the photoinitiator. For the equimolar reaction of **NTA4** with *N*-acetyl cysteine (Ac–Cys–OH) in THF (Table 1, compound 13), complete consumption of the allyl-NTA starting material was observed by TLC in 60 min, with isolation of the conjugate via flash chromatography. The thiol-ene conjugation reaction was then extended to a polymeric system. Water-soluble poly(acryloyl morpholine) (PACMO) was synthesized via RAFT polymerization (MW = 6.0 kg/mol, Đ = 1.08), followed by reduction of the trithiocarbonate with hydrazine[34] to reveal a free thiol on the polymer chain end. Reaction of this polymeric thiol for 70 min with **NTA4** under similar conditions to those described above afforded complete consumption of **NTA4**. The NTA-PACMO conjugate was easily isolated by precipitation (Table 1, compound 14).

To evaluate the scope of thiol-ene reactions with NTAs, we performed the thiol-ene reaction between **NTA4** and bovine serum albumin (BSA), a model protein with a single reduced cysteine residue (Cys34).[35] To accommodate the solubility of BSA a largely aqueous reaction medium was employed. Unfortunately, there was no evidence of NTA consumption by TLC after UV irradiation for up to 2 h under these conditions.

Table 1. Reactions of functional N-substituted NTAs.

	N-substituted NTA	Substrate (equiv)	Product structure
7	**NTA2**	2-azidoethyl benzoate[a] (1)	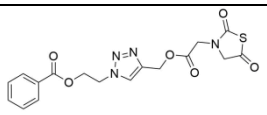
8	**NTA2**	Fmoc–Lys(N_3)–OH[a] (1)	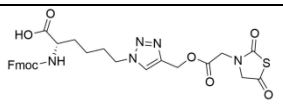
9	**NTA2**	PEG–N_3[a] (0.8)	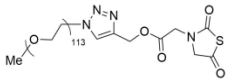
10	**NTA3**	THP–propargyl-OH (1)[a]	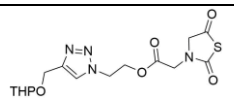
11	**NTA3**	PEG–alkyne (0.8)[a]	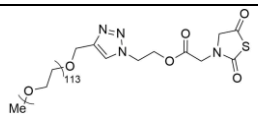
12	**NTA4**	methyl acrylate[b] (2)	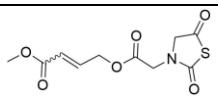
13	**NTA4**	Ac–Cys–OH[c] (1)	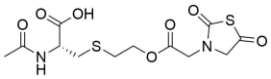
14	**NTA4**	PACMO–SH[d] (0.5)	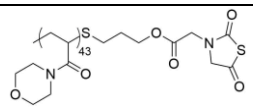
15	**NTA5**	benzyl mercaptan[c] (1)	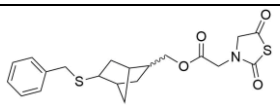
16	**NTA5**	BSA[e] (0.1)	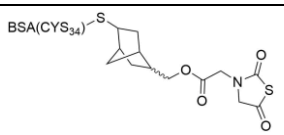

[a]$CuSO_4 \cdot 5H_2O$ (0.4 equiv), sodium ascorbate (5 equiv), THF:H_2O (4:1 v/v), sonication. [b]Hoveyda-Grubbs Gen. II catalyst, CH_2Cl_2, reflux, N_2 atmosphere. [c]TPO (0.1 equiv), THF, UV irradiation. [d]TPO (0.3 equiv), THF, UV irradiation, N_2 atmosphere. [e]TPO (0.05 equiv), H_2O:THF (9:1), UV irradiation.

Figure 1. A) H_2S release from parent functional NTAs (10 µM) in the presence of Gly (100 µM) and CA (800 nM) in 1X PBS buffer (pH 7.4). B) H_2S release from functionalized NTAs 7-15, see

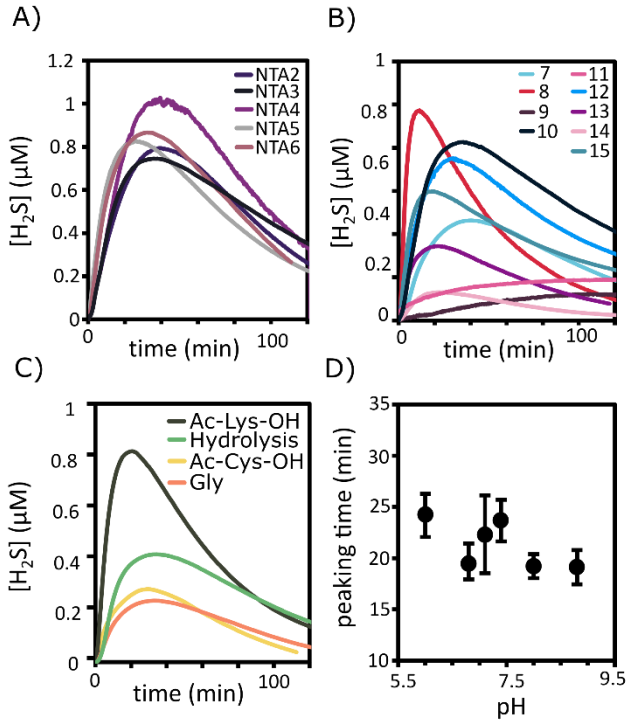

table 1. C) H_2S release for benzyl NTA (10 µM) in the presence of *N*-α-acetyl-L-lysine (Ac–Lys–OH), glycine (Gly), *N*-acetyl cysteine (Ac–Cys–OH) in 1X PBS buffer (pH 7.4). D) Plot of peaking times of benzyl NTA (10 µM) vs pH value in various buffered systems (10 mM).

Previous reports have demonstrated rapid and efficient light-mediated thiol-ene reactions between substituted norbornenes and thiols in aqueous media.[27, 36] This inspired the synthesis of norbornyl-NTA (**NTA5**) to enable thiol-ene under conditions where **NTA4** does not give

appreciable conversion. A small molecule model reaction between **NTA5** and benzyl mercaptan in the presence of TPO progressed smoothly, reaching full conversion in approximately 60 min (Table 1, compound **15**). Using the same reaction conditions with **NTA4** and BSA, we observed complete consumption of **NTA5** by TLC after 2 h of irradiation with UV light in the presence of TPO. After isolation via precipitation, analysis by MALDI-TOF mass spectrometry revealed a shift in the center of the peak observed for pure BSA from 66,200 to 66,700 m/z (Figure S38), indicating that the conjugation reaction was successful. These results are similar to published MALDI-TOF analyses of modified BSA.[37] Successful formation of NTA-functionalized BSA was also confirmed by H_2S release measurements (Figure S40).

H_2S release profiles of the functional NTAs were investigated using an H_2S-selective electrochemical probe in the presence of physiologically relevant concentrations of CA (800 nM). H_2S release profiles for the parent NTAs (**NTAs 2–6**) displayed the typical release profile for small molecule H_2S donors, with a rise to a peak concentration followed by a slow return to baseline (Figure 1A). For **NTAs 2–6** H_2S concentrations peaked between 20–35 min in PBS buffer (pH 7.4) with 100 μM added glycine as a trigger. H_2S release from small molecule NTAs after the various functionalization reactions (compounds **7**, **8**, **10**, **12**, **13**, and **15**) did not show a change in the general shape of the H_2S release profile from their parent, N-substituted NTA, and peaking times remained within a 15–35 min timeframe (Figure 1B). Although fairly small, we attribute the differences in peaking times between non-polymeric products from the same parent NTA (e.g. compound **7** versus **8** and compound **12** versus **13**) to changes in the local environment; for example, the carboxylic acids in compounds **7** and **13** may contribute to their enhanced release rate compared with compounds **8** and **12**. Maximum concentrations of H_2S in these release profiles are related to peaking time, where a faster peaking time generally leads to a larger maximum H_2S

concentration. Overall, these results demonstrate that functionalization of NTAs with small molecules does not substantially alter their H_2S release profile.

A more dramatic change in H_2S release profile was observed for the polymer-NTA conjugates, PEG-NTA (**9** and **11**) and PACMO-NTA (**14**). All of the polymer-NTA conjugates showed substantially lower maximum concentrations of H_2S relative to the small molecule NTAs at the same concentration, with peaking times occurring at 20 min for the PACMO-NTA conjugate (**14**) and approximately 2 h for the PEG-NTA conjugates (**9** and **11**). Despite the differences in peaking times, all of the macromolecular NTA conjugates showed a more gradual return to baseline H_2S concentrations relative to the small molecule NTA donors, demonstrating that polymeric donors are capable of maintaining a sustained concentration of H_2S in solution to a greater degree than the small molecule NTAs. The phenomenon of extended and sustained H_2S release from polymeric H_2S donors has been previously reported, and it likely stems from steric effects of the polymer chain in solution.[21-22, 26]

To gather further insight into the H_2S release kinetics of N-substituted NTAs, benzyl-NTA (**NTA6**) was used as a model substrate in the presence of various biologically relevant nucleophiles and at different pH values. In the first set of experiments with **NTA6**, we explored the effect of various nucleophiles on H_2S release rate under pseudo-first-order conditions (10:1 molar ratio of nucleophile to NTA). The nucleophiles included water only (hydrolysis), glycine, Ac–Lys–OH, and Ac–Cys–OH and were chosen to provide a range of functionalities available *in vivo*. Each nucleophile tested gave a similar release profile to hydrolysis, with addition of Ac–Lys–OH leading to a moderate decrease in peaking time and a greater maximum H_2S concentration (Figure 1C) than the others, indicating a faster overall release.

Release of H_2S from **NTA6** was also measured in buffers at various pH values. Peaking times remained constant within experimental error between pH 6 and 8.8, with peaking times ranging from 20–25 min at each pH value (Figure 1D). Taken together, these results demonstrate that NTAs provide a platform with consistent COS/H_2S release rates under a variety of physiologically relevant pH values.

Figure 2. Viability of H9C2 cardiomyocytes treated with **NTA6** at various concentrations.

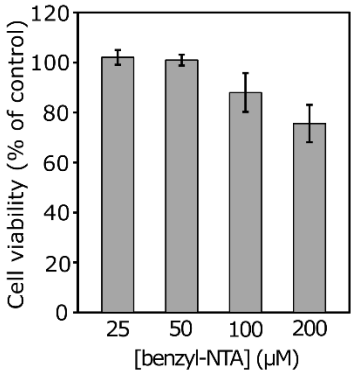

Viability is presented as a percentage relative to a media-only control. Quantification of viability was carried out using Cell Counting Kit-8 (CCK-8). Results are expressed as the mean ± SEM, where 10 trials were run for each treatment group over two independent experiments.

Lastly, we assessed the cytotoxicity of **NTA6** in the presence of H9C2 cardiomyocytes (Figure 2). **NTA6** showed no effect on cell viability at concentrations of ≤50 μM after incubation for 24 h, relative to untreated controls. Slight decreases in viability were seen at 100 and 200 μM, similar to other COS donors. [19, 38-39]

3.5. Conclusions

In summary, we have validated functional N-substituted NTAs as a modular donor platform from which a wide variety of H_2S donor conjugates may be prepared. Herein, we have presented a synthetic route to a variety of functional NTAs, which can subsequently be used to modify existing drugs, macromolecules, or proteins to form COS/H_2S-releasing conjugates. NTAs release H_2S spontaneously in CA-containing water but at a faster rate when triggered with an amine. Synthesis of NTA conjugates in aqueous conditions was successful, which will inform preparation of H_2S-donating proteins or water-soluble polymers. An assortment of H_2S donor systems will further facilitate the study of COS/H_2S physiology and help fully realize the therapeutic benefits of exogenous H_2S delivery.

3.6. Acknowledgements

This work was supported by the National Science Foundation (DMR-1454754), the National Institutes of Health (R01GM123508), and the Dreyfus foundation. The authors acknowledge Dr. Yin Wang for his help with cell culture, Prof. Rich Gandour for critical reading of the manuscript, as well as Dr. Mehdi Ashraf-Khorassani and Dr. Rich Helm for their assistance with high-resolution mass spectrometry.

3.7. References

1. Kalia, J.; Raines, R. T., Advances in Bioconjugation. *Curr. Org. Chem.* **2010,** *14*, 138-147.

2. Binder, W. H.; Sachsenhofer, R., “Click” Chemistry in Polymer and Materials Science. *Macromol. Rapid Commun.* **2007,** *28*, 15-54.

3. Le Droumaguet, B.; Velonia, K., Click Chemistry: A Powerful Tool to Create Polymer-Based Macromolecular Chimeras. *Macromol. Rapid Commun.* **2008,** *29*, 1073-1089.

4. Oladeinde, O. A.; Hong, S. Y.; Holland, R. J.; Maciag, A. E.; Keefer, L. K.; Saavedra, J. E.; Nandurdikar, R. S., "Click" Reaction in Conjunction with Diazeniumdiolate Chemistry: Developing High-Load Nitric Oxide Donors. *Org. Lett.* **2010,** *12*, 4256-4259.

5. Zhang, J.; Song, H.; Ji, S.; Wang, X.; Huang, P.; Zhang, C.; Wang, W.; Kong, D., NO Prodrug-Conjugated, Self-Assembled, pH-responsive and Galactose Receptor Targeted Nanoparticles for Co-Delivery of Nitric Oxide and Doxorubicin. *Nanoscale* **2018,** *10*, 4179-4188.

6. Nguyen, D.; Oliver, S.; Adnan, N. N. M.; Herbert, C.; Boyer, C., Polymer–Protein Hybrid Scaffolds as Carriers for CORM-3: Platforms for the Delivery of Carbon Monoxide (CO). *RSC Advances* **2016,** *6*, 92975-92980.

7. Abe, K.; Kimura, H., The Possible Role of Hydrogen Sulfide as an Endogenous Neuromodulator. *J. Neurosci.* **1996,** *16*, 1066-1071.

8. Cuevasanta, E.; Möller, M. N.; Alvarez, B., Biological Chemistry of Hydrogen Sulfide and Persulfides. *Arch. Biochem. Biophys.* **2017,** *617*, 9-25.

9. Lefer, D. J., A New Gaseous Signaling Molecule Emerges: Cardioprotective Role of Hydrogen Sulfide. *Proc. Natl. Acad. Sci. U. S. A.* **2007,** *104*, 17907.

10. Kaneko, Y.; Kimura, Y.; Kimura, H.; Niki, I., L-cysteine Inhibits Insulin Release from the Pancreatic Beta-Cell: Possible Involvement of Metabolic Production of Hydrogen Sulfide, a Novel Gasotransmitter. *Diabetes* **2006,** *55*, 1391-7.

11. Hu, L.-F.; Lu, M.; Tiong, C. X.; Dawe, G. S.; Hu, G.; Bian, J.-S., Neuroprotective Effects of Hydrogen Sulfide on Parkinson's Disease Rat Models. *Aging Cell* **2010,** *9*, 135-146.

12. Kashfi, K.; Olson, K. R., Biology and Therapeutic Potential of Hydrogen Sulfide and Hydrogen Sulfide-Releasing Chimeras. *Biochem. Pharmacol.* **2013,** *85*, 689-703.

13. Papapetropoulos, A.; Pyriochou, A.; Altaany, Z.; Yang, G.; Marazioti, A.; Zhou, Z.; Jeschke, M. G.; Branski, L. K.; Herndon, D. N.; Wang, R.; Szabó, C., Hydrogen Sulfide is an Endogenous Stimulator of Angiogenesis. *Proc. Natl. Acad. Sci. U. S. A.* **2009,** *106*, 21972-21977.

14. Zhao, Y.; Bhushan, S.; Yang, C.; Otsuka, H.; Stein, J. D.; Pacheco, A.; Peng, B.; Devarie-Baez, N. O.; Aguilar, H. C.; Lefer, D. J.; Xian, M., Controllable Hydrogen Sulfide Donors and Their Activity Against Myocardial Ischemia-Reperfusion Injury. *ACS Chem. Biol.* **2013,** *8*, 1283-1290.

15. Calvert, J. W.; Jha, S.; Gundewar, S.; Elrod, J. W.; Ramachandran, A.; Pattillo, C. B.; Kevil, C. G.; Lefer, D. J., Hydrogen Sulfide Mediates Cardioprotection Through Nrf2 Signaling. *Circ. Res.* **2009,** *105*, 365-374.

16. Whiteman, M.; Cheung, N. S.; Zhu, Y. Z.; Chu, S. H.; Siau, J. L.; Wong, B. S.; Armstrong, J. S.; Moore, P. K., Hydrogen Sulphide: A Novel Inhibitor of Hypochlorous Acid-Mediated Oxidative Damage in the Brain? *Biochem. Biophys. Res. Commun.* **2005,** *326*, 794-798.

17. Zhao, Y.; Biggs, T. D.; Xian, M., Hydrogen sulfide (H_2S) Releasing Agents: Chemistry and Biological Applications. *Chem. Commun.* **2014,** *50*, 11788-11805.

18. Powell, C. R.; Dillon, K. M.; Matson, J. B., A Review of Hydrogen Sulfide (H_2S) Donors: Chemistry and Potential Therapeutic Applications. *Biochem. Pharmacol.* **2018,** *149*, 110-123.

19. Steiger, A. K.; Yang, Y.; Royzen, M.; Pluth, M. D., Bio-Orthogonal "Click-and-Release" Donation of Caged Carbonyl Sulfide (COS) and Hydrogen Sulfide (H_2S). *Chem. Commun.* **2017,** *53*, 1378-1380.

20. Ji, X.; Zhou, C.; Ji, K.; Aghoghovbia, R. E.; Pan, Z.; Chittavong, V.; Ke, B.; Wang, B., Click and Release: A Chemical Strategy toward Developing Gasotransmitter Prodrugs by Using an Intramolecular Diels–Alder Reaction. *Angew. Chem. Int. Ed.* **2016,** *55*, 15846-15851.

21. Foster, J. C.; Matson, J. B., Functionalization of Methacrylate Polymers with Thiooximes: A Robust Postpolymerization Modification Reaction and a Method for the Preparation of H_2S-Releasing Polymers. *Macromolecules* **2014,** *47*, 5089-5095.

22. Xiao, Z.; Bonnard, T.; Shakouri-Motlagh, A.; Wylie, R. A. L.; Collins, J.; White, J.; Heath, D. E.; Hagemeyer, C. E.; Connal, L. A., Triggered and Tunable Hydrogen Sulfide Release from Photogenerated Thiobenzaldehydes. *Chem. Eur. J.* **2017,** *23*, 11294-11300.

23. Urquhart, M. C.; Ercole, F.; Whittaker, M. R.; Boyd, B. J.; Davis, T. P.; Quinn, J. F., Recent advances in the delivery of hydrogen sulfide via a macromolecular approach. *Polym. Chem.* **2018,** *9*, 4431-4439.

24. Lee, M.; McGeer, E.; Kodela, R.; Kashfi, K.; McGeer, P. L., NOSH-Aspirin (NBS-1120), a Novel Nitric Oxide and Hydrogen Sulfide Releasing Hybrid, Attenuates Neuroinflammation Induced by Microglial and Astrocytic Activation: A New Candidate for Treatment of Neurodegenerative Disorders. *Glia* **2013,** *61*, 1724-1734.

25. Hasegawa, U.; Tateishi, N.; Uyama, H.; van der Vlies, A. J., Hydrolysis-Sensitive Dithiolethione Prodrug Micelles. *Macromol. Biosci.* **2015,** *15*, 1512-22.

26. Powell, C. R.; Foster, J. C.; Okyere, B.; Theus, M. H.; Matson, J. B., Therapeutic Delivery of H_2S via COS: Small Molecule and Polymeric Donors With Benign Byproducts. *J. Am. Chem. Soc.* **2016,** *138*, 13477-13480.

27. Fairbanks, B. D.; Schwartz, M. P.; Halevi, A. E.; Nuttelman, C. R.; Bowman, C. N.; Anseth, K. S., A Versatile Synthetic Extracellular Matrix Mimic via Thiol-Norbornene Photopolymerization. *Adv. Mater.* **2009,** *21*, 5005-5010.

28. Qin, L.-H.; Hu, W.; Long, Y.-Q., Bioorthogonal Chemistry: Optimization and Application Updates During 2013-2017. *Tetrahedron Lett.* **2018**.

29. Dragutan, I.; Dragutan, V.; Demonceau, A., Targeted Drugs by Olefin Metathesis: Piperidine-Based Iminosugars. *RSC Advances* **2012,** *2*, 719-736.

30. Sinclair, F.; Alkattan, M.; Prunet, J.; Shaver, M. P., Olefin Cross Metathesis and Ring-Closing Metathesis in Polymer Chemistry. *Polym. Chem.* **2017,** *8*, 3385-3398.

31. Chatterjee, A. K.; Choi, T.-L.; Sanders, D. P.; Grubbs, R. H., A General Model for Selectivity in Olefin Cross Metathesis. *J. Am. Chem. Soc.* **2003,** *125*, 11360-11370.

32. Forman, G. S.; Tooze, R. P., Improved Cross-Metathesis of Acrylate Esters Catalyzed by 2nd Generation Ruthenium Carbene Complexes. *J. Organomet. Chem.* **2005,** *690*, 5863-5866.

33. Willcock, H.; O'Reilly, R. K., End Group Removal and Modification of RAFT Polymers. *Polym. Chem.* **2010,** *1*, 149-157.

34. Shen, W.; Qiu, Q.; Wang, Y.; Miao, M.; Li, B.; Zhang, T.; Cao, A.; An, Z., Hydrazine as a Nucleophile and Antioxidant for Fast Aminolysis of RAFT Polymers in Air. *Macromol. Rapid Commun.* **2010,** *31*, 1444-1448.

35. Oettl, K.; Stauber, R. E., Physiological and Pathological Changes in the Redox State of Human Serum Albumin Critically Influence its Binding Properties. *Br. J. Pharmacol.* **2007,** *151*, 580-590.

36. Lin, C.-C.; Ki, C. S.; Shih, H., Thiol-Norbornene Photo-Click Hydrogels for Tissue Engineering Applications. *J. Appl. Polym. Sci.* **2015,** *132*, 41563.

37. Chen, Y.; Hagerman, A. E., Characterization of Soluble Non-Covalent Complexes Between Bovine Serum Albumin and β-1,2,3,4,6-Penta-O-galloyl-d-glucopyranose by MALDI-TOF MS. *J. Agric. Food Chem.* **2004,** *52,* 4008-4011.

38. Zhao, Y.; Pluth, M. D., Hydrogen Sulfide Donors Activated by Reactive Oxygen Species. *Angew. Chem. Int. Ed.* **2016,** *55,* 14638-14642.

39. Steiger, A. K.; Marcatti, M.; Szabo, C.; Szczesny, B.; Pluth, M. D., Inhibition of Mitochondrial Bioenergetics by Esterase-Triggered COS/H_2S Donors. *ACS Chem. Biol.* **2017,** *12,* 2117-2123.

3.8. Experimental

Materials and Methods

All reagents and solvents were obtained from commercial vendors and used as received unless otherwise stated. NMR spectra were measured on Agilent 400 MHz or Bruker 500 MHz spectrometers. ^{1}H and ^{13}C NMR chemical shifts are reported in ppm relative to internal solvent resonances. Yields refer to compounds as isolated by silica gel chromatography unless otherwise stated. Thin-layer chromatography (TLC) was performed on glass-backed silica plates and visualized by UV. XAA,[1] THP-protected propargyl alcohol,[2] 2-azidoethanol,[3] *rac*-norbornyl alcohol,[4] PEG-N_3,[5] Fmoc-Lys-N_3,[6] and PACMO–SH[7] were synthesized according to literature procedures. For pH studies on H_2S release, buffers were prepared at 10 mM for the following pH ranges: acetate buffer (pH 5.3-6.0), phosphate buffer (pH 6.2-8.1), and carbonate buffer (pH 8.2-8.8). pH was measured by a Fisher Scientific accumet AE150 benchtop pH meter. High-resolution mass spectra were obtained via an Agilent Technologies 6230 TOF LC/MS mass spectrometer. Protein-NTA conjugate analysis was performed using a matrix-assisted laser desorption

ionization−tandem time of flight mass spectrometer (4800 MALDI TOF/TOF; AB Sciex). H_2S release data acquired with a WPI ISO-H2S-100 electrochemical probe set to a constant 100 nA current.

Cell studies were conducted on an adherent H9C2 line of rat embryonic cardiomyocytes (ATCC, Manassas, VA, USA). Cultures were grown in Dulbecco's Modified Eagle Medium (DMEM, VWR, Radnor, PA), supplemented with 10 % fetal bovine serum (FBS, VWR, Radnor, PA). Cells were cultured at 37 °C in 5 % CO_2-air. The cultures were passaged after 70–80 % confluence was achieved. Cells were rinsed with PBS solution, and then released with trypsin and EDTA solution (VWR, Radnor, PA). The suspension of released cells was centrifuged at 1000 rpm for 5 min.

Synthesis of functional N-substituted NTAs

*Synthesis of compound **TCDA***

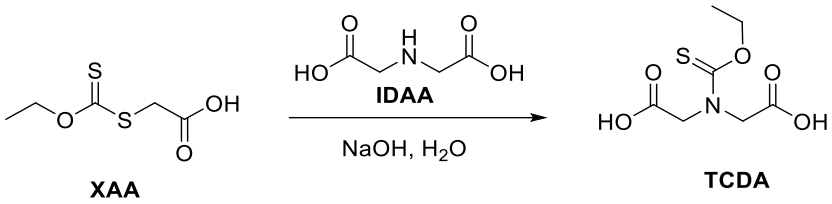

A round bottom flask was charged with **XAA** (6.60 g, 36.6 mmol), **IDAA** (4.87 g, 36.6 mmol), and a magnetic stir bar. An Erlenmeyer flask was charged with NaOH (4.39 g, 110 mmol), and the NaOH was dissolved in water (120 mL). The aqueous NaOH solution was then added slowly, in one portion, to the flask containing **XAA** and **IDAA** while stirring at rt to give a clear, pale yellow solution. The reaction mixture was stirred at rt for 40 h, at which point full consumption of **XAA** was observed by TLC (10 % MeOH in CH_2Cl_2 + 2 % v/v acetic acid). The reaction mixture was

acidified with concentrated HCl until the pH reached ~2 as measured by pH paper (Hydrion). The resulting aqueous solution was extracted with EtOAc (30 mL, 3x). The organic layers were combined, dried over Na_2SO_4, filtered, and concentrated to give a yellow oil. The oil was dissolved in Et_2O (30 mL) and cooled to 0 °C in an ice bath. Hexanes (100 mL) was added, resulting in a white precipitate. The white powder was filtered, triturated with CH_2Cl_2 (50 mL), and filtered again to give thiocarbamate diacetic acid **TCDA** (6.152 g, 27.81 mmol) (m.p. = 131.2-132.7 °C). ^{1}H NMR (DMSO-d_6): δ 12.85 (broad s, 1H), 4.49 (s, 2H), 4.37 (q, J = 7 Hz, 2H), 4.23 (s, 2H), 1.22 (t, J = 7 Hz, 3H). ^{13}C NMR (DMSO-d_6): δ 189.1, 169.7, 1z69.6, 67.6, 54.7, 50.7, 14.0.

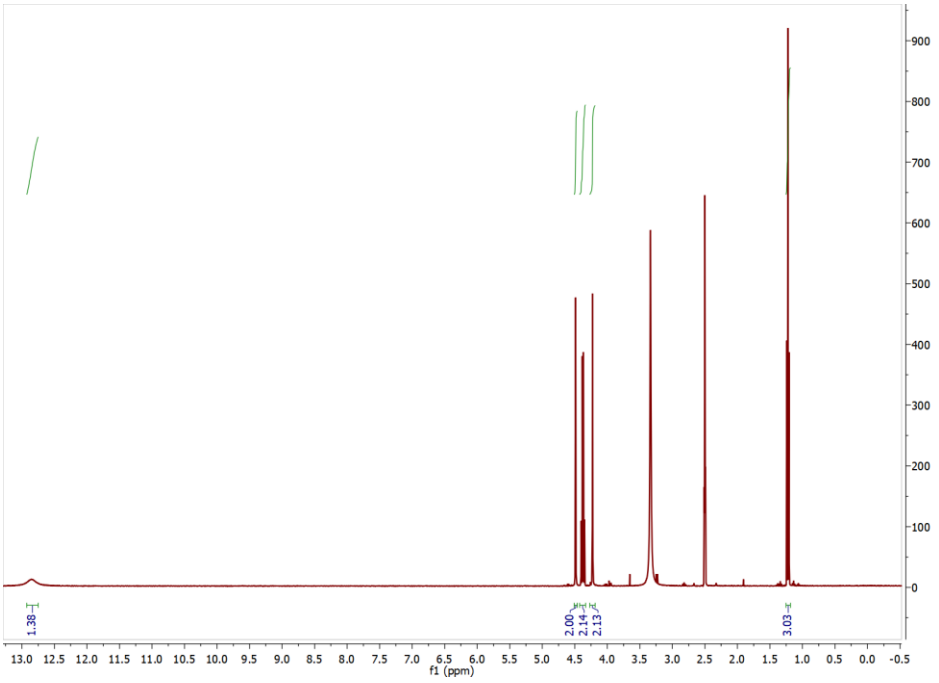

Figure S1. ^{1}H NMR spectrum (DMSO-d_6) of **1**.

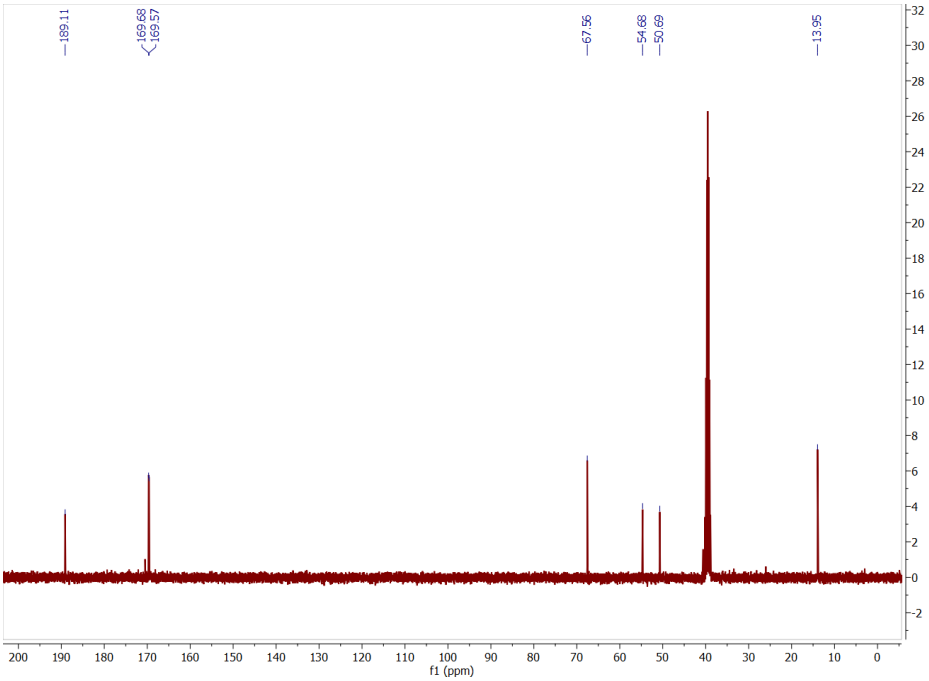

Figure S2. ^{13}C NMR (DMSO-d_6) spectrum of **1**.

*Representative synthetic procedure for NTA precursors **1i-1v***

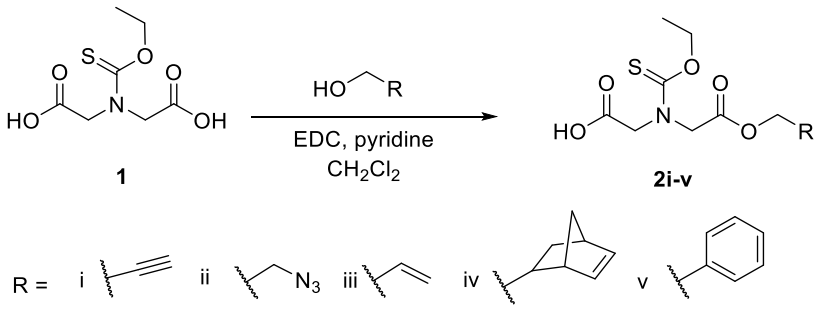

A round bottom flask was charged with iminodiacetic acid thiocarbamate **TCDA** (2.188 g, 9.890 mmol) and a magnetic stir bar. To this flask, CH_2Cl_2 (80 mL) was added to give a suspension of **TCDA**. Pyridine (0.80 mL, 9.9 mmol) was added in one portion, generating a soluble pyridinium salt of **TCDA** as a clear solution. This solution was cooled to 0 °C in an ice bath. A separate round

bottom flask was charged with EDC·HCl (1.896 g, 9.890 mmol) and CH_2Cl_2 (25 mL) to give a suspension of EDC. Allyl alcohol (2.0 mL, 30 mmol) was added to the EDC suspension in one portion, which resulted in a clear, yellow solution. The EDC/alcohol solution was added dropwise to the solution of pyridinium·**TCDA** via addition funnel at 0 °C. The reaction mixture was allowed to warm to rt as the ice melted. Disappearance of starting material **1** was monitored by TLC (5 % MeOH in CH_2Cl_2). After 16 h, complete disappearance of **TCDA** was observed, and the reaction mixture was washed with 1 N HCl (2x) and brine (1x), dried over Na_2SO_4, filtered and concentrated. The resulting yellow oil was purified by silica gel chromatography (CH_2Cl_2) to give the thiocarbamate acid-ester **1iii** (2.147 g, 8.217 mmol). Yields for additional thiocarbamate acid-esters are as follows: **1i** (76 %, pale yellow oil), **1ii** (73 %, yellow oil), **1iv** (81 %, pale yellow oil), **1v** (26 %, pale yellow oil).

1i: ^{1}H NMR ($CDCl_3$): δ 4.79 (dd, *J* = 20, 3 Hz, 2H), 4.70 (d, *J* = 3 Hz, 2H), 4.52 (m, 2H), 4.32 (d, *J* = 8 Hz, 2H), 2.52 (m, 1H), 1.34 (td, *J* = 7, 5 Hz, 3H). ^{13}C NMR ($CDCl_3$): δ 190.4, 173.8, 172.8, 169.0, 167.8, 76.8, 75.9, 75.8, 69.2, 69.1, 55.0, 54.8, 53.3, 53.1, 51.1, 50.6, 14.1.

1ii: ^{1}H NMR ($CDCl_3$): δ 4.69 (d, *J* = 5 Hz, 2H), 4.52 (m, 2H), 4.43-4.28 (m, 4H), 3.60-3.46 (m, 2H), 1.40-1.27 (m, 3H). ^{13}C NMR ($CDCl_3$): δ 190.4, 173.5, 172.4, 169.7, 168.4, 69.3, 69.1, 64.6, 64.3, 55.3, 55.0, 51.6, 50.7, 49.7, 14.2, 14.1.

1iii: ^{1}H NMR ($CDCl_3$): δ 6.03-5.78 (m, 1H), 5.45-5.22 (m, 2H), 4.80-4.60 (m, 4H), 4.59-4.42 (m, 2H), 4.30 (d, *J*= 7Hz, 2H), 1.33 (dt, *J*= 11, 7 Hz, 3H). ^{13}C NMR ($CDCl_3$): δ 190.4, 177.5, 173.5, 170.2, 168.4, 131.3, 131.2, 119.6, 119.5, 69.2, 69.0, 66.9, 66.5, 55.5, 55.1, 52.0, 50.9, 14.2, 14.1.

1iv: ^{1}H NMR ($CDCl_3$): δ 10.22 (broad s, 1H), 6.49-5.53 (m, 2H), 4.72-4.59 (m, 2H), 4.54-4.44 (m, 2H), 4.33-4.19 (m, 2H), 4.07 (m, 1H), 3.01-2.55 (m, 2H), 1.90-1.66 (m, 1H), 1.40-1.11 (m, 5H). ^{13}C NMR ($CDCl_3$): δ 190.3, 173.4, 172.1, 170.4, 168.8, 138.0, 137.8, 137.2, 137.1, 136.2,

136.0, 132.2, 131.9, 70.3, 69.9, 69.7, 69.3, 69.1, 68.8, 55.5, 55.1, 51.9, 51.8, 51.0, 49.6, 49.5, 45.0, 43.9, 43.7, 43.6, 42.3, 41.7, 41.6, 38.0, 37.9, 37.7, 14.1.

1v: ^{1}H NMR ($CDCl_3$): δ 7.42-7.30 (m, 5H), 5.21 (d, *J* = 12 Hz, 2H), 4.70-4.63 (m, 2H), 4.46 (dq, *J* = 33 Hz, 7 Hz, 2H), 4.28 (d, *J* = 4 Hz, 2H), 1.26 (dt, *J*= 48, 7 Hz, 3H). ^{13}C NMR ($CDCl_3$): δ 190.4, 190.3, 172.6, 171.8, 169.9, 168.6, 140.4, 135.0, 134.9, 128.8, 128.7, 128.6, 128.5, 127.8, 127.2, 69.0, 68.9, 67.8, 67.5, 65.2, 55.3, 55.0, 51.4, 51.0, 14.0.

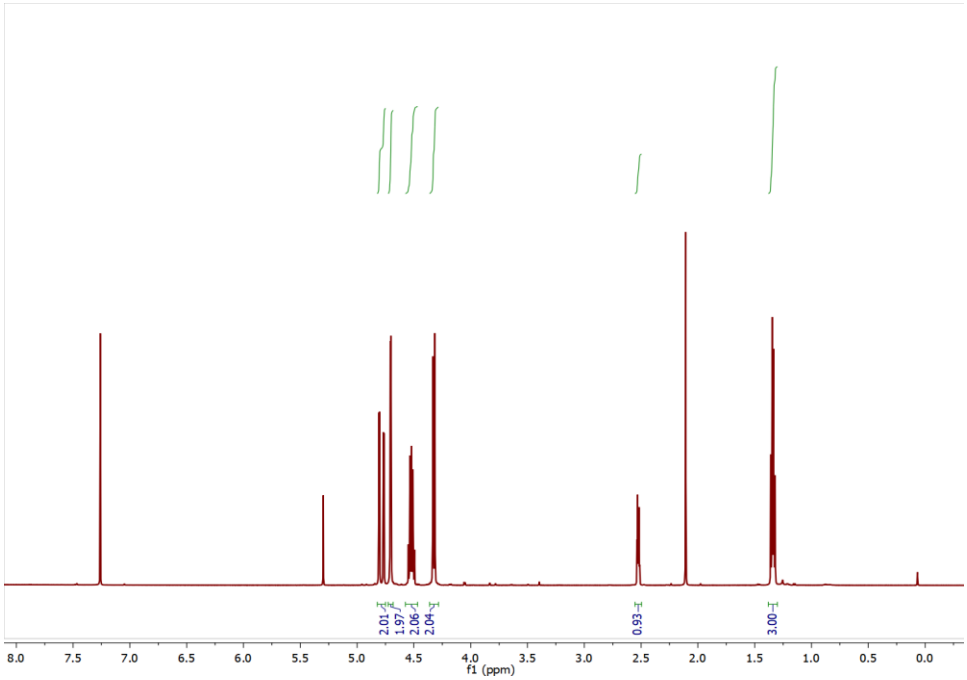

Figure S3. ^{1}H NMR spectrum ($CDCl_3$) of **1i**.

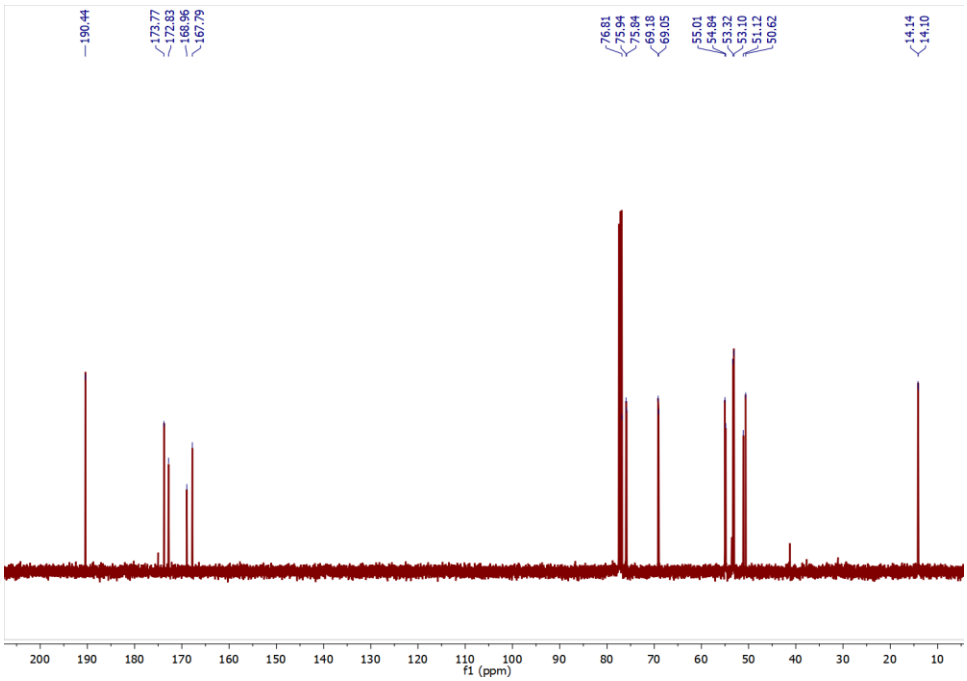

Figure S4. ^{13}C NMR spectrum ($CDCl_3$) of **1i**.

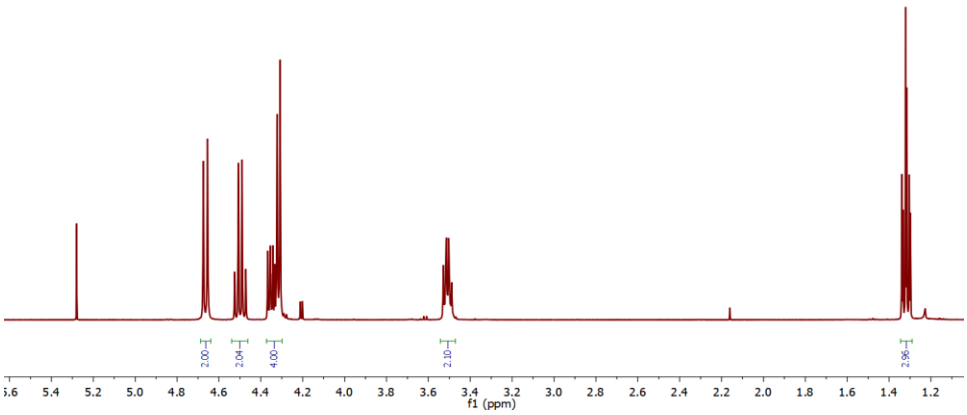

Figure S5. ^{1}H NMR spectrum ($CDCl_3$) of **1ii**.

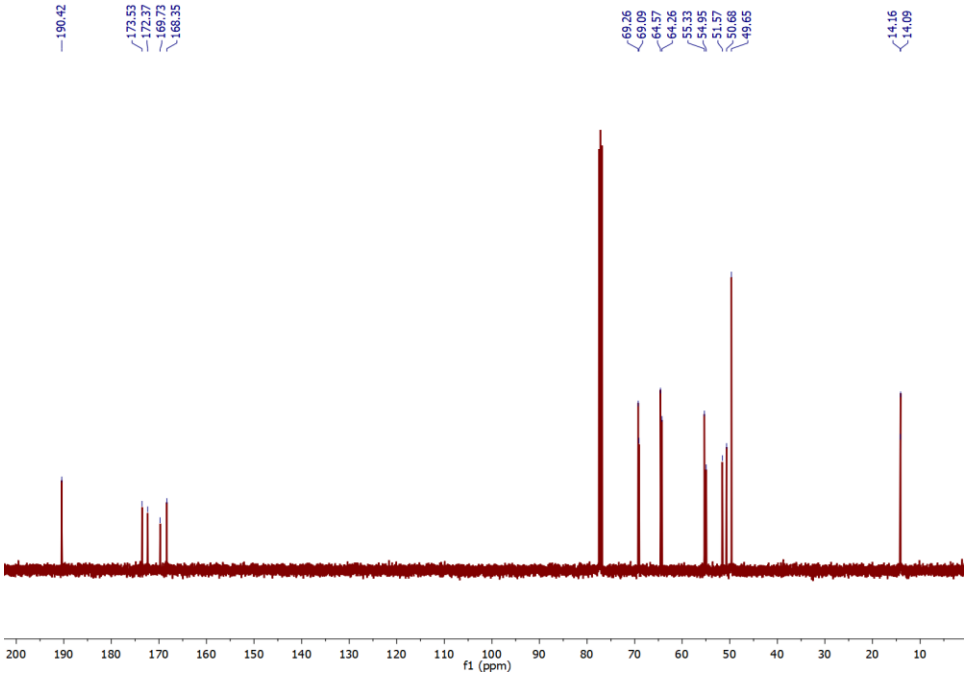

Figure S6. ^{13}C NMR spectrum ($CDCl_3$) of **1ii**.

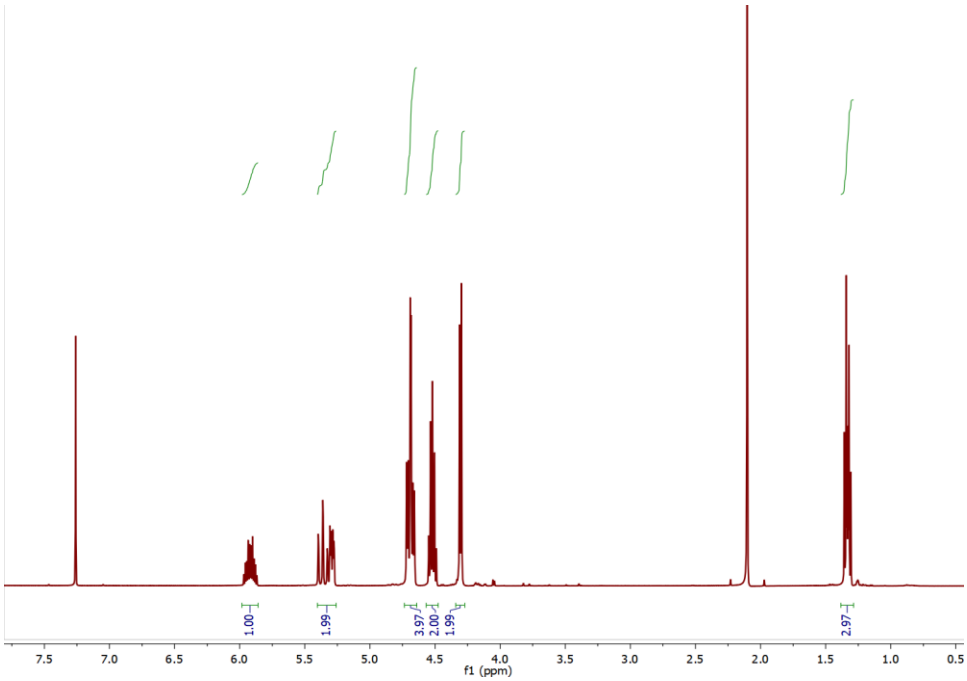

Figure S7. ^{1}H NMR spectrum ($CDCl_3$) of **1iii**.

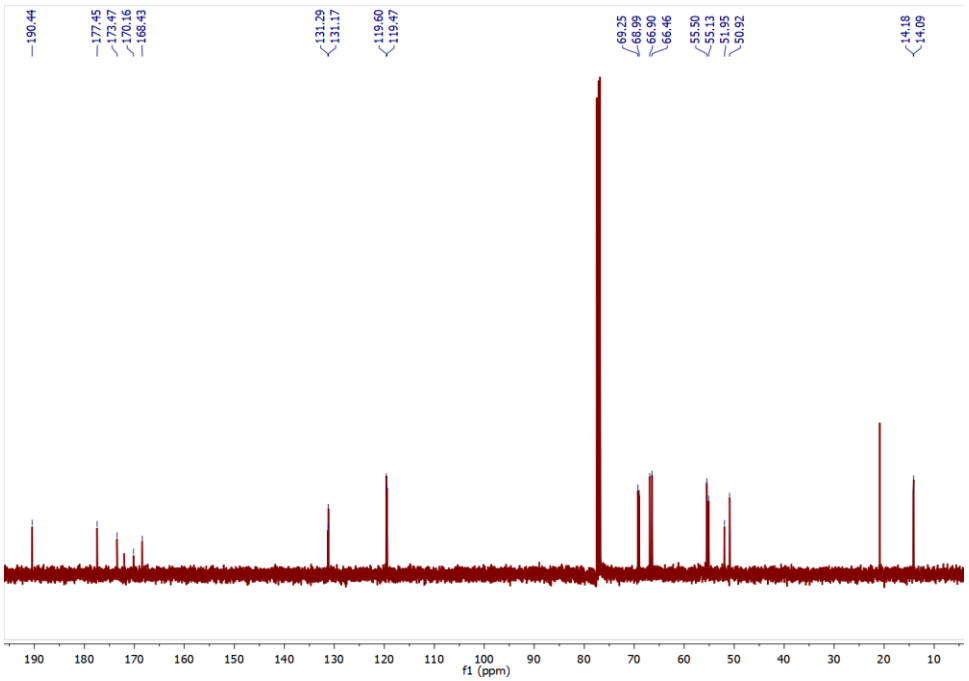

Figure S8. ^{13}C NMR spectrum ($CDCl_3$) of **1iii**.

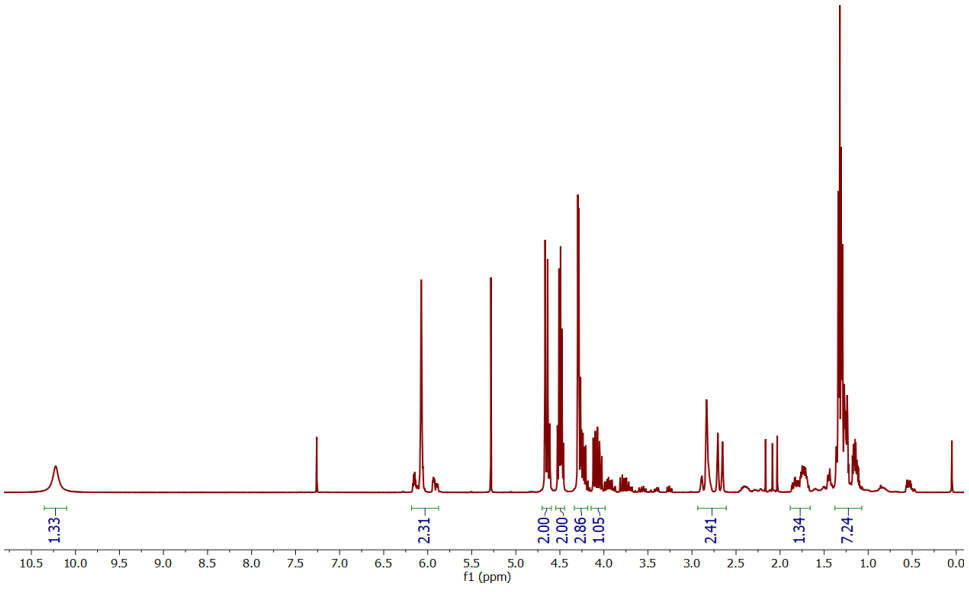

Figure S9. ^{1}H NMR spectrum ($CDCl_3$) of **1iv**.

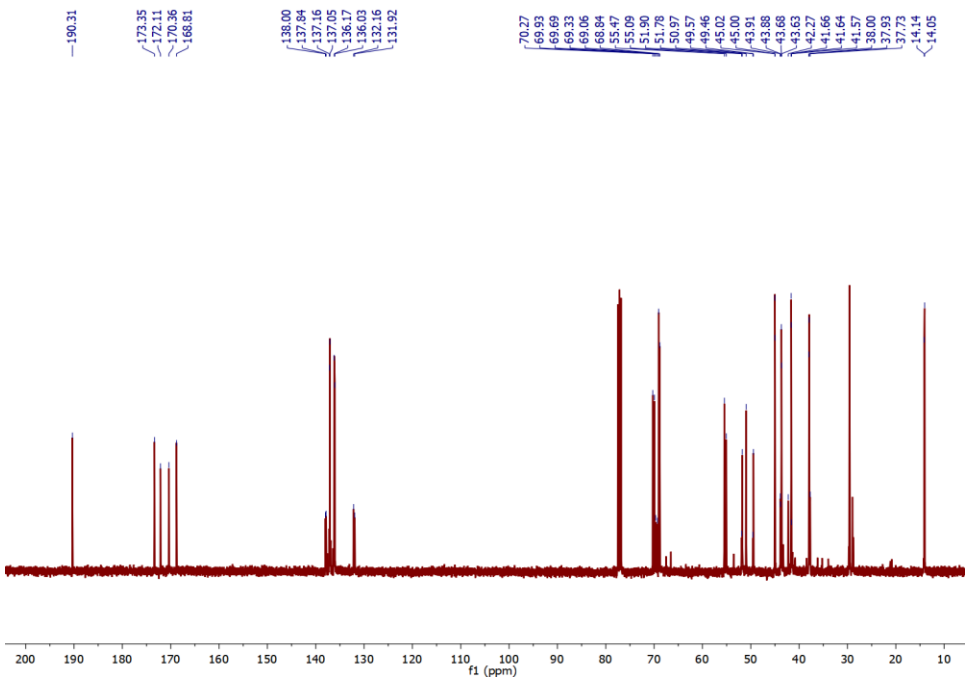

Figure S10. ^{13}C NMR spectrum ($CDCl_3$) of **1iv**.

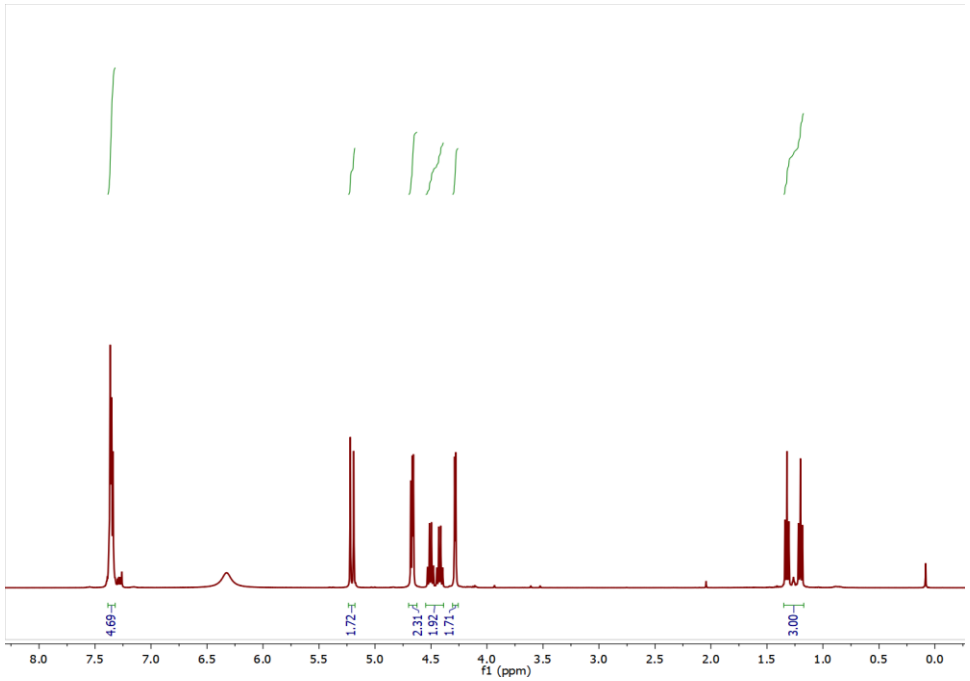

Figure S11. ^{1}H NMR spectrum ($CDCl_3$) of **1v**.

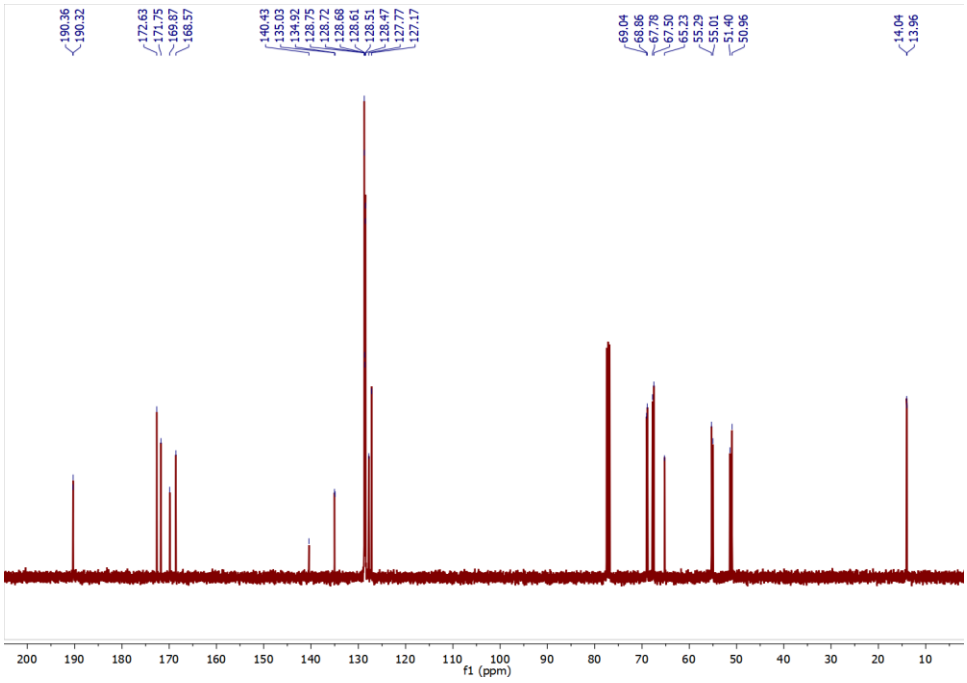

Figure S12. ^{13}C NMR spectrum ($CDCl_3$) of **1v**.

*Representative synthetic procedure for functional N-substituted **NTA** synthesis*

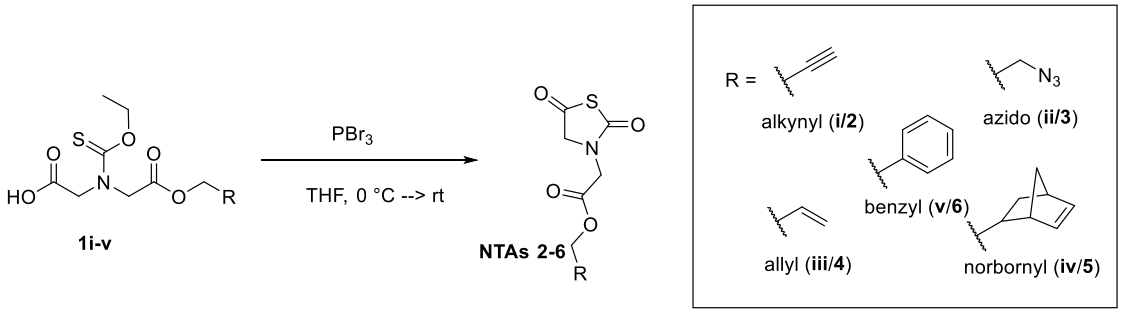

A two-neck round bottom flask equipped with a glass vacuum adaptor and septum was charged with a magnetic stir bar. The reaction vessel was flame-dried under vacuum and backfilled with nitrogen. Dry THF (2mL) (passed through an alumina column and dried over 3 Å molecular sieves) was added to a vial containing thiocarbamate monoester **1iii** (0.372 g, 1.42 mmol). Once fully dissolved, this solution was added to the reaction vessel. The reaction mixture was then diluted

with dry THF (3 mL) to the final reaction volume (5 mL). The clear yellow reaction mixture was placed in an ice bath to cool to 0 °C. Phosphorous tribromide (PBr_3) (0.150 mL, 1.57 mmol) was added dropwise under nitrogen, and the reaction mixture was allowed to stir at 0 °C for 10 min, at which point the ice bath was removed and the reaction mixture was allowed to warm to rt. Once at rt, the reaction mixture was allowed to stir for an additional 45 min. The reaction mixture was again cooled to 0 °C in an ice bath, and MeOH was added dropwise until bubbling ceased to quench excess PBr_3. The reaction mixture was concentrated on a rotary evaporator, and the residue was dissolved in CH_2Cl_2. The CH_2Cl_2 solution was washed with saturated $NaHCO_3$ (2x) and brine (1x), dried over Na_2SO_4, filtered, and concentrated. The crude oil was then purified via silica gel chromatography (CH_2Cl_2) to give **NTA3** as an off-white solid (0.215 g, 0.999 mmol). Yields for specific NTAs are as follows: **NTA2** (63 %, off-white solid) (m.p. = 46.3-46.8 °C), **NTA3** (77 %, clear oil), **NTA4** (70 %, off-white solid) (m.p. = 38.5 – 39.0 °C), **NTA5** (50 %, yellow oil), **NTA6** (59 %, off-white solid) (m.p. = 93.4 – 94.1 °C).

NTA2: ^{1}H NMR ($CDCl_3$): δ 4.77 (d, *J* = 3 Hz, 2H), 4.32 (d, *J* = 5 Hz, 2H), 2.52 (t, *J* = 3 Hz, 1H). ^{13}C NMR ($CDCl_3$): δ 192.9, 166.9, 166.4, 76.6, 76.2, 60.1, 53.4, 44.4.

NTA3: ^{1}H NMR ($CDCl_3$): δ 4.38-4.33 (m, 6H), 3.56-3.52 (m, 2H). ^{13}C NMR ($CDCl_3$): δ 192.9, 167.3, 166.4, 64.5, 60.2, 49.6, 44.5.

NTA4: ^{1}H NMR ($CDCl_3$): δ 5.98-5.84 (m, 1H), 5.39-5.27 (m, 2H), 4.68 (dt, *J* = 6, 1 Hz, 2H), 4.32 (d, *J*= 7 Hz, 4H). ^{13}C NMR ($CDCl_3$): δ 193.1, 167.1, 166.2, 131.1, 119.6, 66.6, 60.1, 44.4.

NTA5: ^{1}H NMR ($CDCl_3$): δ 6.21-5.90 (m, 2H), 4.38-4.21 (m, 5H), 4.09 (dd, *J* = 11, 9 Hz, 1H), 3.99-3.74 (m, 1H), 2.89-2.81 (m, 1H), 2.68 (h, *J* = 2 Hz, 1H), 1.89-1.68 (m, 1H), 1.41-1.35 (m, 1H), 1.33-1.25 (m, 2H), 1.20-1.13 (m, 1H). ^{13}C NMR ($CDCl_3$): δ 193.2, 167.5, 167.4, 166.4, 138.1, 137.2, 136.1, 132.0, 70.2, 69.6, 60.3, 45.1, 44.6, 44.0, 43.7, 42.3, 41.7, 38.0, 37.8.

NTA6: ^{1}H NMR ($CDCl_3$): δ 7.48-7.30 (m, 5H), 5.21 (s, 2H), 4.31 (d, *J* = 3 Hz, 4H). ^{13}C NMR ($CDCl_3$): δ 193.1, 167.4, 166.4, 134.8, 129.0, 128.9, 128.7, 67.9, 60.2, 44.6.

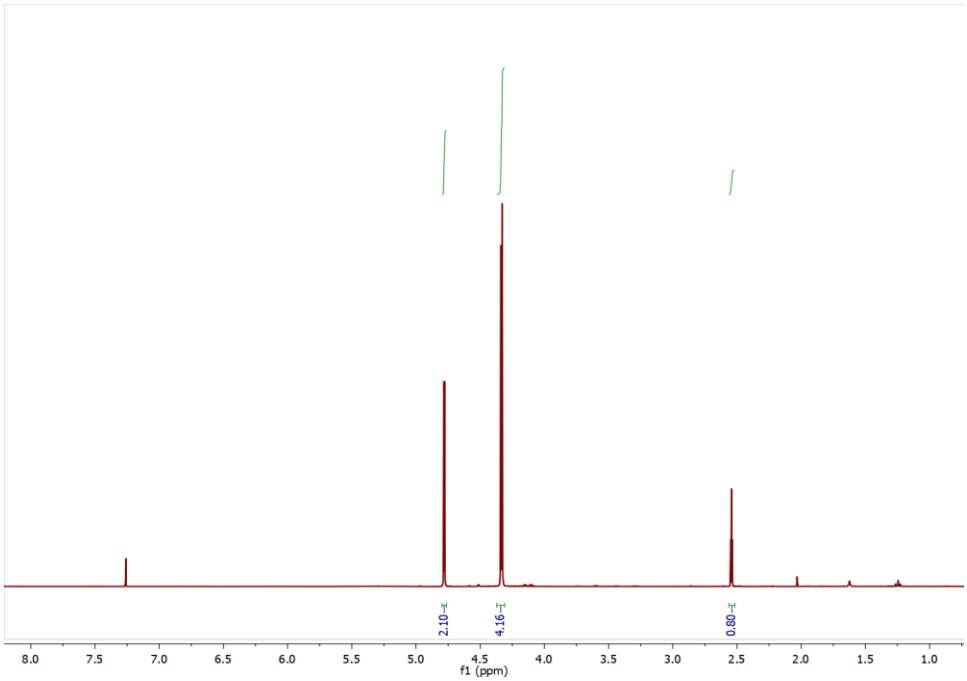

Figure S13. ^{1}H NMR spectrum ($CDCl_3$) of alkynyl NTA, **NTA2**.

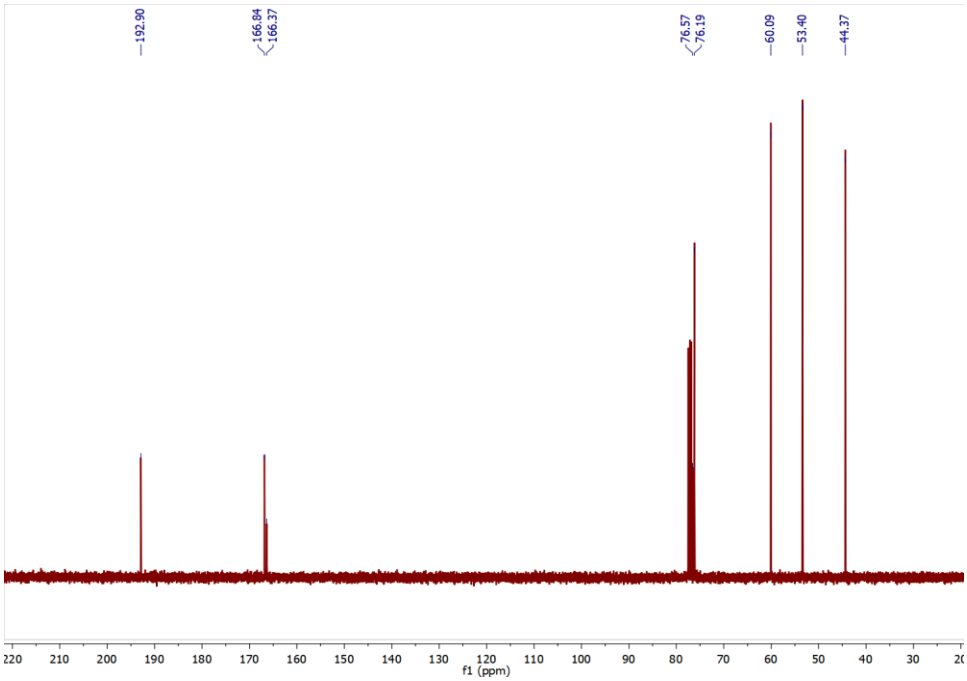

Figure S14. ^{13}C NMR spectrum ($CDCl_3$) of alkynyl NTA, **NTA2**.

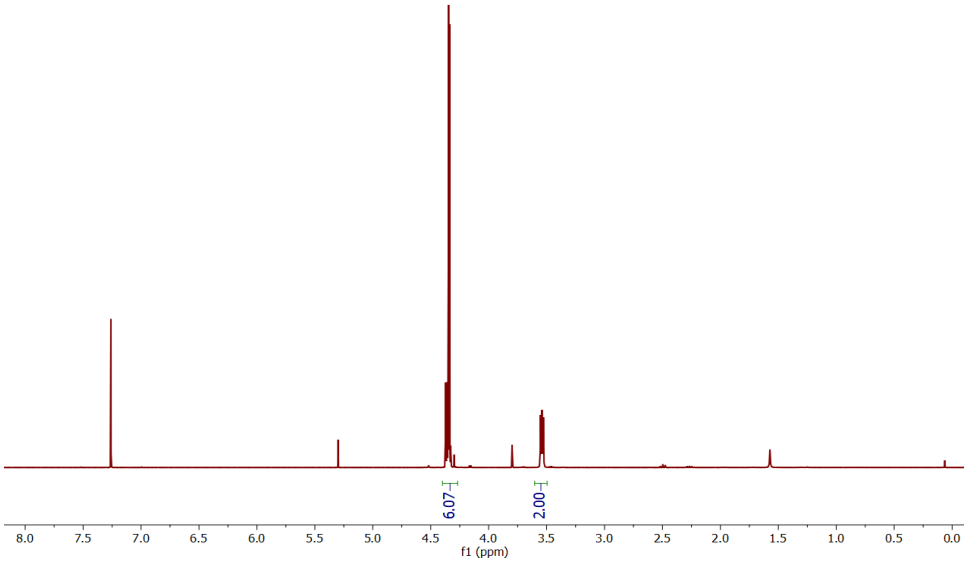

Figure S15. ^{1}H NMR spectrum ($CDCl_3$) of azido NTA, **NTA3**.

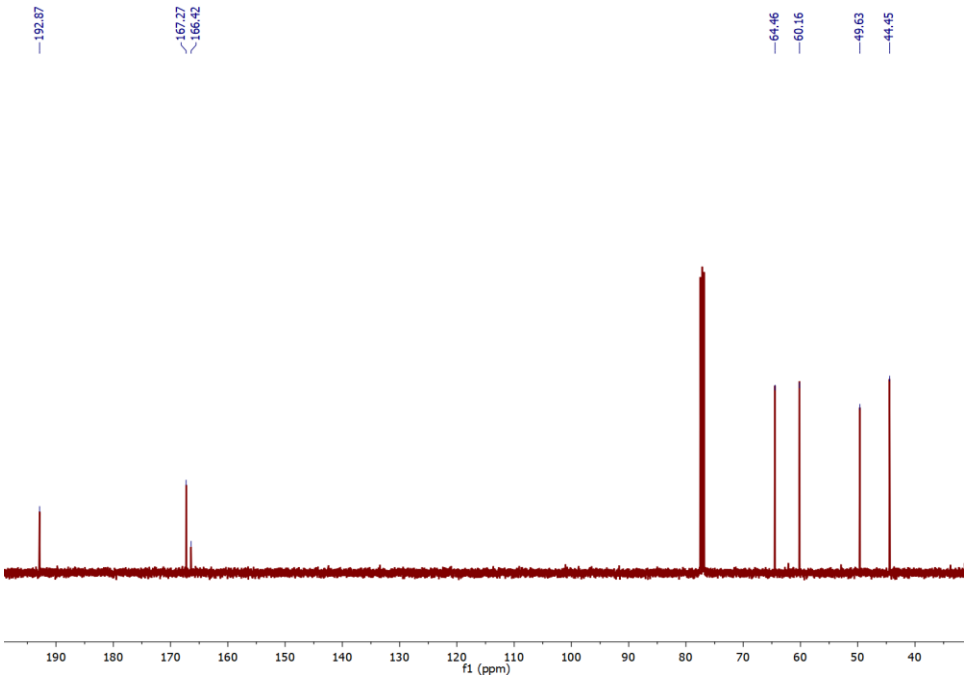

Figure S16. ^{13}C NMR spectrum ($CDCl_3$) of azido NTA, **NTA3**.

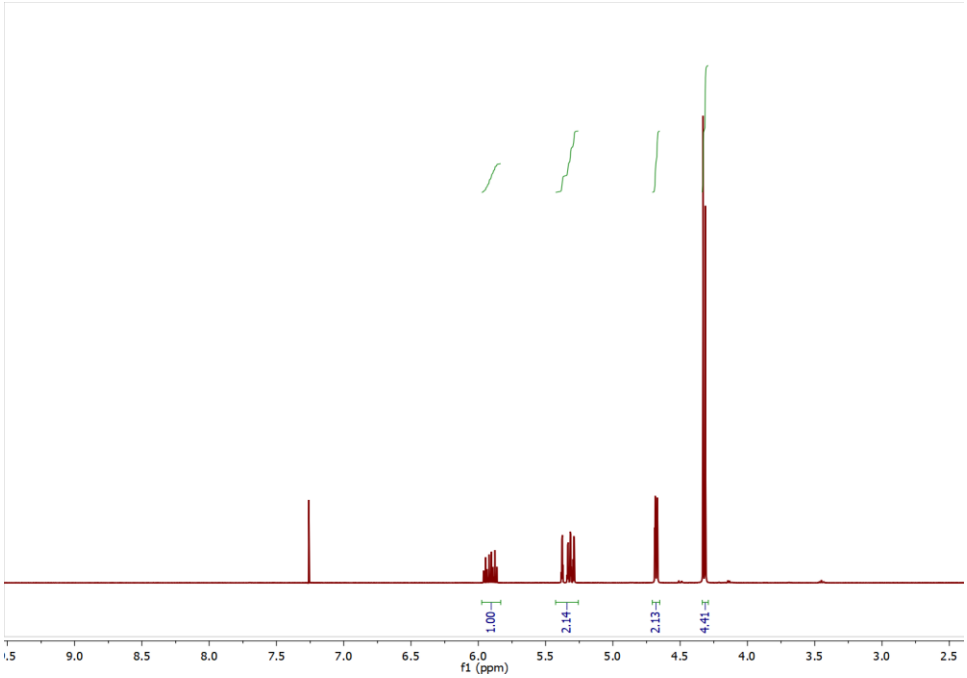

Figure S17. ^{1}H NMR spectrum ($CDCl_3$) of allyl NTA **NTA4**.

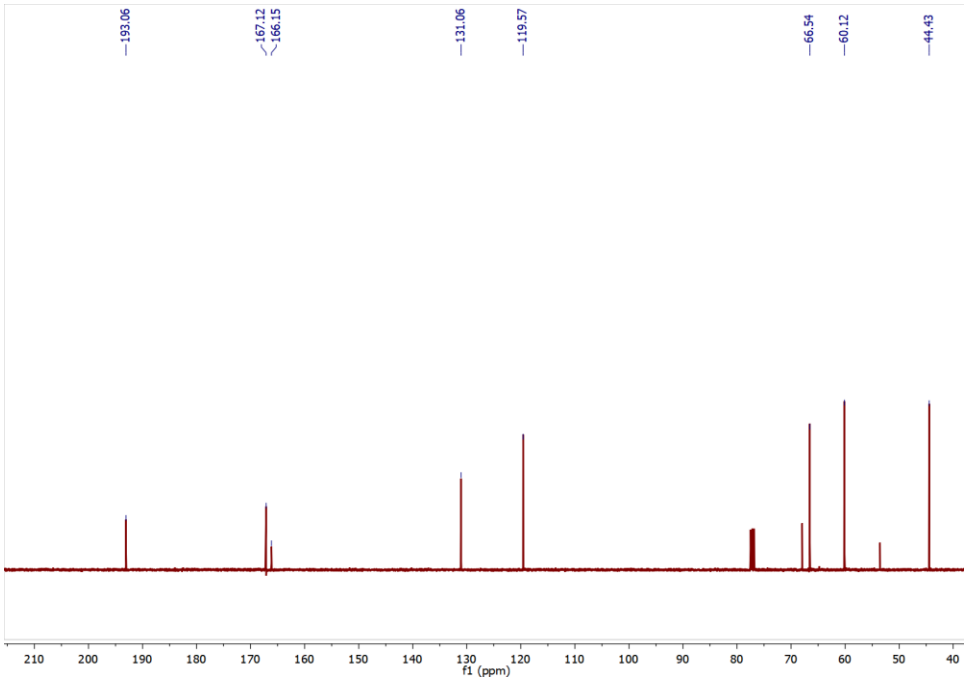

Figure S18. ^{13}C NMR spectrum ($CDCl_3$) of allyl NTA, **NTA4**.

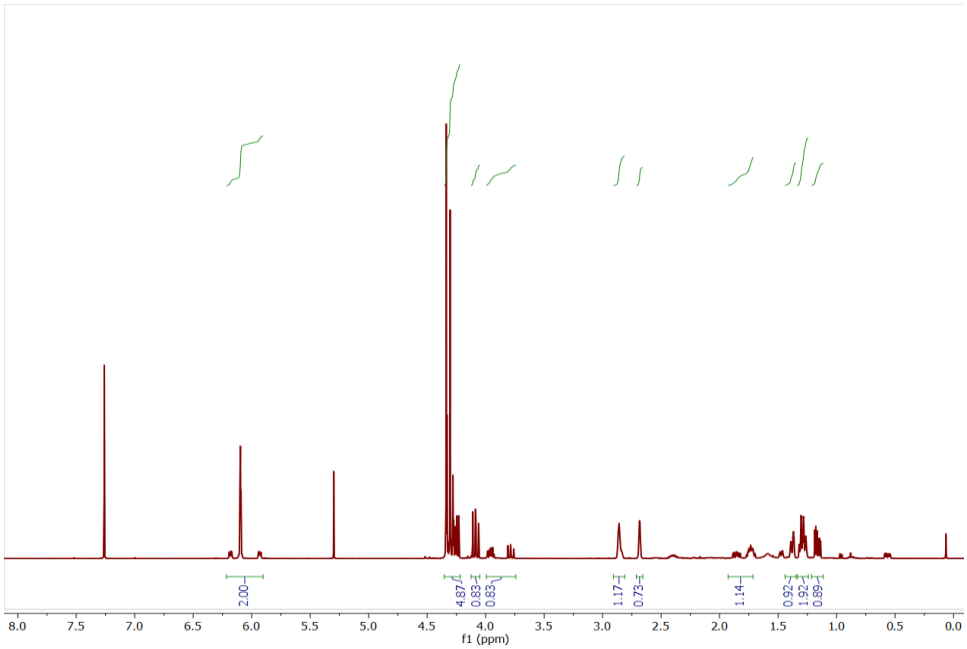

Figure S19. ^{1}H NMR spectrum ($CDCl_3$) of norbornyl NTA, **NTA5**.

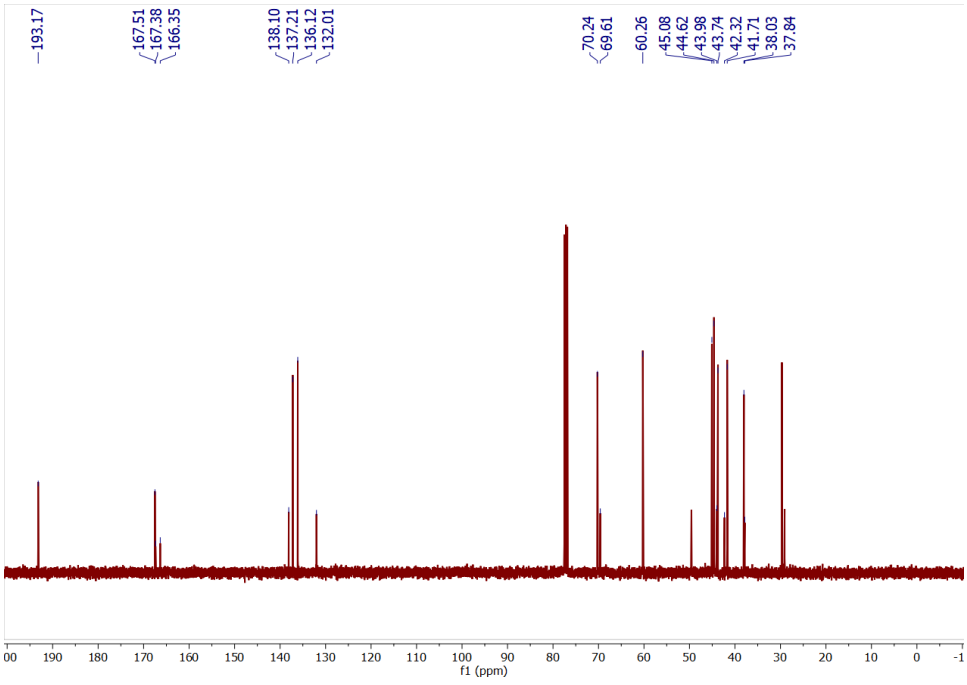

Figure S20. ^{13}C NMR spectrum ($CDCl_3$) of norbornyl NTA, **NTA5**.

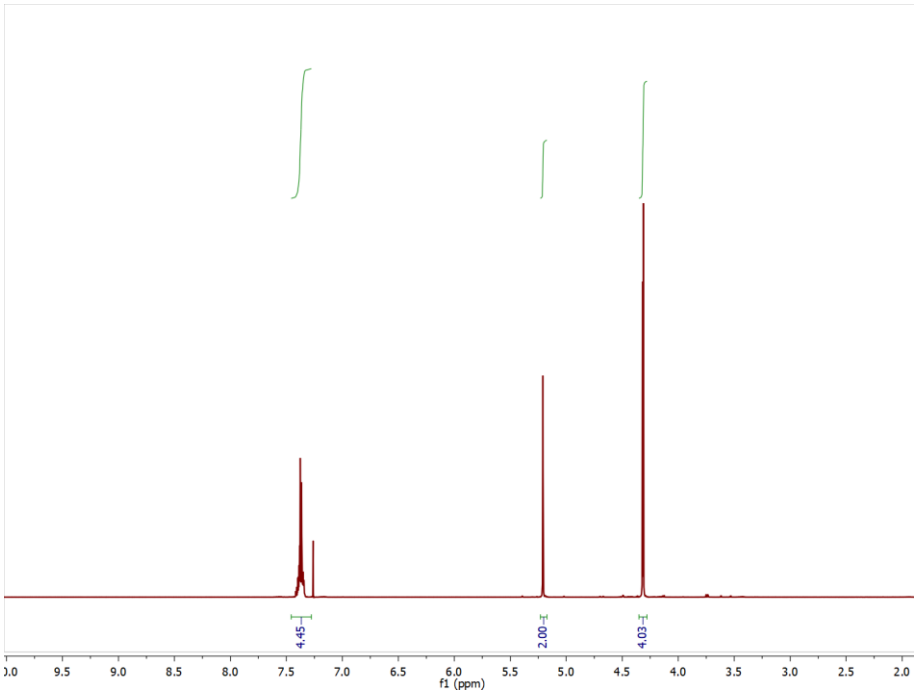

Figure S21. ^{1}H NMR spectrum ($CDCl_3$) of benzyl NTA, **NTA6**.

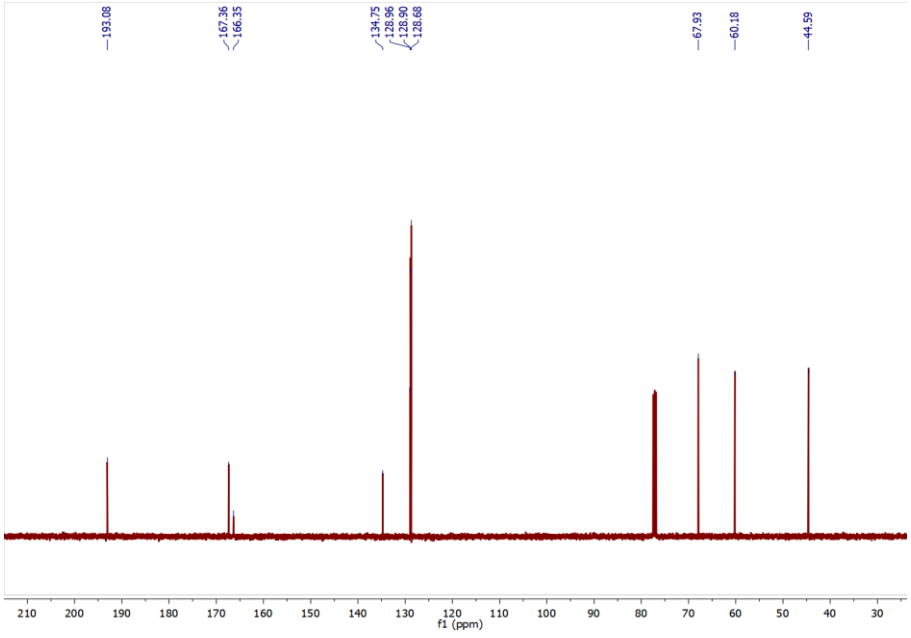

Figure S22. ^{13}C NMR spectrum ($CDCl_3$) of benzyl NTA, **NTA6**.

Functionalization of NTAs

Representative synthetic procedure for Huisgen [3+2] reactions between alkynyl/azido NTAs and small molecule organo-azides/alkynes

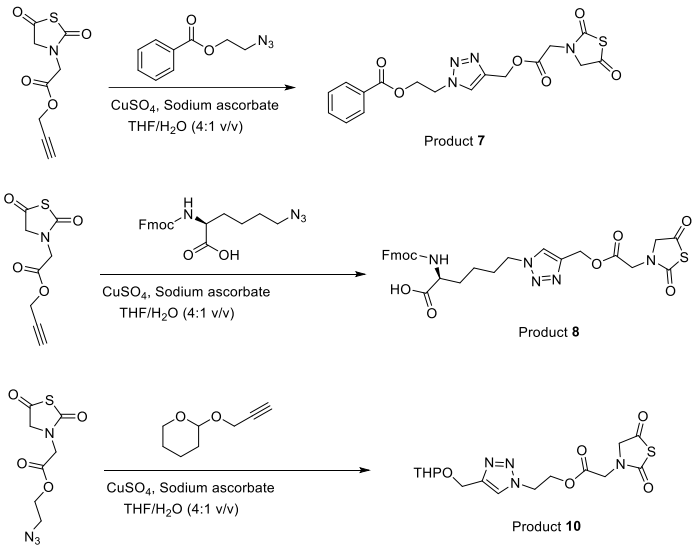

A scintillation vial was charged with alkynyl NTA (**NTA2**) (87 mg, 0.41 mmol) and 2-azidoethyl benzoate (78 mg, 0.41 mmol). The reactants were dissolved in THF (2 mL) to give a clear yellow solution. Copper sulfate pentahydrate ($CuSO_4 \cdot 5H_2O$) (41 mg, 0.16 mmol) was added in one portion. Sodium ascorbate (240 mg, 1.20 mmol) was added to a separate vial and dissolved in water (0.5 mL); this solution was subsequently added to the vial containing the NTA/azide mixture in one portion. Immediately, an insoluble brown precipitate formed. The vial was placed in a bath sonicator (Branson 2510) at rt, and the reaction mixture became a moderately turbid, yellow solution after approximately 10 min. Reaction progress was monitored by TLC (CH_2Cl_2) until the disappearance of **NTA2** was noted (30 min). The reaction mixture was concentrated by rotary evaporation to remove THF, and the residue was diluted with water. The aqueous solution was then extracted with CH_2Cl_2 (3x). The organic layers were combined, dried over Na_2SO_4, and concentrated. The crude product was purified by silica gel chromatography (CH_2Cl_2 and MeOH mixture, with acetic acid added (2 % v/v) to give a white powder (102 mg, 62 % yield) (m.p.

=127.8-130.4 °C). Product **8** (white powder, 42 %) (m.p. = 80.0 – 85.8 °C, possible degradation) and product **10** (clear oil, 35 %).

Product **7**: ^{1}H NMR ($CDCl_3$): δ 7.99-7.94 (m, 2H),7.75-7.72 (s, 1H), 7.61-7.55 (m, 1H), 7.48-7.42 (m, 2H), 5.31 (d, *J* = 1 Hz, 2H), 4.79-4.69 (m, 4H), 4.26 (d, *J* = 3 Hz, 4H). ^{13}C NMR ($CDCl_3$): δ 192.9, 167.4, 166.4, 166.0, 142.2, 133.8, 129.8, 129.2, 128.8, 124.8, 62.9, 60.2, 58.9, 49.6, 44.5. HRMS (ESI-TOF) calcd. for $C_{17}H_{16}N_4O_6S$ $[M+H]^+$ 405.0869, found 405.0866.

Product **8**: ^{1}H NMR ($CDCl_3$): δ 7.72 (d, *J* = 8 Hz, 2H), 7.62-7.45 (m, 3H), 7.40-7.18 (m, 4H), 5.71 (d, *J* = 8 Hz, 1H), 5.23 (s, 1H), 4.50-4.12 (m, 9H), 2.17-1.52 (m, 6H), 1.44-1.14 (m, 2H). ^{13}C NMR ($CDCl_3$): δ 193.2,176.4, 167.6, 166.6, 156.3, 143.9, 143.8, 141.7, 141.4, 127.2, 125.2, 124.4, 120.1, 67.1, 60.3, 58.5, 50.2, 47.2, 44.6, 31.5, 27.0, 22.0, 20.9. HRMS (ESI-TOF) calcd. for $C_{29}H_{30}N_5O_8S$ $[M+H]^+$ 608.1815, found 608.1827.

Product **10**: ^{1}H NMR ($CDCl_3$): δ 7.61 (s, 1H), 4.88 (dd, *J* = 12, 1 Hz, 1H), 4.67-4.59 (m, 6H), 4.27 (d, *J* = 4 Hz, 4H) 3.94-3.87 (m, 1H), 3.59-3.50 (m, 1H), 1.88-1.69 (m, 2H), 1.65-1.49 (m, 5H). ^{13}C NMR ($CDCl_3$): δ 192.7, 167.1, 166.5, 146.0, 123.3, 98.5, 63.6, 62.6, 60.7, 60.2, 48.9, 44.5, 30.6, 25.5, 19.6. HRMS (ESI-TOF): calcd. for $C_{15}H_{20}N_4O_6S$ $[M+H]^+$ 384.1104, found 384.1138.

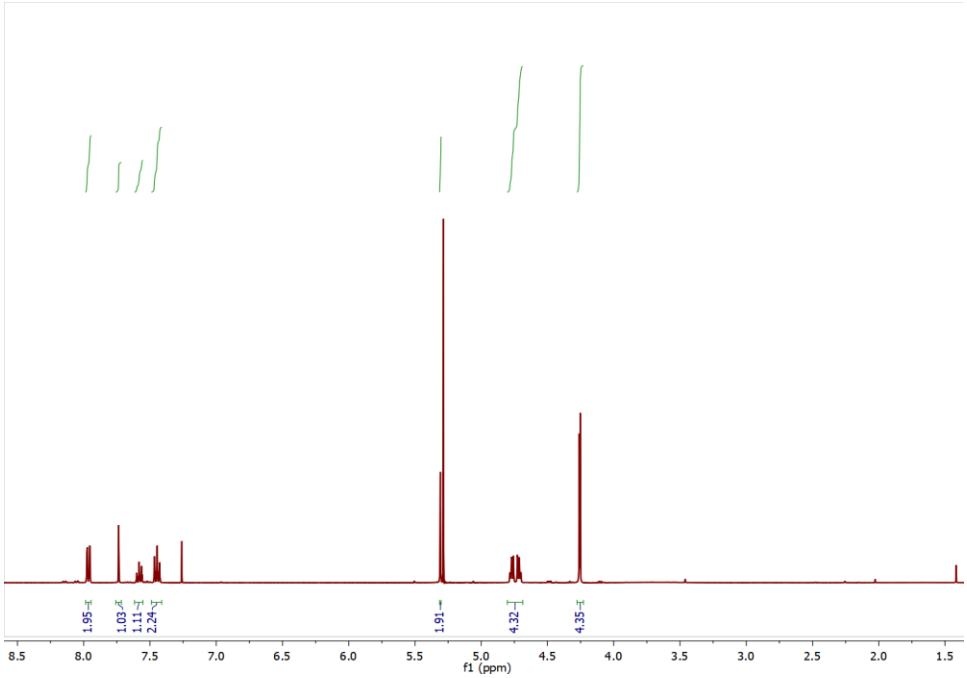

Figure S23. ^{1}H NMR spectrum ($CDCl_3$) of product **7**.

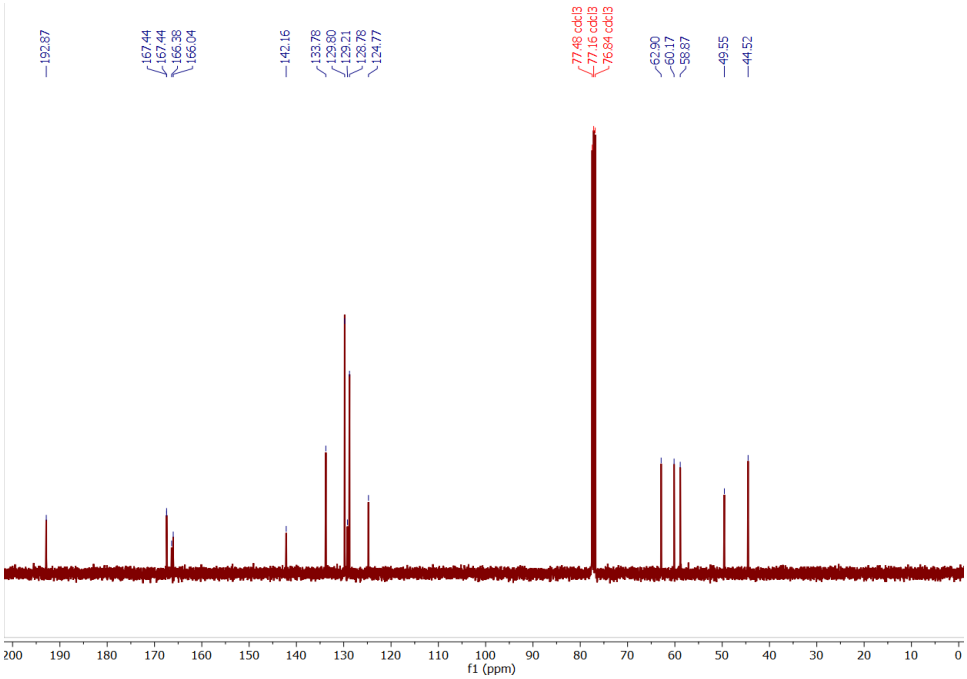

Figure S24. ^{13}C NMR spectrum ($CDCl_3$) of product **7**.

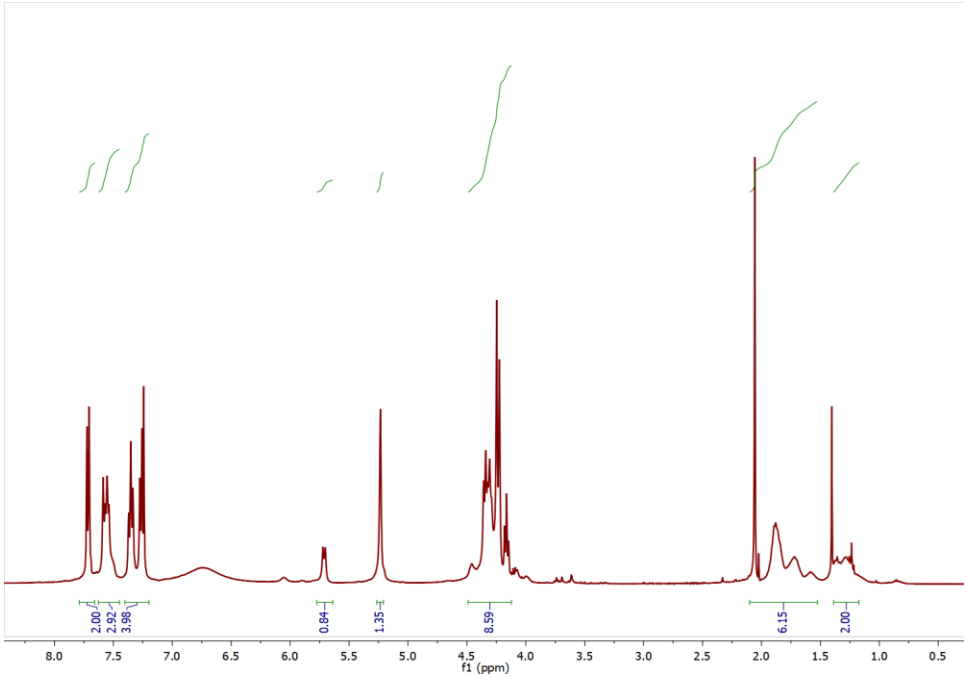

Figure S25. ^{1}H NMR spectrum ($CDCl_3$) of product **8**.

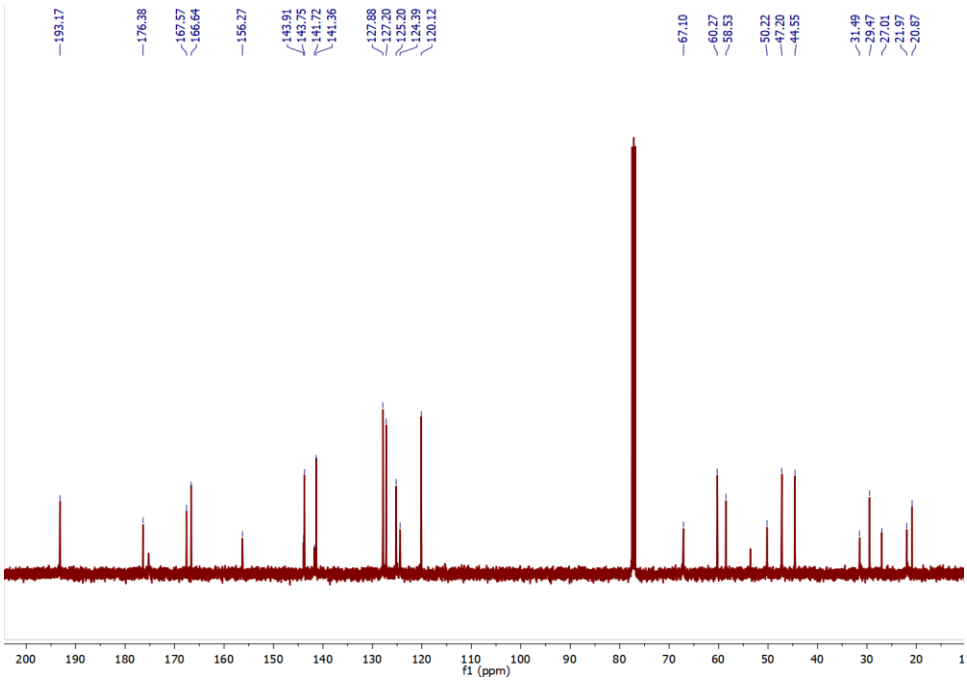

Figure S26. ^{13}C NMR spectrum ($CDCl_3$) of product **8**.

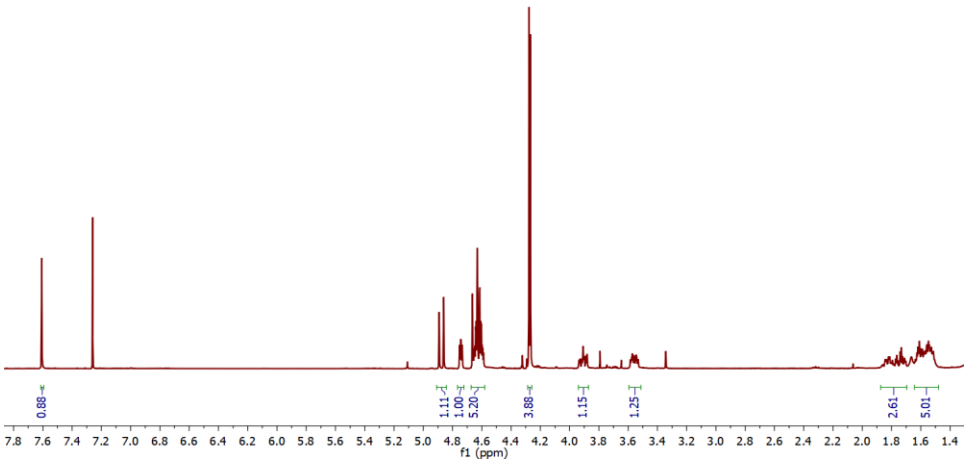

Figure S27. ^{1}H NMR spectrum ($CDCl_3$) of product **10**.

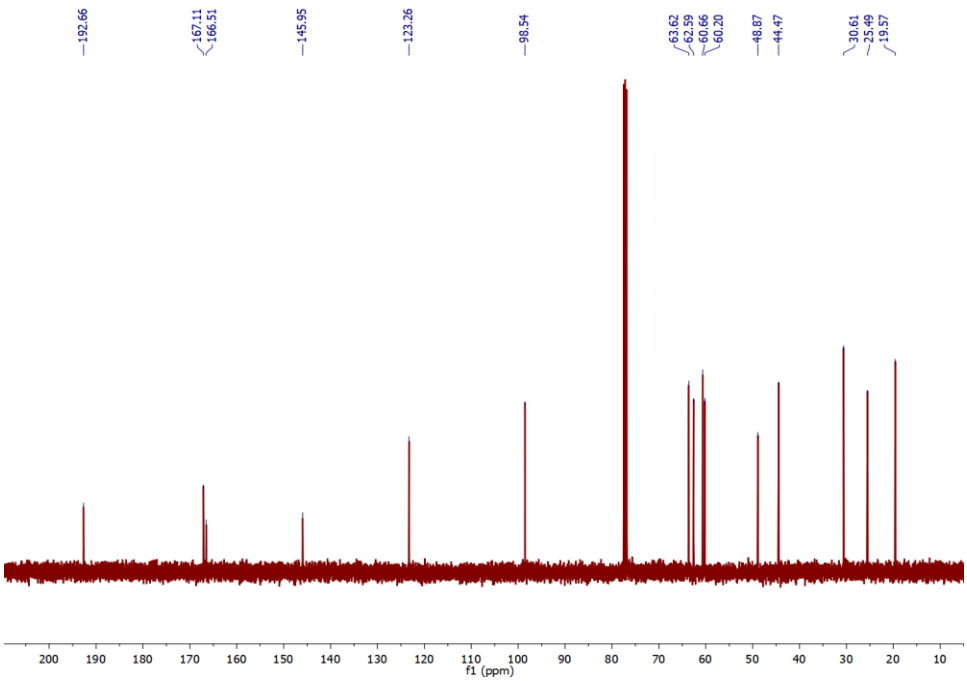

Figure S28. ^{13}C NMR spectrum ($CDCl_3$) of product **10**.

Synthetic procedure for Huisgen [3+2] cycloaddition between alkyne or azido NTA and PEG–N_3 or PEG–alkyne

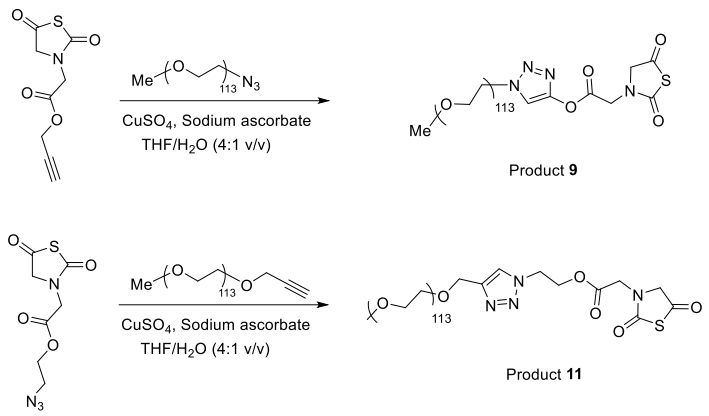

A scintillation vial was charged with alkynyl NTA (**NTA2**) (50 mg, 0.23 mmol) and PEG–N_3 (940 mg, 0.19 mmol), and the reactants were dissolved in THF (6 mL) to give a clear yellow solution. Copper sulfate pentahydrate ($CuSO_4 \cdot 5H_2O$) (23 mg, 0.094 mmol) was added in one portion. Sodium ascorbate (140 mg, 0.70 mmol) was added to a separate vial and dissolved in water (2 mL); this solution was subsequently added to the vial containing the NTA/PEG-N_3 mixture in one portion. Immediately, an insoluble brown precipitate formed. The vial was then placed in a bath sonicator (Branson 2510) at rt, and the reaction mixture became a moderately turbid, yellow solution after approximately 10 min. Reaction progress was monitored by TLC (CH_2Cl_2) until the disappearance of alkynyl NTA was observed after 75 min. The reaction mixture was passed through a column of neutral alumina and diluted with CH_2Cl_2. The organic solution was washed with saturated $NaHCO_3$, dried over Na_2SO_4, and concentrated via rotary evaporator. The crude solid was then dissolved in a minimal amount of CH_2Cl_2 and precipitated into diethyl ether to afford the PEG-NTA conjugate as a white solid (800 mg recovered).

Product **9**: ^{1}H NMR ($CDCl_3$): δ 7.84 (s, 1H), 4.77 (broad s, 2H), 4.54 (t, *J* = 5 Hz, 2H), 4.30 (d, *J* = 6 Hz, 4H), 3.70-3.56 (broad s, 451H), 3.44 (dd, *J* = 6, 4 Hz, 4H), 3.36 (s, 3H).

Product **11**: ^{1}H NMR ($CDCl_3$): δ 7.68 (s, 1H), 4.70-4.56 (m, 6H), 4.27 (d, *J* = 4 Hz, 2H), 3.65-3.60 (broad s, 413H), 3.47-3.43 (m, 4H), 3.36 (s, 3H).

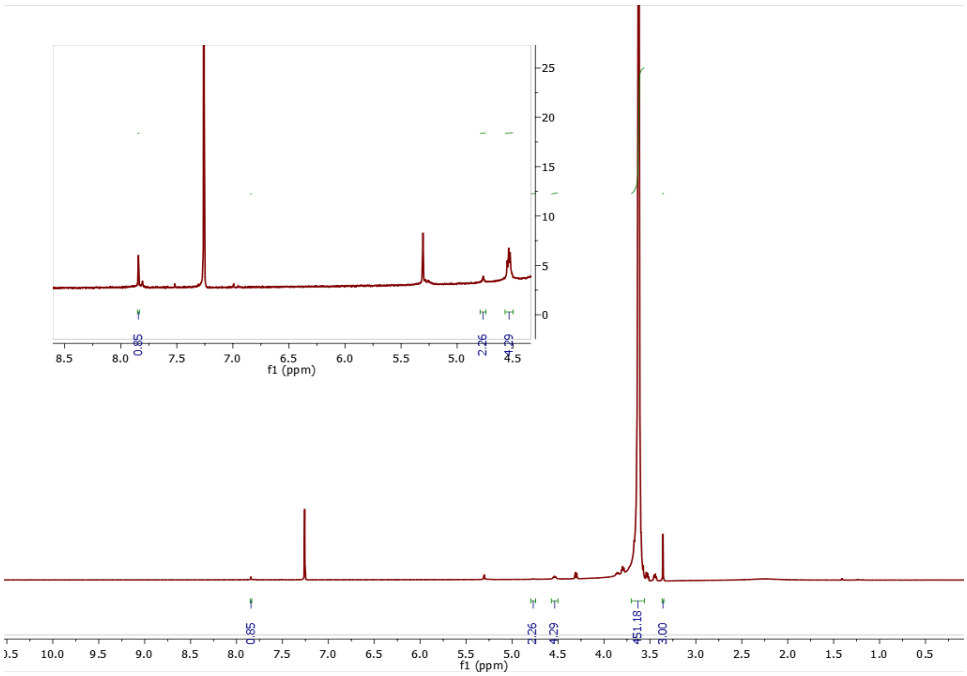

Figure S29. ^{1}H NMR spectrum ($CDCl_3$) of product **9** with inset magnifying region with triazole and NTA methylene peaks.

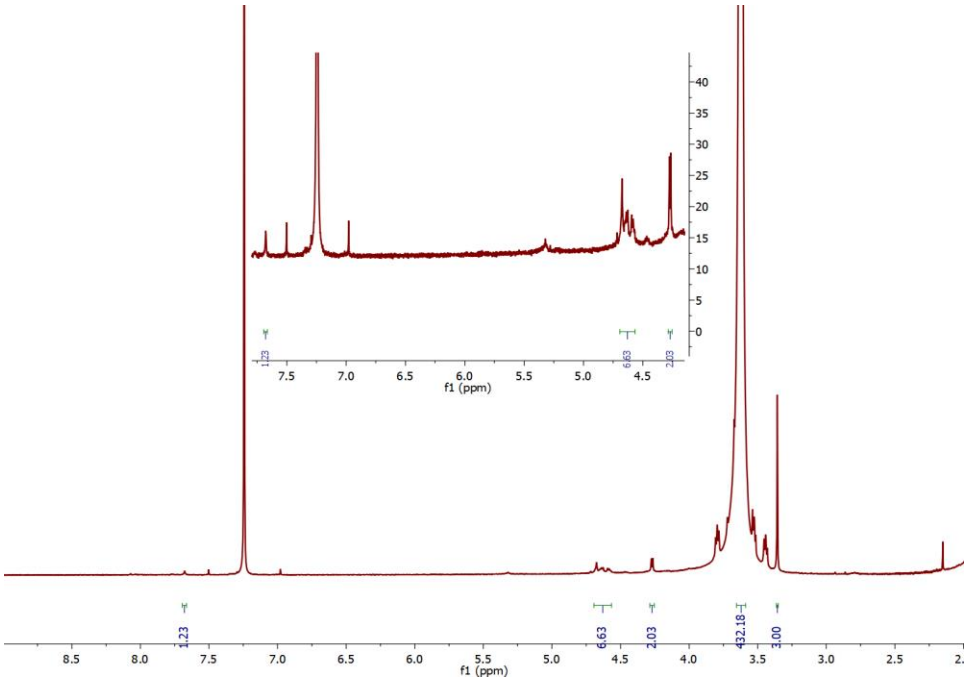

Figure S30. ^{1}H NMR spectrum ($CDCl_3$) of product **11** with inset magnifying region with triazole and NTA methylene peaks.

Synthetic procedure for cross-metathesis (CM) reaction with allyl-NTA

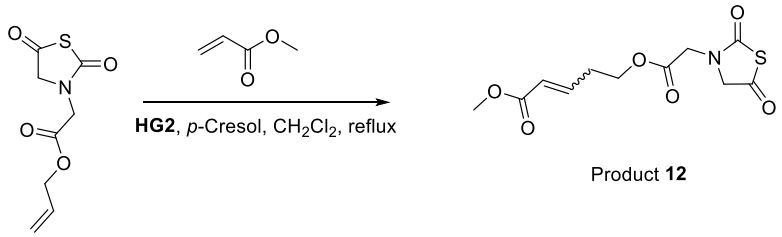

A two-neck round bottom flask equipped with a condenser and a septum was charged with allyl NTA (**NTA4**) (153 mg, 0.711 mmol), *p*-cresol (48.0 mg, 0.444 mmol) and a magnetic stir bar. CH_2Cl_2 (1.5 mL) was added to give a clear, pale yellow solution. Methyl acrylate (0.130 mL, 1.42 mmol) was then added in one portion. The reaction mixture was bubbled with N_2 for 20 min and heated to a gentle reflux. In a separate vial, a stock solution of Hoveyda-Grubbs Gen. II catalyst (1.6 mM in CH_2Cl_2) was prepared and immediately added (0.5 mL) to the refluxing reaction

mixture under N_2 flow. The reaction mixture was allowed to stir at reflux under N_2 until disappearance of allyl NTA was observed by TLC (CH_2Cl_2), 2 h. After completion of the reaction, the round bottom flask was cooled to rt, and the contents were concentrated via rotary evaporation to remove CH_2Cl_2 and any excess methyl acrylate. The residue was purified by silica gel chromatography (hexanes:EtOAc), yielding NTA **12** as a clear, colorless oil (60 mg, 36 % yield). Product **12**: ^{1}H NMR ($CDCl_3$): δ 6.91 (dt, *J* = 16, 5 Hz, 1H, *E* isomer), 6.23 (dt, *J* = 12, 5 Hz, 1H, *Z* isomer), 6.04 (dt, 16, 2 Hz, 1H, *E* isomer), 5.92 (dt, 12, 2 Hz, 1H, *Z* isomer), 4.84 (dd, *J* = 5, 2 Hz, 2H), 4.34 (d, *J* = 7 Hz, 4H), 3.75 (s, 3H). ^{13}C NMR ($CDCl_3$): δ 192.9, 167.0, 166.4, 166.0, 143.1, 139.9, 123.0, 121.4, 64.0, 63.9, 60.2, 60.1, 52.0, 51.8, 44.5, 44.4. HRMS (ESI-TOF): calcd. for $C_{17}H_{16}N_4O_6S$ $[M+H]^+$ 274.0385, found 274.0376.

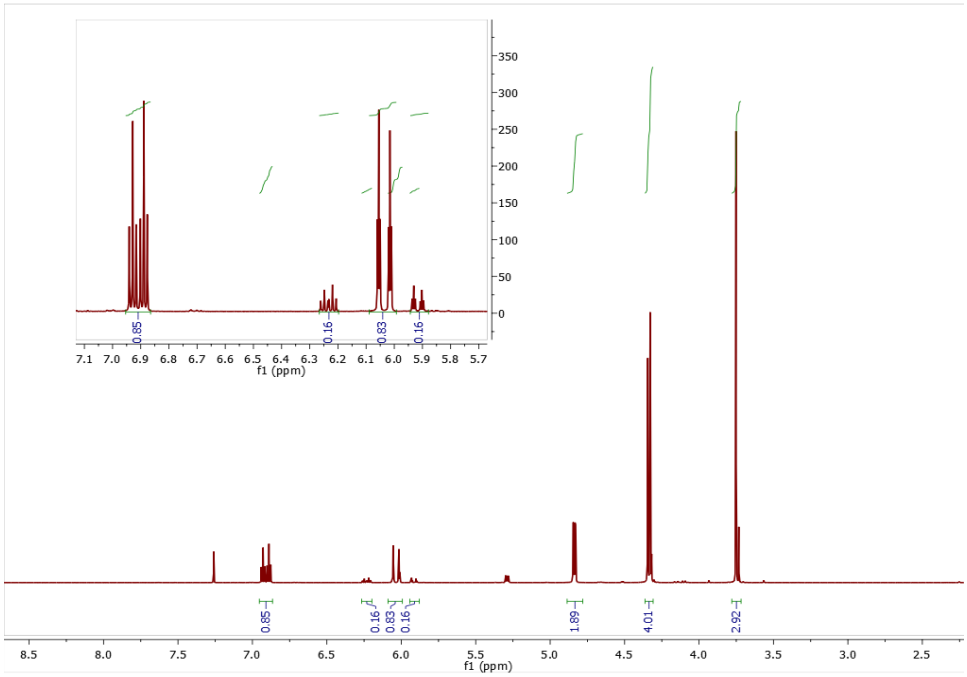

Figure S31. ^{1}H NMR spectrum ($CDCl_3$) of product **12** with inset magnifying region with alkene peaks and integrations (85:15 E/Z).

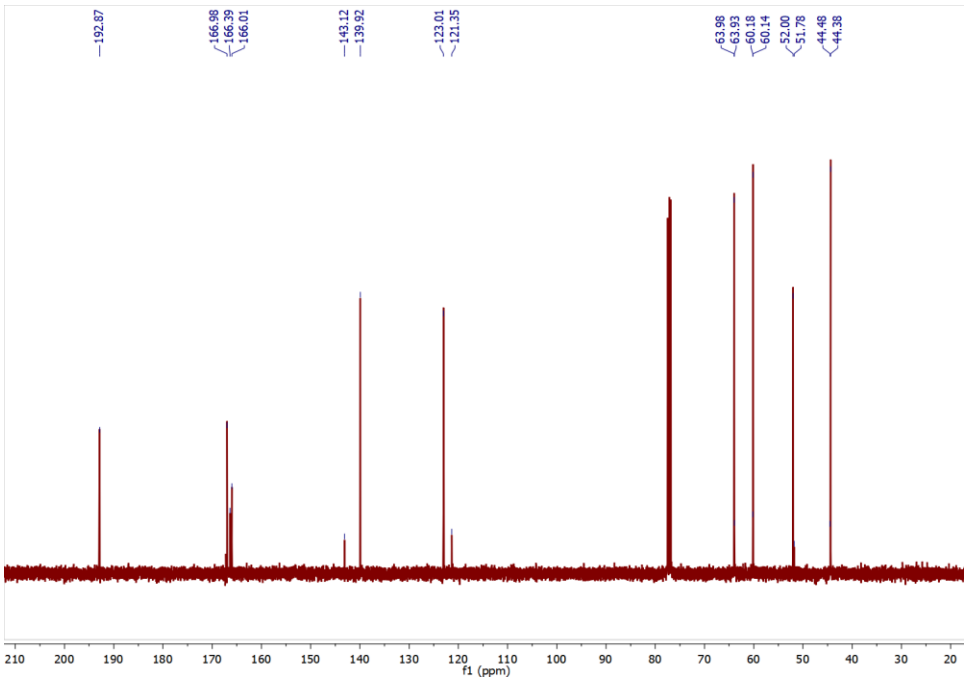

Figure S32. ^{13}C NMR spectrum ($CDCl_3$) of product **12**.

Representative synthetic procedure for thiol-ene reactions of small molecule thiols with NTAs

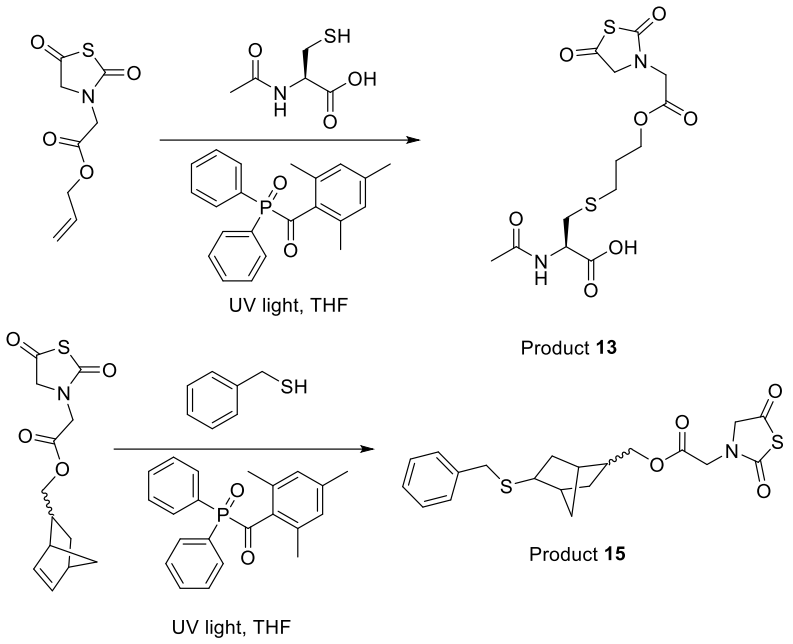

A scintillation vial was charged with norbornyl NTA (**NTA5**) (150 mg, 0.530 mmol) and a magnetic stir bar. The NTA was dissolved in THF (1.7 mL) and allowed to stir at rt. In a separate vial, (diphenylphosphoryl)(mesityl)methanone (TPO) photoinitiator (19 mg, 0.053 mmol) was dissolved in THF (0.3 mL) and added to the vial containing the **NTA5** solution in one portion, affording a pale-yellow solution. Benzyl mercaptan (62 µL, 0.53 mmol) was added to the reaction mixture, and the scintillation vial was capped and placed inside a 250 mL beaker covered in aluminum foil. The top of the beaker was covered with a UV lamp (UVP, Analytik Jena US, long wavelength setting) and allowed to stir at rt under UV irradiation. Reaction progress was monitored by TLC (CH_2Cl_2) until the **NTA5** starting material was consumed, 60 min. The reaction mixture was concentrated by rotary evaporation, and the crude material was purified via silica gel chromatography (CH_2Cl_2:MeOH mixture) to give product **15** as a clear oil (131 mg, 61 % yield). Product **13**: white solid, 17 % yield (m.p. = 130.0 – 132.3 °C). ^{1}H NMR (DMSO-d_6): δ 8.25 (d, J = 8 Hz, 1H), 4.52 (s, 2H), 4.37 (td, 8, 5 Hz, 1H), 4.33 (s, 2H), 4.18 (t, J = 6 Hz, 2H), 2.91-2.68 (m,

4H), 2.58 (t, J = 7 Hz, 2H), 1.86 (s, 3H). ^{13}C NMR (DMSO-d_6): δ 194.2, 172.3, 169.4, 167.7, 165.0, 63.8, 60.8, 52.0, 44.6, 32.8, 27.9, 27.8, 22.4. HRMS (ESI-TOF) **13**: calcd. for $C_{13}H_{19}N_2O_7S_2$ $[M+H]^+$ 379.0634, found 379.0636.

Product **15**: ^{1}H NMR ($CDCl_3$): δ 7.34-7.22 (m, 5H), 4.34-4.21 (m, 4H), 3.92 (dd, J = 2 Hz, 2H), 3.78-3.65 (m, 2H), 2.58-2.41 (m, 1H), 2.33-2.18 (m, 2H), 2.14-2.02 (m, 1H), 1.79-1.57 (m, 3H), 1.41-1.00 (m, 4H). ^{13}C NMR ($CDCl_3$): δ 193.02, 167.41, 166.15, 138.58, 128.81, 128.77, 128.53, 128.50, 126.92, 68.79, 68.69, 60.14, 60.13, 45.92, 45.77, 45.11, 44.46, 44.44, 43.95, 42.15, 41.74, 40.35, 40.07, 38.83, 38.50, 38.41, 37.99, 36.78, 36.61, 36.08, 32.98, 32.55. HRMS (ESI-TOF): calcd. for $C_{20}H_{24}NO_4S_2$ $[M+H]^+$ 406.1147, found 406.1144.

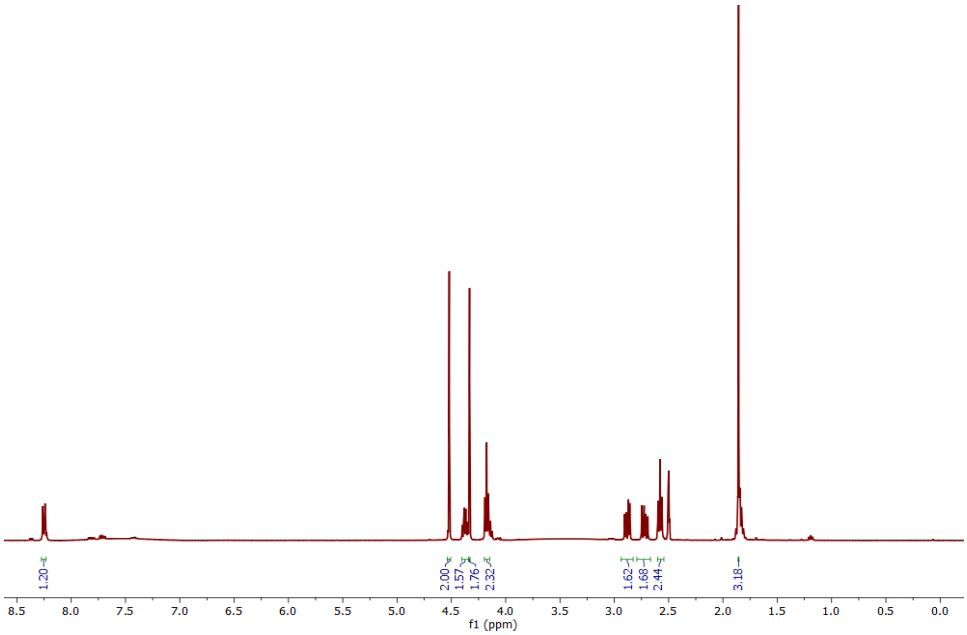

Figure S33. ^{1}H NMR spectrum (DMSO-d_6) of product **13**.

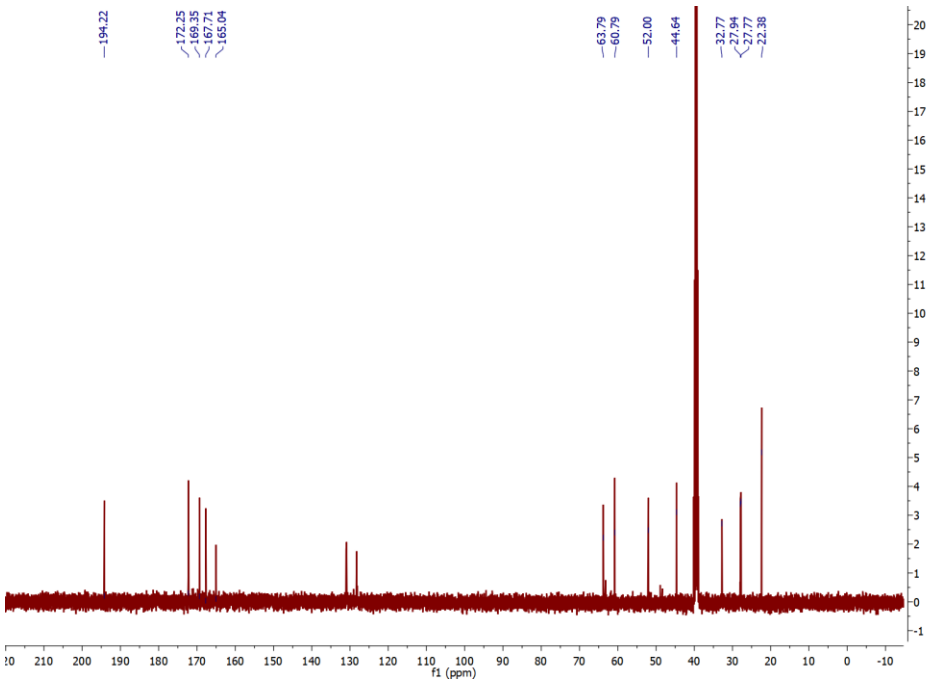

Figure S34. ^{13}C NMR spectrum (DMSO-d_6) of product **13**.

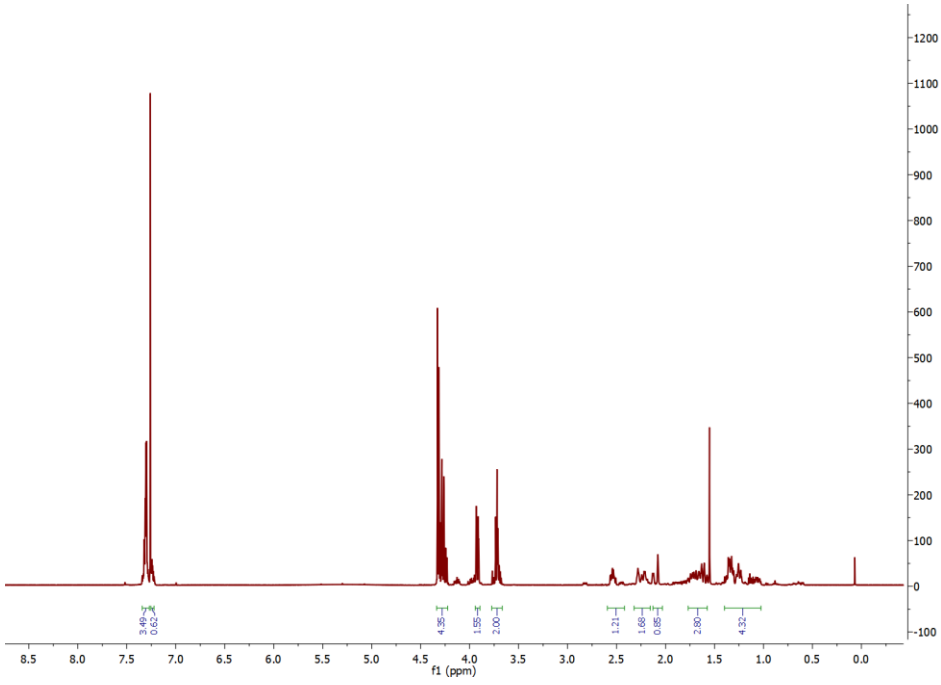

Figure S35. ^{1}H NMR spectrum ($CDCl_3$) of product **15**.

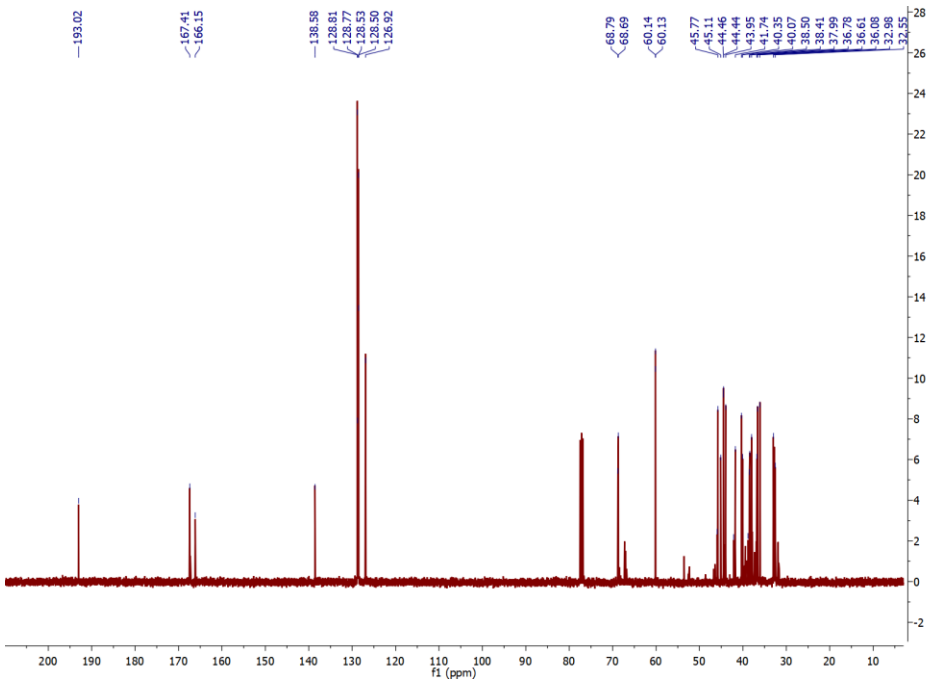

Figure S36. ^{13}C NMR spectrum ($CDCl_3$) of product **15**.

Synthetic procedure for thiol-ene reaction with PACMO-SH

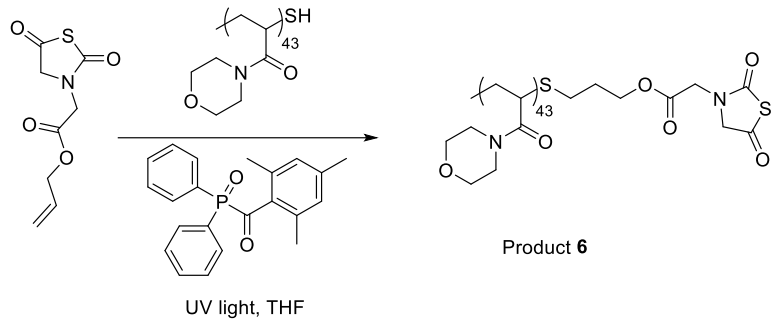

A Schlenk tube was charged with allyl NTA (**NTA4**) (6.6 mg, 31 µmol), PACMO–SH (100 mg, 15 µmol) and a magnetic stir bar. The reactants were dissolved in THF (1.0 mL), and a solution of TPO in THF (0.2 mL, 20 mM) was subsequently added. The flask was subjected to three freeze-pump-thaw cycles and backfilled with N_2. The Schlenk tube was placed in a beaker (500 mL) covered in aluminum foil, and a handheld UV lamp (UVP, Analytik Jena US, long wavelength setting) was placed adjacent to the flask inside the beaker, with the bulb parallel to the Schlenk tube and pointed toward the contents of the reaction mixture. The entire UV lamp ensemble was covered in aluminum foil, and the UV lamp was turned on. The reaction mixture was stirred at rt under UV irradiation. The reaction was monitored by TLC (CH_2Cl_2) until **NTA4** was consumed, 90 min, at which point the flask was opened to air. The reaction mixture was precipitated into cold Et_2O (2x), dried, and collected to give PACMO-NTA (**14**) as a white powder (50 mg).

Product **14**: ^{1}H NMR ($CDCl_3$): δ 4.40-4.27 (m, 4H), 4.05 (s, 2H), 3.82-3.22 (broad, 211H), 2.70-2.35 (broad, 33H), 1.91-1.56 (broad, 74H).

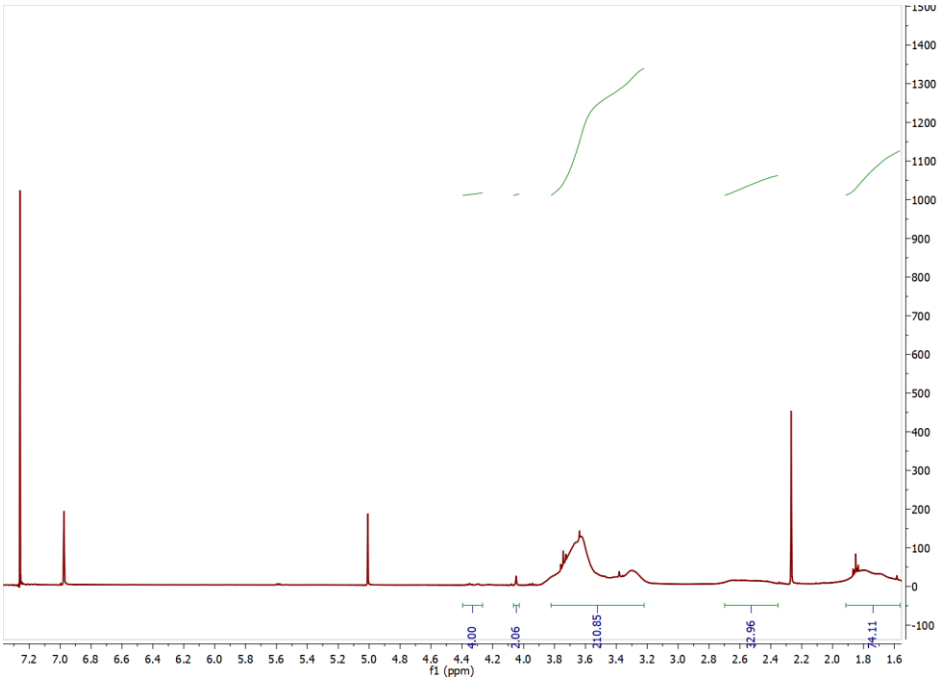

Figure S37. ^{1}H NMR of product **14**.

Synthetic procedure for thiol-ene reaction of bovine serum albumin (BSA) with norbornyl NTA

A scintillation vial was charged with BSA (100 mg) and a magnetic stir bar. The BSA was dissolved in water (0.8 mL) to give a viscous, clear, yellow solution. A solution of norbornyl NTA in THF (50 µL, 0.300 M) was added followed by addition of a solution of TPO in THF (20 µL, 0.038 M). The scintillation vial was capped and placed in a 250 mL beaker covered in aluminum foil, and a UV lamp (UVP, Analytik Jena US, long wavelength setting) was placed on top of the beaker. The reaction mixture was allowed to stir at rt under UV irradiation. After 2 h, the reaction mixture was poured into acetone at 0 °C, resulting in the immediate formation of a white precipitate. The suspension was cooled in a freezer for 20 min and subsequently centrifuged at 2000 rpm for 30 min. The supernatant was decanted off, and the precipitate was collected, washed with cold acetone, and dried via lyophilization.

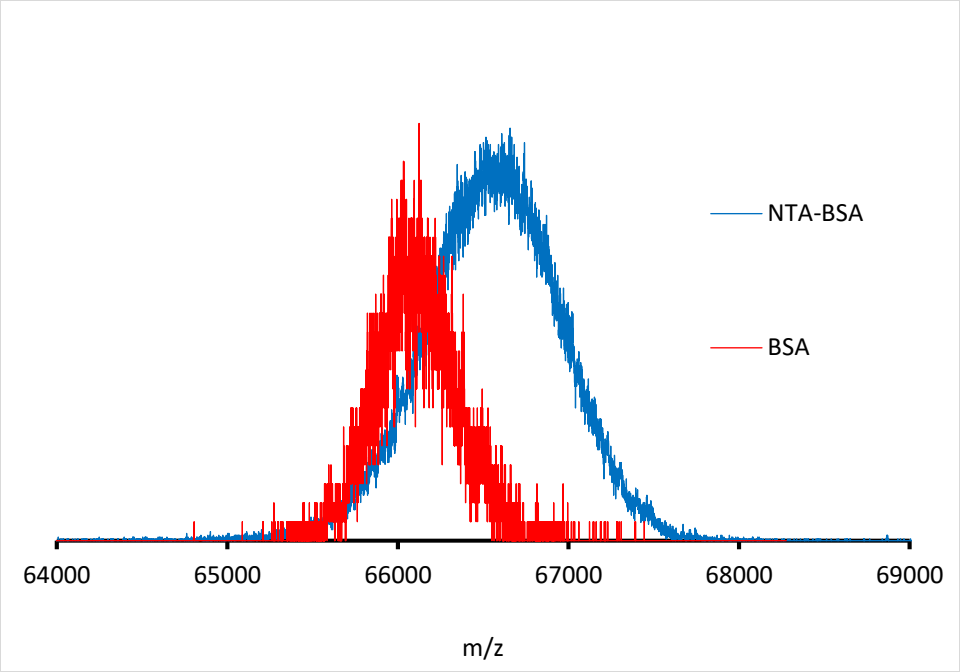

Figure S38. Samples were analyzed by a matrix-assisted laser desorption ionization–tandem time of flight mass spectrometer (4800 MALDI TOF/TOF; AB Sciex). Two µL of alpha-cyano-4-hydroxycinnamic acid matrix (4 mg/mL, 50%/50% ACN/H_2O, 0.1% TFA and 10 mM ammonium chloride) were loaded on a MALDI-target plate, mixed with 1 µL of protein solution (2 mg/mL in H_2O). The sample spot was de-salted via adding 1 µL water onto the sample and immediately wicking the water away with a Kimwipe prior to analysis in linear positive-ion mode (laser intensity 7900). The peak *m*/*z* value of 66200 was obtained for standard BSA, and 66700 was observed for the BSA-NTA conjugate.

H_2S release electrochemical probe data

A scintillation vial was charged with 9.73 mL of 1X PBS buffer (pH 7.4), 4 µL of a solution of nucleophile (0.5 M in H_2O), 250 µL of a solution of CA (33.3 µM in 1X PBS), and a small magnetic stir bar. The probe was submerged in the solution and the voltage was allowed to equilibrate for ~5 minutes. Once equilibrated, 20 µL of a solution of NTA (5 mM in DMSO) were

added. Final concentrations were 10 μM **NTA1,** 100 μM glycine, and 300 nM CA. Once all of the reagents had been added, the probe was immediately inserted into the solution, and the probe current was recorded. This initial current spike was omitted from the reported data. Peaking time of H_2S in solution was measured at the point where the current readout was at a global maximum for the dataset.

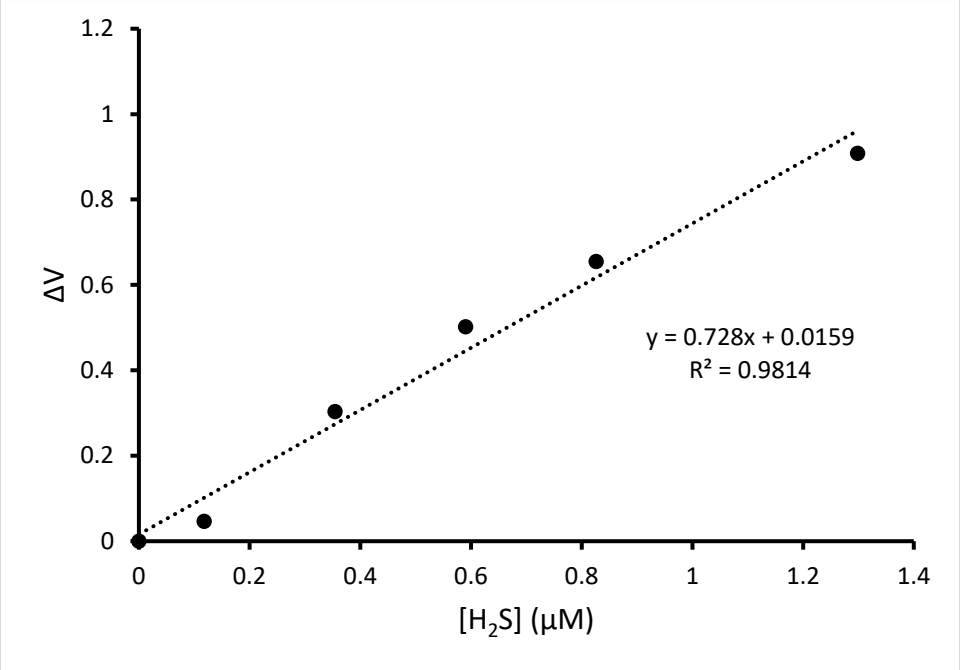

Figure S39. Representative calibration curve constructed for the H_2S-selective electrochemical probe. Values on the x-axis indicate the concentration of Na_2S in solution (PBS buffer, pH 7.4). Values on the y-axis indicate the change in output voltage after each successive addition of Na_2S. Concentration of H_2S calculated via the equation $[H_2S] = [Na_2S]/\{1 + \frac{K_a{}^1}{[H^+]} + \frac{K_a{}^1 K_a{}^2}{[H^+]}\}$ where $pK_a{}^1$ = 6.89 and $pK_a{}^2$ = 19 for the chemical equation [total sulfide] = $[H_2S]$ + $[HS^-]$ + $[S^{2-}]$.[8]

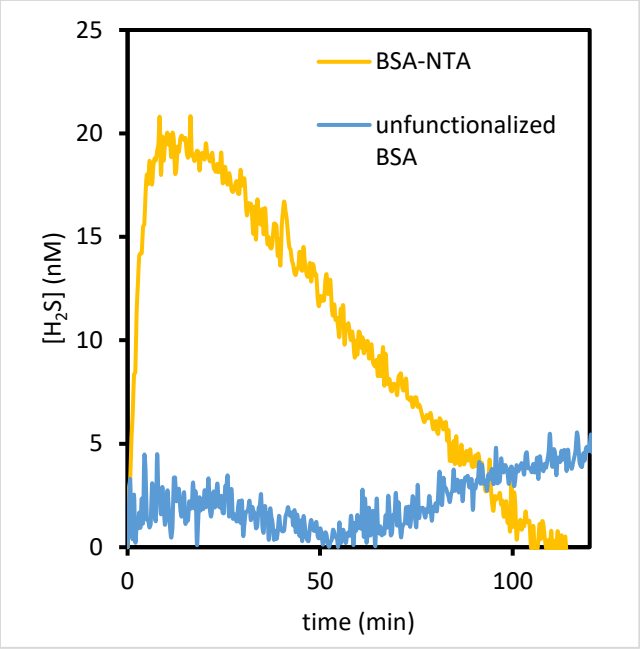

Figure S40. H_2S selective electrochemical probe data of pure (unfunctionalized) BSA (blue) and the BSA-NTA conjugate (yellow) (90 µM) in the presence of glycine (900 µM) and CA (800 nM) in 1X PBS buffer (pH 7.4).

Experimental References

1. J. Cao, D. Siefker, B. A. Chan, T. Yu, L. Lu, M. A. Saputra, F. R. Fronczek, W. Xie and D. Zhang, Interfacial Ring-Opening Polymerization of Amino-Acid-Derived N-Thiocarboxyanhydrides Toward Well-Defined Polypeptides. *ACS Macro Letters*, **2017**, *6*, 836-840.

2. J. J. Caldwell, I. D. Cameron, S. D. R. Christie, A. M. Hay, C. Johnstone, W. J. Kerr, and A. Murray, Total Synthesis of Japanese Hop Ether Using an Efficient Intramolecular Pauson-Khand Reaction. *Synthesis*, **2005**, *2005*, 3293-3296.

3. X. Lu and R. Bittman, Synthesis of a Photoactivatable (2S,3R)-Sphingosylphosphorylcholine Analogue. *J. Org. Chem.*, **2005**, *70*, 4746-4750.

4. R. Sen, D. Gahtory, J. Escorihuela, J. Firet, S. P. Pujari and H. Zuilhof, Approach Matters: The Kinetics of Interfacial Inverse-Electron Demand Diels–Alder Reactions. *Chemistry – A European Journal*, **2017**, *23*, 13015-13022.

5. J. Edward Semple, B. Sullivan, T. Vojkovsky and K. N. Sill, Synthesis and Facile End-Group Quantification of Functionalized PEG Azides *J. Polym. Sci., Part A: Polym. Chem.*, **2016**, *54*, 2888-2895.

6. R. Chapman, K. A. Jolliffe and S. Perrier, Modular Design for the Controlled Production of Polymeric Nanotubes from Polymer/Peptide Conjugates. *Polym. Chem.*, 2011, **2**, 1956-1963.

7. W. Shen, Q. Qiu, Y. Wang, M. Miao, B. Li, T. Zhang, A. Cao and Z. An, Hydrazine as a Nucleophile and Antioxidant for Fast Aminolysis of RAFT Polymers in Air *Macromol. Rapid Commun.*, **2010**, *31*, 1444-1448.

8. B. Meyer, K. Ward, K. Koshlap and L. Peter, Second Dissociation Constant of Hydrogen Sulfide *Inorg. Chem.*, **1983**, *22*, 2345-2346.

Chapter 4: Polycarbonates as Macromolecular Scaffolds for the Delivery of Hydrogen Sulfide

4.1. Authors.

Chadwick R. Powell,[§,†] Haley Young,[§,†] Jake Viar, [§,†] [§,†] and John B. Matson*[§,†]

[§]Department of Chemistry, Virginia Tech, Blacksburg, Virginia 24061, United States
[†]Virginia Tech Center for Drug Discovery, Virginia Tech, Blacksburg, Virginia 24061, United States

4.2. Abstract

Herein we report a novel, biodegradable, polymeric H_2S donor scaffold via the preparation of an azide-functionalized aliphatic polycarbonate by ring-opening polymerization, termed **PC-N_3**. Each repeat unit of the polycarbonate backbone contained an azide, which was used as a functional handle for the Huisgen [3+2] cycloaddition reaction (CuAAC). In two sequential steps, an alkyne-functionalized PEG and an H_2S-releasing alkynyl-NTA (**NTA2**) were appended to the polycarbonate backbone to give water soluble, H_2S releasing polycarbonates.

4.3. Introduction

The application of macromolecules in the field of drug delivery has become a cornerstone in polymer research. Polymers provide an element of controlled, tunable release to a variety of drugs, allowing for more effective dosing schedules over simply delivering a small molecule drug.[1] Polymers are most commonly employed as drug encapsulation agents, wherein the drug is dispersed within a polymer matrix, resulting in diffusion of the drug from the matrix.[2-3] More recently, polymer therapeutics have become increasingly popular wherein the polymer itself is bioactive,[4-6] or more commonly, the drug is covalently attached to an inert polymeric delivery

vehicle.[7-9] As a testament to the viability of these strategies, there are a large number of polymer-drug conjugates that are approved for clinical use or are currently in clinical trials.[10-11]

Drug delivery polymers of particular interest to us are those that deliver hydrogen sulfide (H_2S). H_2S has recently garnered much interest in the area of drug delivery after its discovery as a signaling molecule in mammals.[12] Research into the physiology of H_2S has demonstrated its implication in a variety of disease states including cystic fibrosis,[13] cardiovascular disease,[14] and Alzheimer's.[15] Since this discovery, a wide variety of sulfur-containing functional groups have been developed to enable the release of H_2S from organic compounds (termed H_2S donors) in response to a variety of stimuli.[16] Additionally, considerable effort has gone into preparing H_2S donor systems with tunable, extended release half-lives (from minutes to hours), and polymer-H_2S donor conjugates effectively decrease release rate in aqueous media.[17-19] Current H_2S-releasing macromolecular systems include water-soluble statistical copolymers,[17-18, 20-21] and block copolymer micelles[22-23].

While the current polymeric H_2S donor systems have demonstrated limited toxicity, and positive therapeutic indications in some cases, there is no indication of the toxicity or mode of clearance of the polymeric byproducts after H_2S release. In an effort to alleviate this gap in the H_2S donor literature, we devised a route to a biodegradable polymeric H_2S donor based on an aliphatic poly(carbonate) (PC) platform. PCs synthesized via ring-opening polymerization (ROP) have gained attention recently as modular platforms from which a wide range of functional, aliphatic PCs can be readily prepared.[24] PCs undergo gradual enzymatic degradation *in vivo* to generate alcohols and carbon dioxide as the major byproducts, which contributes to their general biocompatability.[25-26] Additionally, work by Dove, Hedrick, Waymouth, and others, has generated a litany of organocatalysts that are easily applied to the ROP of PCs, eliminating the need for toxic

heavy metal catalysts.[27-29] Additionally, PCs have been employed in a variety of drug delivery applications due to their biocompatibility, biodegradability, and wide range of functionalities which can be accommodated.[30-33]

4.4. Results and Discussion

When devising a synthetic route toward an aliphatic PC-NTA conjugate via ROP, the electrophilicity of the NTA moiety generated the need for a post-polymerization modification strategy. Conjugation of the NTA to the PC monomer prior to ring-opening would result in partial or total loss of the COS/H_2S payload as well as crosslinking via ring opening of the NTA moiety. With this synthetic restriction in mind, we devised a route to a cyclic carbonate azide monomer (**CM-N_3**) (Scheme 1).

CM-N_3 was prepared on the gram scale in five steps from commercially available trimethylolethane (($CH_3C(CH_2OH)_3$). In order to install an azide exclusively on one alcohol of trimethyolethane, an acetonide was utilized as a protecting group for two of the alcohols in the presence of a catalytic amount of acid (cyclic acetal **1**). The unprotected alcohol of product **1** was then tosylated in pyridine to give tosylate **2**. Product **2** was subjected to nucleophilic substitution in the presence of sodium azide (NaN_3) to generate azide **3**. To obtain the desired cyclic carbonate, the acetonide was deprotected in refluxing acid (generating diol **4**) followed by ring closure with ethyl chloroformate to ultimately form the cyclic carbonate monomer **CM-N_3**.

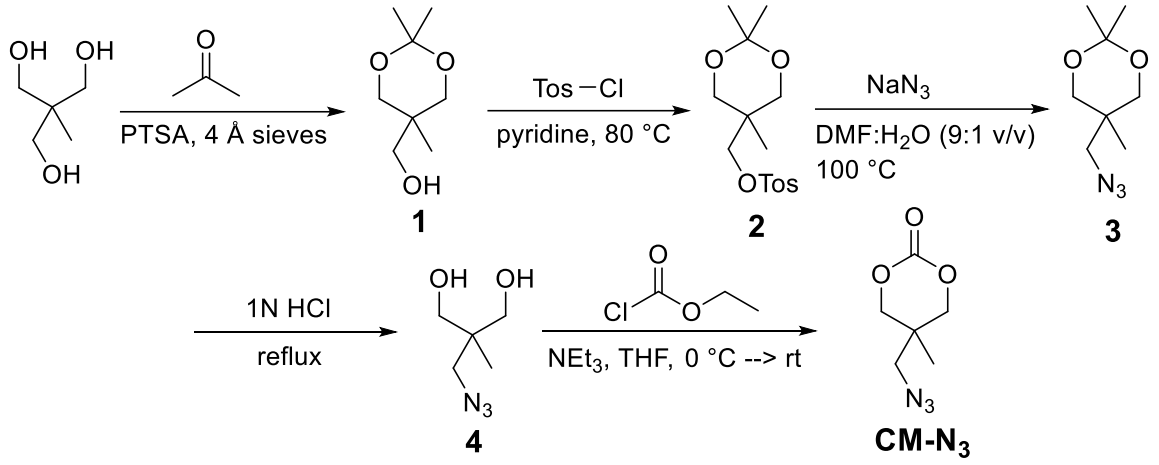

Scheme 1. Synthesis of **CM-N3**.

Polymerization of **CM-N3** was carried out using a dual thiourea (TU)/amine organocatalyst system; DBU was selected as the amine base, as it has been shown to mediate ROP of lactide as well as various lactones.[34-35] In apolar solvents, the TU:DBU catalyst system can effectively mediate ROP initiated by alcohols via an activated monomer mechanism, effectively preventing transesterification/transcarbonation reactions, and thus providing conditions for a living polymerization. Additionally, for polymers of biological interest, the catalysts alleviate the need for heavy metal catalysts, which may be cytotoxic *in vitro* or *in vivo*.

Polymerization of **CM-N3** was conducted in dichloromethane employing benzyl alcohol as the initiating species and the TU:DBU cocatalyst system noted above, targeting a degree of polymerization (DP) of 50 (theoretical M_n = 8.7 kg/mol) (Figure 1A). Polymerizations were conducted for 18 h at rt, reaching > 90 % conversion under these conditions as monitored by ^{1}H NMR spectroscopy. Pure poly(carbonate azide) (**PC-N3**) was readily isolated via precipitation with (M_n = 9.1 kg/mol (^{1}H NMR end group analysis), M_n = 8.4 kg/mol (SEC), Đ = 1.11). The presence of azides on the **PC-N3** repeat unit was confirmed by FTIR spectroscopy (Figure S13). Kinetic

analysis of the polymerization of **PC-N$_3$** displayed living behavior as evidenced by the linear relationship between the natural log of monomer concentration at a given time ([M]) relative to initial monomer concentration ($[M]_0$), subtracting the equilibrium monomer concentration ($[M]_{eq}$) from each, vs. time (Figure 1B). Monomer concentrations were determined by ^{1}H NMR spectroscopy. Additionally, we observed a linear relationship between relative M_n based on SEC analysis (assuming linear relationship between M_n and retention time by SEC) and monomer conversion (Figure 1C).

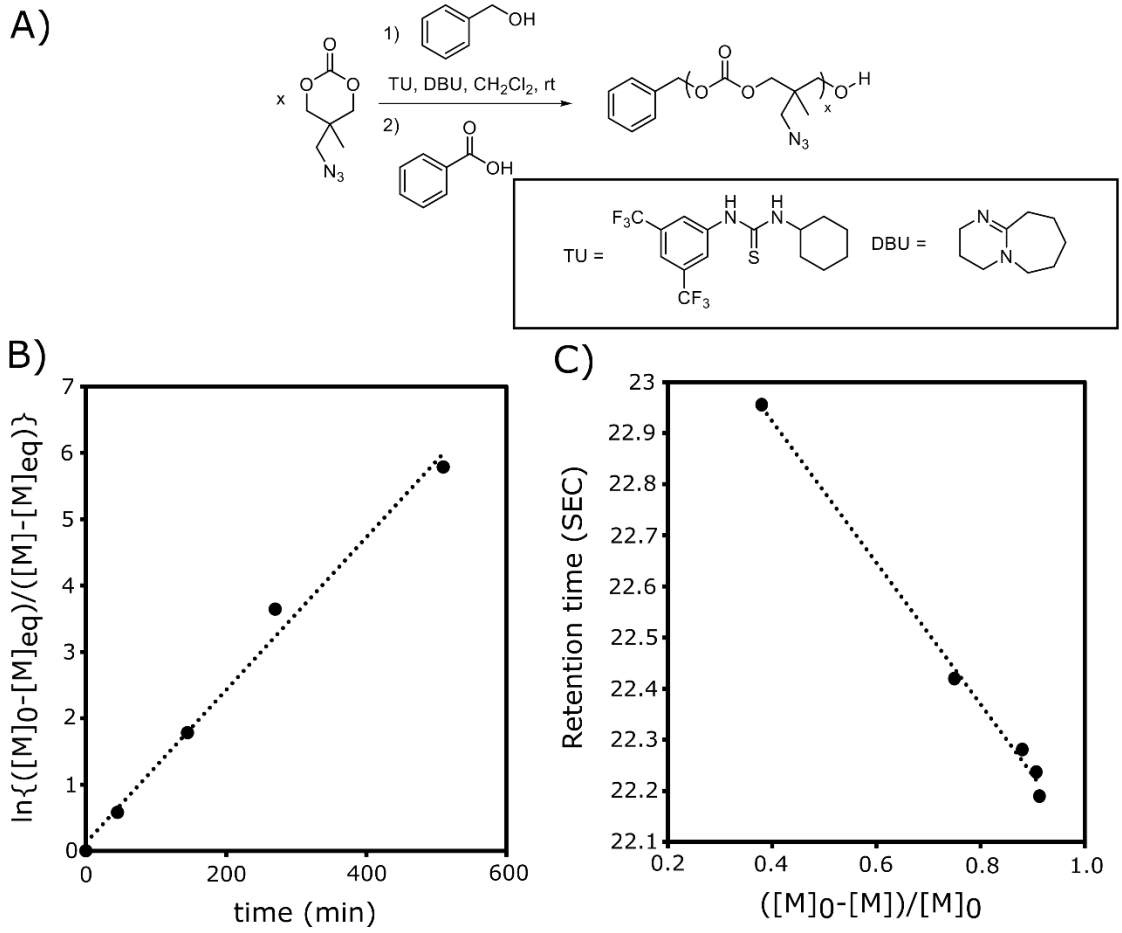

Figure 1. A) Synthesis of **PC-N$_3$** using benzyl alcohol as the initiator and TU:DBU cocatalyst system (50:1:1:1 [M]:[I]:[TU]:[DBU]). B) Plot of monomer conversion versus time determined by

^{1}H NMR spectroscopy. C) Plot of retention time determined by SEC RI traces vs. time. The linear nature of the plots in B and C supports the living nature of the polymerization.

As the **PC-N$_3$** homopolymer was not water soluble, we postulated that introduction of poly(ethylene glycol) (PEG) (M_n = 0.75 kg/mol) grafts would be sufficient to attain adequate water solubility. Thus, an alkyne-terminated PEG$_{750}$ was prepared according to a literature procedure[36] and employed in the copper-mediated Huisgen [3+2] cycloaddition (CuAAC) reaction with **PC-N$_3$**. The best reaction conditions found for the CuAAC reaction between **PC-N$_3$** and PEG were in THF, with copper iodide (CuI) as the copper source, and diisopropylethylamine (DIEA) as the base, at rt. ^{1}H NMR analysis of the product showed a new peak at δ = 8.1 ppm corresponding to the formation of the desired triazole between the PEG$_{750}$ alkyne and **PC-N$_3$**, with integration relative to **PC-N$_3$** end groups corresponding to 96% conversion (Figure S14) under these reaction conditions to give the desired **PC-*graft*-PEG** (Figure 2). Unfortunately, subsequent CuAAC reactions with alkynyl NTA (**NTA2**) were met with limited success, possibly due to steric factors arising from the PEG grafts or poor solubility of **PC-*graft*-PEG**. Attempts to alter reaction conditions for the conjugation of **NTA2** to conditions previously employed to conjugate **NTA2** with PEG chains (Chapter 3) were met with limited success. Previous CuAAC reactions of **NTA2** with PEG azides were performed in a THF/H_2O mixture with copper sulfate pentahydrate ($CuSO_4 \cdot 5H_2O$), sodium ascorbate as a reducing agent, and sonication in lieu of stirring. However, these conditions caused gelation of the **PC-*graft*-PEG**, likely due to chain scission events along the PC backbone induced by the sonicator. When vortex mixing followed by stirring was employed in lieu of sonication, limited conversion of **NTA2** was observed, and an insoluble yellow precipitate formed, which is tentatively assigned to a Cu–**NTA2** complex. Additionally, purification of the

resulting polymer product from the THF/H_2O solvent system as well as the water soluble copper salts and sodium ascorbate proved a challenge as the PEG grafts had imparted water solubility, but also appear to result in the formation of ~10 nm aggregates, as determined by dynamic light scattering (DLS). However, in the most successful attempt to conjugate **NTA4** under these conditions, ~40 % conversion of **NTA2** to **PC-*graft*-PEG** was achieved as determined by ^{1}H NMR spectroscopy (Figure S15).

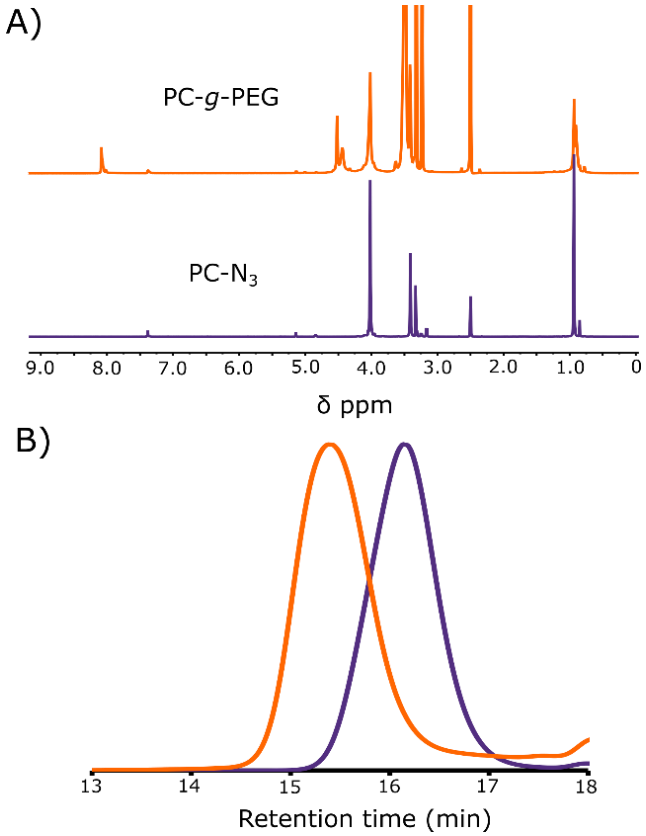

Figure 2. A) Stacked ^{1}H NMR spectra (DMSO-d_6) of PC-N_3 (purple) and **PC-*g*-PEG** (orange) showing successful conjugation of the PEG alkyne to **PC-N_3**, determined by the appearance of a peak corresponding to a 1,4-disubstituted triazole (δ = 8.1 ppm) as well as broad peaks

corresponding to PEG methylenes (δ = 3.45-3.55) and PEG end-group methyl (δ = 3.23). B) SEC traces for **PC-N_3** (purple) and **PC-*g*-PEG** (orange) showing an increase in retention time after the CuAAC reaction, indicating an increase in molecular weight.

Thus, the synthetic strategy was reformed to attempt the CuAAC reaction with **NTA2** prior to appending the PEG_{750} grafts. However, the CuAAC conditions that were successful in installing the PEG_{750} grafts (CuI with DIEA in THF) gave a completely insoluble yellow precipitate within minutes of the addition of the CuI to the reaction medium. Attempts to analyze the product were unsuccessful, and model reactions with **NTA2** and a small molecule organo-azide under these conditions generated the same insoluble material, indicating that the CuI catalyst was incompatible with **NTA2** under these conditions.

However, to demonstrate the importance of macromolecular H_2S donors in modulating H_2S release rate, the moderately successful product of the CuAAC reaction was dissolved in 1X PBS buffer (pH 7.4), and H_2S release was monitored by an H_2S-selective electrochemical probe in the presence of carbonic anhydrase (CA) (800 nM) and glycine (100 μM) (Figure 3). When compared to the H_2S release profile from small molecule **NTA2**, it is clear that at the same concentration of NTA (10 μM) in solution, the macromolecular donor **PC-*graft*-PEG-NTA** is capable of extending the H_2S release from minutes to hours, similar to other macromolecular systems reported from our lab.[17-18] As a control, H_2S release from the **PC-*graft*-PEG**, prior to appending the NTA, was collected under the same conditions and demonstrated no H_2S release, as expected. Despite the limited success of the CuAAC reaction as of now, this is an exciting result.

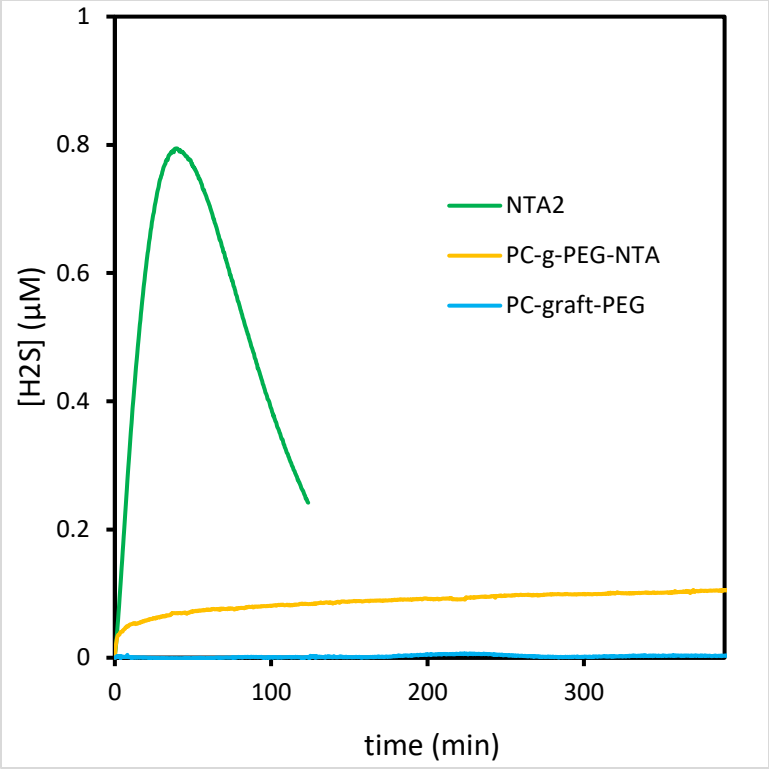

Figure 3. H_2S release using an H_2S-selective electrochemical probe for small molecule **NTA2** (10 µM) (green line) showing a peaking time of 20 min, typical of small molecule NTAs. The **PC-*graft*-PEG-NTA** (2.5 µM, 10 µM [NTA]) (yellow line) showed a peak concentration of H_2S out past 300 min and **PC-*graft*-PEG** (blue line), showed no H_2S release.

4.5. Conclusions

In summary, we have synthesized a biodegradable macromolecular H_2S donor **PC-*g*-PEG-NTA**. Synthesis of the azido-polycarbonate homopolymer **PC-N_3** was successful and demonstrated a living polymerization facilitated by the dual TU:DBU organocatalyst system. Conjugation of PEG_{750} via the CuAAC reaction was successful and went to complete conversion to generate a water-soluble graft polymer **PC-*graft*-PEG**. However, attempts at conjugating **NTA2**

under various CuAAC reaction conditions were met with limited success. However, preliminary H_2S release studies indicated that the **PC-*graft*-PEG-NTA** system successfully extends H_2S release over the small molecule **NTA2**. Current efforts focus on optimizing the CuAAC reaction conditions for the reaction between **NTA2** and **PC-N_3** to incorporate greater NTA loadings onto the water-soluble macromolecular donor.

4.6. Acknowledgements

This work was supported by the National Science Foundation (DMR-1454754) and the National Institutes of Health (R01GM123508). We also thank 3M for support of this work through a Non-Tenured Faculty Award to JBM.

4.7. References

1. Uhrich, K. E.; Cannizzaro, S. M.; Langer, R. S.; Shakesheff, K. M., Polymeric Systems for Controlled Drug Release. *Chem. Rev.* **1999,** *99*, 3181-3198.

2. Langer, R.; Peppas, N. A., Present and Future Applications of Biomaterials in Controlled Drug Delivery Systems. *Biomaterials* **1981,** *2*, 201-214.

3. Verma, R.; Mishra, B.; Garg, S., Osmotically Controlled Oral Drug Delivery. *Drug Dev. Ind. Pharm.* **2000,** *26*, 695-708.

4. Roberts, M.; Bentley, M.; Harris, J., Chemistry for Peptide and Protein PEGylation. *Adv. Drug Del. Rev.* **2012,** *64*, 116-127.

5. Chin, W.; Zhong, G.; Pu, Q.; Yang, C.; Lou, W.; De Sessions, P. F.; Periaswamy, B.; Lee, A.; Liang, Z. C.; Ding, X.; Gao, S.; Chu, C. W.; Bianco, S.; Bao, C.; Tong, Y. W.; Fan, W.; Wu, M.; Hedrick, J. L.; Yang, Y. Y., A Macromolecular Approach to Eradicate Multidrug Resistant

Bacterial Infections While Mitigating Drug Resistance Onset. *Nature communications* **2018,** *9*, 917.

6. Zheng, L.-Y.; Zhu, J.-F., Study On Antimicrobial Activity of Chitosan with Different Molecular Weights. *Carbohydr. Polym.* **2003,** *54*, 527-530.

7. Boyer, C.; Bulmus, V.; Liu, J.; Davis, T. P.; Stenzel, M. H.; Barner-Kowollik, C., Well-Defined Protein−Polymer Conjugates via In Situ RAFT Polymerization. *J. Am. Chem. Soc.* **2007,** *129*, 7145-7154.

8. Satchi-Fainaro, R.; Puder, M.; Davies, J. W.; Tran, H. T.; Sampson, D. A.; Greene, A. K.; Corfas, G.; Folkman, J., Targeting Angiogenesis With a Conjugate of HPMA Copolymer and TNP-470. *Nat. Med.* **2004,** *10*, 255.

9. Khandare, J. J.; Jayant, S.; Singh, A.; Chandna, P.; Wang, Y.; Vorsa, N.; Minko, T., Dendrimer Versus Linear Conjugate: Influence of Polymeric Architecture on the Delivery and Anticancer Effect of Paclitaxel. *Bioconjugate Chem.* **2006,** *17*, 1464-1472.

10. Li, C.; Wallace, S., Polymer-Drug Conjugates: Recent Development in Clinical Oncology. *Adv. Drug Del. Rev.* **2008,** *60*, 886-898.

11. Liechty, W. B.; Kryscio, D. R.; Slaughter, B. V.; Peppas, N. A., Polymers for Drug Delivery Systems. *Annu. Rev. Chem. Biomol. Eng.* **2010,** *1*, 149-173.

12. Abe, K.; Kimura, H., The Possible Role of Hydrogen Sulfide as an Endogenous Neuromodulator. *J. Neurosci.* **1996,** *16*, 1066-1071.

13. Fang, L.; Li, H.; Tang, C.; Geng, B.; Qi, Y.; Liu, X., Hydrogen Sulfide Attenuates the Pathogenesis of Pulmonary Fibrosis Induced by Bleomycin in Rats. *Can. J. Physiol. Pharmacol.* **2009,** *87*, 531-538.

14. Polhemus, D. J.; Li, Z.; Pattillo, C. B.; Gojon, G., Sr.; Gojon, G., Jr.; Giordano, T.; Krum, H., A Novel Hydrogen Sulfide Prodrug, SG1002, Promotes Hydrogen Sulfide and Nitric Oxide Bioavailability in Heart Failure Patients. *Cardiovasc. Ther.* **2015,** *33*, 216-26.

15. Giuliani, D.; Ottani, A.; Zaffe, D.; Galantucci, M.; Strinati, F.; Lodi, R.; Guarini, S., Hydrogen Sulfide Slows Down Progression of Experimental Alzheimer's Disease by Targeting Multiple Pathophysiological Mechanisms. *Neurobiol. Learn. Mem.* **2013,** *104*, 82-91.

16. Powell, C. R.; Dillon, K. M.; Matson, J. B., A Review of Hydrogen Sulfide (H_2S) Donors: Chemistry and Potential Therapeutic Applications. *Biochem. Pharmacol.* **2018,** *149*, 110-123.

17. Foster, J. C.; Matson, J. B., Functionalization of Methacrylate Polymers with Thiooximes: A Robust Postpolymerization Modification Reaction and a Method for the Preparation of H_2S-Releasing Polymers. *Macromolecules* **2014,** *47*, 5089-5095.

18. Powell, C. R.; Foster, J. C.; Okyere, B.; Theus, M. H.; Matson, J. B., Therapeutic Delivery of H_2S via COS: Small Molecule and Polymeric Donors with Benign Byproducts. *J. Am. Chem. Soc.* **2016,** *138*, 13477-13480.

19. Ercole, F.; Mansfeld, F. M.; Kavallaris, M.; Whittaker, M. R.; Quinn, J. F.; Halls, M. L.; Davis, T. P., Macromolecular Hydrogen Sulfide Donors Trigger Spatiotemporally Confined Changes in Cell Signaling. *Biomacromolecules* **2016,** *17*, 371-383.

20. Li, Z.; Li, D.; Wang, L.; Lu, C.; Shan, P.; Zou, X.; Li, Z., Photocontrollable Water-Soluble Polymeric Hydrogen Sulfide (H_2S) Donor. *Polymer* **2019**.

21. Xiao, Z.; Bonnard, T.; Shakouri-Motlagh, A.; Wylie, R. A. L.; Collins, J.; White, J.; Heath, D. E.; Hagemeyer, C. E.; Connal, L. A., Triggered and Tunable Hydrogen Sulfide Release from Photogenerated Thiobenzaldehydes. *Chemistry – A European Journal* **2017,** *23*, 11294-11300.

22. Foster, J. C.; Radzinski, S. C.; Zou, X.; Finkielstein, C. V.; Matson, J. B., H_2S-Releasing Polymer Micelles for Studying Selective Cell Toxicity. *Mol. Pharm.* **2017,** *14*, 1300-1306.

23. Foster, J. C.; Carrazzone, R. J.; Spear, N. J.; Radzinski, S. C.; Arrington, K. J.; Matson, J. B., Tuning H_2S Release by Controlling Mobility in a Micelle Core. *Macromolecules* **2019,** *52*, 1104-1111.

24. Tempelaar, S.; Mespouille, L.; Coulembier, O.; Dubois, P.; Dove, A. P., Synthesis and Post-Polymerisation Modifications of Aliphatic Poly(carbonate)s Prepared by Ring-Opening Polymerisation. *Chem. Soc. Rev.* **2013,** *42*, 1312-1336.

25. Zhu, K.; Hendren, R.; Jensen, K.; Pitt, C., Synthesis, Properties, and Biodegradation of Poly(1, 3-trimethylene carbonate). *Macromolecules* **1991,** *24*, 1736-1740.

26. Edlund, U.; Albertsson, A.-C.; Singh, S.; Fogelberg, I.; Lundgren, B., Sterilization, Storage Stability and In Vivo Biocompatibility of Poly(trimethylene carbonate)/Poly(adipic anhydride) Blends. *Biomaterials* **2000,** *21*, 945-955.

27. Lin, B.; Waymouth, R. M., Urea Anions: Simple, Fast, and Selective Catalysts for Ring-Opening Polymerizations. *J. Am. Chem. Soc.* **2017,** *139*, 1645-1652.

28. Pratt, R. C.; Lohmeijer, B. G. G.; Long, D. A.; Lundberg, P. N. P.; Dove, A. P.; Li, H.; Wade, C. G.; Waymouth, R. M.; Hedrick, J. L., Exploration, Optimization, and Application of Supramolecular Thiourea−Amine Catalysts for the Synthesis of Lactide (Co)polymers. *Macromolecules* **2006,** *39*, 7863-7871.

29. Naumann, S.; Thomas, A. W.; Dove, A. P., Highly Polarized Alkenes as Organocatalysts for the Polymerization of Lactones and Trimethylene Carbonate. *ACS Macro Letters* **2016,** *5*, 134-138.

30. Nederberg, F.; Zhang, Y.; Tan, J. P. K.; Xu, K.; Wang, H.; Yang, C.; Gao, S.; Guo, X. D.; Fukushima, K.; Li, L.; Hedrick, J. L.; Yang, Y.-Y., Biodegradable Nanostructures with Selective Lysis of Microbial Membranes. *Nat. Chem.* **2011,** *3*, 409.

31. Anderski, J.; Mahlert, L.; Sun, J.; Birnbaum, W.; Mulac, D.; Schreiber, S.; Herrmann, F.; Kuckling, D.; Langer, K., Light-Responsive Nanoparticles Based on New Polycarbonate Polymers as Innovative Drug Delivery Systems for Photosensitizers in PDT. *Int. J. Pharm.* **2019,** *557*, 182-191.

32. Wang, H.; Wang, Y.; Chen, Y.; Jin, Q.; Ji, J., A Biomimic pH-Sensitive Polymeric Prodrug Based on Polycarbonate for Intracellular Drug Delivery. *Polym. Chem.* **2014,** *5*, 854-861.

33. Yi, X.; Zhang, Q.; Dong, H.; Zhao, D.; Xu, J.-q.; Zhuo, R.; Li, F., One-Pot Synthesis of Crosslinked Amphiphilic Polycarbonates as Stable but Reduction-Sensitive Carriers for Doxorubicin Delivery. *Nanotechnology* **2015,** *26*, 395602.

34. Dove, A. P.; Pratt, R. C.; Lohmeijer, B. G. G.; Waymouth, R. M.; Hedrick, J. L., Thiourea-Based Bifunctional Organocatalysis: Supramolecular Recognition for Living Polymerization. *J. Am. Chem. Soc.* **2005,** *127*, 13798-13799.

35. Lin, B.; Waymouth, R. M., Organic Ring-Opening Polymerization Catalysts: Reactivity Control by Balancing Acidity. *Macromolecules* **2018,** *51*, 2932-2938.

36. Hiki, S.; Kataoka, K., Versatile and Selective Synthesis of "Click Chemistry" Compatible Heterobifunctional Poly(ethylene glycol)s Possessing Azide and Alkyne Functionalities. *Bioconjugate Chem.* **2010,** *21*, 248-254

4.8. Experimental

Materials and Methods

All reagents were obtained from commercial vendors and used as received unless otherwise stated. NMR spectra were measured on Agilent 400 MHz or Bruker 500 MHz spectrometers. ^{1}H and ^{13}C NMR chemical shifts are reported in ppm relative to internal solvent resonances. CH_2Cl_2 and THF were dried and degassed on solvent columns (MBraun) containing alumina absorbent and stored in a Strauss flask under N_2 before use. Other solvents were used as received unless otherwise noted. Yields refer to chromatographically and spectroscopically pure compounds unless otherwise stated. Thin-layer chromatography (TLC) was performed on glass-backed silica plates and visualized by UV unless otherwise stated. Size exclusion chromatography (SEC) was carried out in THF at 1 mL/min at 30 °C on two Agilent PLgel 10 μM MIXED-B columns connected in series with a Wyatt Dawn Heleos 2 light scattering detector and a Wyatt Optilab Rex refractive index detector. H_2S release was monitored via an ISO-H2S-100 electrochemical probe operating at a constant 100 nA. TU catalyst was synthesized according to literature procedure.[1]

Synthesis of acetonide-protected trimethylolethane **(1)**

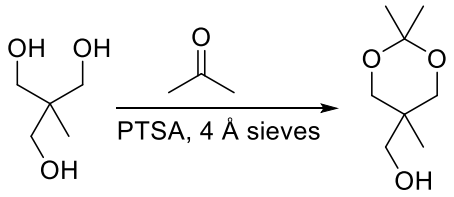

A three-neck round bottom flask equipped with a glass vacuum adaptor and two septa was charged with 4 Å molecular sieves and a stir bar. The flask was flame-dried under vacuum and then put under positive N_2 pressure. Acetone (400 mL) was added to the round bottom flask and allowed to dry over sieves for 24 h. The flask was charged with trimethylolethane (40 g, 250 mmol) and *p*-

toluenesulfonic acid (PTSA) (2.5 g, 15 mmol) and set to stir. The trimethylolethane slowly dissolved over the course of ~20 min to give a clear, colorless solution. The mixture was stirred overnight at rt. To quench the reaction potassium carbonate (K_2CO_3) (5.0 g, 36 mmol) was added and the resulting suspension was stirred for 30 min. The excess K_2CO_3 and molecular sieves were filtered off via vacuum filtration and the filtrate was concentrated via rotary evaporation. The resulting oil was purified by vacuum distillation to give pure **1** was a clear oil (b.p. 75 °C at 400 mtorr, literature value 75 °C at 400 mtorr[2]) (22.03 g, 55 % yield). ^{1}HNMR ($CDCl_3$): δ 3.62 (m, 6H), 2.37 (broad s, 1H), 1.40 (m, 6H), 0.81 (s, 3H). ^{13}C NMR ($CDCl_3$): δ 98.1, 66.4, 65.9, 34.9, 27.4, 20.2, 17.7.

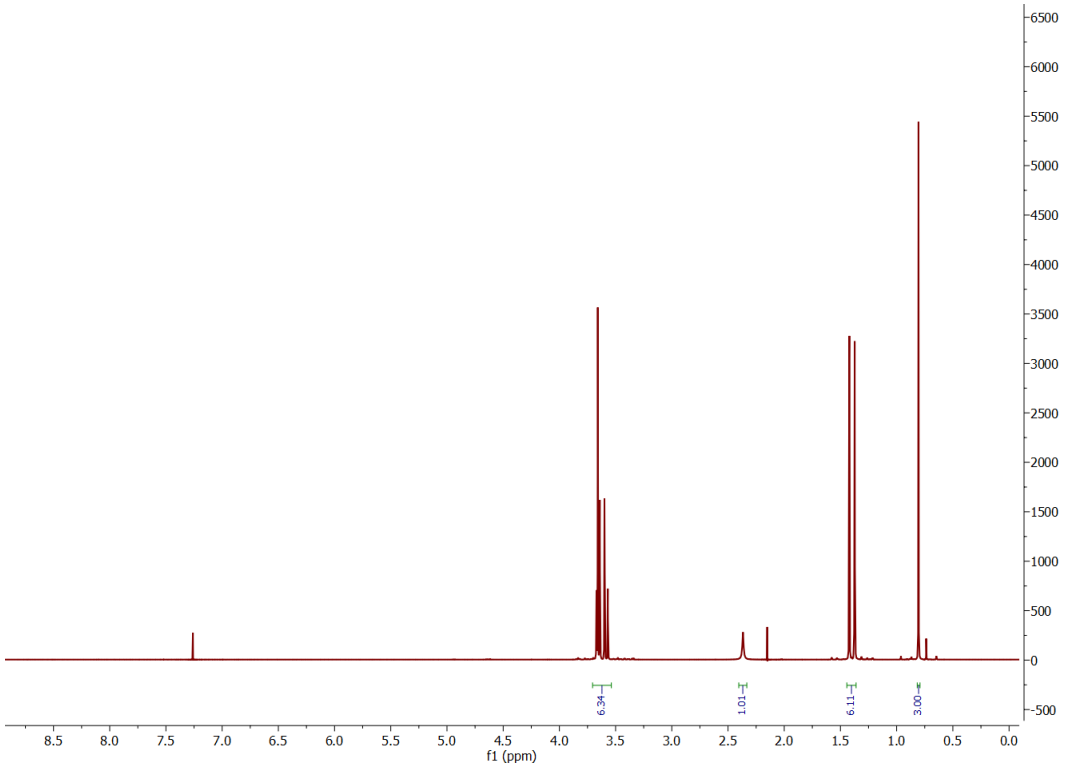

Figure S1. ^{1}H NMR spectrum ($CDCl_3$) of **1**.

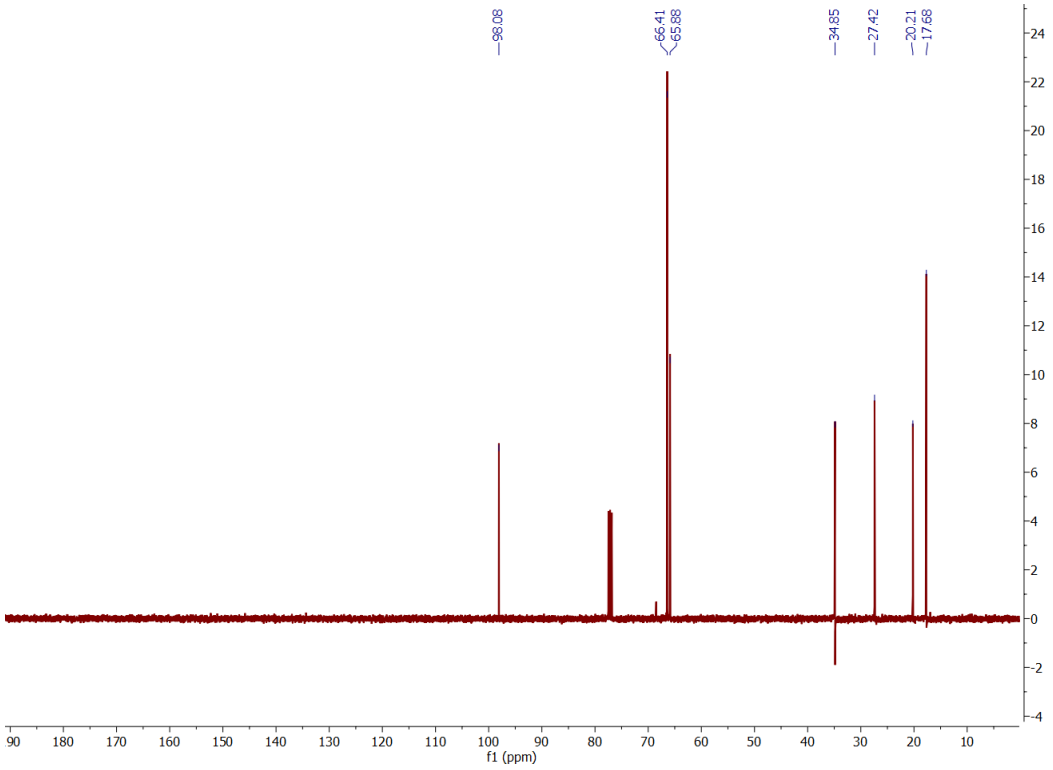

Figure S2. ^{13}C NMR spectrum ($CDCl_3$) of **1**.

Synthesis of acetonide-protected trimethylolethane tosylate **(2)**

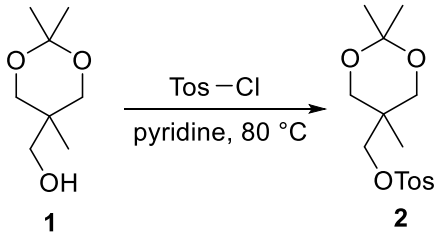

1 **2**

Procedure adapted from Peng et al.[3] A round bottom flask equipped with an addition funnel was charged with **1** (12.86 g, 80.3 mmol), pyridine (40 mL), and a magnetic stir bar to give a clear solution. A separate round bottom flask was charged with *p*-toluene sulfonyl chloride (Tos–Cl) and pyridine to give a clear, yellow solution. The Tos–Cl solution was transferred to the addition funnel and added dropwise to the solution of **1** with vigorous stirring at rt. Once addition of the Tos–Cl solution was complete, the reaction flask was equipped with a condenser and heated to 100

°C in an oil bath. Reaction progress was monitored by TLC (5 % MeOH in CH_2Cl_2) and showed complete consumption of starting material within 30 min. Once complete, the brown reaction solution was removed from the oil bath and cooled to rt, resulting in the formation of colorless crystals. Once cooled the reaction mixture was poured into ice water with vigorous stirring, resulting in the precipitation of **2** as a white solid. The precipitate was isolated via vacuum filtration and washed with ice cold water and dried in vacuo to give **2** as a white solid (11.73 g, 93 % yield). The product was used without further purification. NMR data matches literature precedent.[3] ^{1}H NMR ($CDCl_3$): δ 7.26 (m, 2H) 7.31 (m, 2H), 4.03 (s, 2H), 3.50 (m, 5H), 2.39 (s, 3H), 1.25 (m, 6H), 0.75 (s, 3H). ^{13}C NMR ($CDCl_3$): δ 144.8, 132.4, 129.8, 128.0, 98.0, 72.6, 65.6, 33.8, 27.6, 21.6, 19.2, 17.1.

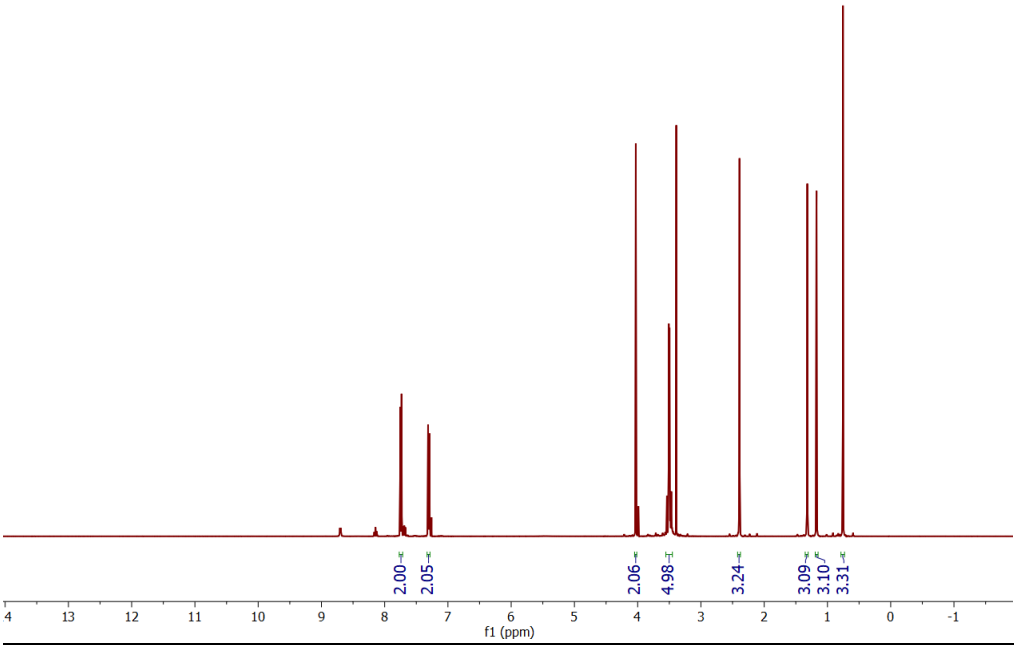

Figure S3. ^{1}H NMR spectrum ($CDCl_3$) of **2**.

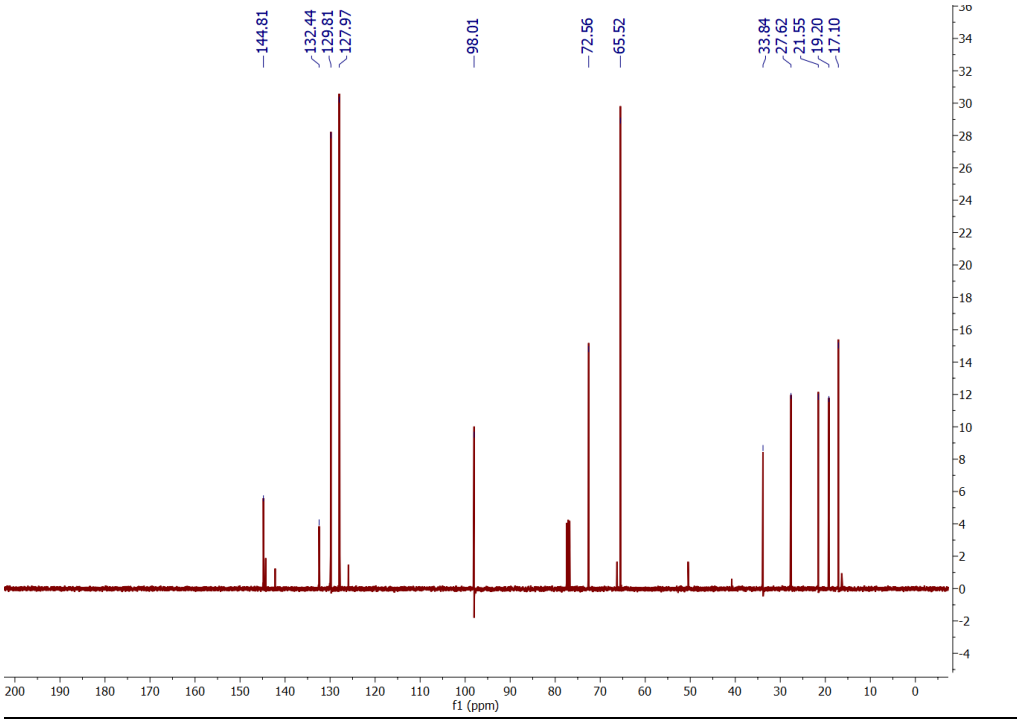

Figure S4. ^{13}C NMR spectrum ($CDCl_3$) of **2**.

Synthesis of acetonide-protected trimethylolethane azide **(3)**

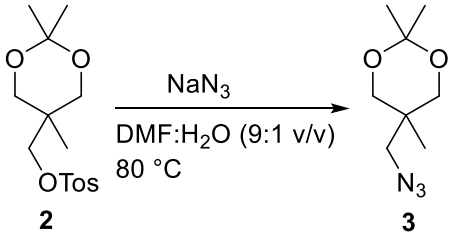

Procedure adapted from Liu et al.[4] A round bottom flask was charged with **2** (9.50 g, 51.3 mmol) and a magnetic stir bar. Product **2** was then dissolved in DMF (50 mL) to give a clear solution. A separate round bottom flask was charged with NaN_3 (6.14 g, 95.0 mmol) dissolved in water (5 mL). The NaN_3 solution was added to the solution of **2** in one portion. The flask containing **2** and NaN_3 was equipped with a condenser and heated to 80 °C in an oil bath. Reaction progress was monitored by TLC (50 % EtOAc in hexanes, visualized by iodine stain) and showed completion

after 32 h. The flask was removed from the oil bath and allowed to cool to rt. The reaction mixture was diluted with water (100 mL), transferred to a separatory funnel, and extracted with Et_2O (5 x, 20 mL). The organics were combined, dried over Na_2SO_4, and concentrated via rotary evaporation to give a crude yellow/brown oil. The crude product was then purified by silica gel chromatography (eluting 20 % EtoAc in hexanes, visualized by iodine stain) to give product **3** (6.84 g, 72 % yield). NMR data matches literature precedent.[4] ^{1}H NMR ($CDCl_3$): δ 7.77 (m, 2H) 7.34 (m, 2H), 3.74 (d, *J* = 8 Hz, 2H), 1.74 (t, *J* = 2 Hz, 1H), 1.34 (s, 12H). ^{13}C NMR ($CDCl_3$): δ 144.43, 135.31, 127.50, 83.90, 29.18, 24.98.

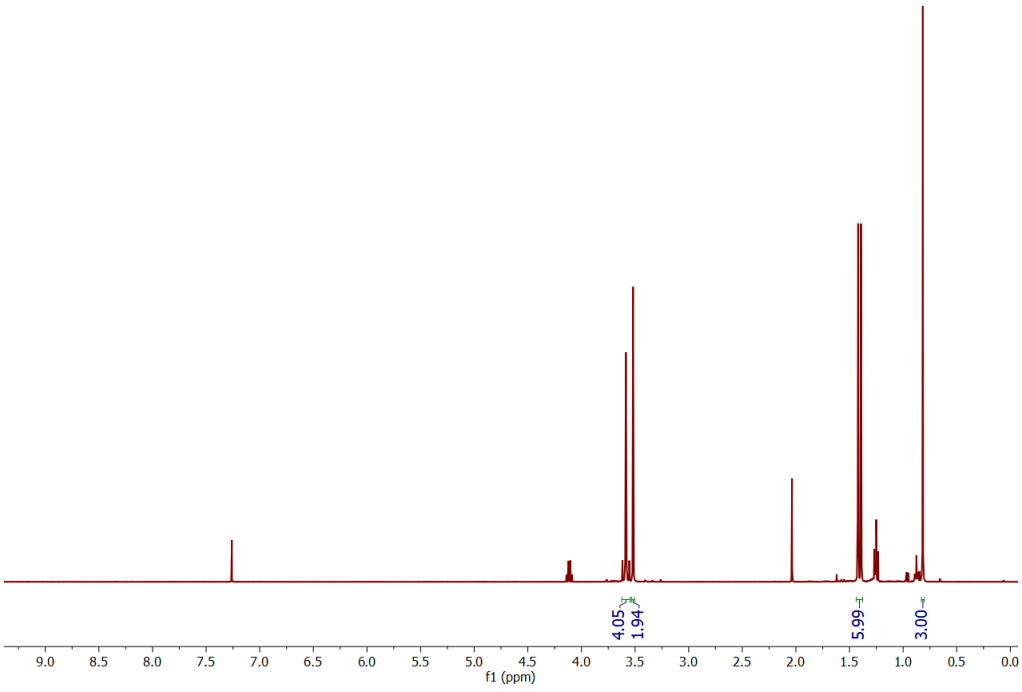

Figure S5. ^{1}H NMR spectrum ($CDCl_3$) of **3**.

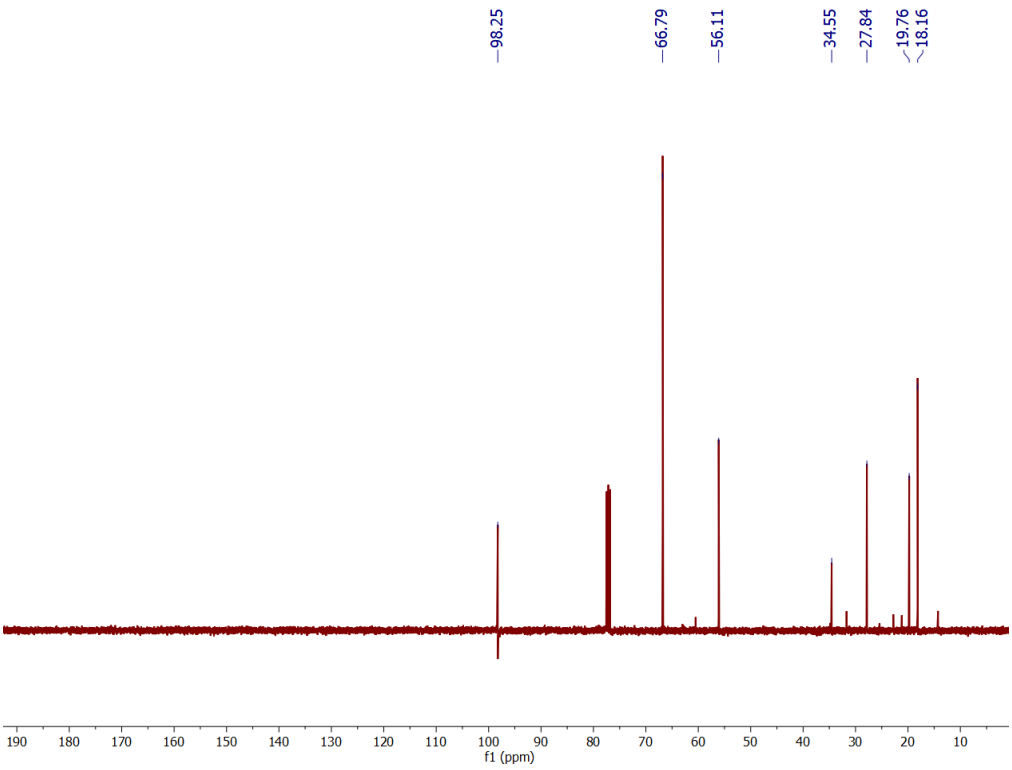

Figure S6. ^{13}C NMR spectrum ($CDCl_3$) of **3**.

Synthesis of 2-(azidomethyl)-2-methylpropane-1,3-diol **(4)**

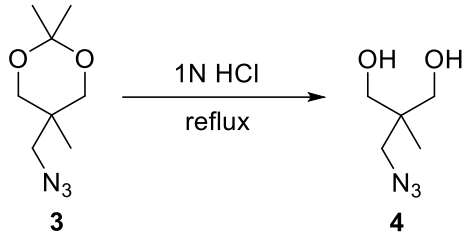

3 **4**

A round bottom flask was charged with **3** (5.42 g, 29.3 mmol) and a magnetic stir bar. Product **3** was dissolved in THF (50 mL) and 9 N HCl (5 mL) was added in one portion. The flask was equipped with a condenser and heated to 90 °C in an oil bath. Reaction progress was monitored by TLC (5 % MeOH in CH_2Cl_2), showing completion after 90 min. The solvent was removed by rotary evaporator to give product **4** (4.25 g, quant.), which was carried forward without further

purification. ^{1}H NMR ($CDCl_3$): δ 4.02 (broad s, 2H), 3.54 (s, 4H), 3.39 (s, 2H) 0.84 (s, 3H). ^{13}C NMR ($CDCl_3$): δ 67.4, 55.5, 41.1, 17.5.

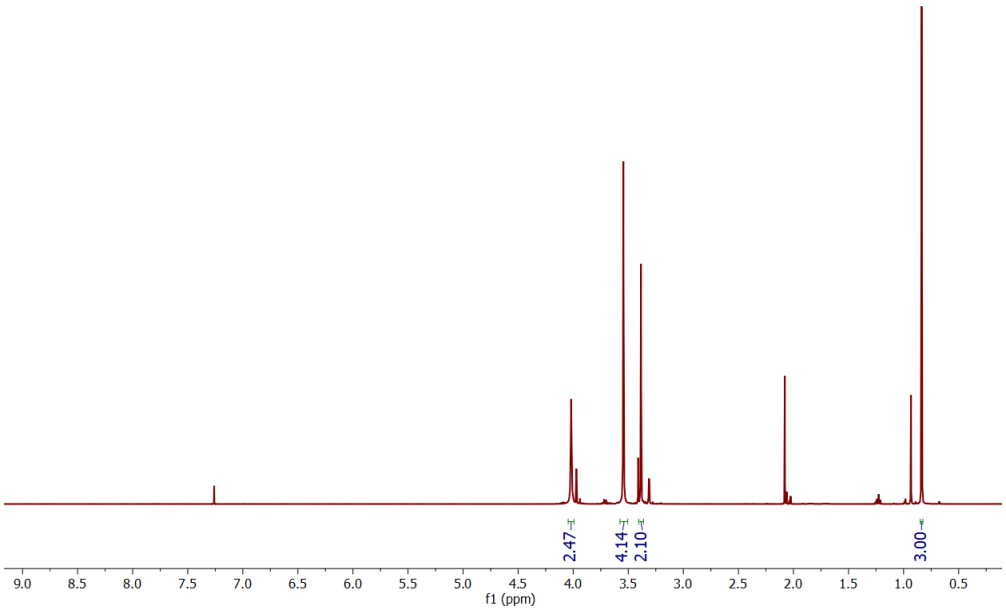

Figure S7. ^{1}H NMR spectrum ($CDCl_3$) product **4**.

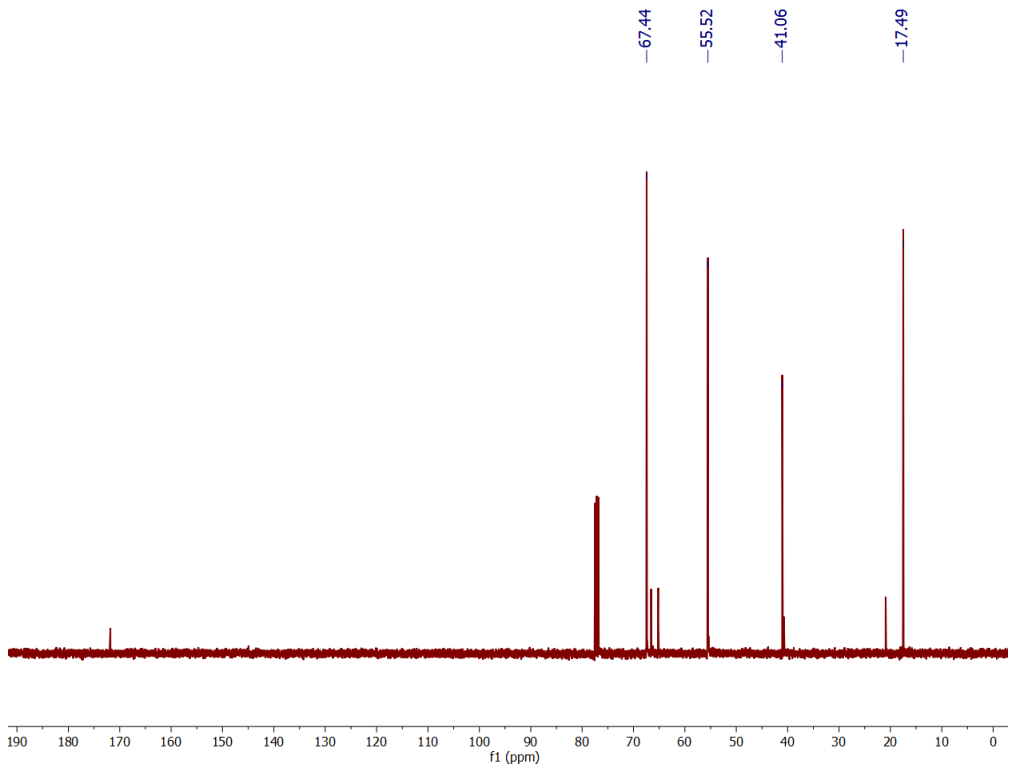

Figure S8. ^{13}C NMR spectrum ($CDCl_3$) of product **4**.

Synthesis of cyclic carbonate azide monomer **(CM-N_3)**

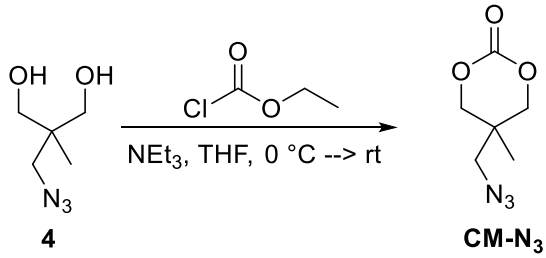

Procedure adapted from Li et al.[5] A three-neck round bottom flask equipped with a glass vacuum adapter, an addition funnel, and a rubber septum was charged with a magnetic stir bar. The flask was flame-dried under vacuum and back-filled with N_2. The flask was charged with **4** (3.80 g, 26.2 mmol) which was subsequently dissolved in THF (150 mL) to give a clear, colorless solution. The solution was cooled to 0 °C in an ice bath. Ethyl chloroformate (5.3 mL, 55 mmol) was added in one portion via syringe at 0 °C and the reaction was allowed to stir for 10 min. Distilled

triethylamine (NEt_3) was then added dropwise via the addition funnel at 0 °C resulting in the formation of the white triethylammonium hydrochloride precpitate. Once addition of NEt_3 was complete, the reaction was allowed to stir at 0 °C for an additional 30 min at which point the flask was removed from the ice bath and the mixture was stirred at rt for 16 h. The triethylammonium salt was filtered off via vacuum filtration and the filtrate was concentrated via rotary evaporation to give a crude off-white product. The crude product was then recrystallized twice from THF to give pure **CM-N_3** (3.34 g, 75 % yield) (m.p. = 79.4 – 82.0 °C). NMR spectra match literature precedent.[5] ^{1}H NMR ($CDCl_3$): δ 4.17 (m, 4H), 3.48 (s, 2H), 1.10 (s, 3H). ^{13}C NMR ($CDCl_3$): δ 147.7, 73.8, 54.1, 32.9, 17.5.

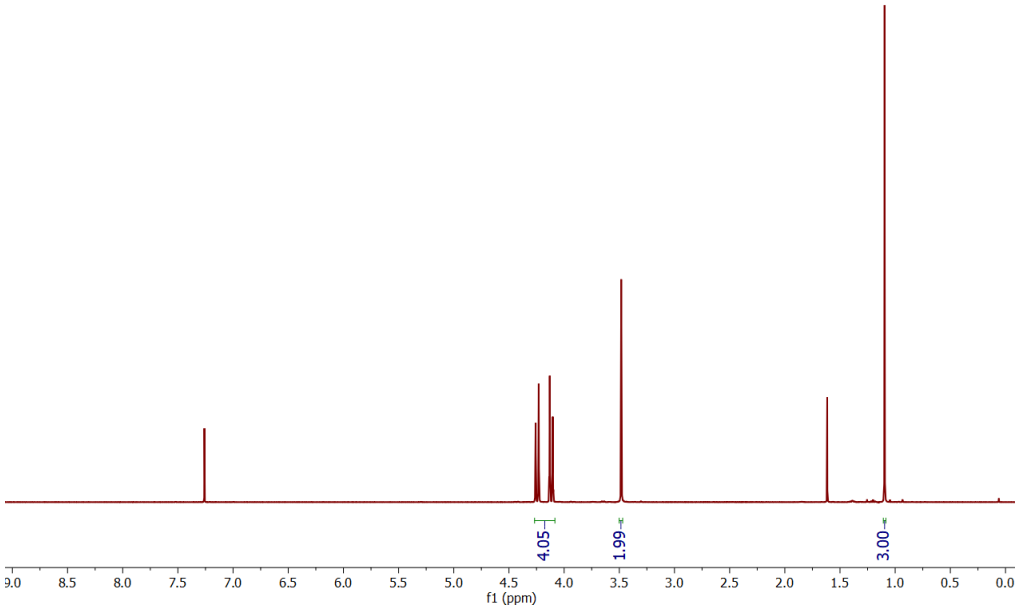

Figure S9. ^{1}H NMR spectrum ($CDCl_3$) of **CM-N_3.**

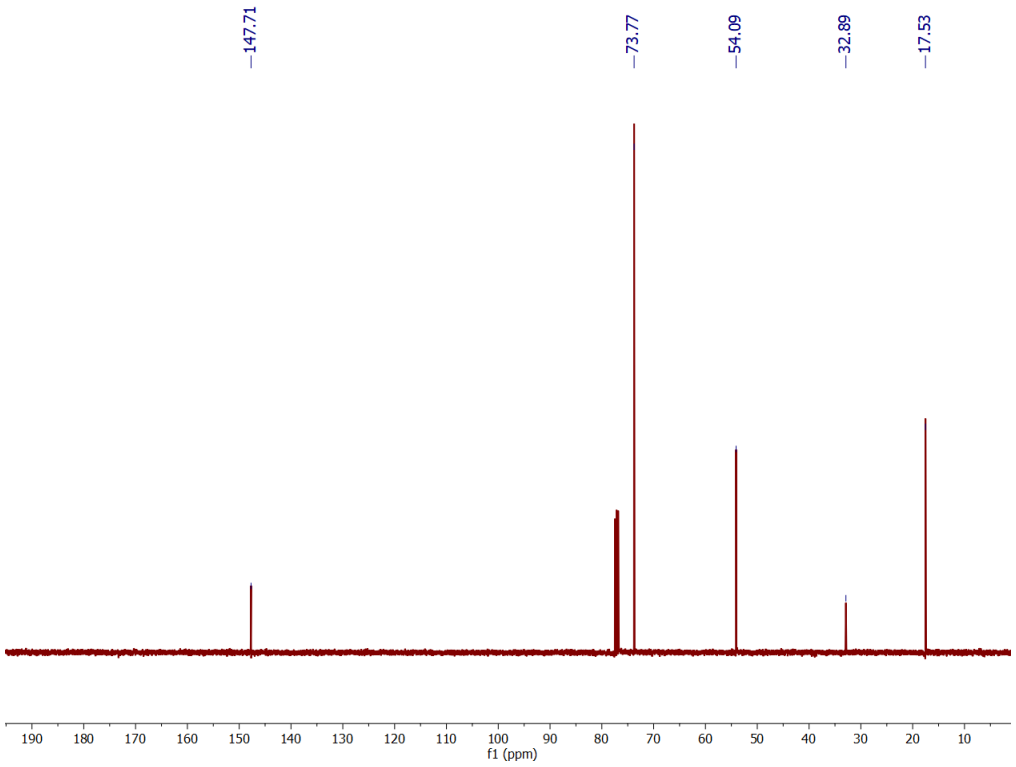

Figure S10. ^{13}C NMR spectrum ($CDCl_3$) of **CM-N$_3$**.

*Polymerization of **CM-N$_3$*** **(PC-N$_3$)**.

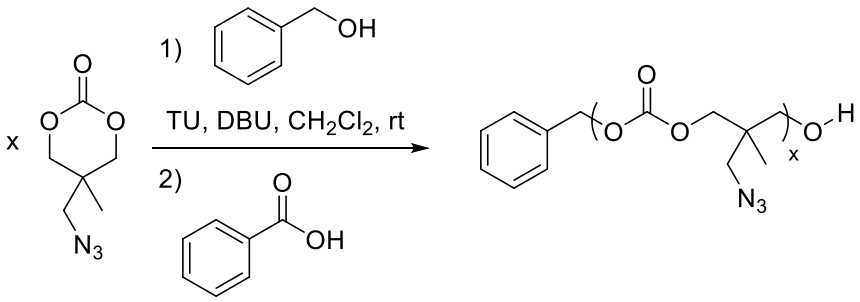

A two-neck round bottom flask equipped with a glass vacuum adapter and a rubber septum was charged with a magnetic stir bar. The flask was flame-dried under vacuum and backfilled with N_2. The flask was then charged with **CM-N$_3$** (0.850 g, 5.0 mmol) and CH_2Cl_2 (9 mL) to give a clear, colorless solution. A separate flame-dried, two-neck round bottom flask was charged with TU (80 mg, 0.2 mmol) and CH_2Cl_2 (2 mL) to give a suspension of TU. Freshly distilled DBU (30 μL, 0.2

mmol) was added to the flask containing TU, resulting in a soluble TU:DBU complex. The stock solution of TU:DBU cocatalysts (1 mL) was added to the polymerization flask in one portion, and the polymerization was set to stir at rt. Conversion was monitored by ^{1}H NMR ($CDCl_3$) removing aliquots and quenching with excess benzoic acid (0.5 M in CH_2Cl_2), removing as much CH_2Cl_2 as possible by passing a stream of air through the vial. Polymerization reached > 90 % conv. in approximately 10 h. To quench, benzoic acid (1 mL, 0.5 M in CH_2Cl_2) was added and stirred for additional 10 min. **PC-N_3** is then precipitated into MeOH at -98 °C by cooling in liquid N_2, collected, and reprecipitated into hexanes (680 mg, 80 % yield).

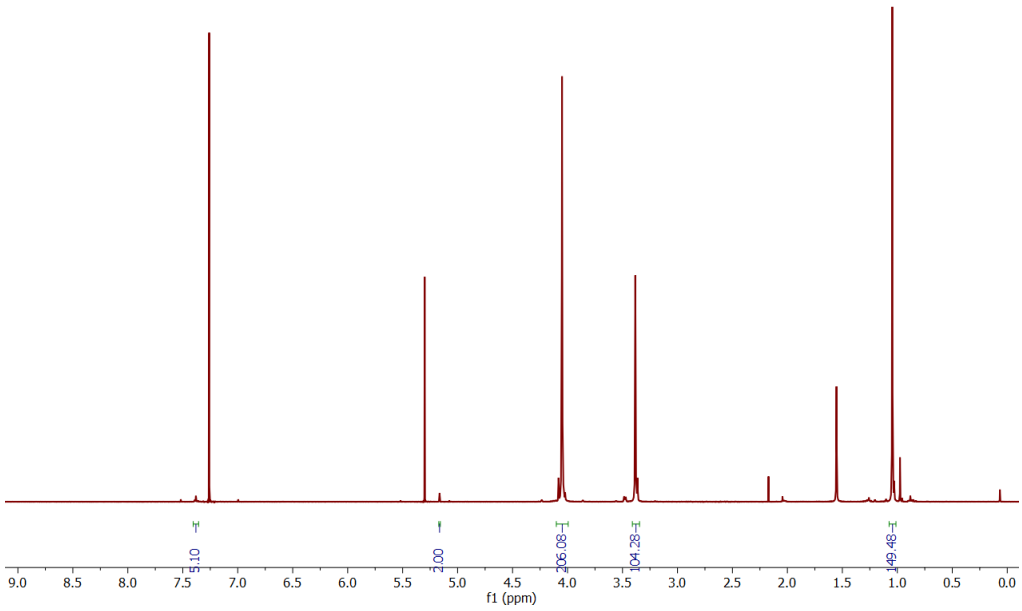

Figure S11. ^{1}H NMR spectrum ($CDCl_3$) of **PC-N_3**.

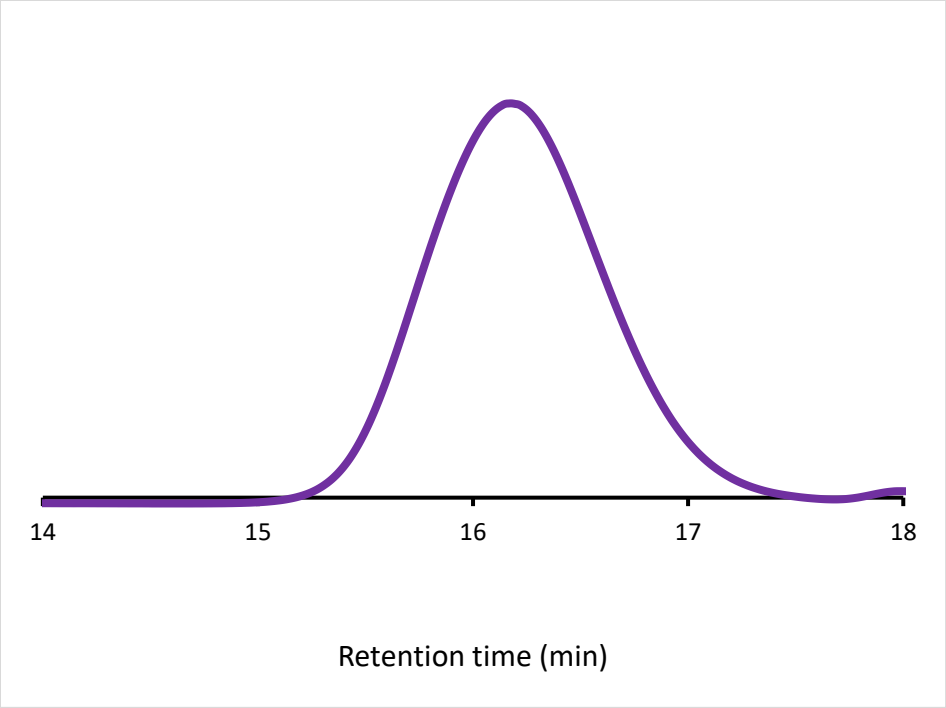

Figure S12. Representatitve SEC (RI trace) of **PC-N$_3$** (M_n = 8.4 kg/mol, Đ = 1.11). M_n calculated by SEC-MALS, d*n*/d*c* value (0.06 in THF) calculated by assuming 100 % mass recovery.

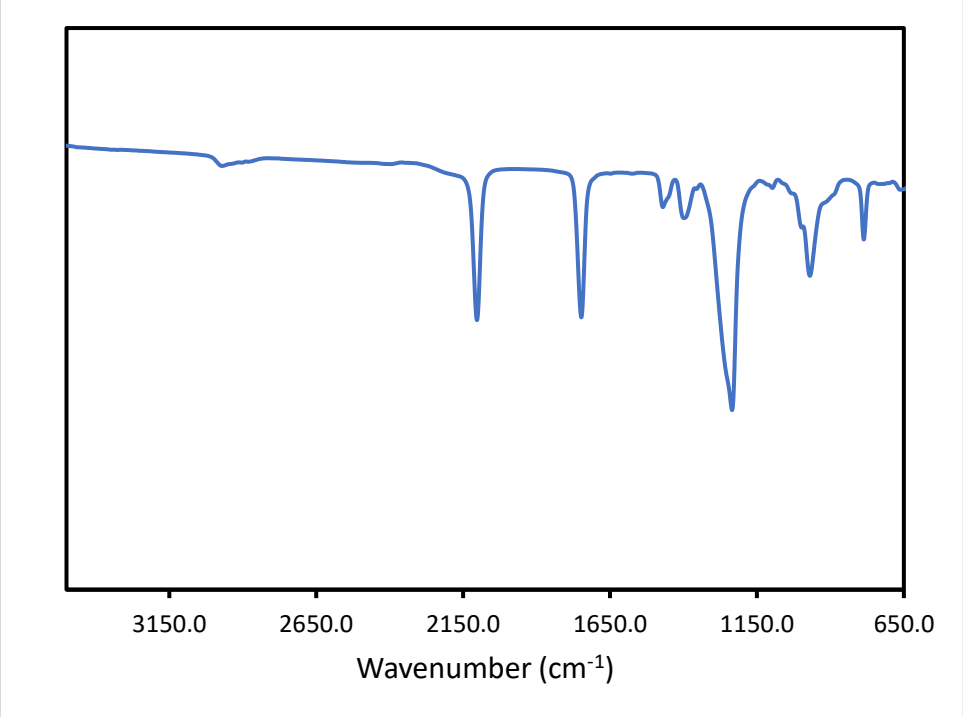

Figure S13. FTIR spectrum of **PC-N$_3$** where the azide stretch absorbance can be seen at 2100 cm^{-1}.

Synthesis of **PC-*graft*-PEG**

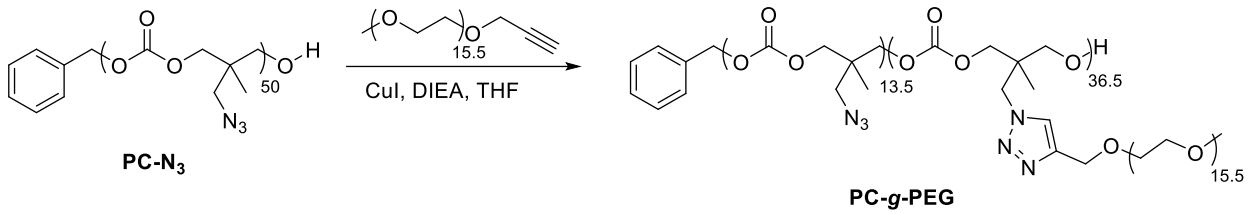

PC-N_3 **PC-*g*-PEG**

A two-neck round bottom flask equipped with a glass vacuum adapter and rubber septum was charged with **PC-N_3** (80 mg, 10 μmol) and a magnetic stir bar. **PC-N_3** was dissolved in THF (1 mL) to give a clear, colorless solution. PEG_{750} alkyne (300 mg, 390 μmol) was added to a separate 1 dram vial and dissolved in THF (1 mL) to give a clear, yellow solution, which was subsequently added to the vial containing **PC-N_3** in one portion. DIEA (20 μL, 120 μmol) was added to the yellow reaction solution. The solution was deoxygenated via bubbling with N_2 for 30 min. CuI (6 mg, 30 μmol) was added under positive N_2 pressure and the reaction was set to stir vigorously at rt for 16 h; reaction conversion was monitored by aliquoting the reaction into $CDCl_3$ and acquiring ^1H NMR spectra. Once complete, the reaction mixture was passed through a column of neutral alumina and concentrated to ~1 mL of THF. The reaction mixture was then precipitated twice into diethyl ether at 0 °C to give **PC-*g*-PEG** (320 mg, 84 % yield) as a viscous yellow oil.

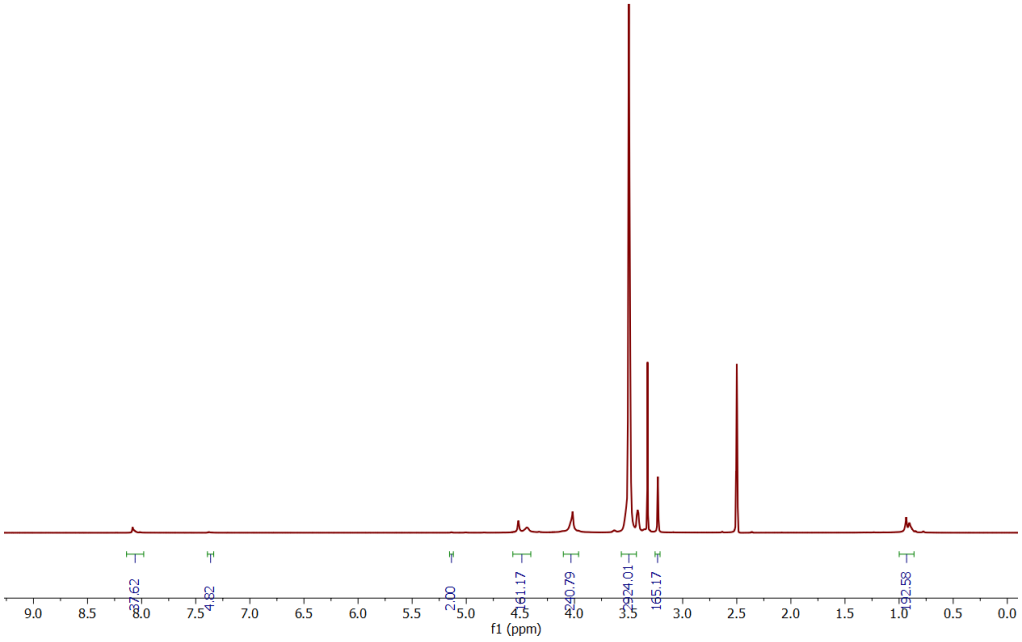

Figure S14. ^{1}H NMR spectrum (DMSO-d_6) of **PC-*g*-PEG** (64 scans, 10 s T_1 relaxation) with integration of the triazole peak (δ = 8.1 ppm) used to calculate conversion of the CuAAC reaction between **PC-N$_3$** and PEG_{750} alkyne.

Synthesis of **PC-*graft*-PEG-NTA**

A two-neck round bottom flask equipped with a glass vacuum adapter and rubber septum was charged with **PC-*g*-PEG** (38 mg, 1.2 μmol) and a magnetic stir bar. **PC-*g*-PEG** was dissolved in THF (2 mL) to give a clear, yellow solution. **NTA4** (5.2 mg, 24 μmol) and DIEA (1.3 μL, 7.3 μmol) were subsequently added and the solution was deoxygenated via bubbling with N_2 for 30 min. CuI (1.2 mg, 6.3 μmol) was added then added and the solution was set to stir vigorously at rt. The reaction was monitored visually and as soon a yellow precipitate began to form the reaction was cooled to 0 °C in an ice bath and diluted with THF. The reaction mixture was passed through

a column of neutral alumina, concentrated to ~1 mL THF and precipitated twice into cold diethyl ether to give **PC-*g*-PEG-NTA** (34 mg).

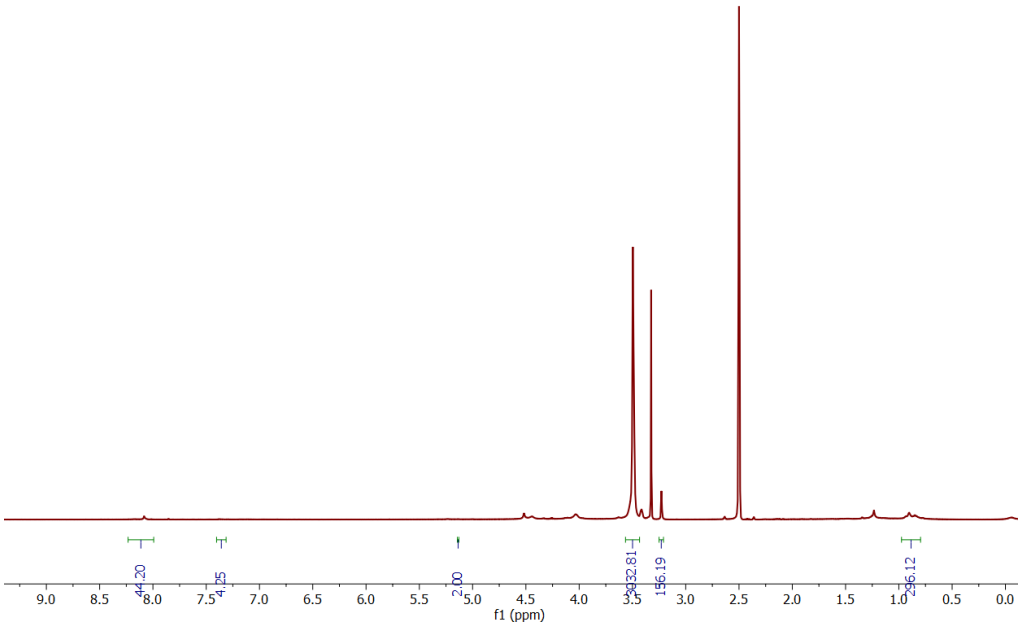

Figure S15. ^{1}H NMR spectrum (DMSO-d_6) of **PC-*g*-PEG-NTA** (64 scans, 10 s T_1 relaxation) with integration of the triazole peak (δ = 8.1 ppm) showing an increase from 37.5 to 44.2 over the integration of **PC-*g*-PEG** under the same ^{1}H NMR experimental conditions. This result indicates that the CuAAC reaction went to ~42 % conversion.

Experimental References

1. Tripathi, C. B.; Mukherjee, S., Lewis Base Catalysis by Thiourea: N-Bromosuccinimide-Mediated Oxidation of Alcohols. *J. Org. Chem.* **2012,** *77*, 1592-1598.
2. Ouchi, M.; Inoue, Y.; Wada, K.; Iketani, S.; Hakushi, T.; Weber, S., Molecular Design of Crown Ethers. 4. Syntheses and Selective Cation Binding of 16-Crown-5 and 19-Crown-6 Lariats. *J. Org. Chem.* **1987**, 52, 2420-2427.
3. Liu, S.-T.; Wang, H.-E.; Cheng, M.-C.; Peng, S.-M., Unusual Tripodal Ligands. Synthesis of 2,2-Bis(diphenylphosphinomethyl)-1-phenylthiopropane and its Group VI Complexes. *J. Organomet. Chem.* **1989,** *376* (2), 333-342.
4. Liu, S. T.; Liu, C. Y., Synthesis of Amino-Containing Phosphines. The Use of Iminophosphorane as a Protecting Group for Primary Amines. *J. Org. Chem.* **1992,** *57* (22), 6079-6080.
5. Dan, Z.; Ma, S.; Yi, X.; Cheng, S.; Zhuo, R.; Li, F., Reversible Core-Crosslinked Nanocarriers with pH-Modulated Targeting and Redox-Controlled Drug Release for Overcoming Drug Resistance. *Journal of Materials Chemistry B* **2017,** *5* (42), 8399-8407.

Chapter 5: A Reactive Oxygen Species (ROS)-Responsive Persulfide Donor: Insights into Reactivity and Therapeutic Potential

Adapted with permission from: Powell, C. R., et al. (2018). "A Reactive Oxygen Species (ROS)-Responsive Persulfide Donor: Insights into Reactivity and Therapeutic Potential" Angewandte Chemie **130**: 6432-6436. Copyright 2018 Wiley-VCH Verlag GmbH & Co. KGaA.

5.1. Authors

Chadwick R. Powell,[§,†] Kearsley M. Dillon,[§,†] Yin Wang, [§,†] Ryan J. Carrazzone, [§,†] and John B. Matson*[§,†]

§Department of Chemistry, Virginia Tech, Blacksburg, Virginia 24061, United States
† Virginia Tech Center for Drug Discovery, Virginia Tech, Blacksburg, Virginia 24061, United States

5.2. Abstract

Persulfides (R–SSH) have been hypothesized as critical components in sulfur-mediated redox cycles and as potential signaling compounds, similar to hydrogen sulfide (H_2S). Hindering the study of persulfides is a lack of persulfide donor compounds with selective triggers that release discrete persulfide species. Herein we report the synthesis and characterization of an ROS-responsive, self-immolative persulfide donor. The donor, termed BDP-NAC, showed selectivity towards H_2O_2 over other potential oxidative or nucleophilic triggers, resulting in the sustained release of the persulfide of *N*-acetyl cysteine (NAC) over the course of 2 h, as measured by LCMS. Exposure of H9C2 cardiomyocytes to H_2O_2 revealed that BDP-NAC mitigated the effects of a highly oxidative environment in a dose-dependent manner over relevant controls and to a greater degree than common H_2S donors sodium sulfide (Na_2S) and GYY4137. BDP-NAC also rescued

cells more effectively than a non-persulfide releasing control compound with a Bpin moiety in concert with common H_2S donors and thiols.

5.3. Introduction

Hydrogen sulfide (H_2S) plays a key signaling role in mammalian biology and has been under investigation as a potential therapeutic via exogenous delivery.[1-4] To help elucidate its biological roles, chemists have synthesized several types of H_2S releasing compounds (termed H_2S donors) with a variety of biologically relevant triggers, including water,[5-8] nucleophiles (e.g., thiols, amines),[9-10] enzymes,[11-13] and light[14-15]. Additionally, compounds that release carbonyl sulfide (COS),[16-17] and sulfur dioxide (SO_2),[18-19] have recently been reported, allowing for the study of other small molecule sulfur species as potential signaling compounds. These donors aid in our understanding of the physiological roles of H_2S and related compounds, and hold potential therapeutic value via exogenous H_2S delivery.[20-22] Interestingly, recent studies into the redox chemistry of sulfur species in the body indicate that persulfides (R–SSH) may have physiological roles similar to H_2S, insinuating that some of the physiological effects ascribed to delivery of H_2S may actually be derived from persulfides.[23-26] Further study of persulfides is needed to differentiate between the roles of H_2S itself and its biological products. Moreover, a clear description of sulfur redox chemistry in a biological context will allow further development of therapeutics that exploit pathways involved in H_2S signaling.

Dean and coworkers first identified persulfides in a biological context in their 1994 report on a protein persulfide intermediate of the cysteine desulfurase NifS.[27] Persulfides are prevalent in mammalian biology, generated via reaction of an oxidized thiol (e.g., a sulfenic acid, R–SOH) with H_2S in a process called S-persulfidation.[28] More nucleophilic than thiols, persulfides have

pK_a values a few units lower than their corresponding thiols,[29] as well as greater reduction potentials,[30] making them highly reactive, transiently stable species. In a biological context, persulfides protect thiols from irreversible oxidation, serve as reactive intermediates in sulfur shuttling,[31] and alter enzymatic activity.[32-33] Some examples of protein persulfidation and the resulting changes in protein activity include: an increased parkin activity upon S-persulfidation resulting in a decrease in Parkinson's symptoms,[34] an increase in activity of GAPDH, protecting cells from apoptosis,[35] and H-Ras activation in cardiac tissue, regulating cellular redox signaling.[36] More recently, studies have confirmed the presence of endogenously produced small molecule persulfides (e.g., cysteine persulfide and glutathione persulfide) with reported concentrations as high as 150 μM in human and mouse tissue.[23] Small molecule persulfides likely play a role in regulating cellular redox balance and mediating cellular signaling.[25] A major barrier in the study of the biological roles of persulfides is a lack of chemical tools capable of generating well-defined persulfide species in response to specific, biologically relevant triggers. Our understanding of H_2S biology has been aided immensely by the synthesis of organic H_2S donors; analogous to H_2S, persulfide donors will be vital tools for understanding how persulfides fit into the overall web of redox signaling.

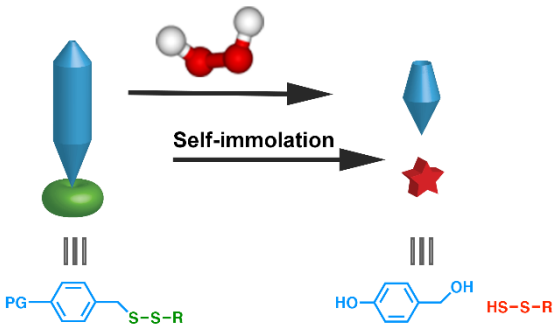

Figure 1. Cartoon schematic representing the proposed release of a discrete persulfide species from a generalized self-immolative prodrug (PG = protecting group) in the presence of a trigger (H_2O_2 shown here).

Polysulfides ($RS–(S)_n–SR$), such as naturally occurring diallyl trisulfide (DATS), are perhaps the best known type of persulfide donor, but their reactivity in biological systems is complex, leading to generation of other redox-active species, including H_2S.[37-39] As a result, polysulfides are not ideal persulfide donors for use in studying persulfide biology, and the complex product mixture may limit their therapeutic potential. Free persulfides (i.e., R–SSH) have been isolated, but they suffer from poor stability under storage conditions and poor water solubility, and thus have relatively low utility in a practical sense.[39] Persulfides are also proposed intermediates in several types of H_2S donors,[9-10] but these compounds all require conditions that cause rapid conversion of the persulfide into H_2S. To date there exist only two families of compounds capable of generating discrete persulfides: Wang and coworkers developed esterase-triggered persulfide prodrugs capable of releasing either a persulfide or hydrogen persulfide (HSSH) and Galardon and coworkers developed a pH-triggered persulfide analog of the nitrosothiol SNAP.[40-42] These donors generate persulfides without concomitant generation of H_2S and can be viewed as spontaneous persulfide donors due to the ubiquity of esterases *in vitro* and *in vivo*.

5.4. Results and Discussion

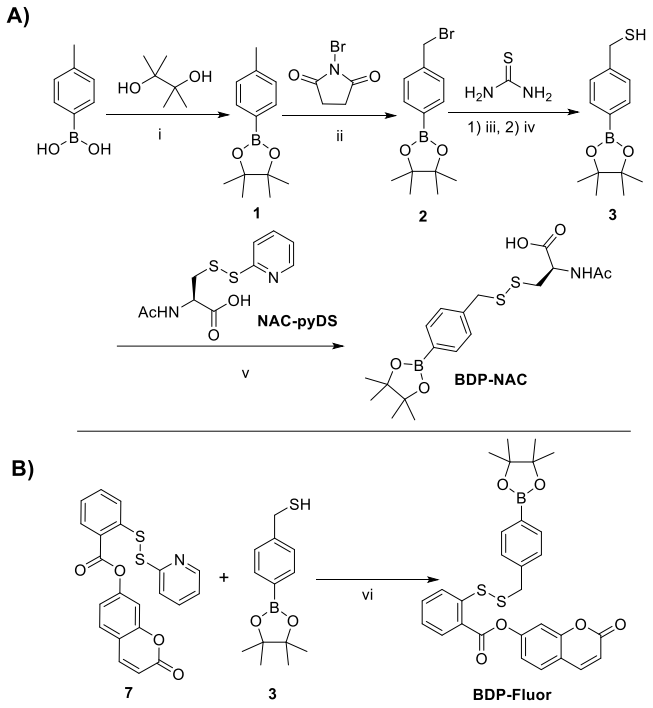

Scheme 1. A) Synthetic route to **BDP-NAC**. Conditions: i) $MgSO_4$, Et_2O, rt, 16 h; ii) AIBN, C_6H_{12}, reflux, 16 h; iii) 1) EtOH, rt, 4 h; iv) 1 N NaOH, reflux, 45 min; v) NEt_3, $CHCl_3$, rt, 3 h; B) Synthetic route to **BDP-Fluor**. Conditions: vi) $CHCl_3$:MeOH (1:1 v/v), rt, 40 h.

We sought to synthesize a discrete persulfide donor scaffold, inert under normal physiological conditions but capable of self-immolation in response to a specific trigger, revealing a discrete persulfide species (Figure 1). As the triggering moiety and persulfide could be readily tuned, this system would enable persulfide generation in response to many types of triggers, providing a valuable set of laboratory tools similar to the self-immolative COS donors recently reported by Pluth and coworkers.[43] In addition to their use as biological tools to study persulfide reactivity, persulfide prodrugs are exciting from a therapeutic standpoint because the reduction potential of persulfides is higher than that of thiols or H_2S, making them prime candidates for

scavenging and reducing the harmful effects resulting from high levels of reactive oxygen species (ROS). Therefore, we aimed to synthesize an ROS-responsive persulfide prodrug as a proof of concept. This would allow for a two-stage quenching of ROS: the initial reaction of the ROS with the prodrug to trigger release, followed by the release of the persulfide. We envisioned that such an ROS-triggered persulfide prodrug would be ideal for cytoprotection against harmful levels of ROS.

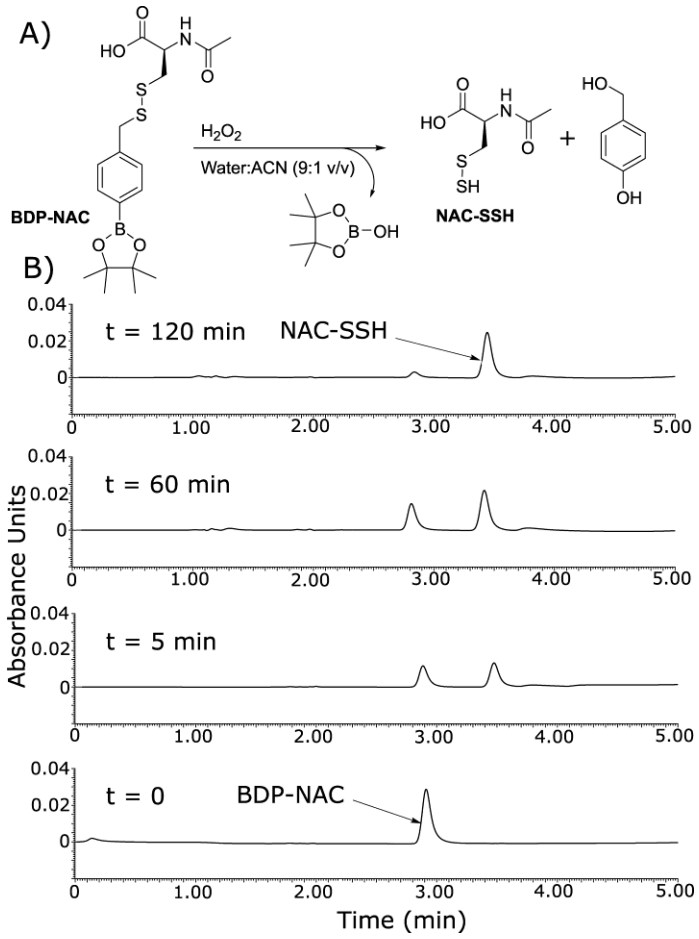

Figure 2. A) Proposed reaction of **BDP-NAC** in the presence of H_2O_2 leading to the release of **NAC–SSH**. B) LC chromatograms highlighting the conversion of **BDP-NAC** into NAC persulfide (**NAC-SSH**) in the presence of H_2O_2. Timepoints are noted above each LC chromatogram. The peak eluting at 2.9 min corresponds to **BDP-NAC**, and the peak at 3.4 min corresponds to **NAC-SSH** (see Figure S20 for corresponding mass spectrometry data).

Aryl boronic esters are relatively easy to synthesize, generally biocompatible, and react selectively with ROS in a B–C bond cleavage reaction to reveal the corresponding phenolate. Therefore, we set out to synthesize a self-immolative persulfide donor containing an aryl boronic ester as an ROS-sensitive trigger. The desired persulfide donor (termed **BDP-NAC** for Bpin-disulfide prodrug-*N*-acetyl cysteine) was synthesized from commercially available 4-tolylboronic acid in four steps (Scheme 1A). Theoretically, any thiol may be installed on the distal end of the disulfide bond from the trigger/self-immolation moiety. Our choice of *N*-acetyl cysteine (NAC) was motivated by its biocompatibility as well as its ability to protect cells in vitro in highly oxidative environments.[44-45]

The ability of **BDP-NAC** to mediate the release of the desired NAC persulfide (**NAC-SSH**) in response to ROS was analyzed by LCMS (Figure 2). Aliquots of the reaction mixture of **BDP-NAC** with H_2O_2 were injected at various time points until the peak attributed to **BDP-NAC** (2.9 min) had subsided, revealing near complete decomposition of **BDP-NAC** within 2 h. A peak corresponding to **NAC–SSH** (3.4 min) increased in intensity over the course of the reaction, consistent with our proposed mechanism of persulfide generation. Mass spectrometry evidence also confirmed the presence of the other byproduct of the reaction, 4-hydroxybenzyl alcohol (a result of addition of water to the quinone methide), but the chromatogram peak was weak, likely due to low absorbance at the monitoring wavelength.

In addition to LCMS, we also investigated the reaction of **BDP-NAC** with H_2O_2 utilizing ^{1}H NMR spectroscopy. Experiments were conducted in DMSO-d_6:D_2O (9:1 v/v) due to the hydrophobic nature of **BDP-NAC** and the increased concentration required in NMR spectroscopy compared with LCMS. Shortly after the addition of H_2O_2 to the **BDP-NAC** solution, two new sets of peaks in the aryl region of the ^{1}H NMR spectrum appeared. One was consistent with 4-

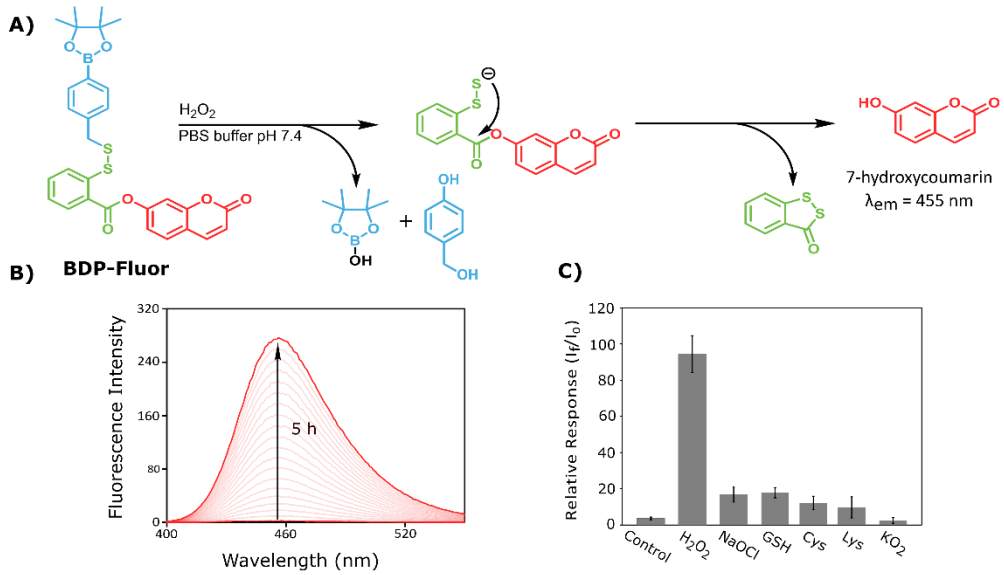

Figure 3. A) Proposed reaction mechanism for the release of 7-hydroxycoumarin from **BDP-Fluor** in the presence of H_2O_2. B) Representative overlay of the fluorescence spectra of **BDP-Fluor** in the presence of 100-fold excess H_2O_2 resulting from the release of 7-hydroxycoumarin over the course of 5 h. C) Relative response of **BDP-Fluor** (3.3 μM) to each potential trigger (330 μM) or control (no trigger added) represented as the ratio of the final fluorescence (I_f) intensity after 5 h to the initial fluorescence intensity (I_0), showing an increased selectivity for H_2O_2 over other potential triggers.

hydroxybenzyl alcohol, and the other was attributed to the slow hydrolysis of the Bpin moiety of **BDP-NAC**, yielding a boronic acid; boronic acids react with H_2O_2 in a similar fashion as pinacol boronic esters.[46] The reaction was considerably slower under these conditions than in the LCMS experiments. This retardation in reaction rate is likely a result of the high organic solvent content in the reaction.[47] Further insights into the stability of **BDP-NAC** as a persulfide prodrug as well as pertinent controls without the Bpin triggering moiety can be found in the SI (Figure S25 and S26).

To further evaluate the reactivity and trigger selectivity of **BDP-NAC**, a profluorophore (**BDP-Fluor**, Scheme 1B) was synthesized. Drawing inspiration from Xian and coworkers' turn-on fluorescence probe (compound **7**) used for detection of sulfane sulfur species (HSSH, RS–$(S)_n$–SR, or S_8), the self-immolative **BDP-Fluor** has the same general structure as **BDP-NAC**, but with a coumarin-based fluorophore as the distal thiol species.[48] As shown in Figure 3A, we expected self-immolation to trigger release of a discrete persulfide, which would then cyclize to form a 5-membered benzodithiolone species, resulting in the release of 7-hydroxycoumarin. Because **BDP-Fluor** itself is not fluorescent, an increase in fluorescence at the characteristic emission wavelength of 7-hydroxycoumarin should only result from persulfide release and subsequent intramolecular cyclization, providing secondary confirmation of persulfide release from these self-immolative prodrug systems.

We tested this design by exposing **BDP-Fluor** to a variety of potential triggers. **BDP-Fluor** showed no evidence of self-immolative behavior (i.e., low fluorescence signal) in the absence of a trigger, but addition of H_2O_2 (100-fold excess) led to a 90-fold increase in fluorescence intensity at the characteristic wavelength of 7-hydroxycoumarin after incubation for 5 h in PBS buffer (Figure 3B and C). When **BDP-Fluor** was treated with other potential triggers, including sodium hypochlorite (NaOCl), cysteine (Cys), glutathione (GSH), lysine (Lys), and potassium superoxide (KO_2), the response was significantly lower, with H_2O_2 showing a greater than 20-fold response over all of these potential triggers, and a greater than 90-fold response over Lys and KO_2.

As the increase in fluorescence response to thiols was unexpected, further investigation indicated that the fluorescence increase may be attributed to nucleophilic attack by cysteine at the aryl ester position, resulting in the release of 7-hydroxycoumarin. For more discussion on the probe response to thiols and relevant controls, see the SI (Figure S22). Taken together, these results

confirm release of the desired persulfide species and demonstrate the selectivity of H_2O_2 as a trigger.

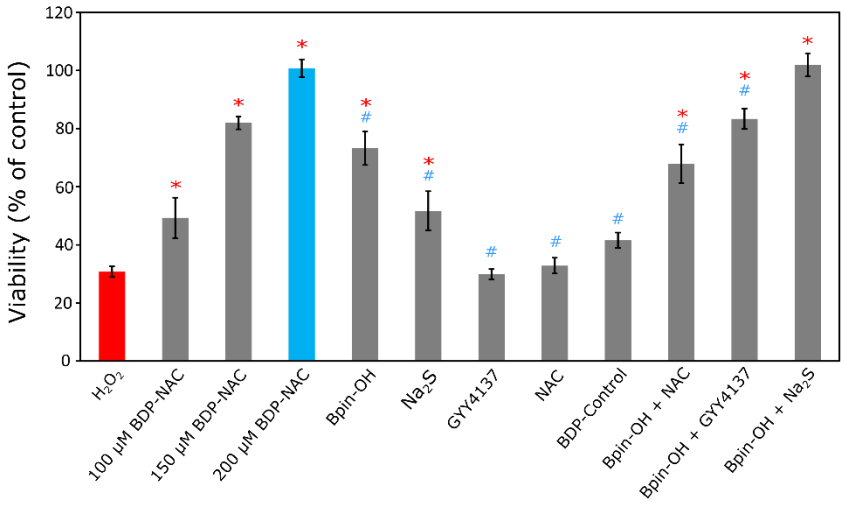

Figure 4. Viability of H9C2 cardiomyoctyes treated with **BDP-NAC** or various controls and related compounds concurrent with exposure to H_2O_2 (100 μM) for 1 h. Each control compound was applied at a concentration of 200 μM (except for Na_2S (100 μM) in the Bpin-OH + Na_2S treatment group). Quantification of viability was carried out using Cell Counting Kit-8 (CCK-8). Results are expressed as the mean ± SEM (n = 10–15 for each treatment group) with 2–3 independent experiments. *P<0.01 for comparisons with the H_2O_2 treatment group and #P<0.01 for comparisons with the **BDP-NAC** (200 μM) treatment group. Group comparisons are indicated as determined by a one-way analysis of variance (ANOVA) with a Student-Newman-Keuls comparisons post-hoc test.

We next aimed to analyze **BDP-NAC** in a biological context. In vitro cytotoxicity studies on H9C2 cardiomyocytes showed that **BDP-NAC** is non-toxic up to 200 μM (Figure S27). As mentioned previously, persulfides have greater reducing potential than their corresponding thiols as well as H_2S. Thus, we envisioned that **BDP-NAC** might be effective in rescuing cells under

oxidative stress, either via direct reduction of H_2O_2 or via upregulation of antioxidant pathways mediated by persulfide signaling.[23, 32] To this end, we evaluated the protective effects of **BDP-NAC** on H9C2 cells in culture via exogenous delivery of H_2O_2, which stresses the cells and promotes apoptosis (Figure 4). In the absence of **BDP-NAC**, cell viability drastically decreased after exposure to H_2O_2 (100 μM) for 1 h. However, simultaneous application of **BDP-NAC** (100–200 μM) with H_2O_2 showed a dose-dependent increase in cell viability, with no cytotoxicity observed after treatment with 200 μM **BDP-NAC**. At longer treatment times (2 h), **BDP-NAC** rescued a similar percentage of cells compared to H_2O_2-only controls (Figure S29). These results indicate that **BDP-NAC** can successfully mitigate the deleterious effects of a hyperoxidative environment in culture.

To further ensure that persulfide release imparts protection to the cardiomyocytes in the presence of H_2O_2, several control studies were carried out. Exposure of the cells to H_2O_2 with added 4-(hydroxymethyl)benzeneboronic acid pinacol ester (Bpin-OH), a non-persulfide releasing compound with a Bpin moiety, showed an increase in viability compared to H_2O_2 alone but did not rescue cells to the same extent as **BDP-NAC**. We also compared **BDP-NAC** to sodium sulfide (Na_2S), a fast-releasing H_2S donor, and GYY4137, a slow-releasing H_2S donor, under the same experimental conditions. Na_2S had a limited ability to rescue cells while GYY4137 had no effect on viability. Interestingly, **BDP-NAC** was more effective at rescuing cells than Na_2S, even while Na_2S enhanced H9C2 proliferation in the absence of H_2O_2 (Figure S28). This provides further evidence that persulfides may serve to maintain redox homeostasis in cells to a greater extent than H_2S. NAC, a potential thiol byproduct after reaction of **BDP-NAC**, also had no effect on viability. To confirm that **BDP-NAC** derives its activity from ROS-triggered persulfide release, the cardiomyocytes were treated with **BDP-Control**, which has an identical structure to **BDP-NAC**,

but without the Bpin triggering moiety. **BDP-Control** also did not rescue cells exposed to H_2O_2 under identical conditions to the previous experiments.

Finally, to recreate the synergistic effects of the Bpin moiety of **BDP-NAC** and the resultant persulfide release, cells were treated with Bpin-OH simultaneously with either NAC, GYY4137, or Na_2S. Each of these combinations was able to mitigate the effects of H_2O_2 on cell viability, but not to the same degree as **BDP-NAC**, with the exception of Bpin-OH + Na_2S. We suspect that simultaneous treatment of the cardiomyocytes with Bpin-OH and Na_2S gives a greater instantaneous concentration of potential antioxidants than **BDP-NAC**, considering its sustained release. In a system with continuous generation of ROS, delivery of Bpin-OH and Na_2S would likely have a diminished ability to rescue cells compared to sustained release from **BDP-NAC**.

5.5. Conclusions

In summary, we have synthesized a self-immolative prodrug that releases a discrete persulfide species (**BDP-NAC**) in the presence of H_2O_2. Persulfide release and trigger specificity were characterized by LCMS, NMR, and fluorescence spectroscopy, demonstrating that sustained release of the persulfide is selectively triggered by H_2O_2. In vitro studies using H9C2 cardiomyocytes under oxidative stress showed that **BDP-NAC** mitigates the harmful effects of highly oxidative environments with greater potency than commonly used H_2S donors Na_2S and GYY4137 as well as relevant controls. **BDP-NAC** not only shows promise therapeutically, but it also provides a modular system for persulfide donors that may be triggered under a variety of conditions. We envision that a library of persulfide donors based on the **BDP-NAC** template will enable the study of persulfide biology in greater depth than is currently possible, providing insight into sulfur redox cycles and sulfur-mediated cell signaling.

5.6. Acknowledgements

This work was supported by the National Science Foundation (DMR-1454754) and the National Institutes of Health (R01GM123508). We also thank 3M for support of this work through a Non-Tenured Faculty Award to JBM. We thank Dr. Tijana Grove and Dr. Webster Santos and their students for experimental assistance as well as Dr. Mehdi Ashraf-Khorassani for help with the LCMS.

5.7. References

1. Wang, R., Two's Company, Three's a Crowd: Can H_2S Be the Third Endogenous Gaseous Transmitter? *FASEB J.* **2002,** *16*, 1792-8.

2. Papapetropoulos, A.; Pyriochou, A.; Altaany, Z.; Yang, G.; Marazioti, A.; Zhou, Z.; Jeschke, M. G.; Branski, L. K.; Herndon, D. N.; Wang, R.; Szabó, C., Hydrogen Sulfide is an Endogenous Simulator of Angiogenesis. *Proc. Natl. Acad. Sci. U. S. A.* **2009,** *106*, 21972-21977.

3. Mustafa, A. K.; Gadalla, M. M.; Snyder, S. H., Signaling by Gasotransmitters. *Sci. Signal* **2009,** *2*, re2-re2.

4. Predmore, B. L.; Lefer, D. J.; Gojon, G., Hydrogen Sulfide in Biochemistry and Medicine. *Antioxid. Redox Signal* **2012,** *17*, 119-40.

5. Zhao, W.; Zhang, J.; Lu, Y.; Wang, R., The Vasorelaxant Effect of H_2S as a Novel Endogenous Gaseous K(ATP) Channel Opener. *EMBO J.* **2001,** *20*, 6008-6016.

6. Nicolau, L. A. D.; Silva, R. O.; Damasceno, S. R. B.; Carvalho, N. S.; Costa, N. R. D.; Aragão, K. S.; Barbosa, A. L. R.; Soares, P. M. G.; Souza, M. H. L. P.; Medeiros, J. V. R., The Hydrogen Sulfide Donor, Lawesson's Reagent, Prevents Alendronate-Induced Gastric Damage in Rats. *Braz. J. Med. Biol. Res.* **2013,** *46*, 708-714.

7. Li, L.; Whiteman, M.; Guan, Y. Y.; Neo, K. L.; Cheng, Y.; Lee, S. W.; Zhao, Y.; Baskar, R.; Tan, C.-H.; Moore, P. K., Characterization of a Novel, Water-Soluble Hydrogen Sulfide–Releasing Molecule (GYY4137). *Circulation* **2008,** *117*, 2351-2360.

8. Zanatta, S. D.; Jarrott, B.; Williams, S. J., Synthesis and Preliminary Pharmacological Evaluation of Aryl Dithiolethiones with Cyclooxygenase-2-Selective Inhibitory Activity and Hydrogen Sulfide-Releasing Properties. *Aust. J. Chem.* **2010,** *63*, 946-957.

9. Zhao, Y.; Wang, H.; Xian, M., Cysteine-Activated Hydrogen Sulfide (H_2S) Donors. *J. Am. Chem. Soc.* **2011,** *133*, 15-17.

10. Foster, J. C.; Powell, C. R.; Radzinski, S. C.; Matson, J. B., S-Aroylthiooximes: A Facile Route to Hydrogen Sulfide Releasing Compounds with Structure-Dependent Release Kinetics. *Org. Lett.* **2014,** *16*, 1558-1561.

11. Zheng, Y.; Yu, B.; Ji, K.; Pan, Z.; Chittavong, V.; Wang, B., Esterase-Sensitive Prodrugs with Tunable Release Rates and Direct Generation of Hydrogen Sulfide. *Angew. Chem. Int. Ed. Engl.* **2016,** *55*, 4514-8.

12. Li, Z.; Organ, C. L.; Zheng, Y.; Wang, B.; Lefer, D. J., Abstract 17903: Novel Esterase-Activated Hydrogen Sulfide Donors Attenuate Myocardial Ischemia/Reperfusion Injury. *Circulation* **2016,** *134*, A17903-A17903.

13. Chauhan, P.; Bora, P.; Ravikumar, G.; Jos, S.; Chakrapani, H., Esterase Activated Carbonyl Sulfide/Hydrogen Sulfide (H_2S) Donors. *Org. Lett.* **2017,** *19*, 62-65.

14. Devarie-Baez, N. O.; Bagdon, P. E.; Peng, B.; Zhao, Y.; Park, C.-M.; Xian, M., Light-Induced Hydrogen Sulfide Release from "Caged" gem-Dithiols. *Org. Lett.* **2013,** *15*, 2786-2789.

15. Fukushima, N.; Ieda, N.; Sasakura, K.; Nagano, T.; Hanaoka, K.; Suzuki, T.; Miyata, N.; Nakagawa, H., Synthesis of a Photocontrollable Hydrogen Sulfide Donor using Ketoprofenate Photocages. *Chem. Commun.* **2014,** *50*, 587-589.

16. Powell, C. R.; Foster, J. C.; Okyere, B.; Theus, M. H.; Matson, J. B., Therapeutic Delivery of H_2S via COS: Small Molecule and Polymeric Donors with Benign Byproducts. *J. Am. Chem. Soc.* **2016,** *138*, 13477-13480.

17. Steiger, A. K.; Pardue, S.; Kevil, C. G.; Pluth, M. D., Self-Immolative Thiocarbamates Provide Access to Triggered H_2S Donors and Analyte Replacement Fluorescent Probes. *J. Am. Chem. Soc.* **2016,** *138*, 7256-7259.

18. Wang, W.; Ji, X.; Du, Z.; Wang, B., Sulfur dioxide prodrugs: triggered release of SO 2 via a click reaction. *Chem. Commun.* **2017,** *53*, 1370-1373.

19. Day, J. J.; Yang, Z.; Chen, W.; Pacheco, A.; Xian, M., Benzothiazole Sulfinate: a Water-Soluble and Slow-Releasing Sulfur Dioxide Donor. *ACS Chem. Biol.* **2016,** *11*, 1647-1651.

20. Zheng, Y.; Yu, B.; De La Cruz, L. K.; Roy Choudhury, M.; Anifowose, A.; Wang, B., Toward Hydrogen Sulfide Based Therapeutics: Critical Drug Delivery and Developability Issues. *Med. Res. Rev.* **2018,** *38*, 57-100.

21. Powell, C. R.; Dillon, K. M.; Matson, J. B., A Review of Hydrogen Sulfide (H_2S) Donors: Chemistry and Potential Therapeutic Applications. *Biochem. Pharmacol.* **2017**, *149*, 110-123.

22. Zhao, Y.; Biggs, T. D.; Xian, M., Hydrogen Sulfide (H_2S) Releasing Agents: Chemistry and Biological Applications. *Chem. Commun.* **2014,** *50*, 11788-11805.

23. Ida, T.; Sawa, T.; Ihara, H.; Tsuchiya, Y.; Watanabe, Y.; Kumagai, Y.; Suematsu, M.; Motohashi, H.; Fujii, S.; Matsunaga, T.; Yamamoto, M.; Ono, K.; Devarie-Baez, N. O.; Xian, M.;

Fukuto, J. M.; Akaike, T., Reactive Cysteine Persulfides and S-polythiolation Regulate Oxidative Stress and Redox Signaling. *Proc. Natl. Acad. Sci. U. S. A.* **2014,** *111*, 7606-11.

24. Yadav, P. K.; Martinov, M.; Vitvitsky, V.; Seravalli, J.; Wedmann, R.; Filipovic, M. R.; Banerjee, R., Biosynthesis and Reactivity of Cysteine Persulfides in Signaling. *J. Am. Chem. Soc.* **2016,** *138*, 289-99.

25. Cuevasanta, E.; Möller, M. N.; Alvarez, B., Biological Chemistry of Hydrogen Sulfide and Persulfides. *Arch. Biochem. Biophys.* **2017,** *617*, 9-25.

26. Filipovic, M. R.; Zivanovic, J.; Alvarez, B.; Banerjee, R., Chemical Biology of H_2S Signaling through Persulfidation. *Chem. Rev.* **2018,** *118*, 1253-1337.

27. Zheng, L.; White, R. H.; Cash, V. L.; Dean, D. R., Mechanism for the Desulfurization of L-Cysteine Catalyzed by the nifS Gene Product. *Biochemistry* **1994,** *33*, 4714-4720.

28. Filipovic, M. R., Persulfidation (S-sulfhydration) and H_2S. In *Chemistry, Biochemistry and Pharmacology of Hydrogen Sulfide*, Moore, P. K.; Whiteman, M., Eds. Springer International Publishing: Cham, 2015; pp 29-59.

29. Cai, Y.-R.; Hu, C.-H., Computational Study of H_2S Release in Reactions of Diallyl Polysulfides with Thiols. *J. Phys. Chem. B* **2017,** *121*, 6359-6366.

30. Francoleon, N. E.; Carrington, S. J.; Fukuto, J. M., The Reaction of H_2S with Oxidized Thiols: Generation of Persulfides and Implications to H_2S Biology. *Arch. Biochem. Biophys.* **2011,** *516*, 146-153.

31. Flint, D. H., Escherichia coli Contains a Protein that is Homologous in Function and N-Terminal Sequence to the Protein Encoded by the nifS Gene of Azotobacter vinelandii and that can Participate in the Synthesis of the Fe-S Cluster of Dihydroxy-acid Dehydratase. *J. Biol. Chem.* **1996,** *271*, 16068-74.

32. Millikin, R.; Bianco, C. L.; White, C.; Saund, S. S.; Henriquez, S.; Sosa, V.; Akaike, T.; Kumagai, Y.; Soeda, S.; Toscano, J. P.; Lin, J.; Fukuto, J. M., The Chemical Biology of Protein Hydropersulfides: Studies of a Possible Protective Function of Biological Hydropersulfide Generation. *Free Radic. Biol. Med.* **2016,** *97*, 136-147.

33. Mueller, E. G., Trafficking in Persulfides: Delivering Sulfur in Biosynthetic Pathways. *Nat. Chem. Biol.* **2006,** *2*, 185-194.

34. Vandiver, M. S.; Paul, B. D.; Xu, R.; Karuppagounder, S.; Rao, F.; Snowman, A. M.; Ko, H. S.; Lee, Y. I.; Dawson, V. L.; Dawson, T. M.; Sen, N.; Snyder, S. H., Sulfhydration Mediates Neuroprotective Actions of Parkin. *Nat. Commun.* **2013,** *4*, 1626.

35. Mustafa, A. K.; Gadalla, M. M.; Sen, N.; Kim, S.; Mu, W.; Gazi, S. K.; Barrow, R. K.; Yang, G.; Wang, R.; Snyder, S. H., H_2S Signals Through Protein S-Sulfhydration. *Sci. Signal* **2009,** *2*, ra72-ra72.

36. Nishida, M.; Sawa, T.; Kitajima, N.; Ono, K.; Inoue, H.; Ihara, H.; Motohashi, H.; Yamamoto, M.; Suematsu, M.; Kurose, H.; van der Vliet, A.; Freeman, B. A.; Shibata, T.; Uchida, K.; Kumagai, Y.; Akaike, T., Hydrogen Sulfide Anion Regulates Redox Signaling via Electrophile Sulfhydration. *Nat. Chem. Biol.* **2012,** *8*, 714-24.

37. Benavides, G. A.; Squadrito, G. L.; Mills, R. W.; Patel, H. D.; Isbell, T. S.; Patel, R. P.; Darley-Usmar, V. M.; Doeller, J. E.; Kraus, D. W., Hydrogen Sulfide Mediates the Vasoactivity of Garlic. *Proc. Natl. Acad. Sci. U. S. A.* **2007,** *104*, 17977-17982.

38. Cerda, M. M.; Hammers, M. D.; Earp, M. S.; Zakharov, L. N.; Pluth, M. D., Applications of Synthetic Organic Tetrasulfides as H_2S Donors. *Org. Lett.* **2017,** *19*, 2314-2317.

39. Park, C.-M.; Weerasinghe, L.; Day, J. J.; Fukuto, J. M.; Xian, M., Persulfides: Current Knowledge and Challenges in Chemistry and Chemical Biology. *Mol. Biosyst.* **2015,** *11*, 1775-1785.

40. Zheng, Y.; Yu, B.; Li, Z.; Yuan, Z.; Organ, C. L.; Trivedi, R. K.; Wang, S.; Lefer, D. J.; Wang, B., An Esterase-Sensitive Prodrug Approach for Controllable Delivery of Persulfide Species. *Angew. Chem. Int. Ed.* **2017,** *56*, 11749-11753.

41. Yu, B.; Zheng, Y.; Yuan, Z.; Li, S.; Zhu, H.; De La Cruz, L. K.; Zhang, J.; Ji, K.; Wang, S.; Wang, B., Toward Direct Protein S-Persulfidation: A Prodrug Approach That Directly Delivers Hydrogen Persulfide. *J. Am. Chem. Soc.* **2018**, *140*, 30-33.

42. Artaud, I.; Galardon, E., A Persulfide Analogue of the Nitrosothiol SNAP: Formation, Characterization and Reactivity. *ChemBioChem* **2014,** *15*, 2361-4.

43. Zhao, Y.; Henthorn, H. A.; Pluth, M. D., Kinetic Insights into Hydrogen Sulfide Delivery from Caged-Carbonyl Sulfide Isomeric Donor Platforms. *J. Am. Chem. Soc.* **2017,** *139*, 16365-16376.

44. Zafarullah, M.; Li, W.; Sylvester, J.; Ahmad, M., Molecular Mechanisms of N-Acetylcysteine Actions. *Cell. Mol. Life Sci.* **2003,** *60*, 6-20.

45. Murphy, N. P.; Lampe, K. J., Fabricating PLGA microparticles with High Loads of the Small Molecule Antioxidant N-Acetylcysteine that Rescue Oligodendrocyte Progenitor Cells from Oxidative Stress. *Biotechnol. Bioeng.* **2018,** *115*, 246-256.

46. Kuivila, H. G., Electrophilic Displacement Reactions. III. Kinetics of the Reaction between Hydrogen Peroxide and Benzeneboronic Acid. *J. Am. Chem. Soc.* **1954,** *76*, 870-874.

47. Schmid, K. M.; Jensen, L.; Phillips, S. T., A Self-Immolative Spacer That Enables Tunable Controlled Release of Phenols under Neutral Conditions. *J. Org. Chem.* **2012,** *77*, 4363-4374.

48. Chen, W.; Liu, C.; Peng, B.; Zhao, Y.; Pacheco, A.; Xian, M., New Fluorescent Probes for Sulfane Sulfurs and the Application in Bioimaging. *Chem. Sci.* **2013,** *4*, 2892-2896.

5.8. Experimental

Materials and Methods

All reagents were obtained from commercial vendors and used as received unless otherwise stated. NMR spectra were measured on Agilent 400 MHz or Bruker 500 MHz spectrometers. ^{1}H and ^{13}C NMR chemical shifts are reported in ppm relative to internal solvent resonances. CH_2Cl_2 was dried and degassed on solvent columns (MBraun) containing alumina absorbent and stored in a Strauss flask under N_2 before use. Other solvents were used as received unless otherwise noted. Yields refer to chromatographically and spectroscopically pure compounds unless otherwise stated. Thin-layer chromatography (TLC) was performed on glass-backed silica plates and visualized by UV unless otherwise stated. Thiosalicylic acid-pyDS and GYY4137 were synthesized according to literature procedures.[1,2] LCMS experiments were performed on a Waters Acquity UPLC system equipped with a Waters Polarity C_{18}-functionalized silica column, diode array detector, and ESI mass spectrometer. Fluorescence spectra were recorded in a 1 cm quartz cuvette on a Cary Eclipse fluorescence spectrophotometer equipped with a PMT detector (600 V), excitation and emission slit widths of 5 nm, 600 nm/min scan speed, and 1.00 nm step. High-resolution mass spectra were taken on an Agilent Technologies 6230 TOF LC/MS mass spectrometer.

Cell studies were conducted on an adherent H9C2 line of rat embryonic cardiomyocytes (ATCC, Manassas, VA, USA). Cultures were grown in Dulbecco's Modified Eagle Medium (DMEM, VWR, Radnor, PA), supplemented with 10 % fetal bovine serum (FBS, VWR, Radnor, PA). Cells were cultured at 37 °C in 5 % CO_2-air. The cultures were passaged after 70–80 % confluence was

achieved. Cells were rinsed with PBS solution, and then released with trypsin and EDTA solution (VWR, Radnor, PA). The suspension of released cells was centrifuged at 1000 rpm for 5 min.

Synthesis of p-Tolylboronic Acid Pinacol Ester **(1)**

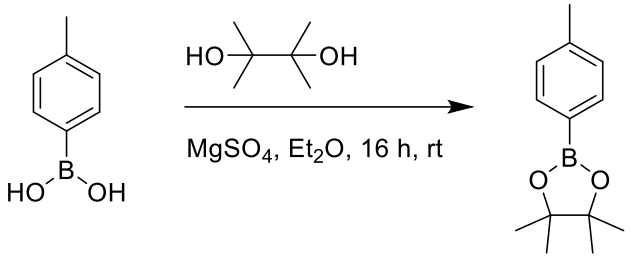

1

A round bottom flask equipped with a septum was charged with diethyl ether (300 mL), *p*-tolylboronic acid (10 g, 74 mmol), and a stir bar. The white suspension was stirred until all solids dissolved (30 min – 1 h). $MgSO_4$ (15 g, 125 mmol) and pinacol (8.9 g, 75 mmol) were then added sequentially to the solution while stirring. The reaction mixture was stirred at rt for 16 h, at which point the reaction was complete by TLC (50:50 hexanes:EtOAc). The resulting white suspension was then filtered, rinsed with diethyl ether (250 mL), and concentrated via rotary evaporation, yielding compound **1** (12.9 g, 87% yield) as white crystals. This product was used in the next reaction step without further purification. Spectroscopic data agree with literature precedent.[3] ^{1}H-NMR ($CDCl_3$): δ 7.70 (m, 2H), 7.19 (m, 2H), 2.37 (s, 3H), 1.34 (s, 12H). ^{13}C-NMR ($CDCl_3$): δ 141.5, 134.9, 128.6, 83.7, 25.0, 21.9.

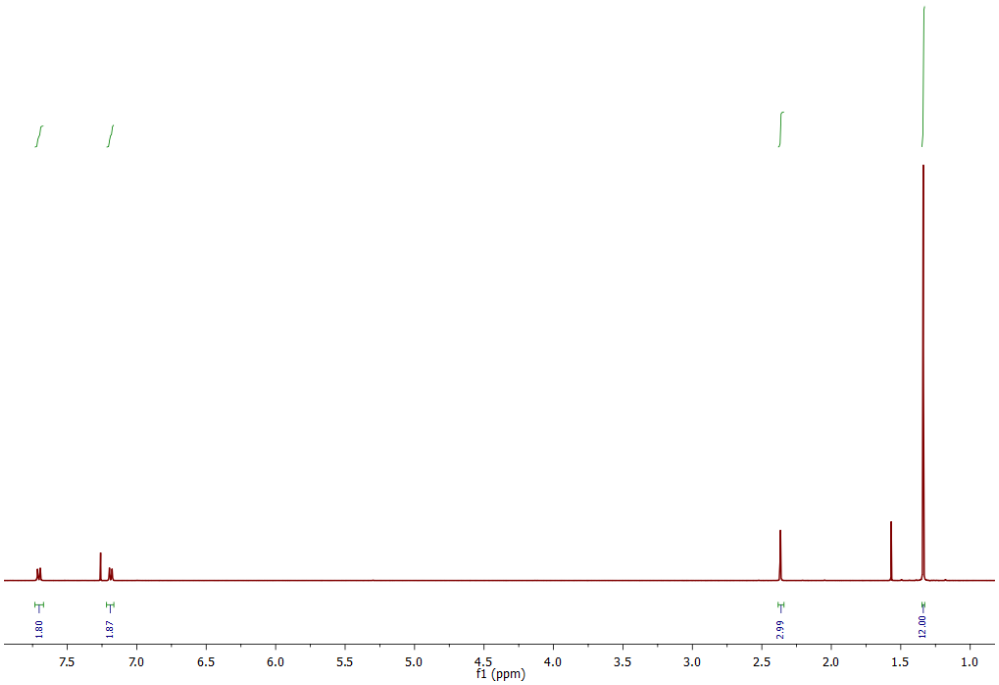

Figure S1. ^{1}H NMR spectrum ($CDCl_3$) of **1**.

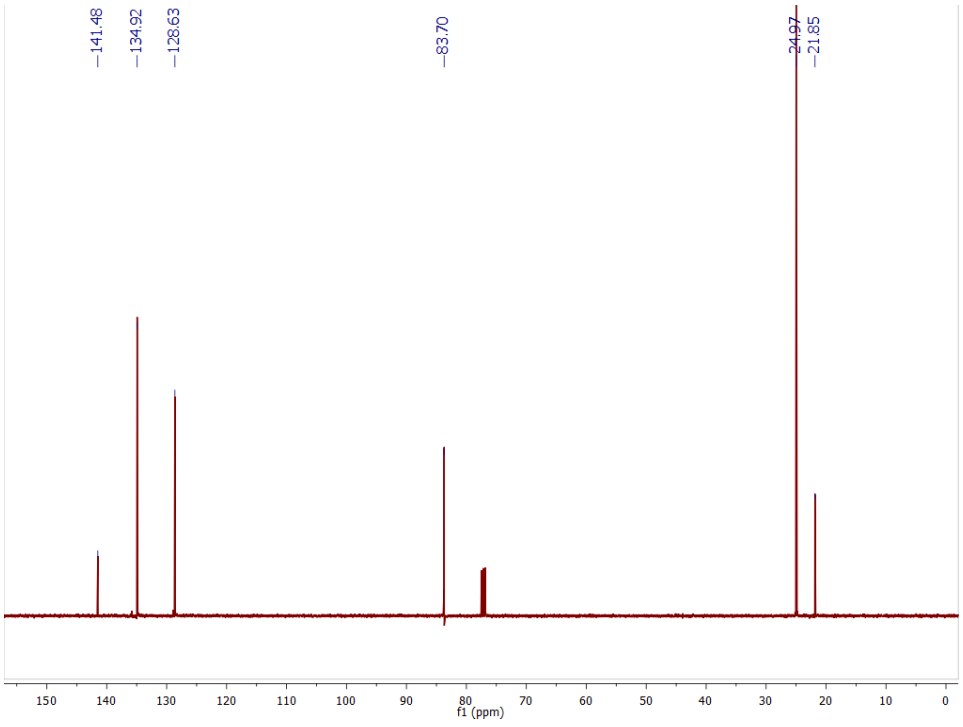

Figure S2. ^{13}C NMR spectrum ($CDCl_3$) of **1**.

Synthesis of p-Benzylboronic Acid Pinacol Ester Bromide **(2)**

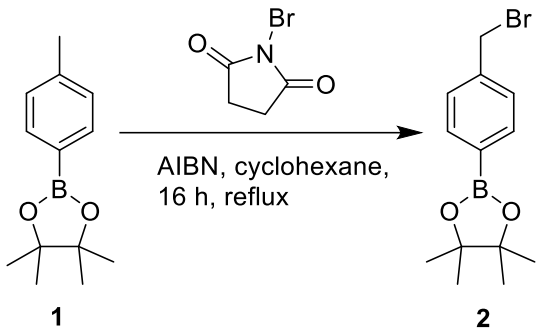

1 **2**

A flame-dried, 2-neck round bottom flask equipped with a septum and condenser was charged with compound **1** (7.87 g, 36.1 mmol), dry, degassed (stored over activated molecular sieves overnight, bubbled with N_2 for 1 h) cyclohexane (120 mL), and *N*-bromosuccinimide (7.07 g, 39.7 mmol) under N_2 flow. The mixture was stirred until the solids fully dissolved to give a clear, light brown solution. Azobisisobutyronitrile (AIBN) (0.593 g, 3.61 mmol) was added in one portion under N_2 flow, and the reaction mixture was heated at reflux. The reaction was monitored by TLC (50:50 hexanes:EtOAc) until starting material was consumed (16 h). The reaction mixture was cooled to rt and washed successively with saturated $NaHCO_3$ (2 x 30 mL), ice water (2 x 30 mL), and brine (30 mL). The organic layer was separated, dried over Na_2SO_4, and then concentrated via rotary evaporation to yield a pale-yellow powder. This crude product was then recrystallized from cyclohexane to yield product **2** (6.04 g, 73 % yield) as an off white solid (m.p. = 81.1- 92.0 °C). Spectroscopic data agree with literature precedent.[4] ^{1}H NMR ($CDCl_3$): δ 7.80 (m, 2H) 7.39 (m, 2H), 4.49 (s, 2H), 1.35 (s, 12H). ^{13}C NMR ($CDCl_3$): δ 140.8, 135.3, 128.4, 84.0, 33.4, 25.0.

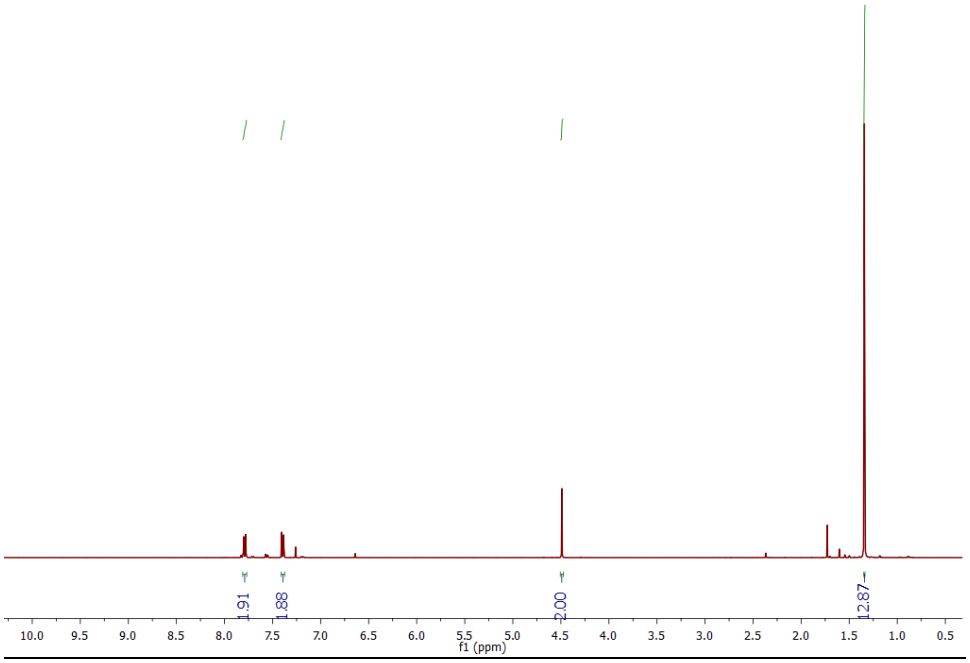

Figure S3. ^{1}H NMR spectrum ($CDCl_3$) of **2**.

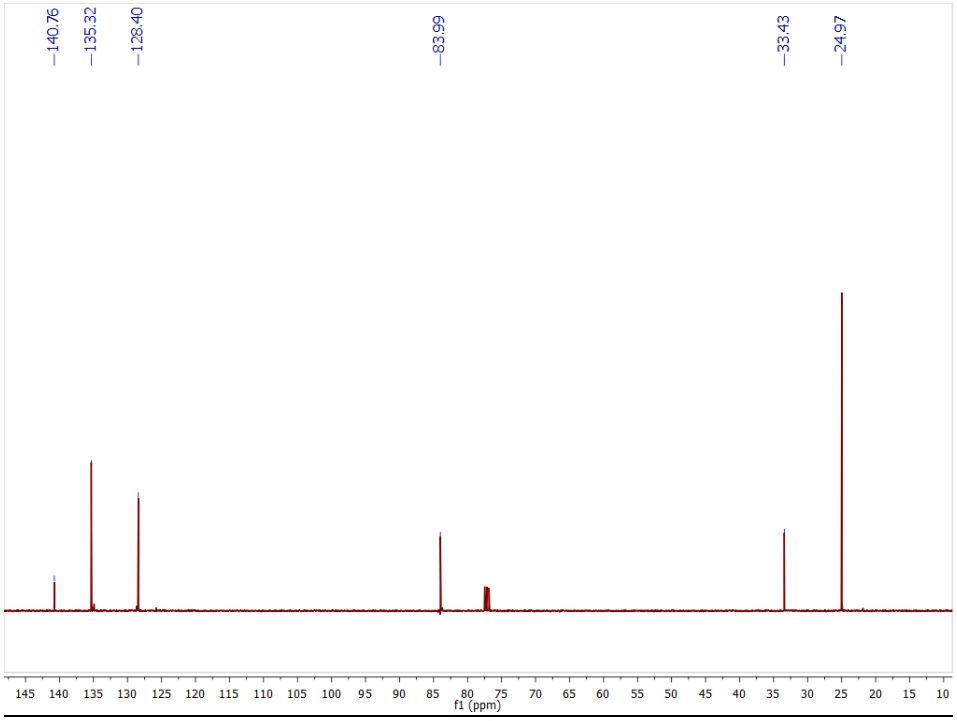

Figure S4. ^{13}C NMR of **2**.

Synthesis of p-Benzylboronic Acid Pinacol Ester Thiol **(3)**

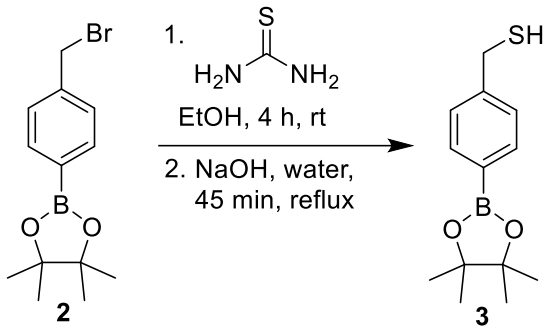

A two-neck round bottom flask equipped with a vacuum adaptor, and a septum was charged with compound **2** (3.47 g, 11.7 mmol), EtOH (30 mL), and a stirbar. The resulting suspension was bubbled with N_2 for 30 min. Thiourea (0.940 g, 12.3 mmol) was then added in one portion under N_2, and the reaction mixture was stirred at rt. The solids dissolved slowly over the course of 1 h to give a clear, colorless solution. Reaction progress was monitored by TLC (50:50 hexanes:EtOAc) until starting material was consumed (4 h). The reaction mixture was then concentrated via rotary evaporation, and the thiouronium intermediate was subsequently dissolved in DI H_2O (20 mL). A reflux condenser was added to the flask, and the suspension was bubbled with N_2 for 30 min. NaOH pellets (1.90 g, 46.7 mmol) were then added under N_2, and the resulting yellow solution was refluxed for 45 min. The reaction mixture was cooled to rt and then placed in an ice bath. HCl (1 N) was added dropwise at 0 °C, resulting in the formation of a white precipitate. HCl addition was continued until the pH of the solution was ~2. The aqueous suspension was then extracted with $CHCl_3$ (5 x 20 mL), and the organic layer was separated and dried over Na_2SO_4. The product was then further purified by silica gel chromatography, eluting with 30 % EtOAc in hexanes, yielding an off-white solid (2.15 g, 74 % yield) (m.p. = 80.3-81.3 °C). Spectroscopic data agree with literature precedent.[5] ^{1}H NMR ($CDCl_3$): δ 7.77 (m, 2H) 7.34 (m, 2H), 3.74 (d, J = 8 Hz, 2H), 1.74 (t, J = 2 Hz, 1H), 1.34 (s, 12H). ^{13}C NMR ($CDCl_3$): δ 144.4, 135.3, 127.5 83.9, 29.2, 25.0.

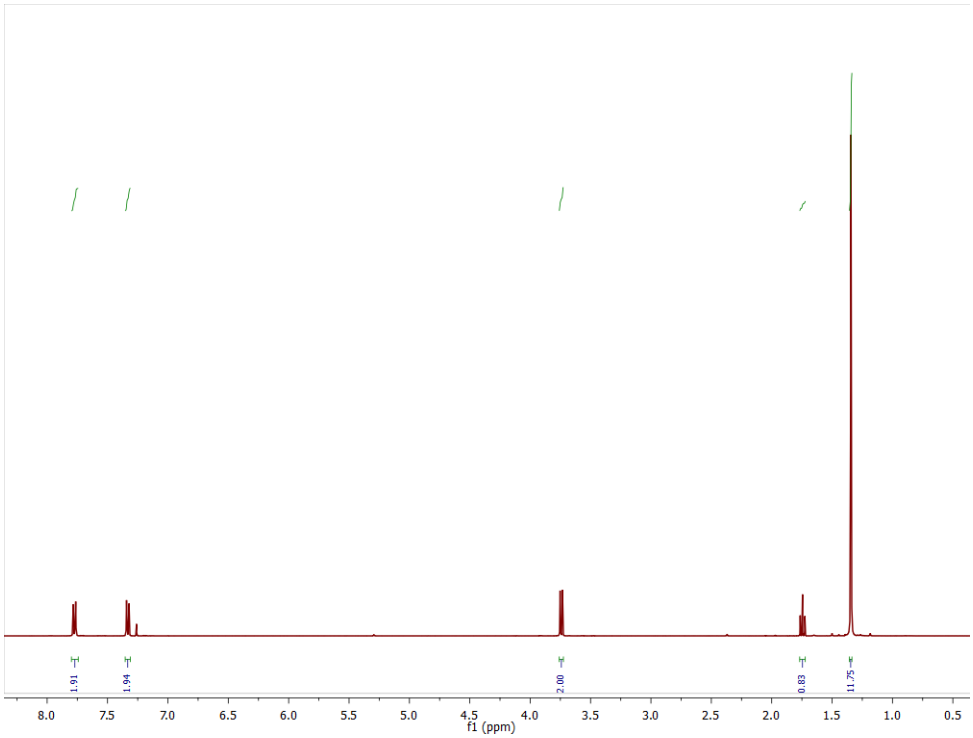

Figure S5. ^{1}H NMR spectrum ($CDCl_3$) of **3**.

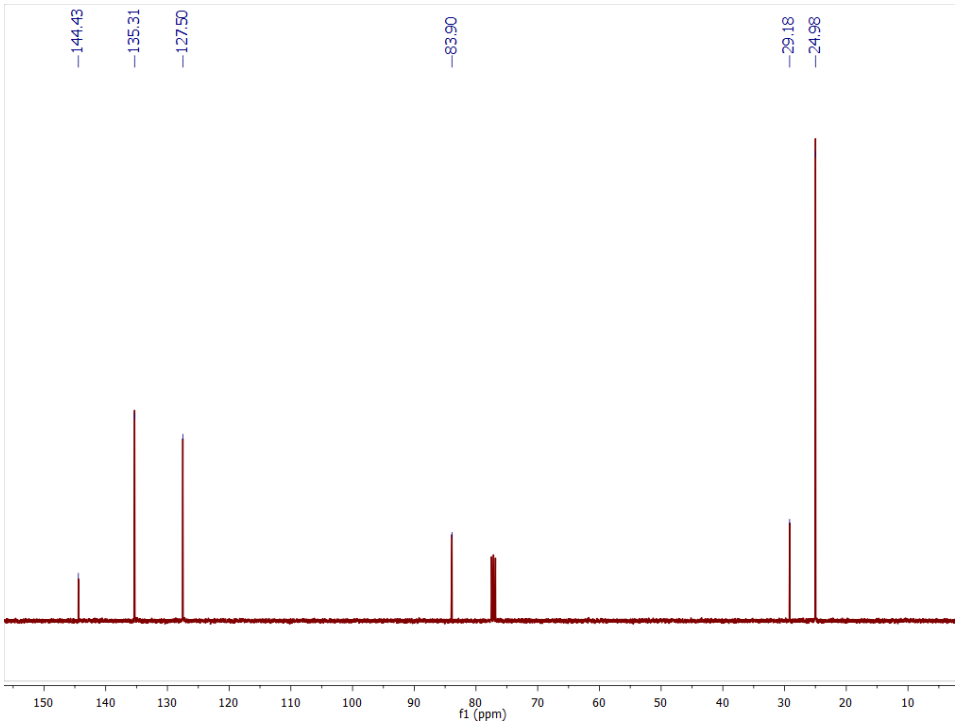

Figure S6. ^{13}C NMR spectrum ($CDCl_3$) of **3**.

Synthesis of Activated N-Acetylcysteine Disulfide **(NAC-pyDS)**

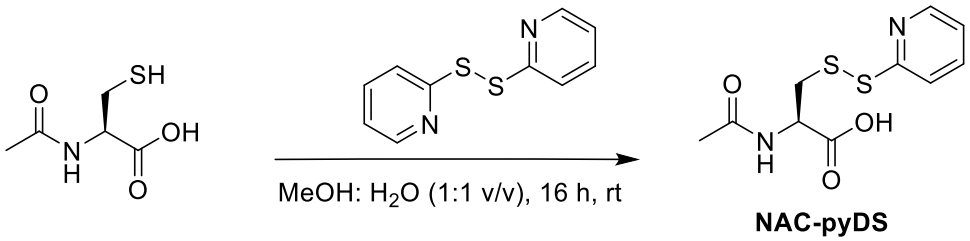

NAC-pyDS

A round bottom flask was charged with *N*-acetylcysteine (2.00 g, 12.3 mmol), H_2O (17 mL), and a stirbar to give a clear solution. A solution of 2,2'-dipyridyl disulfide (5.40 g, 24.5 mmol) in MeOH (17 mL) was added in one portion, resulting in a clear, yellow solution. The reaction mixture was stirred at rt (16 h). Reaction progress was monitored by TLC (EtOAc), showing complete consumption of starting material. The resulting yellow solution was concentrated via rotary evaporation and extracted with DCM (3 x 30 mL). The organic layers were combined, dried over Na_2SO_4, and concentrated by rotary evaporation. The crude product, obtained as a yellow solid, was then purified by silica gel chromatography eluting with 5 % to 15 % MeOH in CH_2Cl_2, yielding a light-yellow powder (2.30 g, 69% yield). Spectroscopic data agree with literature precedent.[6] ^{1}H NMR (DMSO-d_6): δ 12.97 (s, 1H), 8.46 (m, 1H), 8.42 (d, *J* = 8 Hz, 1H), 7.81 (m, 1H), 7.75 (m, 1H), 7.24 (m, 1H), 4.47 (m, 1H), 3.15 (m, 2H), 1.86 (s, 3H). ^{13}C NMR (DMSO-d_6): δ 171.9, 169.5, 158.8, 149.7, 137.9, 121.3, 119.3, 51.4, 39.9, 22.4.

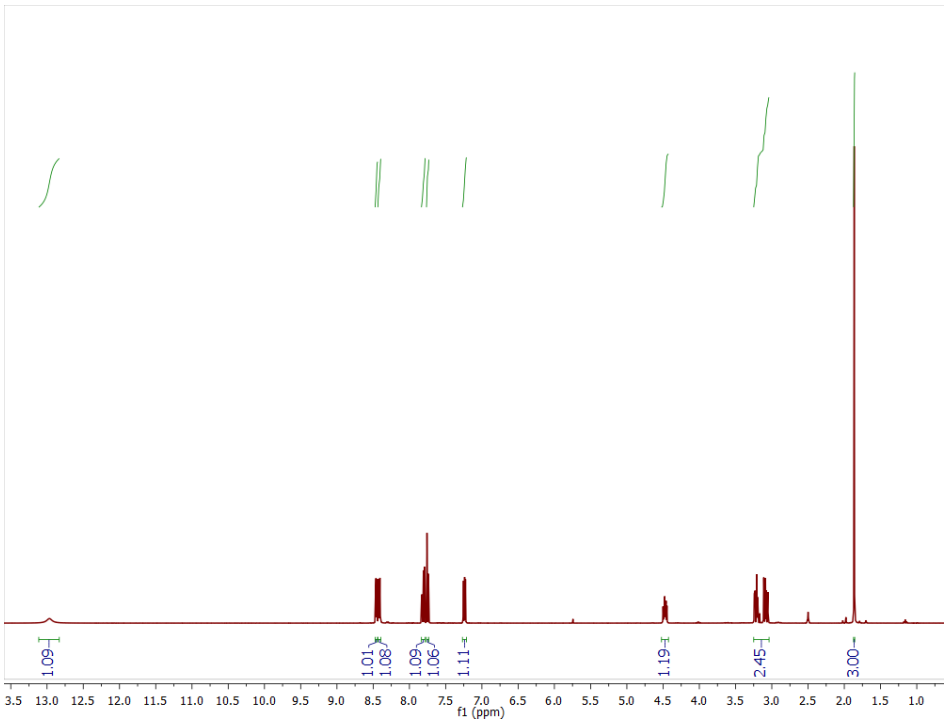

Figure S7. ^{1}H NMR spectrum ($CDCl_3$) of **NAC-pyDS**.

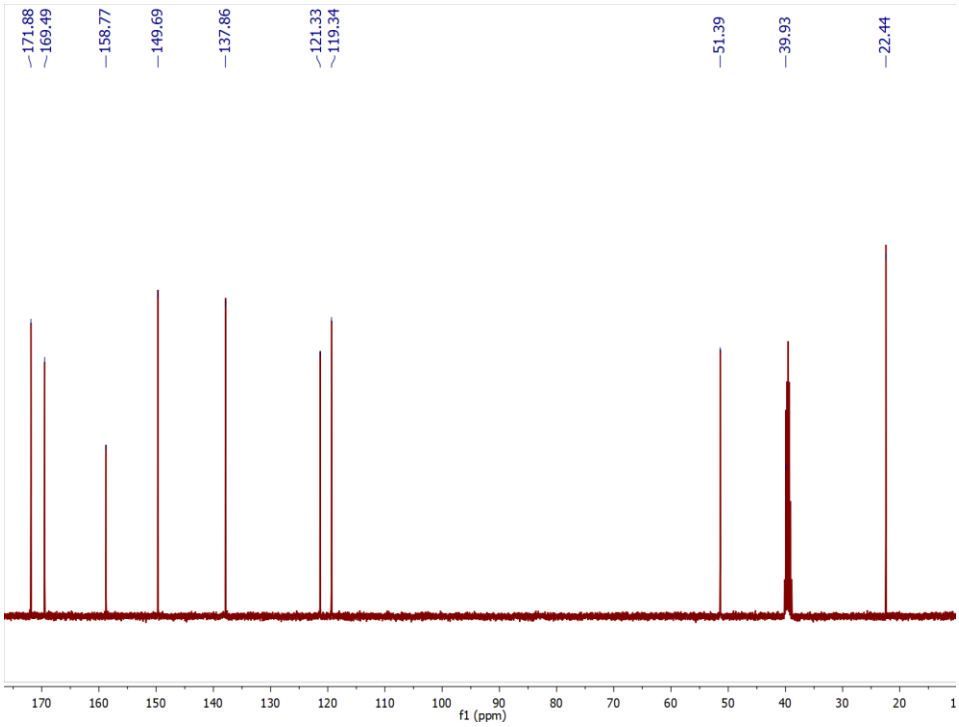

Figure S8. ^{13}C NMR spectrum ($CDCl_3$) of **NAC-pyDS**.

Synthesis of p-Benzylboronic Acid Pinacol Ester N-Acetalcysteine Disulfide **(BDP-NAC)**

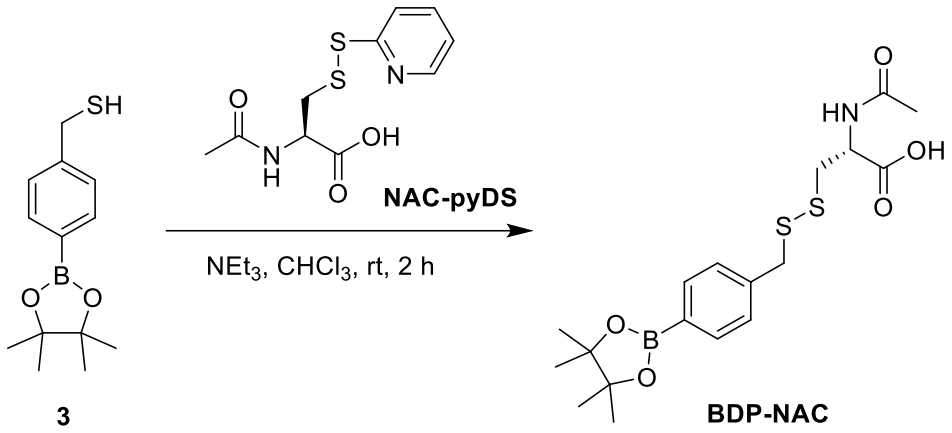

A single-neck round bottom flask was charged with compound **3** (0.412 g, 1.65 mmol), $CHCl_3$ (8 mL), and a stirbar, resulting in a light-yellow solution. **NAC-pyDS** (0.900 g, 3.29 mmol), and triethylamine (NEt_3) (0.460 mL, 3.30 mmol) were added sequentially, resulting in a yellow solution. The reaction was stirred for 2 h at rt, monitoring reaction progress with TLC (50:50 hexanes:EtOAc). Once complete, the reaction mixture was diluted with $CHCl_3$ (10 mL) and washed sequentially with 1 N HCl (2 x 5 mL) and brine (5 mL). The organic layer was then dried over Na_2SO_4, concentrated via rotary evaporation, and purified by silica gel chromatography (30% EtOAc in hexanes), yielding a yellow solid (0.375 g, 56 % yield). ^{1}H NMR (DMSO-d_6): δ 12.89 (s, 1H), 8.30 (d, J = 8, 1H), 7.62 (m, 2H), 7.33 (m, 2H), 4.47 (m, 1H), 3.98 (d, J = 3 Hz, 2H), 3.02-2.94 (m, 1H), 2.81-2.74 (m, 1H), 1.86 (s, 3H), 1.28 (s, 12H). ^{13}C NMR (DMSO-d_6): δ 172.1, 169.4, 140.9, 134.6, 128.8, 83.7, 51.2, 41.8, 39.4, 24.7, 22.4. HRMS (ESI-TOF) calcd. for $C_{18}H_{27}BNO_5S_2$ $[M+H]^+$ 412.1429, found 412.1422. Calcd. for $C_{18}H_{26}BKNO_5S_2$ $[M+K]^+$ 450.0946, found 450.0980.

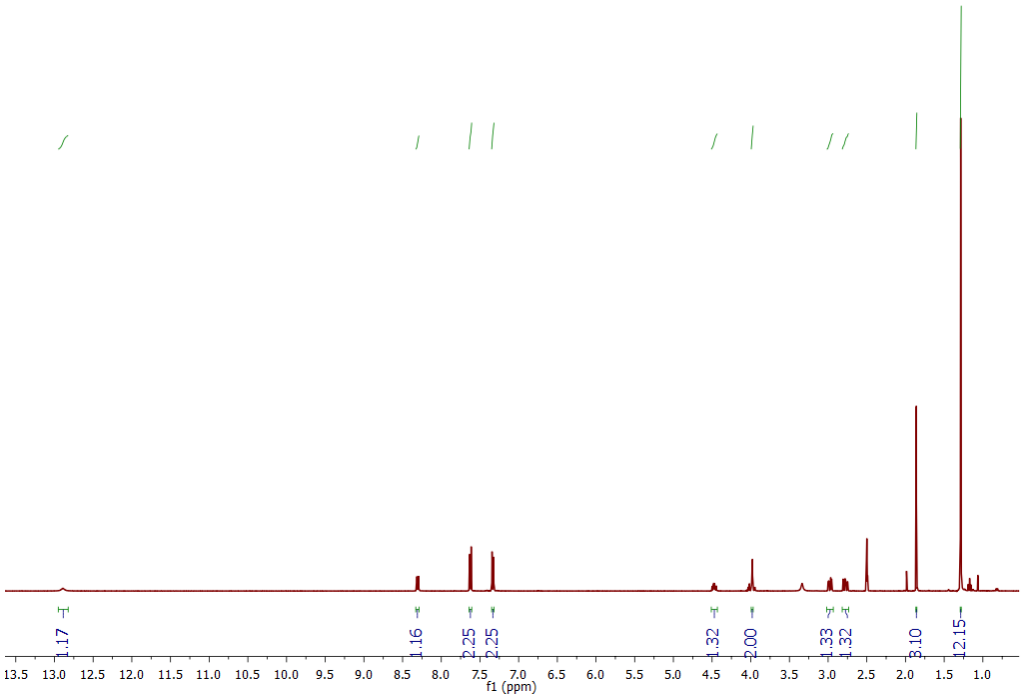

Figure S9. ^{1}H NMR spectrum (DMSO-d_6) of **BDP-NAC**.

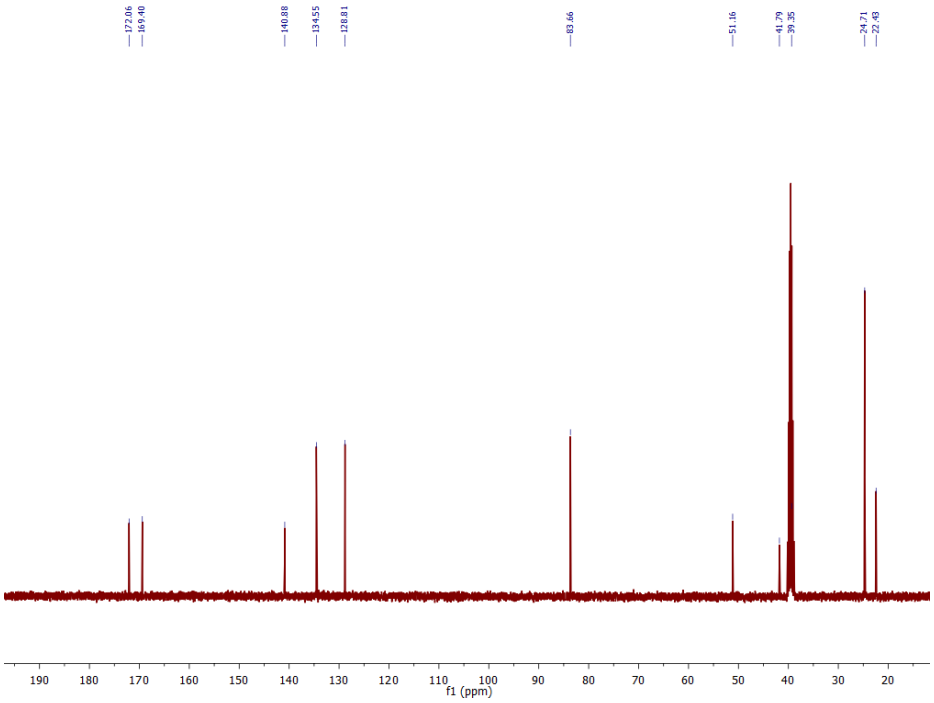

Figure S10. ^{13}C NMR spectrum (DMSO-d_6) of **BDP-NAC**.

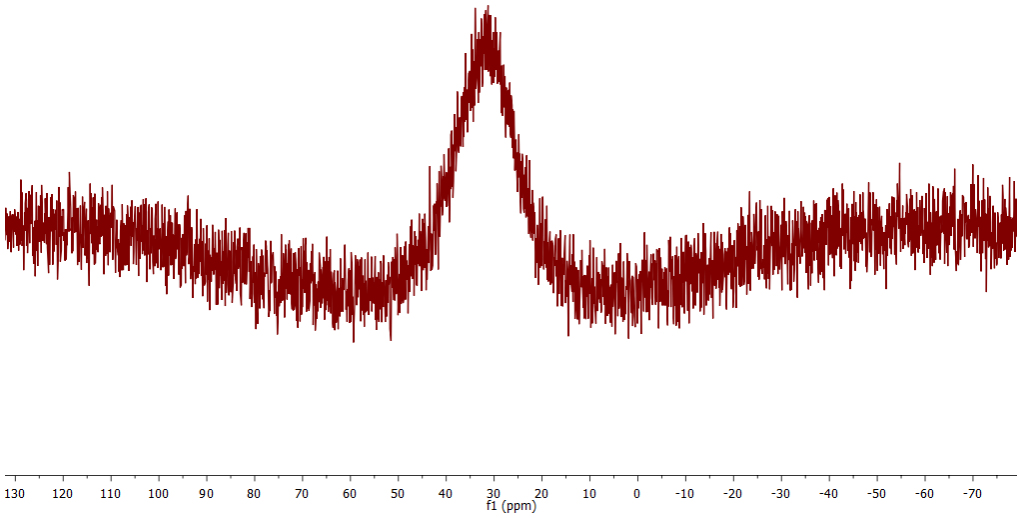

Figure S11. ^{11}B NMR spectrum of **BDP-NAC** in 90 % (v/v) DMSO-d_6:D_2O.

Synthesis of Benzyl N-Acetylcysteine Disulfide **(BDP-Control)**

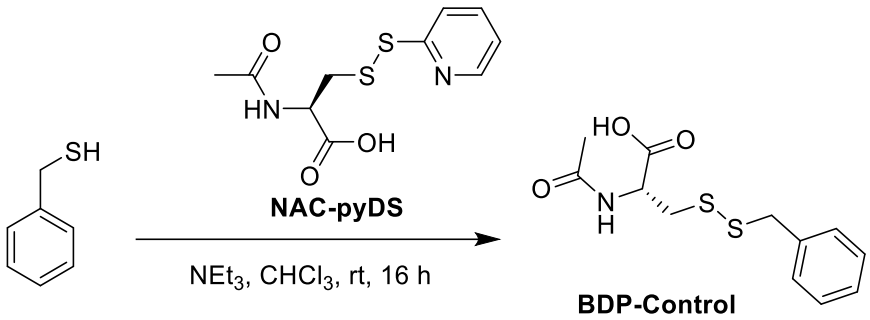

A single neck round bottom flask was charged with **NAC-pyDS** (1.3 g, 4.8 mmol) and $CHCl_3$ (10 mL) to form a suspension. Benzyl mercaptan (0.52 mL, 4.0 mmol) and NEt_3 (0.83 mL, 6.0 mmol) were added sequentially. Upon addition of NEt_3, a clear, yellow solution formed. The reaction was

stirred for 4 h at rt, monitoring reaction progress by TLC (30 % EtOAc in hexanes). Once complete, the reaction mixture was diluted with $CHCl_3$ (10 mL), washed successively with 1 N HCl (2 x 5 mL) and brine (5 mL), dried over Na_2SO_4, and concentrated by rotary evaporation. The resulting yellow powder was purified by silica gel chromatography eluting with a gradient of 0% to 10 % MeOH in EtOAc, yielding a light brown solid (0.688 g, 60 % yield) (m.p. = 121.2 -130.5 °C). ^{1}H NMR (DMSO-d_6): δ 12.94 (s, 1H), 8.30 (d, J = 5, 1H), 7.37-7.23 (m, 5H), 4.46 (m, 1H), 3.97 (m, 2H), 2.99-2.71 (m, 2H), 1.86 (s, 3H). ^{13}C NMR (DMSO-d_6): δ 172.10, 169.39, 137.37, 129.30, 128.44, 127.31, 51.25, 41.92, 39.45, 22.45. HRMS (ESI-TOF) calcd. for $C_{12}H_{16}NO_3S_2$ $[M+H]^+$ 286.0571, found 286.0566. Calcd. for $C_{12}H_{15}NNaO_3S_2$ $[M+Na]^+$ 309.0414, found 309.0414.

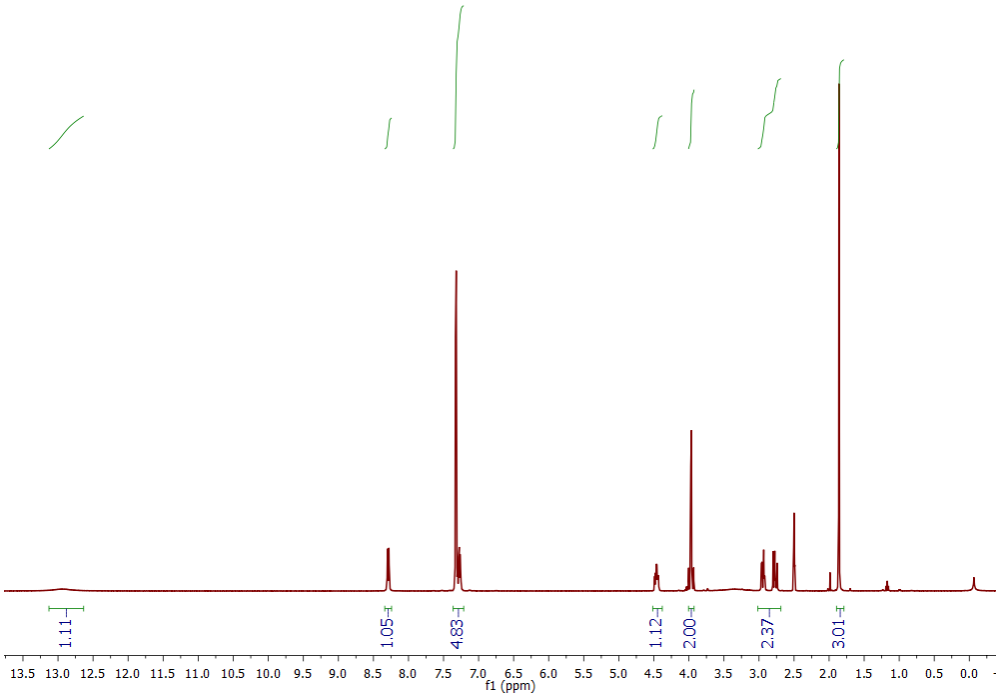

Figure S12. ^{1}H NMR spectrum (DMSO-d_6) of **BDP-Control**.

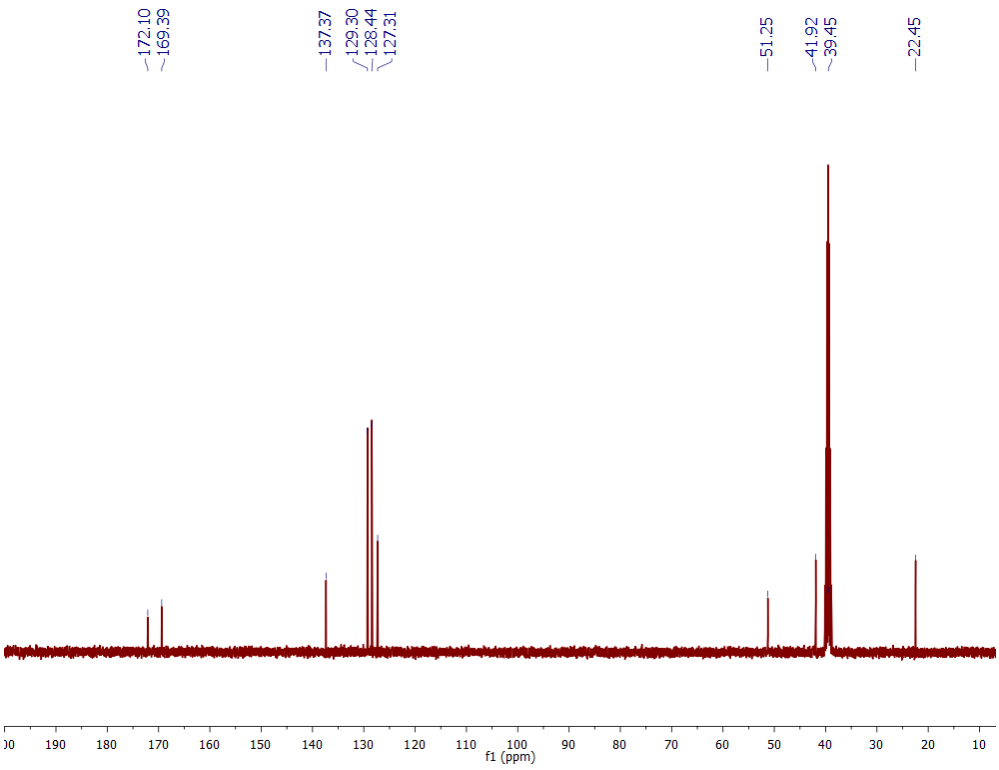

Figure S13. ^{13}C NMR spectrum (DMSO-d_6) of **BDP-Control**.

Synthesis of Activated Persulfide Probe **(4)**

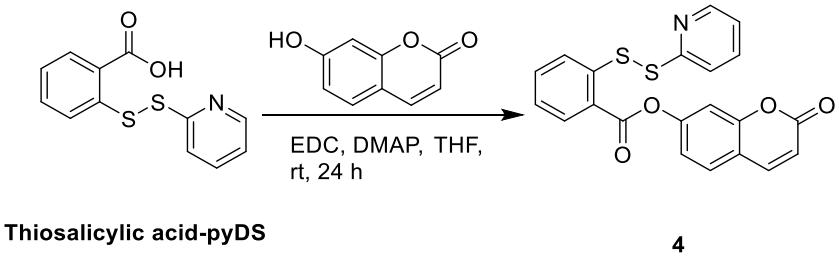

Thiosalicylic acid-pyDS **4**

A single-neck round bottom flask was charged with **Thiosalicylic acid-pyDS** (4.0 g, 15 mmol) and THF (150 mL) to give a light yellow solution. To this solution, EDC (4.7 g, 30 mmol), and DMAP (122 mg, 1 mmol) were added sequentially and stirred until the solution was homogeneous. Next, 7-hydroxycoumarin (2.6 g, 17 mmol) was added, and the reaction mixture was stirred at rt (16 h). Reaction progress monitored by TLC (EtOAc) until starting material was consumed. The resulting amber solution was concentrated via rotary evaporation, and the residue was dissolved

in $CHCl_3$ (200 mL). This solution was washed successively with saturated $NaHCO_3$ (2 x 50 mL), DI H_2O (100 mL), and brine (100 mL), and then separated and dried over Na_2SO_4. The resulting crude product was purified by silica gel chromatography eluting with 20 % EtOAc in CH_2Cl_2 to yield an off-white solid (2.9 g, 47% yield). Spectroscopic data agree with literature precedent.[1] ^{1}H NMR ($CDCl_3$) δ 8.46 (m, 1H), 8.29 (m, 1H), 7.98 (m, 1H), 7.73 (d, *J* = 10 Hz, 1H), 7.60-7.50 (m, 4H), 7.35 (m, 1H), 7.29-7.21 (m, 2H), 7.10 (m, 1H), 6.42 (d, *J* = 10 Hz, 1H). ^{13}C NMR ($CDCl_3$) δ 164.1, 160.3, 158.9, 158.7, 154.8, 153.0, 149.6, 142.8, 141.9, 137.4, 134.2, 132.1, 128.7, 126.3, 125.9, 121.1, 119.6, 118.6, 117.0, 116.3, 110.7.

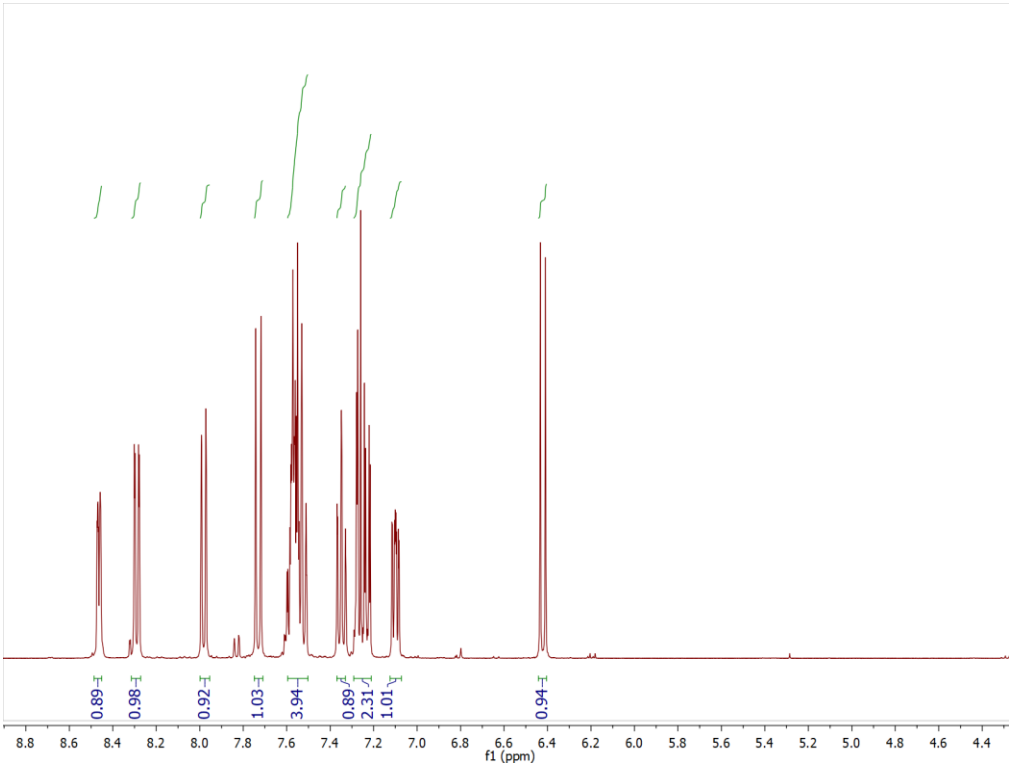

Figure S14. ^{1}H NMR spectrum ($CDCl_3$) of **7**.

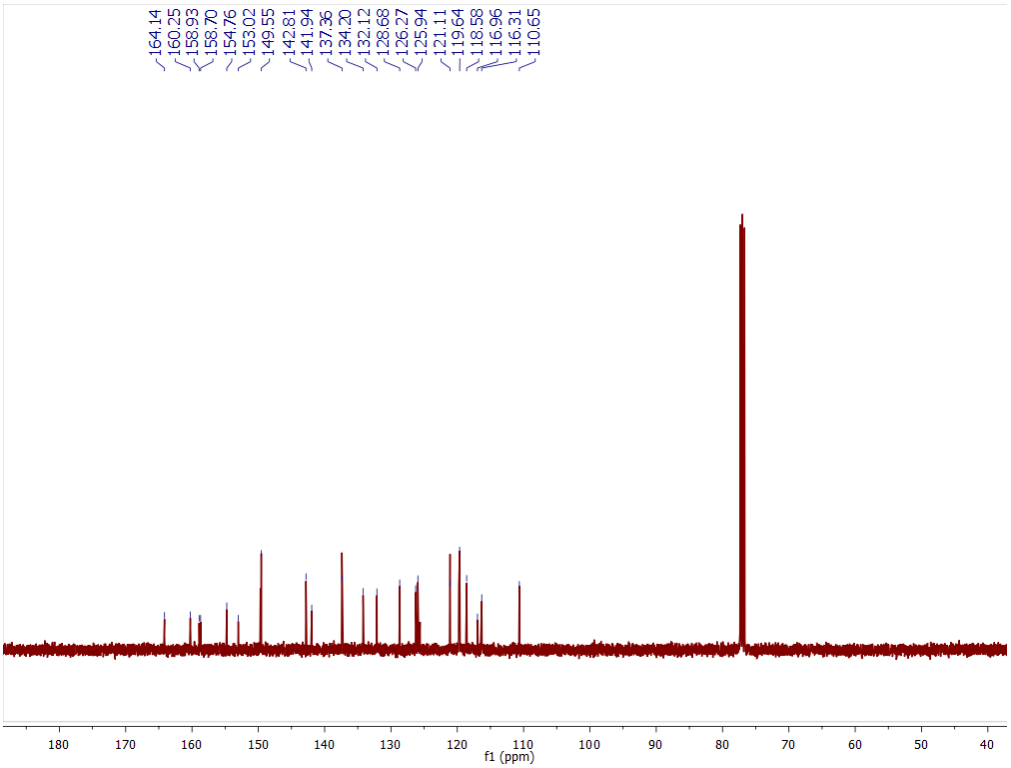

Figure S15. ^{13}C NMR spectrum ($CDCl_3$) of **7**.

Synthesis of Probe-Bpin Disulfide **(BDP-Fluor)**

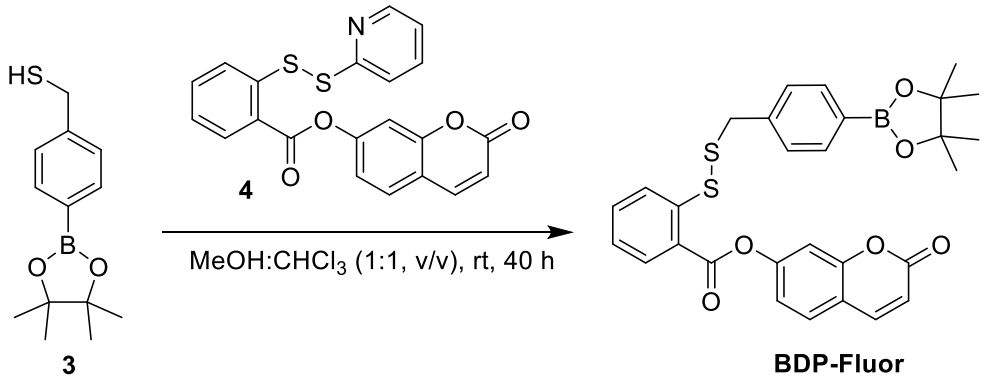

A round bottom flask was charged with compound **4** (538 mg, 1.32 mmol), MeOH (5 mL) and a stir bar to give a clear suspension. Thiol **3** (300 mg, 1.20 mmol) was added as a solution in $CHCl_3$ (5 mL), and the resultant yellow suspension was stirred for 40 h at rt. Reaction progress was monitored by TLC (70 % EtOAc in hexanes). Once complete, the reaction mixture was

concentrated via rotary evaporation and purified on a silica column eluting with 30% EtOAc:hexanes, yielding **BDP-Fluor** as a waxy off-white solid (34 mg, 5.4% yield). ^{1}H NMR ($CDCl_3$) δ 8.19 (m, 1H), 8.07 (m, 1H), 7.72 (m, 1H), 7.69 (m, 2H), 7.57-7.51 (m, 2H), 7.31-7.25 (m, 5H), 7.21 (m, 1H), 6.42 (d, *J* = 10, 1H) 3.95 (s, 2H), 1.34 (s, 12H). ^{13}C NMR ($CDCl_3$): δ 164.1, 160.5, 154.9, 153.3, 143.2, 143.0, 139.4, 137.6, 135.1, 133.8, 132.1, 126.4, 125.64, 125.4, 121.3, 119.8, 118.8, 117.0, 116.33, 110.8, 84.0, 43.5, 25.0. HRMS (ESI-TOF) calcd. for $C_{29}H_{28}{}^{11}BO_6S_2$ $[M+H]^+$ 547.1415, found 547.1452. Calcd. for $C_{29}H_{31}{}^{11}BNO_6S_2$ $[M+NH_4]^+$ 564.1686, found 564.1705. Calcd. for $C_{29}H_{27}{}^{11}BNaO_6S_2$ $[M+Na]^+$ 569.1234, found 569.1267. Calcd. for $C_{29}H_{27}{}^{11}BKO_6S_2$ $[M+K]^+$ 585.0974, found 585.1059.

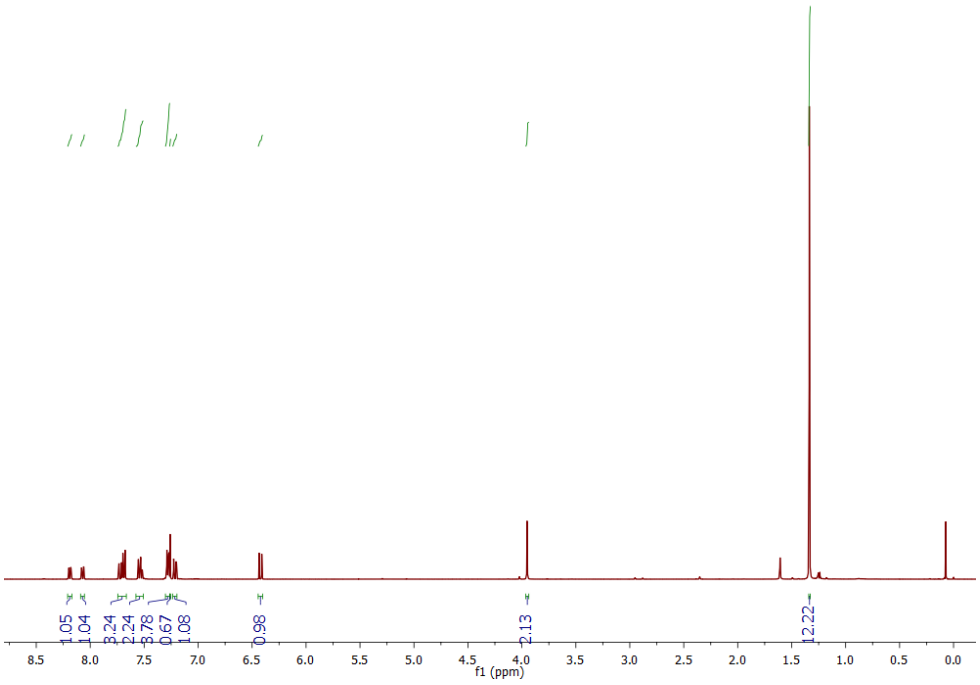

Figure S16. ^{1}H NMR spectrum ($CDCl_3$) of **BDP-Fluor.**

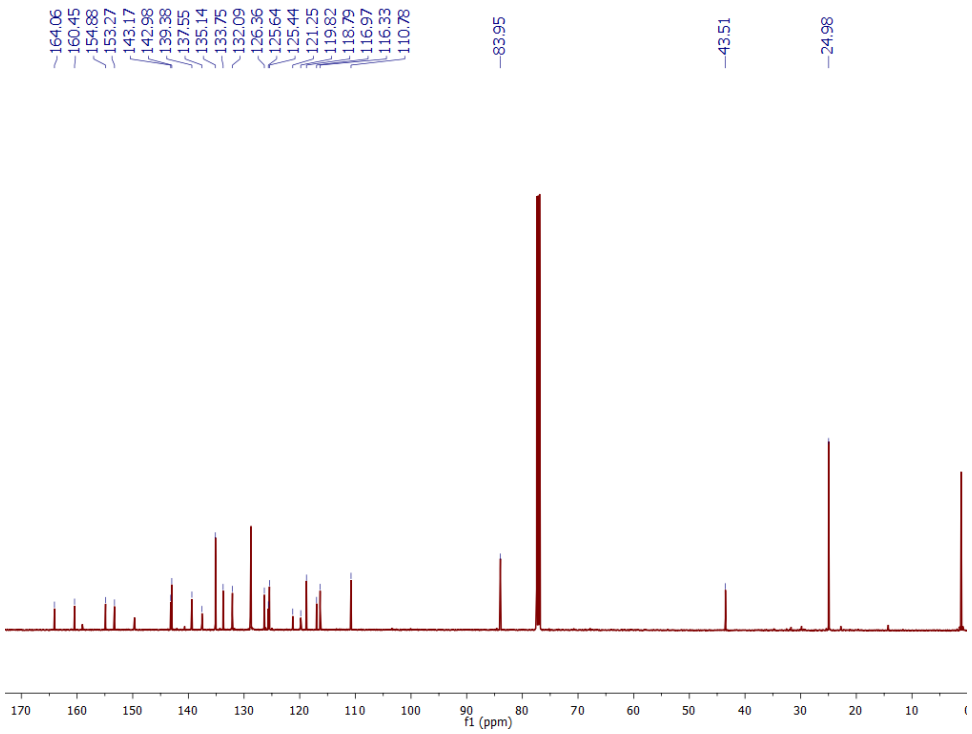

Figure S17. ^{13}C NMR spectrum ($CDCl_3$) of **BDP-Fluor.**

Synthesis of Probe-Control Disulfide **(5)**

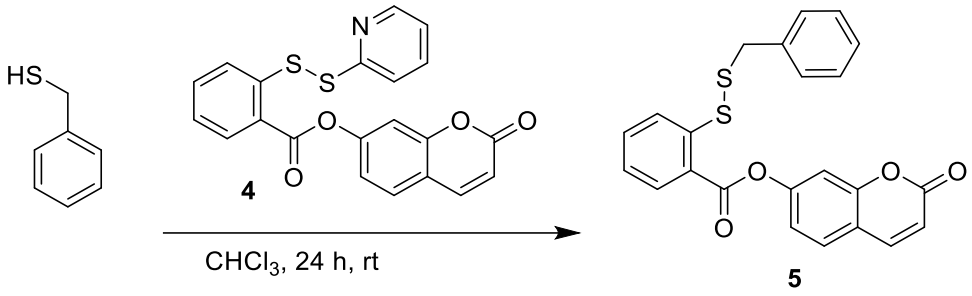

A single-neck round bottom flask was charged with benzyl mercaptan (0.075 mL, 0.64 mmol) and **4** (248 mg, 0.590 mmol), $CHCl_3$ (1 mL), and MeOH (1 mL). The resulting clear, yellow reaction mixture was stirred for 24 h at rt; reaction progress was monitored by TLC (CH_2Cl_2). The reaction mixture was then concentrated by rotary evaporation, and the resultant yellow solid was purified by silica gel chromatography, eluting with 30% EtOAc:hexanes, yielding **5** as a yellow solid (64 mg, 23 % yield). ^1H NMR ($CDCl_3$): δ 8.21 (m, 1H), 8.07 (m, 1H), 7.73 (d, 1H), 7.54 (m, 2H),

7.32-7.27 (m, 5H), 7.25-7.19 (m, 3H), 6.43 (d, J = 10, 1H), 3.96 (s, 2H). ^{13}C NMR ($CDCl_3$): δ 164.1, 160.5, 154.9, 153.3, 143.2, 143.0, 136.4, 133.8, 132.1, 129.4, 128.8, 127.8, 126.2, 125.6, 125.5, 118.8, 117.0, 116.4, 110.8, 43.5. HRMS (ESI-TOF) calcd. for $C_{23}H_{17}O_4S_2$ $[M+H]^+$ 421.0563, found 421.0585. Calcd. for $C_{29}H_{27}{}^{11}BNaO_6S_2$ $[M+Na]^+$ 443.0382, found 443.0416.

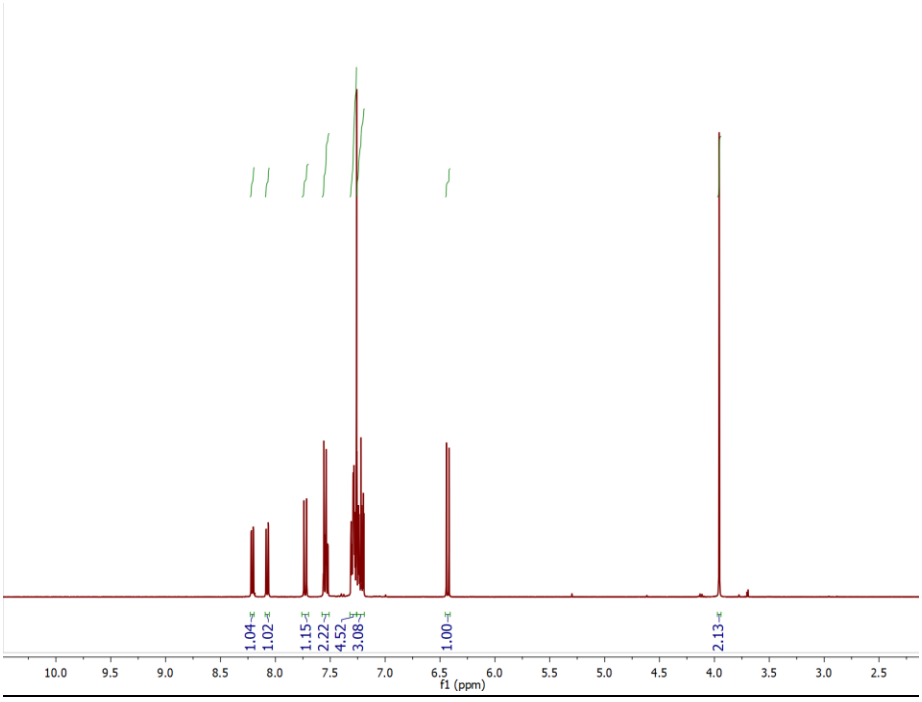

Figure S18. ^{1}H NMR spectrum ($CDCl_3$) of compound **5**.

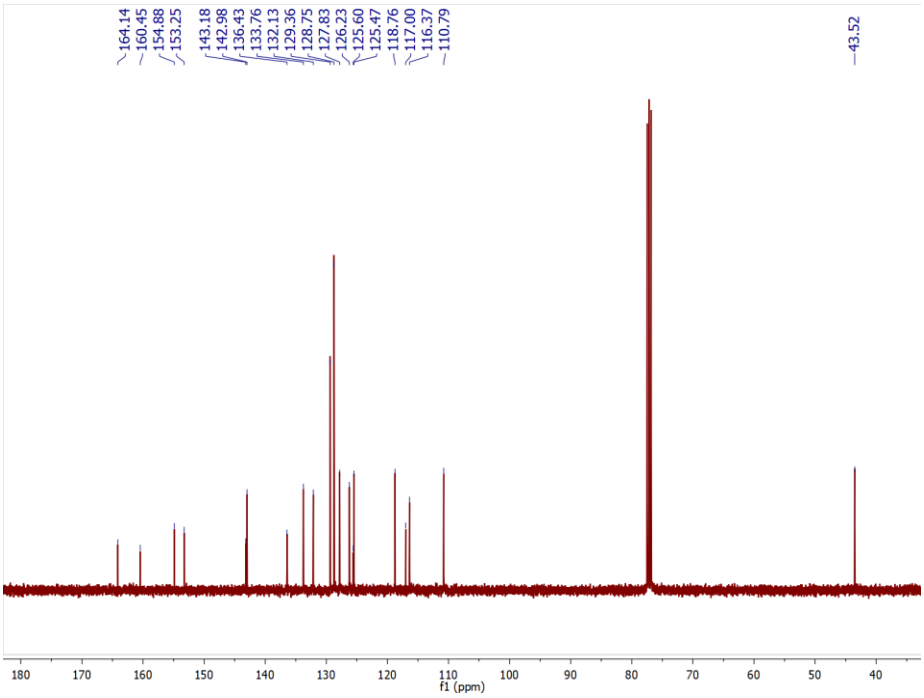

Figure S19. ^{13}C NMR spectrum ($CDCl_3$) of compound **5**.

Analysis of persulfide release by LCMS

A one-dram vial was charged with a solution of **BDP-NAC** (100 µL; 20 mM in ACN) and diluted with water (0.9 mL) to give a clear, colorless solution. An aliquot (50 µL) was removed and diluted into water (0.4 mL) in a vial equipped with a screw cap lid with a rubber septum, which served as the "zero" time point. The aliquot was then analyzed by LCMS. The LCMS method is as follows: 2 µL injection volume, eluting 5 to 90 % ACN in water with 10 mM NH_4OH over the course of 6 min, followed by a 4-min column equilibration in 5 % ACN in water with 10 mM NH_4OH. After acquisition of the zero time point H_2O_2 (30 µL, 3.5 wt %) was added to the reaction mixture. The vial was shaken thoroughly, and after 1 min the first aliquot was removed and diluted with water and injected into the LCMS in the same fashion as the zero min time point (we estimate 5 min for total reaction time based on sample prep and autosampler time). Aliquots were then taken at the 60 and 120 min marks until the peak attributed to **BDP-NAC** subsided. The UV detector readout

was set to 220 nm, and mass spectra were collected by direct infusion into the mass spectrometer in ESI negative mode.

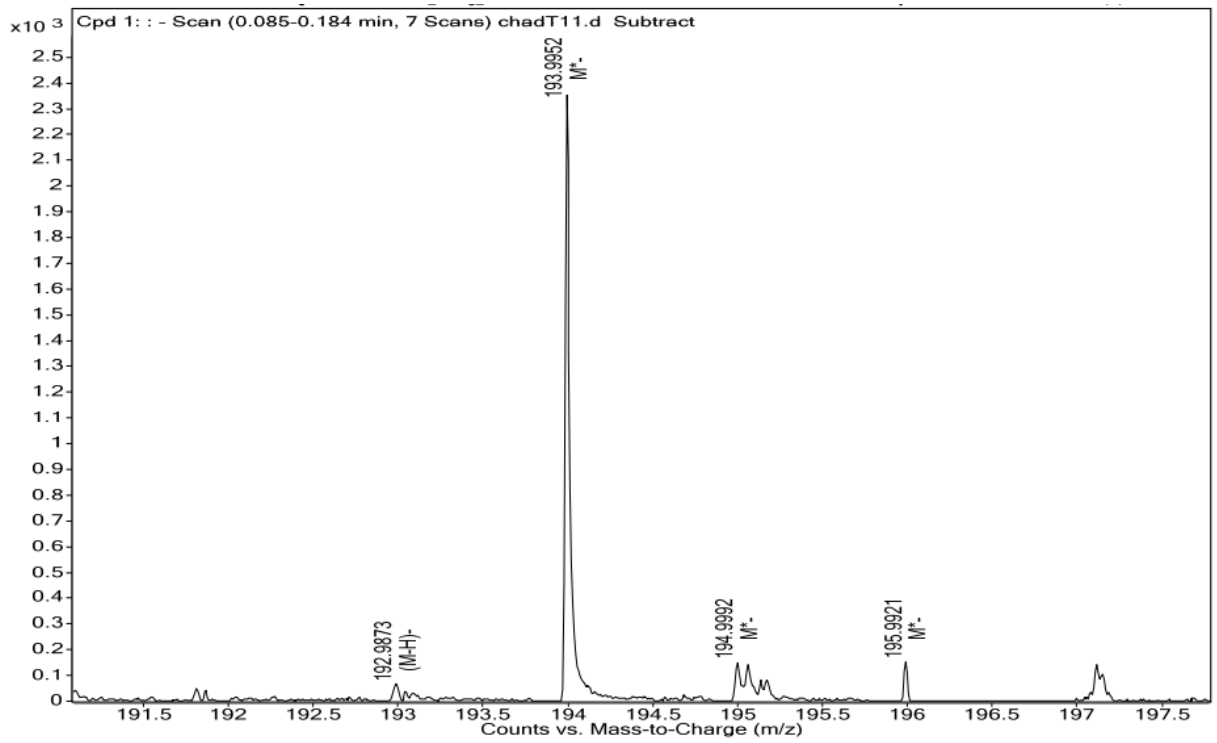

Figure S20. HRMS of the peak eluting at 3.4 min (Figure 2) corresponding to the persulfide of NAC (exact mass calculated to be 193.9551).

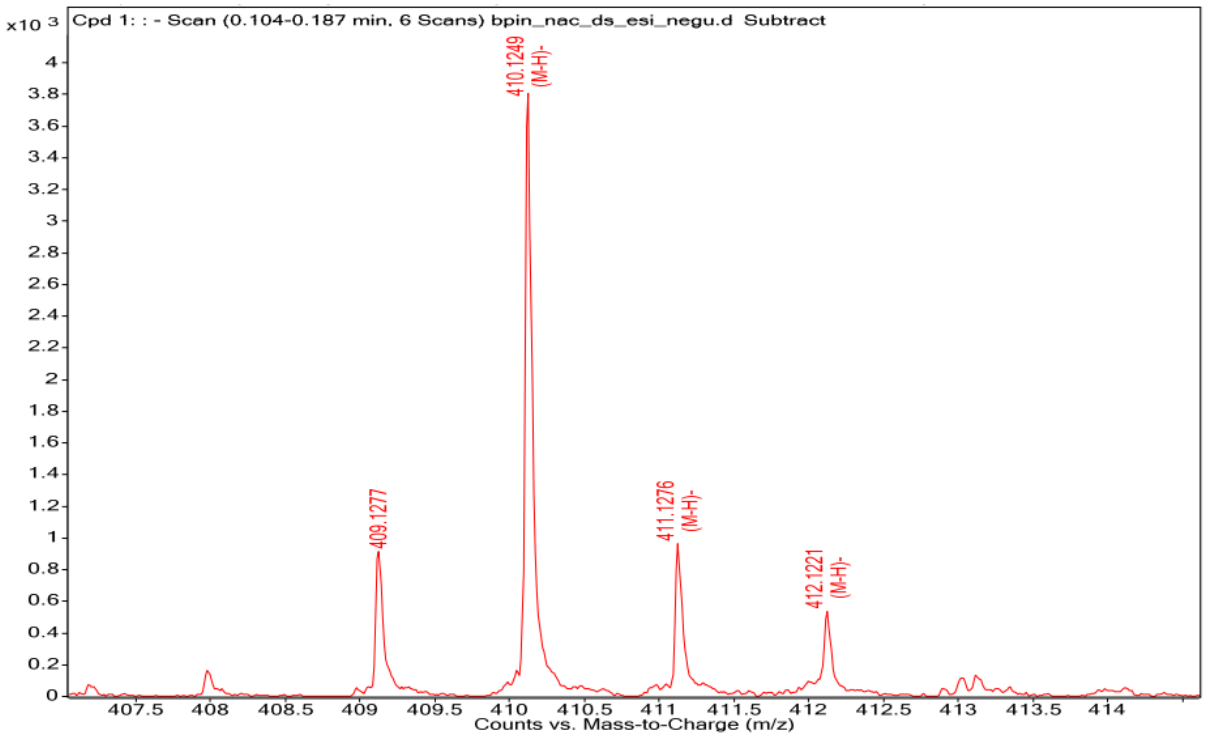

Figure S21. HRMS of **BDP-NAC** (exact mass calculated to be 411.1345).

Analysis of persulfide release by Fluorescence spectroscopy

Fluorescence assays were prepared in a 3 mL quartz cuvette with a threaded lid containing 1.98 mL 1X PBS buffer (pH 7.4), 1.0 mL cetyltrimethylammonium bromide solution (CTAB) (3 mM in PBS buffer), and 0.020 mL **BDP-Fluor** or **5** probe solution (0.50 mM in DMSO). The fluorescence spectrum of this mixture was collected from 400 to 600 nm (λ_{ex} = 380 nm) as the t = 0 timepoint. To this solution was added 5 μL of trigger solution (200 mM in PBS buffer). The cuvette was capped and shaken to mix the solution. The cuvette was then placed in the fluorimeter, and fluorescence spectra from 400-600 nm were collected every 10 min from. Analysis was completed by comparing the fluorescence intensity at 460 nm at the 5 h timepoint (I_f) to the fluorescence intensity at t_0 (I_0). Each measurement was run in triplicate and reported values are the average of these runs; error bars are represented by the standard error of the mean.

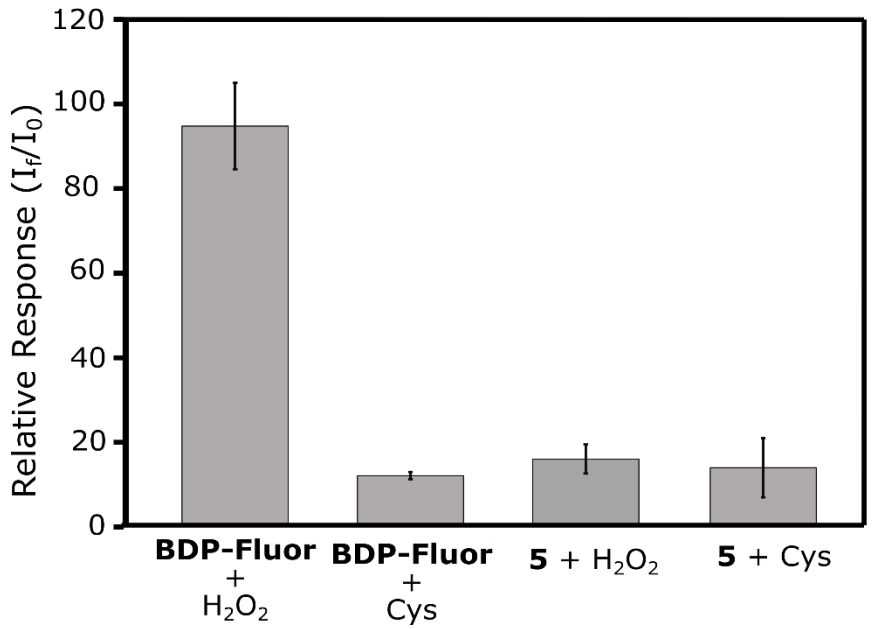

Figure S22. Relative response (I_f / I_0) of **BDP-Fluor** and control fluorescent compound **5** (3.3 μM) to H_2O_2 and Cys (both 330 μM) measured at 460 nm. The increased response of **BDP-Fluor** relative to other potential triggers (Figure 3) is a result of nucleophilic attack of the Cys thiol on the aryl ester bond, liberating 7-hydroxycoumarin. As compound **5** does not have the oxidative-labile Bpin moiety, it does not respond to H_2O_2 to the same degree as **BDP-Fluor**, but it shows an equal response to Cys. These results indicate that nucleophilic attack by cysteine likely causes release of the 7-hydroxycoumarin, leading to a slightly increased response of **BDP-Fluor** to Cys.

*NMR kinetics analysis of **BDP-NAC***

For ^{1}H NMR experiments, **BDP-NAC** (10 mg, 0.024 mmol) or **BDP-Control** (10 mg, 0.036 mmol) was added to a vial and dissolved in DMSO-d_6 (900 μL). Upon full dissolution, D_2O (100 μL) was added to the vial, and the solution was transferred to an NMR tube. A ^{1}H NMR spectrum was collected at this time, which served as the zero time point (t_0). After the addition of H_2O_2 solution (20 μL, 30 wt.% in H_2O), ^{1}H NMR spectra were recorded at various time intervals. The

kinetics of **BDP-NAC** oxidation by H_2O_2 is displayed as a pseudo first-order kinetics plot, where p represents the disappearance of the aryl peaks attributed to **BDP-NAC** (a, a'). The concentration of BDP-NAC (relative to concentration at t_0) was obtained by normalizing the integral values of a + a' to the integral values at t_0, relative to the NAC methyl peak. The data were fitted to a first-order kinetics equation given by $y = 1 - e^{-kt}$, where k is the slope and t is time.

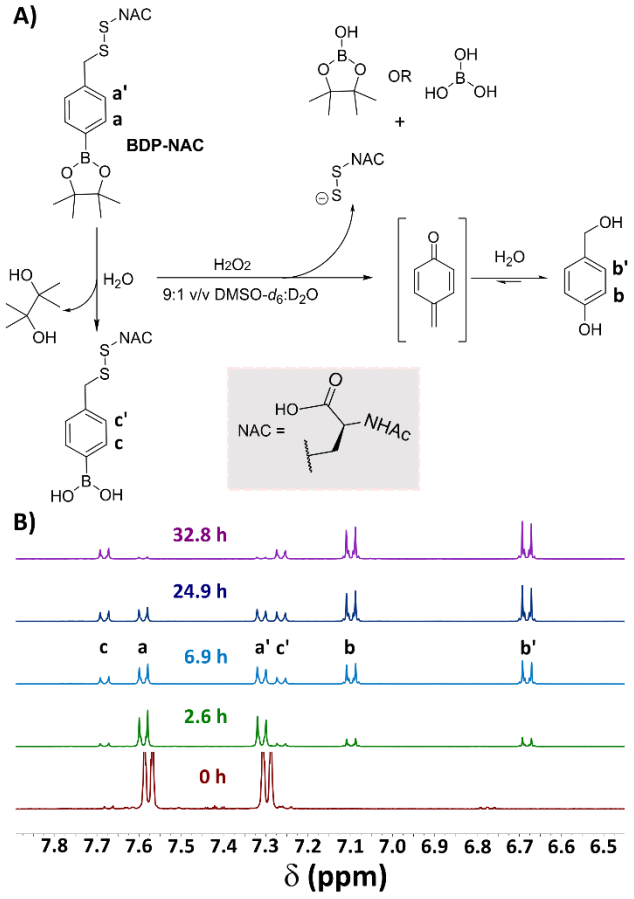

Figure S23. A) Proposed reaction scheme for persulfide release from **BDP-NAC**. B) Stacked ^{1}H NMR spectra showing the formation of *p*-hydroxybenzyl alcohol. Conditions: **BDP-NAC** (10 mg/mL) in 90% (v/v) DMSO-d_6/D_2O with 10-fold molar excess of H_2O_2.

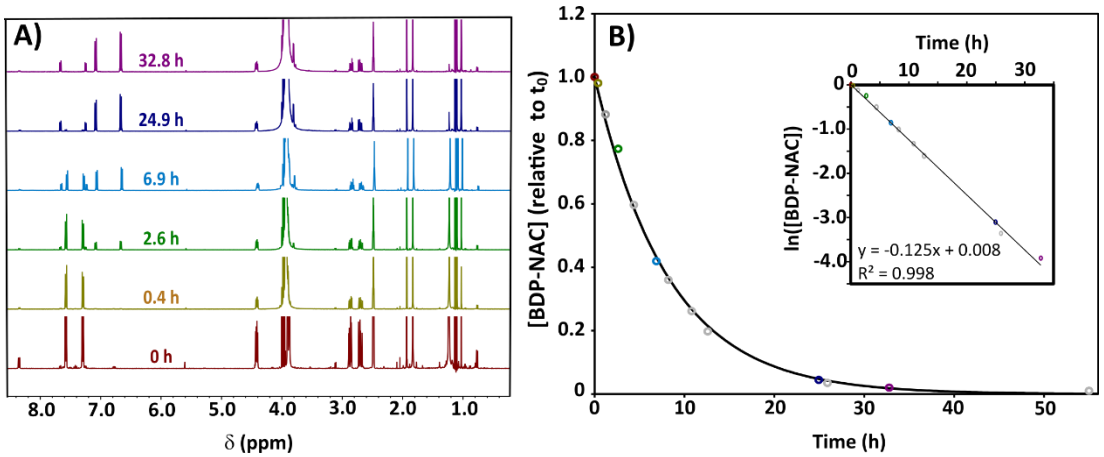

Figure S24. (A) Expanded time dependent ^{1}H NMR spectra and (B) pseudo first-order kinetics plot of **BDP-NAC** (24.3 mM) in 90% (v/v) DMSO-d_6/D_2O with 10-fold excess of H_2O_2. Data points denoted in gray do not have a representative NMR spectrum shown. Inset shows pseudo-first order kinetics plot where [BDP-NAC] was determined by normalizing the data from each time point to the integral value of the BDP-NAC aryl peaks (a, a') of the t_0 time point. The half-life for this reaction was calculated to be 7.5 ± 0.3 h based on the slope of the pseudo-first order kinetics plot ($t_{1/2} = \ln(2)/k_{obs}$).

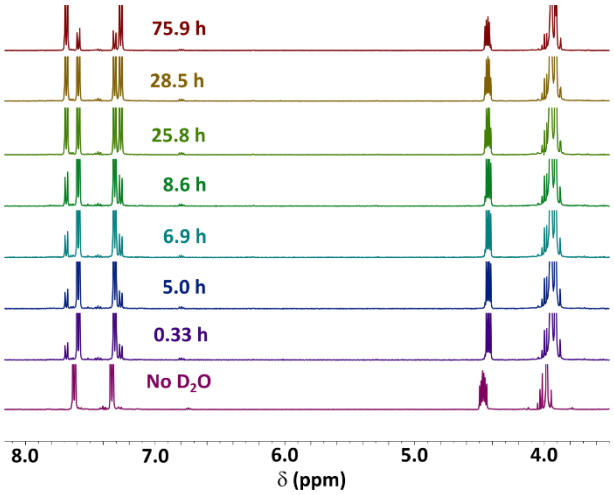

Figure S25. Time dependent ^{1}H NMR spectra of **BDP-NAC** in 90% (v/v) DMSO-d_6/D_2O without addition of H_2O_2. Hydrolysis of the Bpin moiety was followed by monitoring the change in peaks in the aryl region (7.6-7.2 ppm) and the alkyl region (1.1-0.9 ppm). A half-life of hydrolysis was calculated to be 33 h by following the disappearance of the **BDP-NAC** aryl peaks and fitting these data to a pseudo-first order kinetic equation.

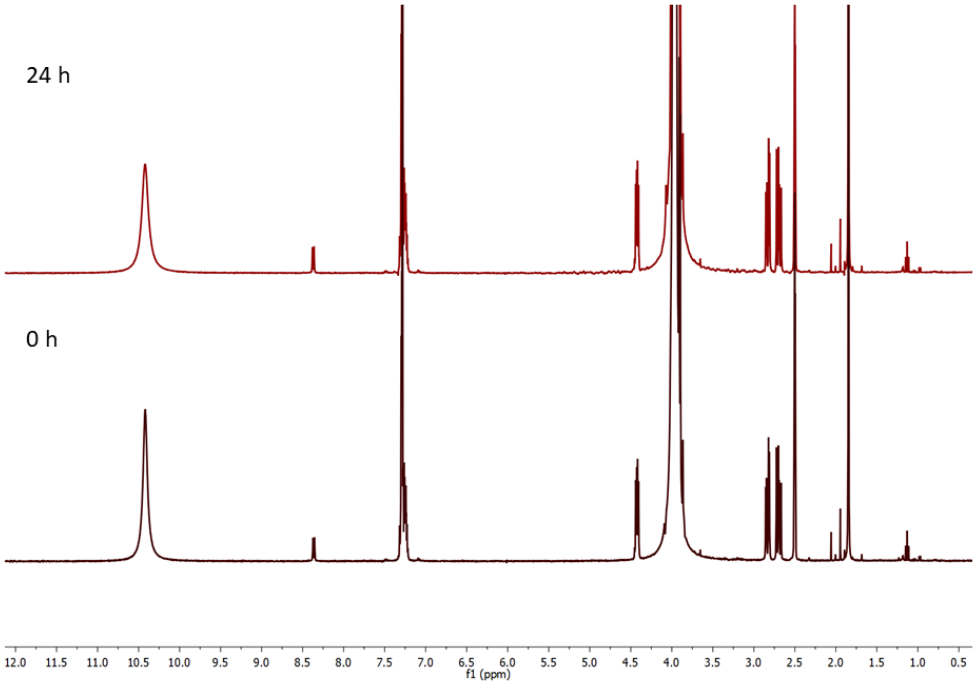

Figure S26. Time dependent ^{1}H NMR spectra of **BDP-Control** in 90% (v/v) DMSO-d_6/D_2O immediately following the addition of H_2O_2 (10-fold excess) (black spectrum), and 24 h after addition of H_2O_2 (red spectrum). No changes in the NMR spectra were observed, indicating that H_2O_2 does not cause persulfide release without the Bpin triggering moiety.

Cell Viability Assays

H9C2 cells were plated at a density of 5000 cells per well in a volume of 180 μL serum-containing media per well in a 96-well plate and cultured for 24 h before treatment. Cell viability data was analyzed using a BioTek Synergy Mx plate reader (BioTek, Winooski, VT).

Cell viability assays were performed by using Cell counting kit 8 (CCK-8, Dojindo, Rockville, Md.). H9C2 cardiomyocytes in a 96-well plate (n = 5 for each group) were treated with various concentrations of **BDP-NAC**, GYY4137, Na_2S, **BDP-Control**, 4-(hydroxymethyl)benzeneboronic acid pinacol ester, *N*-acetylcysteine, or any combination indicated (20 μL) with or without H_2O_2 (200 μM) for 1 h in serum-containing media. For treatment groups containing **BDP-NAC**, **BDP-Control**, 4-(hydroxymethyl)benzeneboronic acid pinacol ester, or NAC, DMSO was used as a vehicle to enable full solubility of these compounds in the stock solutions. Final concentration of DMSO in these treatment groups is 0.2 v/v % in DMEM. After incubation with the aforementioned compounds for 1 h, the cardiomyocytes were then washed with 1X PBS buffer three times. After washing, fresh DMEM (100 μL) without FBS and 10 v/v % CCK-8 solution was added, and the cells were incubated for 3 h. Absorbance was recorded then at 450 and 750 nm. Data were graphed using GraphPad InStat, version 3 (GraphPad Software, Inc., San Diego, CA). For data analysis, multiple comparisons were done using one-way ANOVA followed by Student-Newman-Keuls post-hoc tests for multiple pairwise examinations. Changes were identified as significant if p was less than 0.05. Mean values are reported together with the standard error of mean (SEM) representing the combination of 2–3 different experimental runs (n = 10–15 for each treatment group).

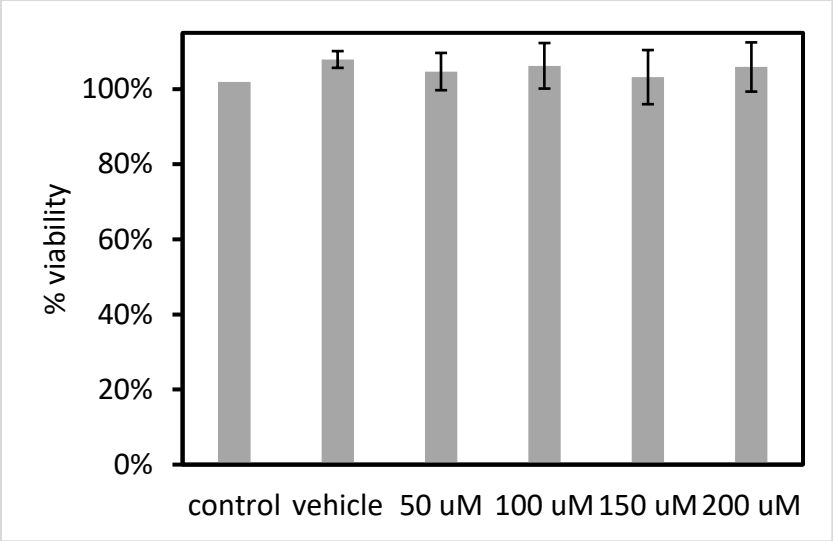

Figure S27. H9C2 cardiomyocyte viability after treatment with **BDP-NAC** (50-200 μM) without H_2O_2.

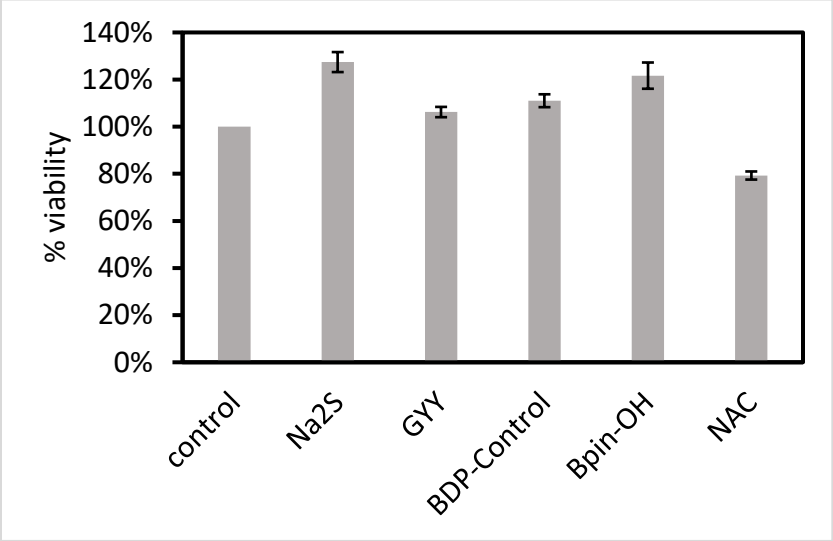

Figure S28. H9C2 cardiomyocyte viability after treatment with compound Na_2S, GYY4137, **BDP-Control**, Bpin-OH, and NAC (200 μm) without H_2O_2.

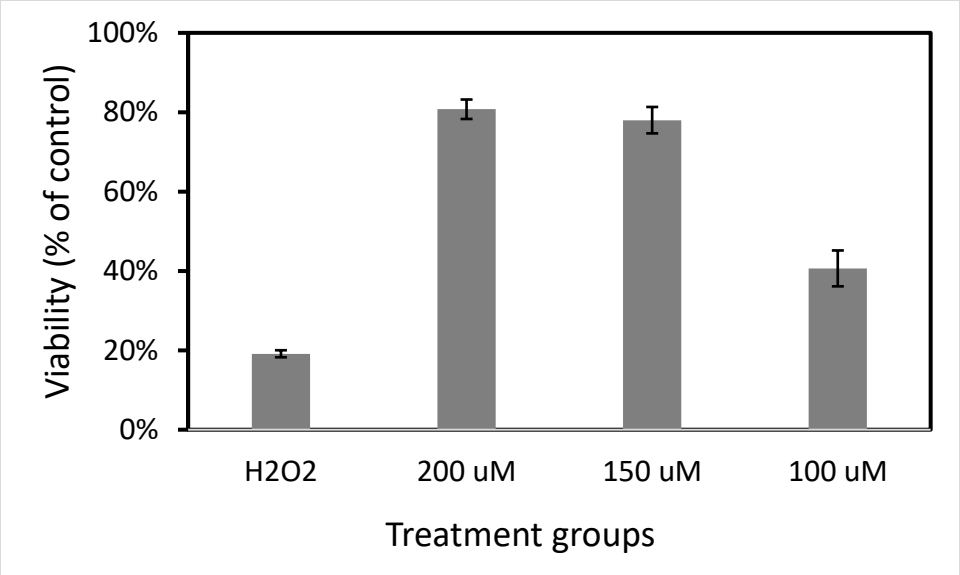

Figure S29. H9C2 cardiomyocyte viability after treatment with **BDP-NAC** (100-200 μM) concurrently with 100 μM H_2O_2 for 2 h.

Experimental References

1. Chen, W.; Liu, C.; Peng, B.; Zhao, Y.; Pacheco, A.; Xian, M., New Fluorescent Probes for Sulfane Sulfurs and the Application in Bioimaging. *Chem. Sci.* **2013,** *4*, 2892-2896.

2. Li, L.; Whiteman, M.; Guan, Y. Y.; Neo, K. L.; Cheng, Y.; Lee, S. W.; Zhao, Y.; Baskar, R.; Tan, C.-H.; Moore, P. K., Characterization of a Novel, Water-Soluble Hydrogen Sulfide–Releasing Molecule (GYY4137). *Circulation* **2008,** *117*, 2351-2360.

3. White, J. R.; Price, G. J.; Schiffers, S.; Raithby, P. R.; Plucinski, P. K.; Frost, C. G., A Modular Approach to Catalytic Synthesis using a Dual-Functional Linker for Click and Suzuki Coupling Reactions. *Tetrahedron Lett.* **2010,** *51*, 3913-3917.

4. Zhang, C.; Zheng, G.; Fang, L.; Li, Y., Efficient Synthesis of Valsartan, a Nonpeptide Angiotensin II Receptor -Antagonist. *Synlett* **2006,** *2006*, 0475-0477.

5. Benati, L.; Capella, L.; Montevecchi, P. C.; Spagnolo, P., Free-Radical Addition of Alkanethiols to Alkynes. Rearrangements of the Intermediate β-(Vinylthio) Radicals. *J. Org. Chem.* **1994,** *59,* 2818-2823.

6. Navath, R. S.; Wang, B.; Kannan, S.; Romero, R.; Kannan, R. M., Stimuli-Responsive Star Poly(ethylene glycol) Drug Conjugates for Improved Intracellular Delivery of the Drug in Neuroinflammation. *J. Controlled Release* **2010,** *142,* 447-456.

Chapter 6: Self-Amplified Depolymerization of Oligo(thiourethanes) for the Release of COS/H_2S

Adapted from C. R. Powell, J. C. Foster, S. N. Swilley, K. Kaur, S. J. Scannelli, D. Troya and J. B. Matson, Polym. Chem., 2019, Advance Article, DOI: 10.1039/C9PY00354A with permission from The Royal Society of Chemistry.

6.1. Authors.

Chadwick R. Powell,[§,†] Jeffrey C. Foster,[§,†] Sarah N. Swilley,[§,†] Kuljeet Kaur,[§,†] Samantha J. Scannelli,[§,†], Diego Troya,[§] and John B. Matson*[§,†]

[§]Department of Chemistry, Virginia Tech, Blacksburg, Virginia 24061, United States

[†]Macromolecules Innovation Institute, Virginia Tech, Blacksburg, Virginia 24061, United States

6.2. Abstract.

Herein we report the self-amplified depolymerization of an aryl oligo(thiourethane) (OTU) for the release of COS/H_2S. The OTU was synthesized via polyaddition of 4-isothiocyanatobenzyl alcohol and end-capped with an aryl azide. The aryl azide chain-end was reduced by tris(2-carboxyethyl)phosphine or H_2S to the corresponding aniline, resulting in depolymerization (i.e., self-immolation) and the release of COS/H_2S. Depolymerization was monitored by ^{1}H NMR and UV-Vis spectroscopy, and the released COS was converted into H_2S by the ubiquitous enzyme carbonic anhydrase in aqueous media, generating an amplified response.

6.3. Introduction

Depolymerizable or degradable polymers (i.e., self-immolative polymers) are a class of materials that depolymerize in the presence of a specific stimulus, typically resulting in the release of small molecules.[1] These stimuli-responsive depolymerizable polymers are comprised of three discrete portions: a triggering moiety, a spacer, and an output.[2] The triggering moiety is a functional group that responds to a specific stimulus such as light,[3] redox reactions,[4] or a small molecule.[5-6] Application of the stimulus results in the formation of an unstable intermediate, typically on the polymer chain-end, which causes the depolymerization of a single monomer unit and the subsequent regeneration of the unstable intermediate (Scheme 1A). This process repeats until each monomer unit in the polymer chain has depolymerized. The utility of depolymerizable polymers derives from the release of the output molecule, which occurs concurrently with depolymerization. Output molecules are often quantifiable (i.e., fluorescent small molecules), making depolymerizable polymers intriguing motifs for signal detection and amplification.[7-8] Despite this progress in depolymerizable polymers for detection of biological events, few depolymerizable polymers have been developed that release biologically active output molecules.[1,9] Here we envisioned developing an depolymerizable polymer capable of releasing hydrogen sulfide (H_2S), a biological signaling gas.

In 1996 H_2S was established as a critical signalling molecule in mammals.[10] As such, alterations in H_2S production in the body have systemic consequences and have been linked to a variety of disease states including cardiovascular disease,[11] cystic fibrosis,[12] and diabetes,[13] among others.[14] A commonality in these disease states is a decrease in endogenous H_2S production.[15] As a result, exogenous delivery of H_2S through inorganic donor salts (NaSH, Na_2S) or synthetic donor compounds may mitigate disease

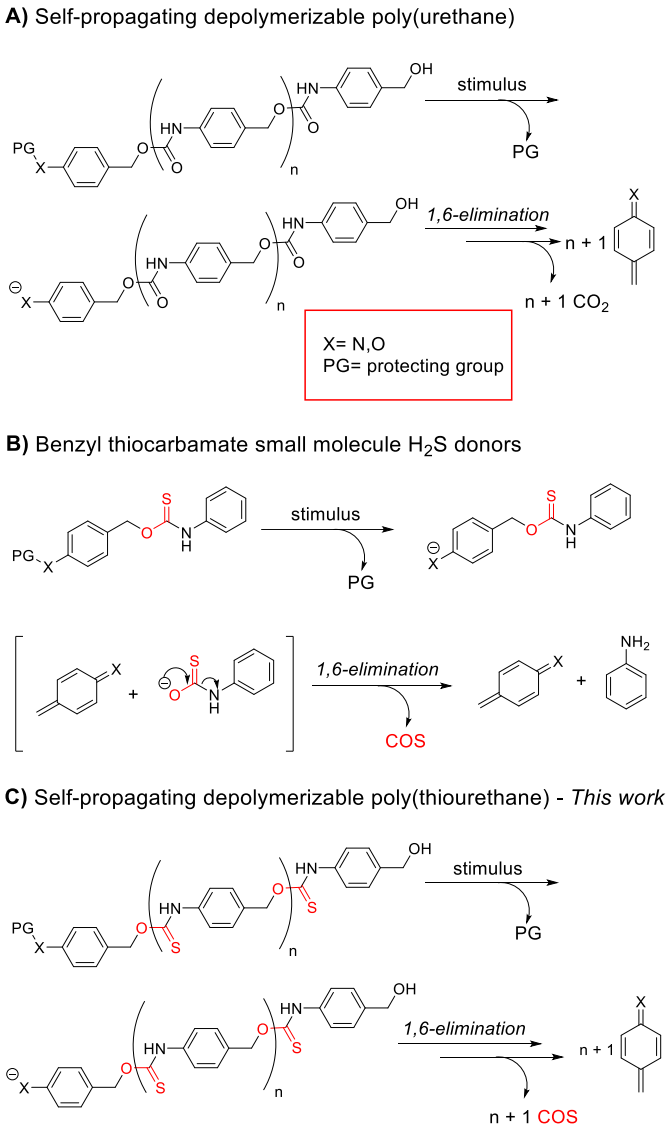

Scheme 1. A) Depolymerizable aryl poly(urethanes). B) Small molecule benzyl thiocarbamate COS/H_2S donors developed by Pluth and coworkers.[27] C) Proposed COS/H_2S-releasing depolymerizable poly(thiourethane).

symptoms and improve healing.[16-19] To aid in understanding H_2S physiology and investigate possible benefits of H_2S therapy, several types of small molecule and polymeric H_2S donors have been developed over the past few years.[20-24] However, many classes of synthetic donors release only one equivalent of H_2S per equivalent of consumed trigger,

which is often a redox-active thiol. This net neutral redox balance may ultimately limit the long-term efficacy of common of synthetic donors and complicate *in vivo* analysis.[25-26] Thus, H_2S donors that release multiple equivalents of H_2S per triggering event may be critical in furthering the therapeutic benefit of exogenous H_2S delivery.

In an effort to develop a depolymerizable polymer that can release multiple equivalents of H_2S in response to low concentrations of H_2S itself, we were inspired by Pluth and coworkers' 2016 report that introduced benzyl thiocarbamates as a class of small molecule, dual carbonyl sulfide (COS)/H_2S donors based on the benzyl elimination reaction (Scheme 1B).[27] These benzyl thiocarbamates released COS via a 1,6-benzyl elimination reaction triggered by a reducing stimulus, such as H_2S itself. The elimination reaction led to release of the desired COS payload via an unstable thiocarbamic acid intermediate (Scheme 1B). The released COS was then rapidly hydrolyzed to H_2S via the action of the ubiquitous enzyme carbonic anhydrase (CA). Since this seminal work on small molecule thiocarbamates as dual COS/H_2S donors, Pluth and coworkers have demonstrated the ability to trigger COS/H_2S release in the presence of other stimuli including hydrogen peroxide,[28] cysteine,[29] light,[30] and others.[29, 31] We envisioned that leveraging benzyl thiocarbamates as the repeat unit of a depolymerizable polymer would provide an exciting opportunity for a platform from which endogenous H_2S production may be amplified, creating a self-amplified depolymerizable polymer (SADP) (Scheme 1C).

6.4. Results and Discussion.

In order to synthesize a COS/H_2S-donating SADP, we first set out to prepare a monomer that could undergo a step-growth polyaddition to make the desired

poly(thiourethane) (PTU). Typically, PTUs are prepared as S-alkyl thiocarbamates through the reaction of thiols and isocyanates mediated by the soft Lewis-acid catalyst dibutyltin dilaurate (DBTDL).[32-34] Unfortunately, the *S*-alkyl thiocarbamate isomer is a less efficient COS donor than the *O*-alkyl isomer, likely stemming from an unfavorable Gibbs free energy (ΔG) for the COS-releasing reaction.[35] In contrast, the *O*-alkyl thiourethane isomer readily decomposes to form COS via the 1,6-benzyl elimination. Accordingly, synthesis of a depolymerizable *O*-alkyl thiourethane repeating unit would require a monomer containing both an aryl isothiocyanate (Ar–NCS) and a benzyl alcohol to facilitate efficient COS release.

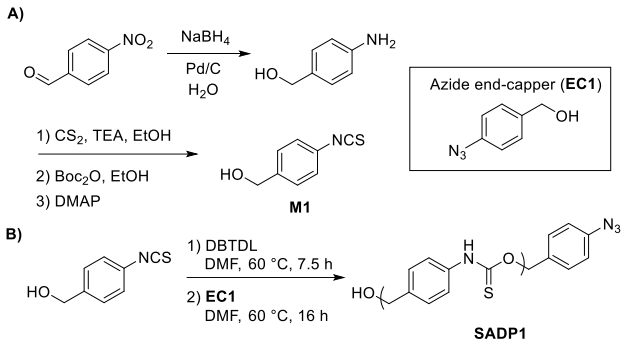

Scheme 2. A) Synthesis of **M1**. B) Synthesis of aryl azide end-capped **SADP1**.

To meet this challenge, we designed and synthesized a bifunctional monomer containing the desired aryl isothiocyanate and benzyl alcohol functional groups (**M1**, Scheme 2). Starting from 4-nitrobenzaldehyde, a one-pot reduction of both the nitro and aldehyde groups was accomplished by addition of sodium borohydride ($NaBH_4$) and palladium on carbon (Pd/C, 5 mol %) in water to give 4-aminobenzyl alcohol (**4-AB**). To access the aryl isothiocyanate, a method

developed by Boas and coworkers[36] was employed wherein the aniline of **4-AB** was converted into the corresponding dithiocarbamate salt by reaction with carbon disulfide in the presence of triethylamine, followed by addition of Boc anhydride, which led to the spontaneous evolution of COS gas and *tert*-butyl alcohol and the formation of the desired aryl isothiocyanate (**M1**).

With the desired AB monomer in hand, we envisioned that it would undergo polyaddition in the presence of DBTDL, as this catalyst has been used successfully in analogous, non-sulfur-containing systems. Thus, the polymerization of **M1** was carried out in dry DMF (1 M) at 60 °C under N_2 in the presence of DBTDL (5 mol %). Under these conditions we observed a plateau in monomer conversion (p) after 7.5 h at approximately 85 % (Figure S11). At this stage in the polymerization, 1 equiv of 4-azidobenzylalcohol (**EC1**) was added as an end-capping reagent, and the reaction mixture was allowed to stir overnight. The azide end-capped SADP (**SADP1**) was then isolated as a yellow powder after precipitating from Et_2O. The presence of the aryl azide on the oligomer chain end was confirmed by FTIR spectroscopy (Figure S9), and the oligomer M_n was measured to be 1.6 kg/mol by ^{1}H NMR end-group analysis (degree of polymerization (X_n) of ~7), which is consistent with the expected M_n for 85% conversion. Size exclusion chromatography (SEC) with light scattering detection was attempted, but the low molecular weight of the oligomer coupled with its low d*n*/d*c* value in the elution solvent (THF) prevented accurate analysis.

To explain the limited conversion of monomer under these conditions, the reaction Gibbs energy for a model small molecule reaction between benzyl alcohol and phenyl isothiocyanate was calculated using density functional theory. The 60 ^{o}C reaction Gibbs energy using the M06-2X functional and aug-cc-pVDZ basis set with implicit DMF solvation is -2.28 kcal/mol. Combining Carothers' equation for step-growth

polymerizations with the reaction Gibbs energy relationship to the equilibrium constant (K) (equation 1) we calculated p to be 0.85 for this system under ideal conditions. These calculations indicate a maximum degree of polymerization (X_n) of 6.7. The polymerization of **M1** routinely yielded oligomers with X_n ~7, in good agreement with the predictions. Therefore, the limited conversion observed experimentally appears to be due to the small polymerization exoergicity under the experimental conditions.

$$p_{eq} = \frac{\sqrt{e^{\frac{-\Delta G}{RT}}}}{1 + \sqrt{e^{\frac{-\Delta G}{RT}}}} \quad (Equation\ 1)$$

We next investigated the depolymerization of azide-terminated **SADP1** by ^{1}H NMR spectroscopy. For these experiments, tris(2-carboxyethyl)phosphine (TCEP, 1.7 equiv with respect to azide chain ends) was employed as an organo-soluble reducing agent to facilitate the reduction of the chain-end aryl azide, leading to depolymerization and ultimately COS release. In order to follow the reaction, changes in the peaks attributed to **SADP1** were monitored as well as the generation of **4-AB**, an expected major byproduct of **SADP1** depolymerization. Due to the low water solubility of **SADP1** at concentrations required for NMR spectroscopy, ^{1}H NMR analysis was performed in DMSO-d_6, which dramatically decreases reaction rates for 1,6-elimination reactions relative to water.[37] However, despite the low reaction rate, ^{1}H NMR analysis revealed a decrease in the broad heteroatomic peak attributed to the thiocarbamate repeating unit proton (Ar–N**H**C(S)O) as well as the appearance of well resolved aromatic doublets consistent with **4-AB**. Under the same conditions, depolymerization of a benzyl alcohol end-capped control SADP (**Ctrl-SADP**)

occurred more slowly in the presence of TCEP (Figures S12 and S13), indicating that reduction of the chain-end azide is critical for initiating depolymerization.

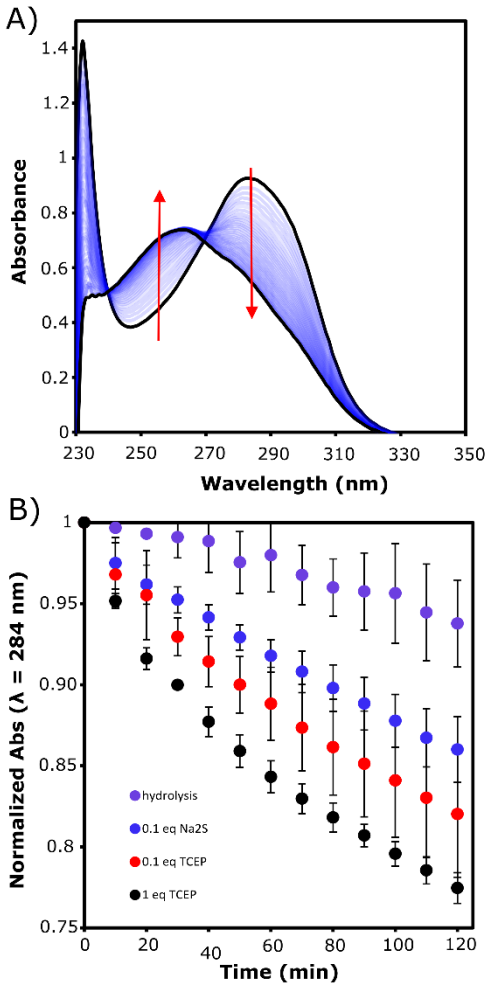

Figure 1. A) Representative UV-Vis spectra of **SADP1** (10 µM) prior to the addition of reducing agent (λ_{max} = 284 nm) and 2 h after the addition of reducing agent (λ_{max} = 254 nm). B) Change in absorbance of **SADP1** at 284 nm over time in the presence and absence of reducing agents. Data are normalized to the absorbance at t_0, prior to the addition of reducing agent. All depolymerisation experiments were run in PBS buffer (pH 7.4) with 2% DMSO, 1 mM CTAB, and 300 nM CA.

Monitoring depolymerization by UV-Vis spectroscopy allowed for use of aqueous media because lower concentrations of **SADP1** could be employed than in the ^{1}H NMR spectroscopy

experiments. For these experiments, **SADP1** was dissolved in PBS buffer (pH 7.4) containing DMSO (2 % v/v) and cetrimonium bromide (CTAB) to aid in solubility. Prior to adding a reducing agent, a broad absorbance for **SADP1** was observed at 284 nm (Figure 1A). Upon addition of a reducing agent (TCEP or Na_2S), the absorbance maximum began to gradually shift to lower wavelength over the course of 2 h. We attribute the shift in λ_{max} for the oligomer to depolymerization and the generation of **4-AB**. Isosbestic points at 240 and 271 nm were observed, although they shifted slightly during the course of the analysis, which we attribute to low MW SADP species and oxidized byproducts of **4-AB**.

In order to better evaluate the depolymerization kinetics of **SADP1,** a series of UV-Vis experiments was conducted using varying amounts of TCEP, Na_2S, and no trigger (hydrolysis) in the presence of CA (which converts COS into H_2S). By plotting the change in absorbance at 284 nm (λ_{max} of **SADP1**) over time, a clear trend in reaction kinetics was observed. Addition of 1 equiv TCEP relative to aryl azide **SADP1** chain-end gave the greatest decrease in absorbance for **SADP1** over the course of 2 h. When the amount of TCEP was reduced to 0.1 equiv, a concomitant decrease in rate was observed. Addition of Na_2S (0.1 equiv) as an alternative means of reducing the **SADP1** chain-end gave data similar to that for the addition of 0.1 equiv TCEP, indicating that TCEP and Na_2S are roughly equal in reduction capacity under these conditions and that both generate multiple equivalents of H_2S per equivalent of added trigger. Additionally, the same shift in λ_{max} was observed without the addition of any reducing agent, albeit at a much lower rate, indicating that hydrolysis, likely of the thiourethane units, contributes to the depolymerization of **SADP1**.

In light of the data indicating that hydrolysis is a viable mechanism for depolymerization of **SADP1**, UV-Vis experiments of **Ctrl-SADP** were conducted to

investigate whether the reducing agent (Na_2S) or the H_2S released in the depolymerization reaction might also contribute to degradation of the benzyl thiocarbamate moiety. The spectral profile of **Ctrl-SADP** is very similar to **SADP1**, with a broad absorbance centred at 284 nm (Figure S14). However, there was no significant change in the absorbance spectrum of **Ctrl-SADP** in the presence or absence of Na_2S, indicating that sulfide does not degrade the benzyl thiocarbamate moiety. Therefore, we conclude that the observed enhanced rate of **SADP1** depolymerization in the presence of Na_2S compared with water is due to the reduction of the chain-end azide and subsequent depolymerization.

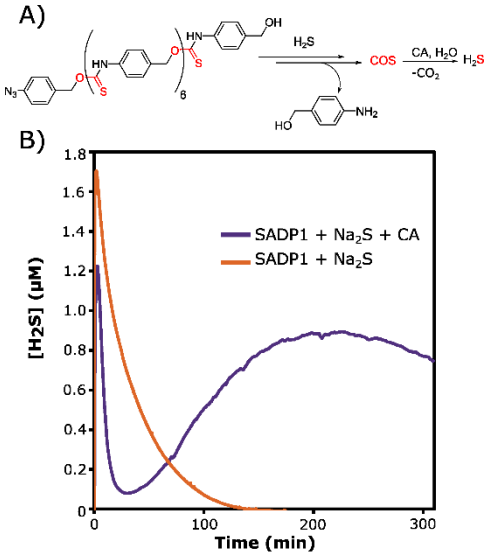

Figure 2. A) Scheme depicting H_2S release data from **SADP1**. B) H_2S release data from **SADP1** (100 μM) in the presence of Na_2S (0.1 equiv) with 300 nM CA (purple curve) and without CA (orange curve).

Lastly, analysis of the H_2S release profile for **SADP1** was performed using an H_2S-selective electrochemical probe. H_2S release experiments were performed in PBS buffer

(pH 7.4) at 100 μM **SADP1** with the addition of CTAB, similar to the UV-Vis experiments. Addition of Na_2S (0.1 equiv) as the reducing agent to a solution of **SADP1** containing CA generated an initial spike in H_2S due to the presence of Na_2S, followed by a rapid decrease in H_2S concentration, followed by steady generation of H_2S, ultimately reaching a peak concentration after 220 min (Figure 2, purple curve). In contrast, addition of Na_2S (0.1 equiv) to a solution of **SADP1** in the absence of CA generated a spike in H_2S concentration followed by a rapid return to baseline, similar to probe response when only Na_2S is added (orange curve). This result indicates that the released COS from **SADP1** was not converted into H_2S, as expected when CA is not present. The apparently low peak H_2S concentration (0.9 μM) is due to the long peaking time of **SADP1**, where low peak concentration is a result of slow H_2S generation combined with COS/H_2S volatilization and H_2S oxidation. Taken together, results from these H_2S release experiments demonstrate that **SADP1** successfully generates H_2S in the presence of submolar quantities of a Na_2S trigger, acting in an autoinductive self-propagating amplification reaction[38] where H_2S derived from hydrolysis of COS generates increasing amounts of H_2S.

6.5. Conclusions

The first COS/H_2S-releasing SADP is reported. The depolymerizable oligo(thiourethane) was synthesized in a polyaddition reaction from a bifunctional monomer containing an aryl isothiocyanate and a benzyl alcohol. The oligomer structure was confirmed by ^1H NMR and FTIR spectroscopy. Aryl azide-terminated **SADP1** underwent depolymerization in the presence of reducing agents, with a greater concentration of reducing agent resulting in an enhanced reaction rate. Additionally, upon

addition of submolar concentrations of reducing agents, including Na_2S, **SADP1** demonstrated COS release, which was converted to H_2S in the presence of CA, generating multiple equivalents of H_2S per triggering event in a manner consistent with signal amplification.

6.6. Acknowledgements

This work was supported by the National Science Foundation (DMR-1454754), the National Institutes of Health (R01GM123508), and the Dreyfus foundation. The authors acknowledge Ryan Carrazzone for help with polymer analysis. Advanced Research Computing at Virginia Tech is gratefully acknowledged for providing computational resources and technical support that have contributed to the results reported within this manuscript.

6.7. References

1. Peterson, G. I.; Larsen, M. B.; Boydston, A. J., Controlled Depolymerization: Stimuli-Responsive Self-Immolative Polymers. *Macromolecules* **2012,** *45*, 7317-7328.

2. Carl, P. L.; Chakravarty, P. K.; Katzenellenbogen, J. A., A Novel Connector Linkage Applicable in Prodrug Design. *J. Med. Chem.* **1981,** *24*, 479-480.

3. de Groot, F. M. H.; Albrecht, C.; Koekkoek, R.; Beusker, P. H.; Scheeren, H. W.; Amir, R. J.; Pessah, N.; Shamis, M.; Shabat, D., Cover Picture: "Cascade-Release Dendrimers" Liberate All End Groups upon a Single Triggering Event in the Dendritic Core / Self-Immolative Dendrimers. *Angew. Chem. Int. Ed.* **2003,** *42*, 4411-4411.

4. Weinstain, R.; Baran, P. S.; Shabat, D., Activity-Linked Labeling of Enzymes by Self-Immolative Polymers. *Bioconjugate Chem.* **2009,** *20*, 1783-1791.

5. Seo, W.; Phillips, S. T., Patterned Plastics That Change Physical Structure in Response to Applied Chemical Signals. *J. Am. Chem. Soc.* **2010,** *132,* 9234-9235.

6. Zhang, H.; Yeung, K.; Robbins, J. S.; Pavlick, R. A.; Wu, M.; Liu, R.; Sen, A.; Phillips, S. T., Self-Powered Microscale Pumps Based on Analyte-Initiated Depolymerization Reactions. *Angew. Chem. Int. Ed.* **2012,** *51,* 2400-2404.

7. Sagi, A.; Weinstain, R.; Karton, N.; Shabat, D., Self-Immolative Polymers. *J. Am. Chem. Soc.* **2008,** *130,* 5434-5435.

8. Redy, O.; Kisin-Finfer, E.; Sella, E.; Shabat, D., A Simple FRET-Based Modular Design for Diagnostic Probes. *Org. Biomol. Chem.* **2012,** *10,* 710-715.

9. Shabat, D., Self-Immolative Dendrimers as Novel Drug Delivery Platforms. *J. Polym. Sci., Part A: Polym. Chem.* **2006,** *44,* 1569-1578.

10. Abe, K.; Kimura, H., The Possible Role of Hydrogen Sulfide as an Endogenous Neuromodulator. *J. Neurosci.* **1996,** *16,* 1066-1071.

11. Lefer, D. J., A New Gaseous Signaling Molecule Emerges: Cardioprotective Role of Hydrogen Sulfide. *Proc. Natl. Acad. Sci. U. S. A.* **2007,** *104,* 17907.

12. Fang, L.; Li, H.; Tang, C.; Geng, B.; Qi, Y.; Liu, X., Hydrogen Sulfide Attenuates the Pathogenesis of Pulmonary Fibrosis Induced by Bleomycin in Rats. *Can. J. Physiol. Pharmacol.* **2009,** *87,* 531-538.

13. Szabo, C., Roles of Hydrogen Sulfide in the Pathogenesis of Diabetes Mellitus and its Complications. *Antioxidants & redox signaling* **2012,** *17,* 68-80.

14. Powell, C. R.; Dillon, K. M.; Matson, J. B., A Review of Hydrogen Sulfide (H_2S) Donors: Chemistry and Potential Therapeutic Applications. *Biochem. Pharmacol.* **2018,** *149,* 110-123.

15. Wang, R., Two's Company, Three's a Crowd: Can H_2S be the Third Endogenous Gaseous Transmitter? *FASEB J.* **2002,** *16*, 1792-8.

16. Zhao, W.; Zhang, J.; Lu, Y.; Wang, R., The Vasorelaxant Effect of H_2S as a Novel Endogenous Gaseous K_{ATP} Channel Opener. *The EMBO Journal* **2001,** *20*, 6008-6016.

17. Whiteman, M.; Cheung, N. S.; Zhu, Y. Z.; Chu, S. H.; Siau, J. L.; Wong, B. S.; Armstrong, J. S.; Moore, P. K., Hydrogen Sulphide: A Novel Inhibitor of Hypochlorous Acid-Mediated Oxidative Damage in the Brain? *Biochem. Biophys. Res. Commun.* **2005,** *326*, 794-798.

18. Zhao, Y.; Yang, C.; Organ, C.; Li, Z.; Bhushan, S.; Otsuka, H.; Pacheco, A.; Kang, J.; Aguilar, H. C.; Lefer, D. J.; Xian, M., Design, Synthesis, and Cardioprotective Effects of N-Mercapto-Based Hydrogen Sulfide Donors. *J. Med. Chem.* **2015,** *58*, 7501-7511.

19. Li, Z.; Organ, C. L.; Zheng, Y.; Wang, B.; Lefer, D. J., Abstract 17903: Novel Esterase-Activated Hydrogen Sulfide Donors Attenuate Myocardial Ischemia/Reperfusion Injury. *Circulation* **2016,** *134*, A17903-A17903.

20. Foster, J. C.; Powell, C. R.; Radzinski, S. C.; Matson, J. B., S-Aroylthiooximes: A Facile Route to Hydrogen Sulfide Releasing Compounds with Structure-Dependent Release Kinetics. *Org. Lett.* **2014,** *16*, 1558-1561.

21. Powell, C. R.; Foster, J. C.; Okyere, B.; Theus, M. H.; Matson, J. B., Therapeutic delivery of H_2S via COS: small molecule and polymeric donors with benign byproducts. *J. Am. Chem. Soc.* **2016,** *138*, 13477-13480.

22. Xiao, Z.; Bonnard, T.; Shakouri-Motlagh, A.; Wylie, R. A. L.; Collins, J.; White, J.; Heath, D. E.; Hagemeyer, C. E.; Connal, L. A., Triggered and Tunable Hydrogen Sulfide Release from Photogenerated Thiobenzaldehydes. *Chem. Eur. J.* **2017,** *23*, 11294-11300.

23. Ercole, F.; Mansfeld, F. M.; Kavallaris, M.; Whittaker, M. R.; Quinn, J. F.; Halls, M. L.; Davis, T. P., Macromolecular Hydrogen Sulfide Donors Trigger Spatiotemporally Confined Changes in Cell Signaling. *Biomacromolecules* **2016,** *17*, 371-383.

24. Zheng, Y.; Yu, B.; Ji, K.; Pan, Z.; Chittavong, V.; Wang, B., Esterase-Sensitive Prodrugs with Tunable Release Rates and Direct Generation of Hydrogen Sulfide. *Angew. Chem. Int. Ed. Engl.* **2016,** *55*, 4514-8.

25. Zhao, Y.; Wang, H.; Xian, M., Cysteine-Activated Hydrogen Sulfide (H_2S) Donors. *J. Am. Chem. Soc.* **2011,** *133*, 15-17.

26. Martelli, A.; Testai, L.; Citi, V.; Marino, A.; Pugliesi, I.; Barresi, E.; Nesi, G.; Rapposelli, S.; Taliani, S.; Da Settimo, F.; Breschi, M. C.; Calderone, V., Arylthioamides as H_2S Donors: l-Cysteine-Activated Releasing Properties and Vascular Effects in Vitro and in Vivo. *ACS Med. Chem. Lett.* **2013,** *4*, 904-908.

27. Steiger, A. K.; Pardue, S.; Kevil, C. G.; Pluth, M. D., Self-Immolative Thiocarbamates Provide Access to Triggered H_2S Donors and Analyte Replacement Fluorescent Probes. *J. Am. Chem. Soc.* **2016,** *138*, 7256-7259.

28. Zhao, Y.; Pluth, M. D., Hydrogen Sulfide Donors Activated by Reactive Oxygen Species. *Angew. Chem. Int. Ed.* **2016,** *55*, 14638-14642.

29. Zhao, Y.; Steiger, A. K.; Pluth, M. D., Cysteine-activated hydrogen sulfide (H_2S) delivery through caged carbonyl sulfide (COS) donor motifs. *Chem. Commun.* **2018,** *54*, 4951-4954.

30. Zhao, Y.; Bolton, S. G.; Pluth, M. D., Light-Activated COS/H_2S Donation from Photocaged Thiocarbamates. *Org. Lett.* **2017,** *19*, 2278-2281.

31. Steiger, A. K.; Yang, Y.; Royzen, M.; Pluth, M. D., Bio-orthogonal "Click-and-Release" Donation of Caged Carbonyl Sulfide (COS) and Hydrogen Sulfide (H_2S). *Chem. Commun.* **2017,** *53*, 1378-1380.

32. Kultys, A.; Rogulska, M.; Pikus, S., The Synthesis and Characterization of New Thermoplastic Poly(Thiourethane-Urethane) s. *J. Polym. Sci., Part A: Polym. Chem.* **2008,** *46*, 1770-1782.

33. Eglin, D.; Griffon, S.; Alini, M., Thiol-Containing Degradable Poly(thiourethane-urethane)s for Tissue Engineering. *Journal of Biomaterials Science -- Polymer Edition* **2010,** *21*, 477-491.

34. Campiñez, M. D.; Ferris, C.; de Paz, M. V.; Aguilar-de-Leyva, A.; Galbis, J.; Caraballo, I., A New Biodegradable Polythiourethane as Controlled Release Matrix Polymer. *Int. J. Pharm.* **2015,** *480*, 63-72.

35. Zhao, Y.; Henthorn, H. A.; Pluth, M. D., Kinetic Insights into Hydrogen Sulfide Delivery from Caged-Carbonyl Sulfide Isomeric Donor Platforms. *J. Am. Chem. Soc.* **2017,** *139*, 16365-16376.

36. Munch, H.; Hansen, J. S.; Pittelkow, M.; Christensen, J. B.; Boas, U., A New Efficient Synthesis of Isothiocyanates from Amines using Di-tert-butyl Dicarbonate. *Tetrahedron Lett.* **2008,** *49*, 3117-3119.

37. Schmid, K. M.; Jensen, L.; Phillips, S. T., A Self-Immolative Spacer That Enables Tunable Controlled Release of Phenols under Neutral Conditions. *J. Org. Chem.* **2012,** *77*, 4363-4374.

38. Sun, X.; Shabat, D.; Phillips, S. T.; Anslyn, E. V., Self-Propagating Amplification Reactions for Molecular Detection and Signal Amplification: Advantages, Pitfalls, and Challenges. *J. Phys. Org. Chem.* **2018,** *31*, e3827.

6.7. Experimental

Materials and Methods

All reagents and solvents were obtained from commercial vendors and used as received unless otherwise stated. NMR spectra were measured on Agilent 400 MHz or Bruker 500 MHz spectrometers. ^{1}H and ^{13}C NMR chemical shifts are reported in ppm relative to internal solvent resonances. Yields refer to compounds as isolated after requisite purification unless otherwise stated. Thin-layer chromatography (TLC) was performed on glass-backed silica plates and visualized by UV. UV-Vis experiments were conducted on a Varian Cary 100 Bio UV-Vis spectrophotometer with a scan rate of 600 nm/min (1 nm data intervals) with 0 and 100 % transmittance baseline corrections. H_2S release data acquired with a WPI ISO-H2S-100 electrochemical probe set to a constant 10 nA current.

Synthetic Procedures

Synthesis of 4-aminobenzyl alcohol (**4-AB**)**.**

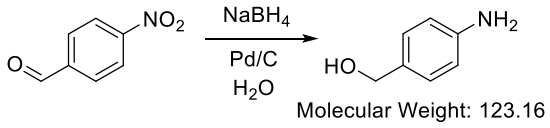

$NaBH_4$ (1.50 g, 40 mmol) was dissolved in H_2O (40 mL) in a 2-necked round bottom flask under N_2 flow. To the flask was added 4-nitrobenzaldehyde (2.00 g 13.2 mmol) in one portion. Pd/C (0.070, 0.66 mmol) was then added slowly to the flask (***CAUTION: this step leads to vigorous H_2 gas evolution; a plastic spatula should be used to add Pd/C to reduce the risk of sparking***). The reaction mixture was stirred at rt until all of the solids dissolved (~ 1 h) to give a clear yellow solution. The reaction mixture was then filtered through packed Celite. The aqueous solution was

extracted with EtOAc (3x, 30 mL), and the combined organic layers were dried over Na_2SO_4. The solvent was removed by rotary evaporation, and the crude product was purified by column chromatography on silica gel eluting with CH_2Cl_2. The pure product was obtained as an off-white solid (1.30 g, 80 % yield). ^{1}H NMR ($CDCl_3$): δ 7.14 (m, 2H), 6.66 (m, 2H), 4.53 (s, 2H) 3.60 (broad s, 2H). ^{13}C NMR ($CDCl_3$): δ 146.11, 131.16, 128.86, 115.24, 65.34.

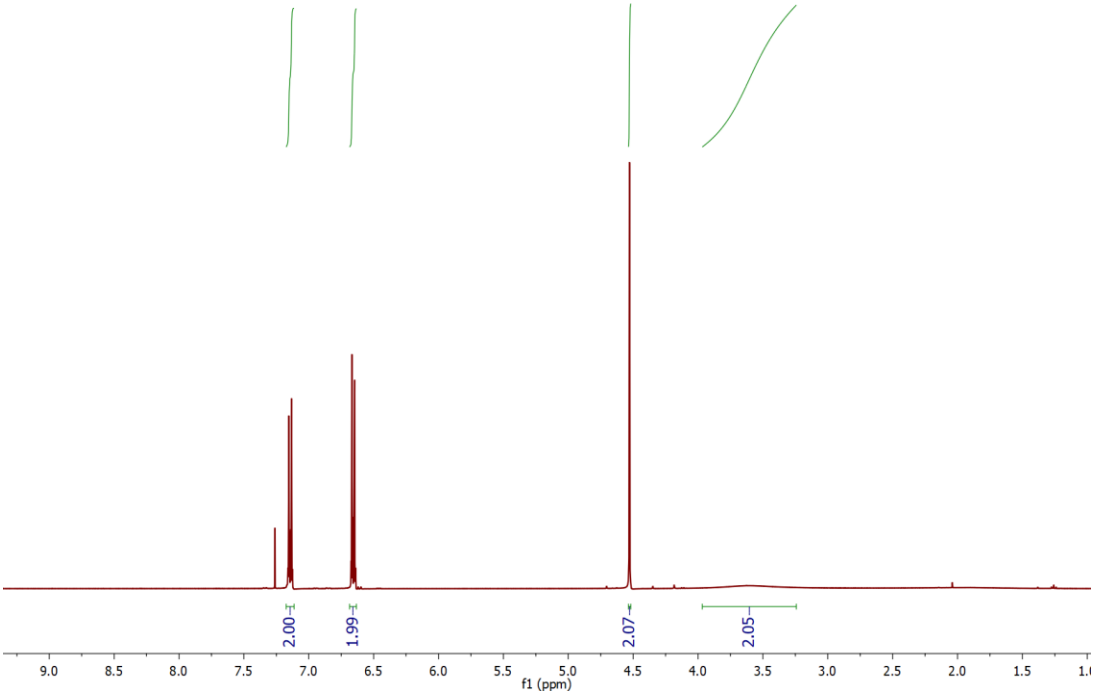

Figure S1. ^{1}H NMR spectrum ($CDCl_3$) of 4-aminobenzyl alcohol.

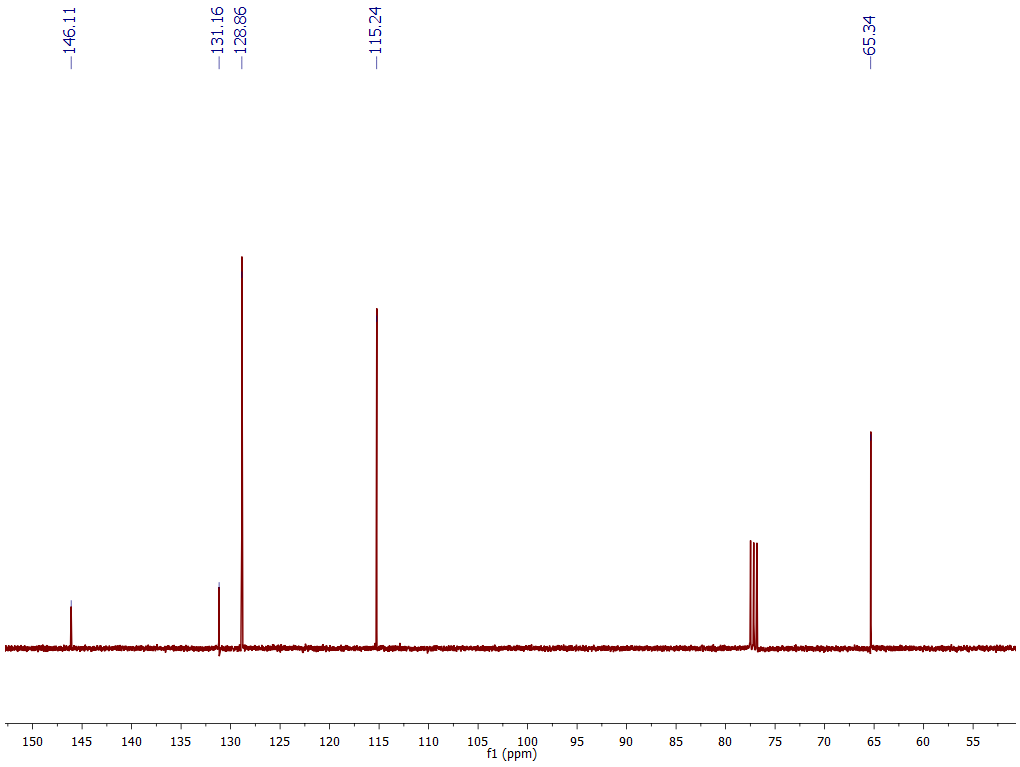

Figure S2. ^{13}C NMR spectrum ($CDCl_3$) of 4-aminobenzyl alcohol.

Synthesis of 4-isocyanatobenzyl alcohol **(M1)**

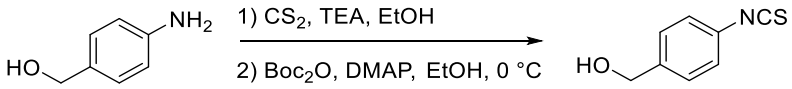

The procedure was adapted from a published procedure by Boas et al.[1] **4-AB** (2.0 g, 16 mmol) was dissolved in EtOH (40 mL) in a round bottom flask. To the flask was added CS_2 (10 mL, 170 mmol) followed by $N(Et)_3$ (2.3 mL, 17 mmol) resulting immediately in a clear yellow solution. The reaction mixture was allowed to stir at rt for 30 min. Reaction progress was monitored via TLC (2 % MeOH in CH_2Cl_2). Upon complete consumption of **4-AB**, the reaction vessel was cooled to 0 °C in an ice bath. A solution of Boc_2O (3.2g, 15 mmol) in 10 mL of EtOH was added dropwise

at 0 °C. DMAP (40 mg, 0.32 mmol) was subsequently added, and the reaction mixture was allowed to warm to rt while stirring for an additional 30 min. The reaction mixture was then diluted with CH_2Cl_2, washed with H_2O and brine, dried over Na_2SO_4, and concentrated by rotary evaporation to give a yellow-brown solid. The crude product was purified by a silica column, eluting with CH_2Cl_2 to yield a yellow/white solid. The solid was then recrystallized twice from hexanes to yield white, needle-like crystals (1.48 g, 56 % yield) (m.p. = 73.9 – 74.6 °C). ^{1}H NMR ($CDCl_3$): δ 7.33 (m, 2H), 7.20 (m, 2H), 4.67 (s, 2H) 1.99 (t, 1H). ^{13}C NMR ($CDCl_3$): δ 140.23, 135.37, 130.47, 128.05, 125.95, 64.56.

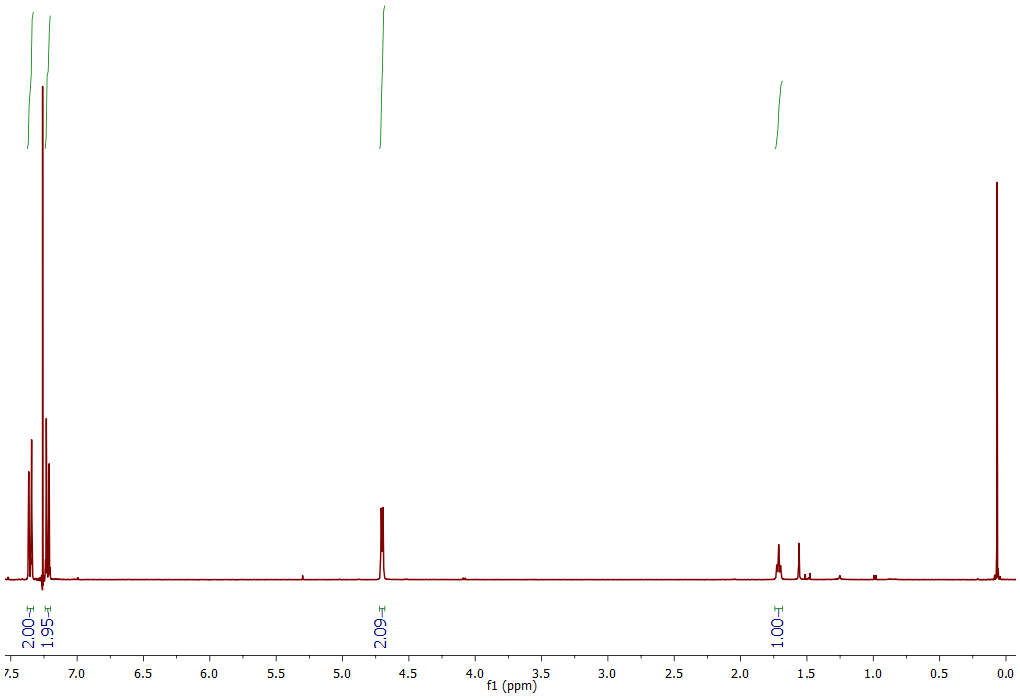

Figure S3. ^{1}H NMR spectrum ($CDCl_3$) of **M1**.

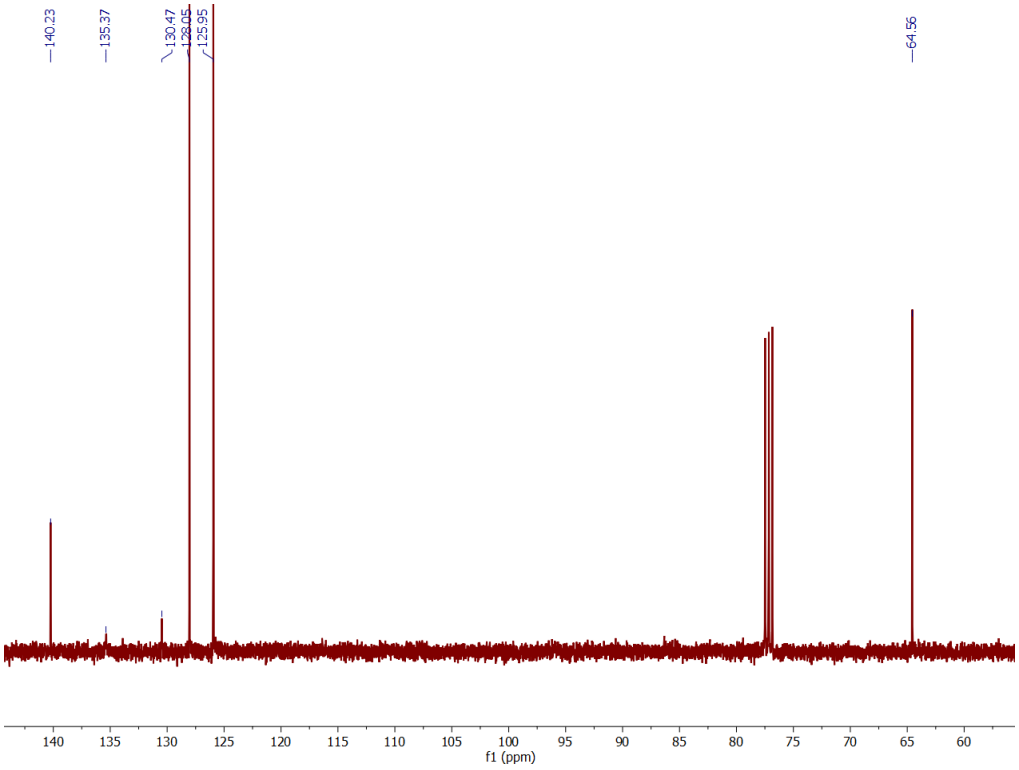

Figure S4. ^{13}C NMR spectrum ($CDCl_3$) of **M1**.

Synthesis of (4-azidophenyl)methanol (**EC1**)

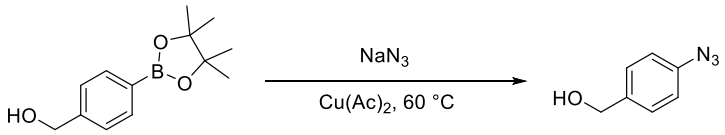

The procedure was adapted from published procedures by Aldrich et al.[2] A round bottom flask was charged with 4-(hydroxymethyl)phenyl boronic acid pinacol ester (0.500 g, 2.16 mmol) and a stirbar. The pinacol boronic ester starting material was dissolved in methanol (10 mL). Sodium azide (0.211 g, 3.25 mmol) was added followed by copper(II) acetate monohydrate (0.43 g, 0.22 mmol). The resulting suspension was warmed to 60 °C in an oil bath and stirred vigorously. The reaction was monitored by TLC (20 % MeOH in EtOAc). Once complete, the mixture was cooled to rt, silica gel was added, and the reaction was concentrated to dryness by rotary evaporation. The

dry-loaded crude product was purified on a silica gel column (eluting with Et_2O) to obtain the pure product as a yellow oil (0.220 g, 70 % yield). ^{1}H NMR ($CDCl_3$): δ 7.36 (m, 2H), 7.02 (m, 2H), 4.67 (d, *J* = 6 Hz, 2H) 1.68 (t, *J* = 6 Hz, 1H). ^{13}C NMR ($CDCl_3$): δ 139.53, 137.71, 128.69, 119.27, 64.90.

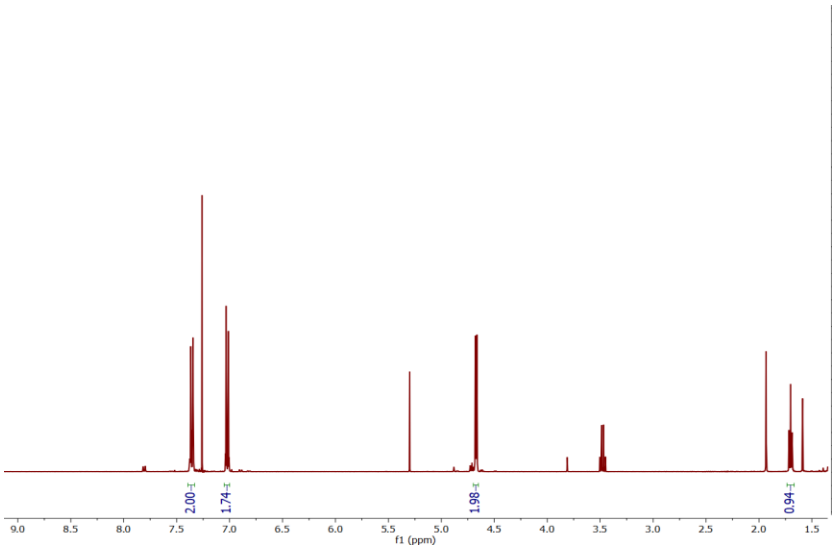

Figure S5. ^{1}H NMR spectrum ($CDCl_3$) of **EC1**.

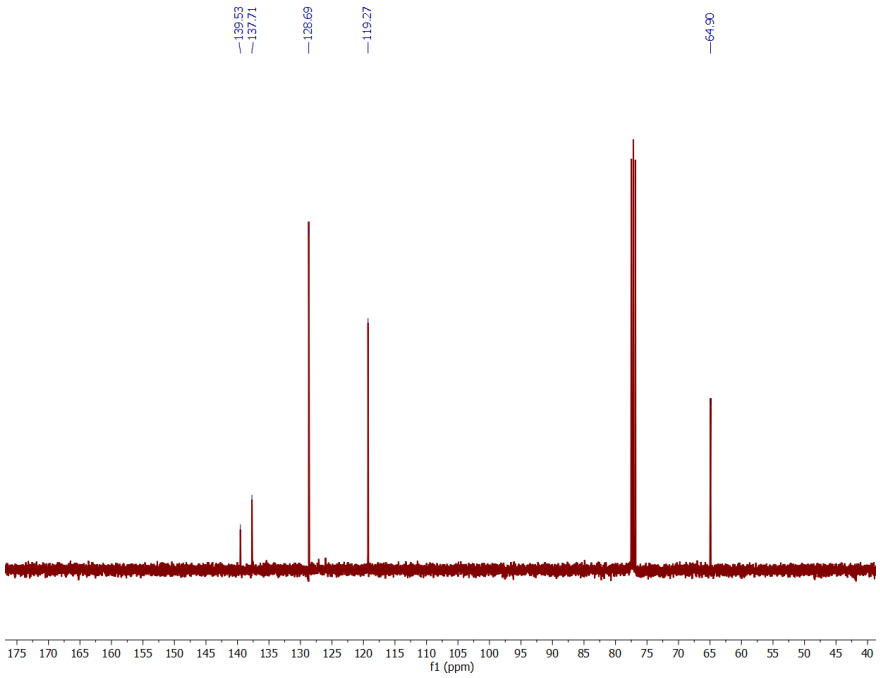

Figure S6. ^{13}C NMR spectrum ($CDCl_3$) of **EC1**.

Representative polymerization of **SADP1**

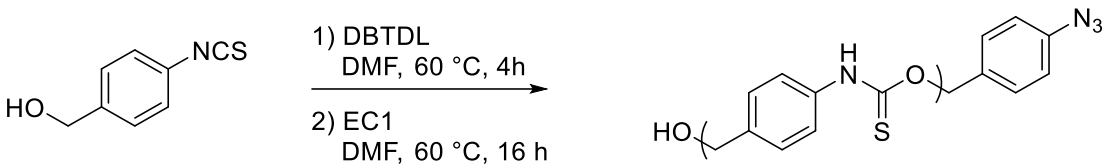

The procedure was adapted from published procedures by Shabat et al.[3] A two-neck round bottom flask equipped with a glass stopper and vacuum adapter was charged with a magnetic stirbar and flame-dried under vacuum. The flask was then put under positive N_2 pressure and charged with **M1** (60 mg, 0.36 mmol). **M1** was then dissolved in dry DMF (0.4 mL) to give a clear, colorless solution. The solution was then heated to 60 °C in an oil bath, and DBTDL (11 μL, 0.018 mmol) was added at temperature. The reaction mixture was allowed to stir at 60 °C under N_2 atmosphere for 7.5 h, resulting in a clear, yellow solution. In a separate flask, **EC1** (54 mg, 0.36 mmol) was dissolved in dry DMF (0.4 mL) and subsequently added to the reaction mixture. The reaction mixture was stirred for 14 h at 60 °C. The mixture was then cooled to rt and precipitated twice into Et_2O to afford **SADP1** as a yellow/brown solid (32 mg).

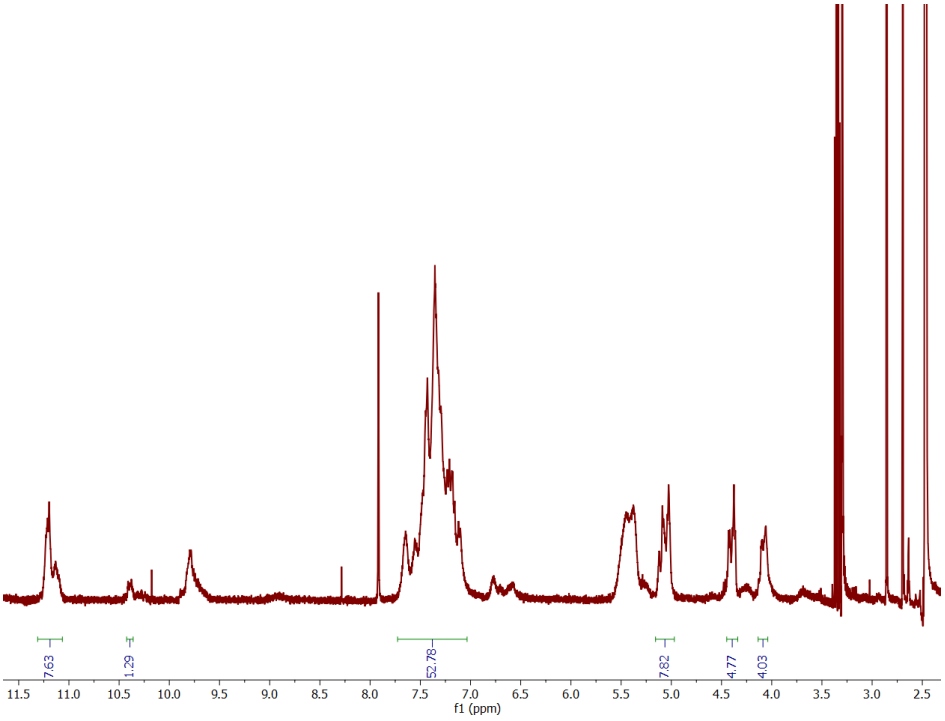

Figure S7. ^{1}H NMR spectrum (DMSO-d_6) of **SADP1.**

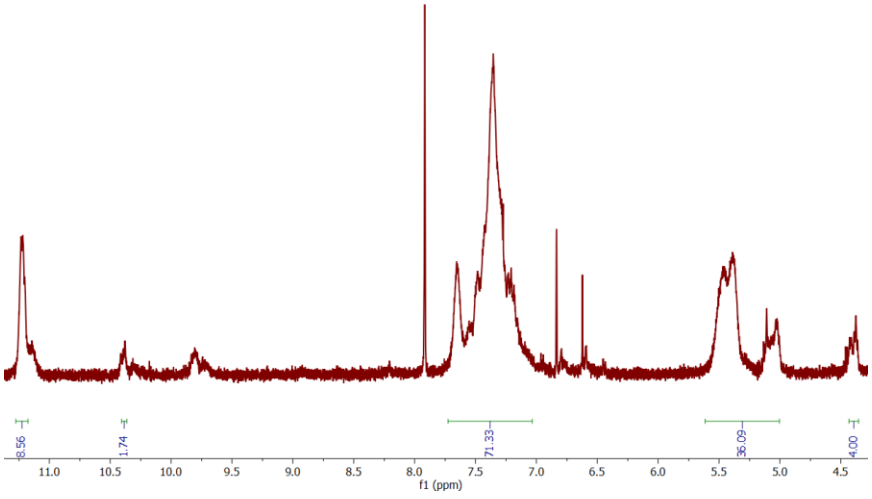

Figure S8. ^{1}H NMR spectrum (DMSO-d_6) of **Ctrl-SIP**.

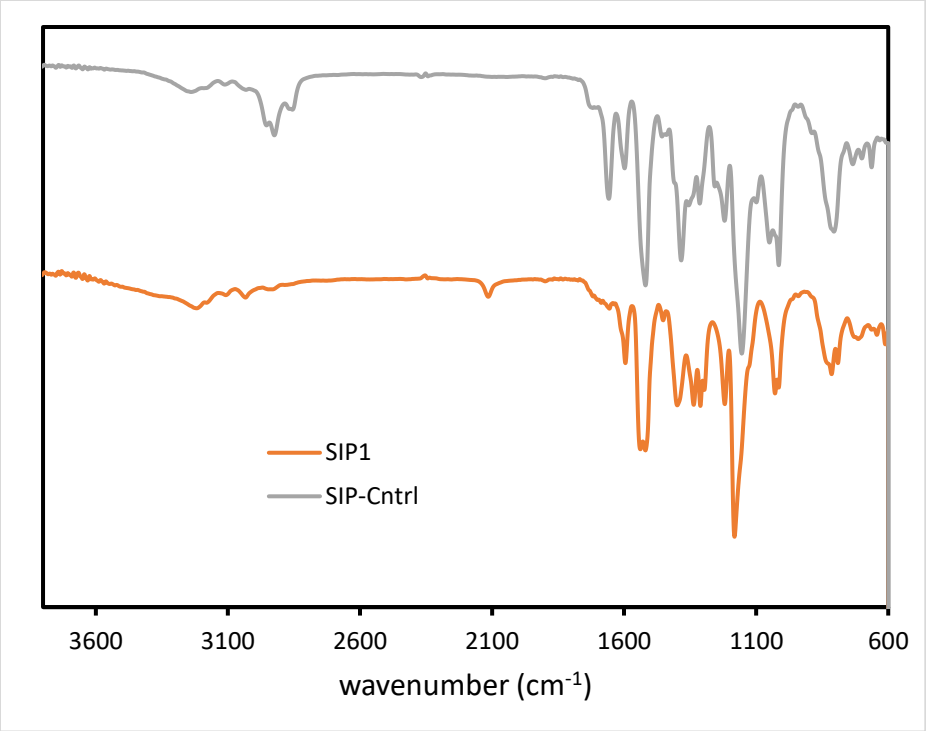

Figure S9. Offset FTIR spectra of **SADP1** and **SADP-Ctrl**. The absorbance band at ~2100 cm^{-1} confirms the presence of the aryl azide end group of **SADP1**.

Polymerization kinetics

Polymerizations were performed as described in *Representative polymerization of SIPs* with 1,3,5-trimethoxybenzene added to the reaction mixture as an internal standard. The polymerization was monitored by removing aliquots from the reaction mixture at predetermined timepoints via an N_2-purged syringe. Aliquots were cooled rapidly in an ice bath and then dissolved in DMSO-d_6 (0.6 mL) for ^{1}H NMR spectroscopic analysis. ^{1}H NMR analysis was done on a Bruker 500 MHz spectrometer (64 scans; T_1 relaxation = 5 s).

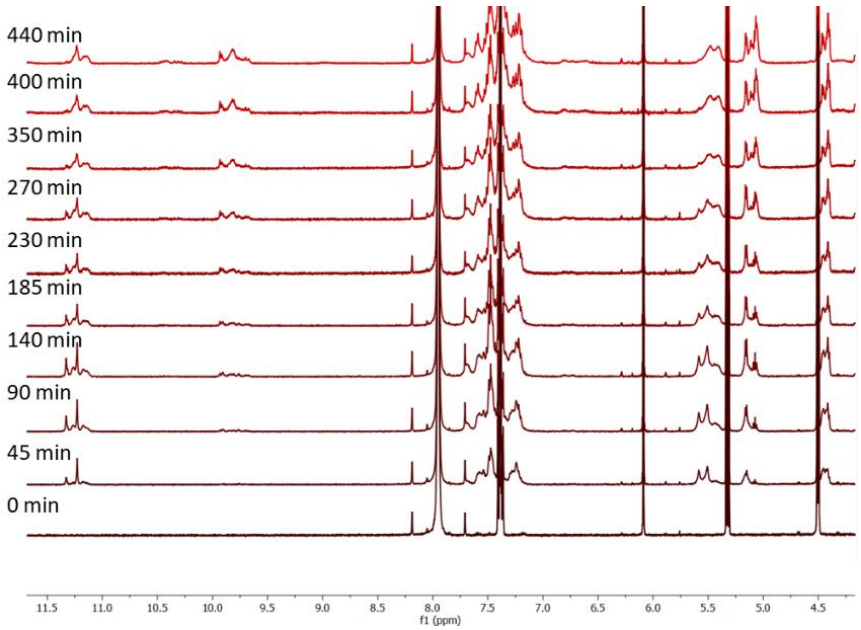

Figure S10. Stacked ^{1}H NMR spectra for the polymerization kinetic analysis of **M1** (**M1** monomer on bottom; time increasing going upward). 1,3,5-trimethoxybenzene (δ = 6.09, 7.38 ppm) was added as an internal standard. Monomer concentration was determined by integrating the methoxy proton signal for 1,3,5-trimethoxybenzene relative to the methylene of **M1** (δ = 4.50).

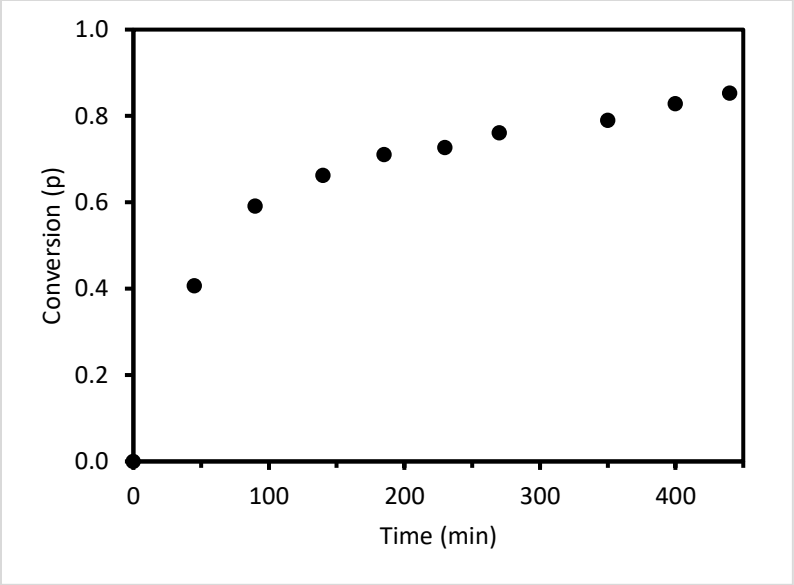

Figure S11. Plot of monomer conversion (p) over time for the polymerization of **M1**. Monomer conversion was determined by the measuring concentration of monomer remaining in the reaction mixture at a given timepoint relative to the internal standard using ^{1}H NMR spectroscopy.

Depolymerization analysis – ^{1}H NMR spectroscopy

In a 1-dram vial, a stock solution of TCEP (6.5 mg) and $N(Et)_3$ (7.25 µL), in DMSO-d_6 (500 µL) was prepared. In a separate vial, a solution of **SADP1** (2.4 mg) was prepared by dissolving it in DMSO-d_6 (958 µL). A t_0 timepoint was then recorded on a Bruker Avance II 500 MHz spectrometer (32 scans, 5 s T_1 relaxation time). The stock solution of TCEP/$N(Et)_3$ (53.5 µL) was then added to the NMR tube containing **SADP1**, and the tube was capped. This solution was mixed, and the NMR tube cap was wrapped with Parafilm. ^{1}H NMR spectra were collected using the aforementioned protocol every day for eight days.

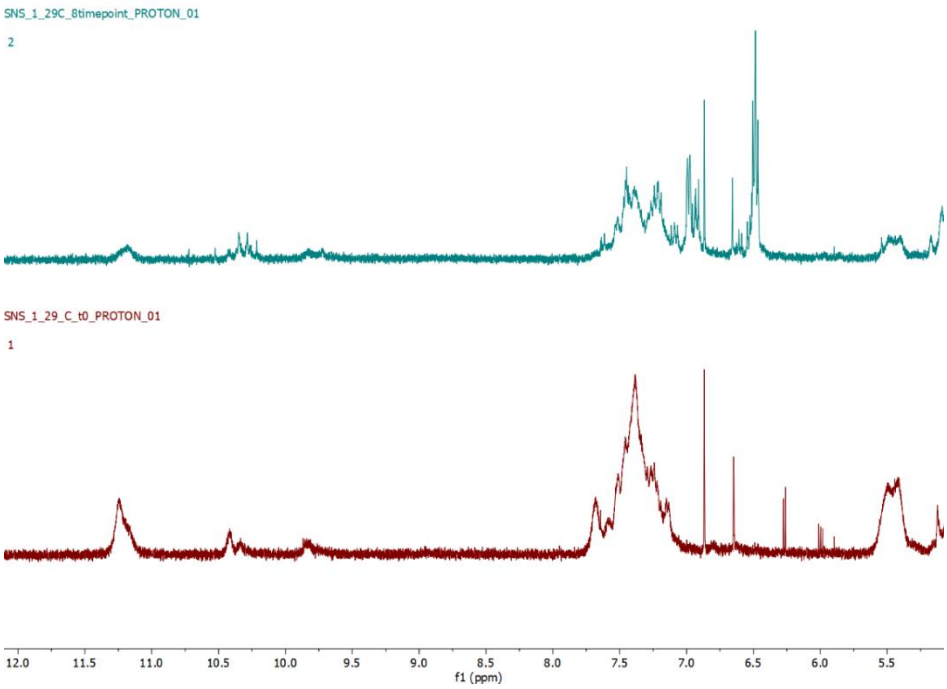

Figure S12. ^{1}H NMR spectra of **SADP1** in the presence of TCEP (1.5 equiv) and $N(Et)_3$ at time 0 (red) and after 8 days (blue). A decrease in the peak attributed to the thiocarbamate repeat unit (Ar–N**H**C(S)O) (δ = 11.25 ppm) as well as peaks attributed to **4-AB** growing in (d, δ = 6.5, 7.0) were observed, indicating depolymerization.

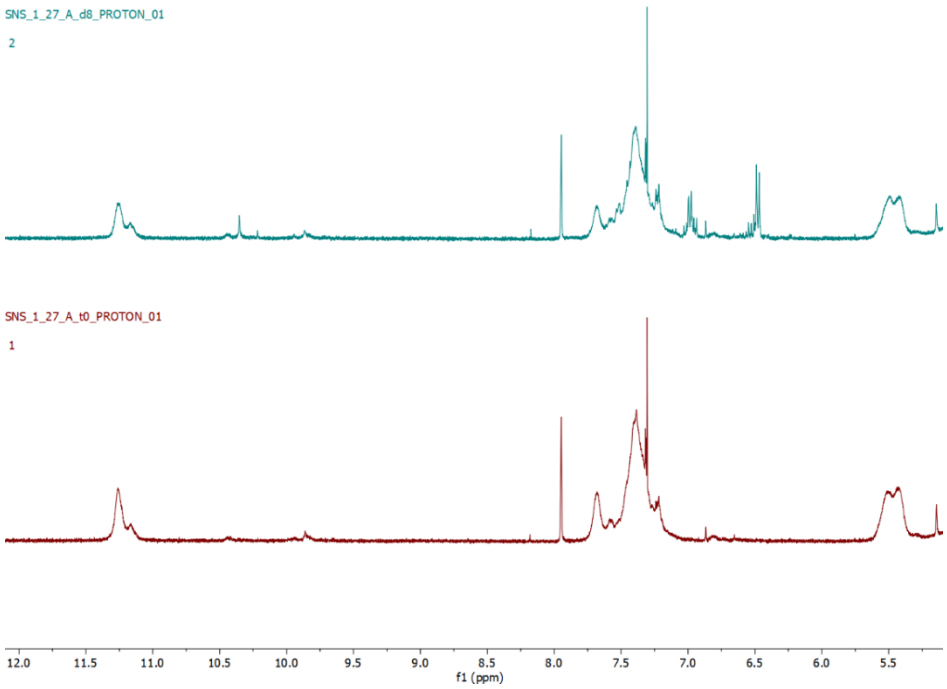

Figure S13. ^{1}H NMR spectra of **Cntrl-SADP** in DMSO-d_6 in the presence of TCEP (1.5 eq) and $N(Et)_3$ (1.5 eq) at t_0 (red) and after 8 days (blue). A small amount of hydrolysis under these conditions is evidenced by the appearance of peaks attributed to **4-AB** (d, δ = 6.5, 7.0).

Depolymerization analysis – UV-Vis

A vial was charged with 1X PBS (1.48 mL, pH 7.4), CTAB (1 mL, 3 mM in PBS), DTPA (0.5 mL, 60 μM in PBS), and CA (20 μL, 75 μM in PBS). **SADP1** (81 μL, 370 μM) was added to the vial, and the contents were transferred to a quartz cuvette with a threaded lid. The cuvette was capped, and an absorption spectrum was recorded as the zero timepoint (t_0). To the vial the desired reducing agent was added (10 μL), and then the vial was shaken to mix and placed back into the spectrometer. Absorbance spectra were recorded every 10 min after the addition of reducing agent for 5 h total. Kinetic analysis was performed by normalizing the absorbance (λ = 284 nm) of each timepoint to the t_0 timepoint.

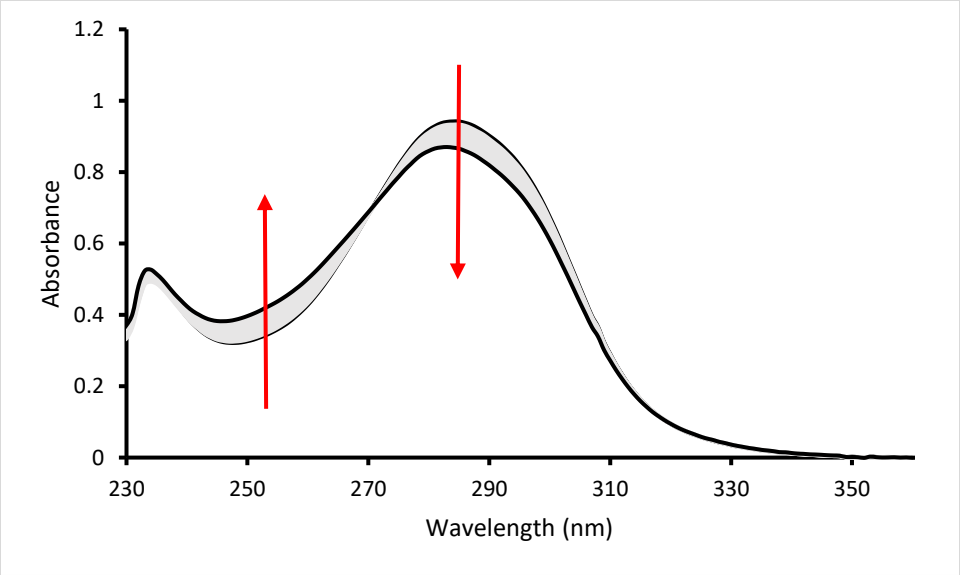

Figure S14. Representative absorbance spectra of **Ctrl-SADP** in the presence of Na_2S (0.1 equiv) during the course of a depolymerization kinetic analysis by UV-Vis (2 h). Similar to **SADP1**, a broad absorbance band (λ_{max} = 284 nm) can be observed prior to addition of Na_2S, followed by a gradual red shift after the addition of Na_2S.

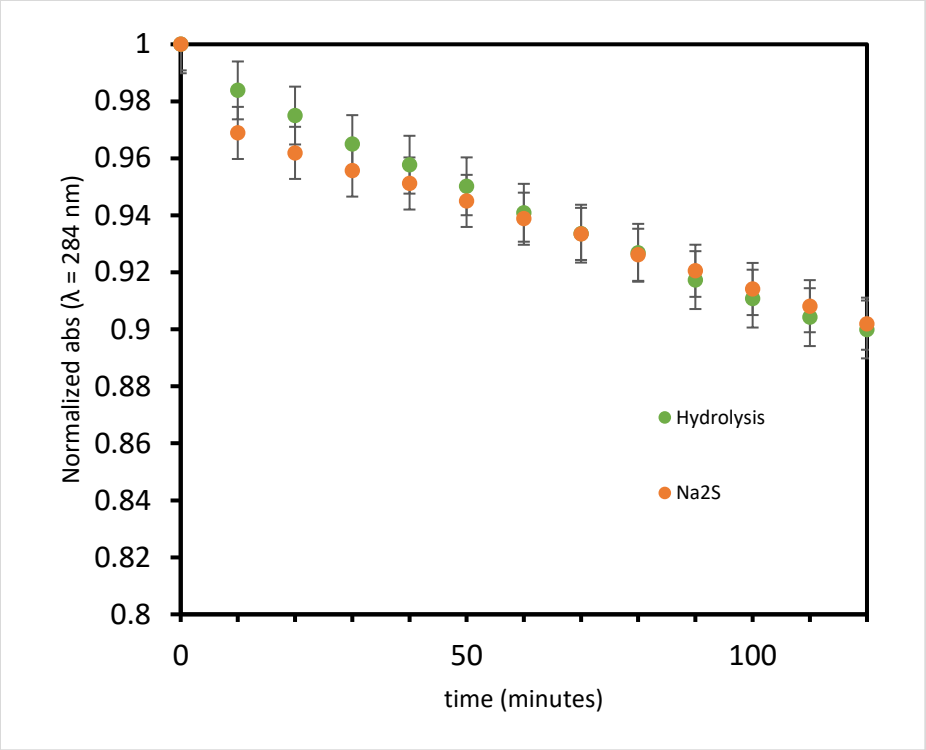

Figure S15. UV-Vis depolymerization data for **Ctrl-SADP** in the presence and absence of Na_2S (0.1 equiv). No significant difference between the two set of conditions was observed, indicating that sulfide does not degrade the benzyl thiocarbamate moiety.

H_2S release data

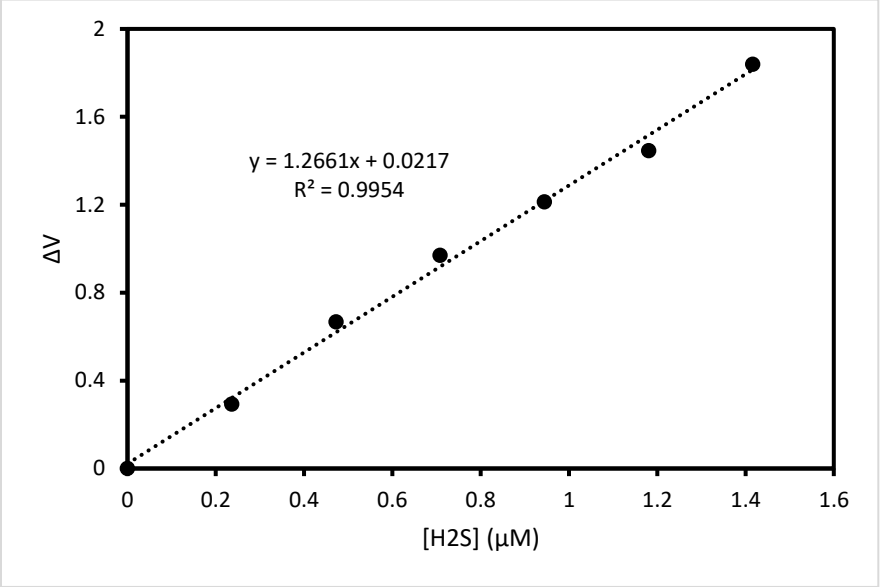

Figure S16. Calibration curve constructed for the H_2S-selective electrochemical probe. Values on the x-axis indicate the concentration of Na_2S in solution (PBS buffer, pH 7.4). Values on the y-axis indicate the change in output voltage after each successive addition of Na_2S. Concentration of H_2S calculated via the equation $[H_2S] = [Na_2S]/\{1 + \frac{K_a{}^1}{[H^+]} + \frac{K_a{}^1 K_a{}^2}{[H^+]}\}$where $pK_a{}^1$ = 6.89 and $pK_a{}^2$ = 19 for the chemical equation [total sulfide] = $[H_2S]$ + $[HS^-]$ + $[S^{2-}]$.[4]

A scintillation vial was charged with 8.31 mL of 1X PBS buffer (pH 7.4), 0.25 mL of DMSO, 400 µL of **SADP1** solution (2.5 mM in DMSO), 1.0 mL CTAB solution (10 mM in 1X PBS), and a small magnetic stir bar. Final concentrations in the reaction vial were 100 µM **SADP1** and 1 mM CTAB. Once all of the reagents had been added, the probe was immediately inserted into the solution, and the output voltage was recorded. After allowing the probe to equilibrate for about 10 min, 20 µL of CA solution (150 µM in 1X PBS) was added to the reaction vial amounting to a final concentration of 300 nM. Following this, 20 µL Na_2S solution (5 mM in PBS) was added

into the reaction vial with final concentration of 10 µM. Peaking times of H_2S in solution were measured at the point where the current readout reached a global maximum for the dataset. Δ

Theoretical calculations of ΔG

The density functional theory calculations were performed using the Gaussian 09[5] suite of software. Geometries and harmonic frequencies for phenyl isothiocyanate, benzyl alcohol, and benzyl thiocarbamate were optimized using the M06-2X functional, the aug-cc-pVDZ basis set, and an ultrafine integration grid, and considered implicit DMF solvation (PCM model). The Gibbs energies listed in **Table S1** below were calculated at 60 °C.

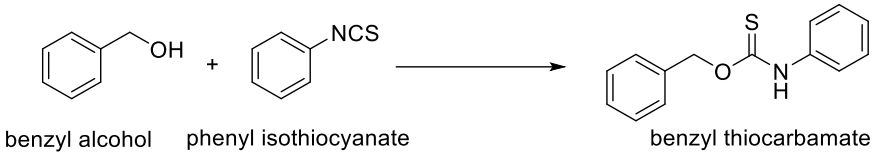

Scheme S1. Small molecule analog reaction modeled by Gaussian for theoretical value of ΔG.

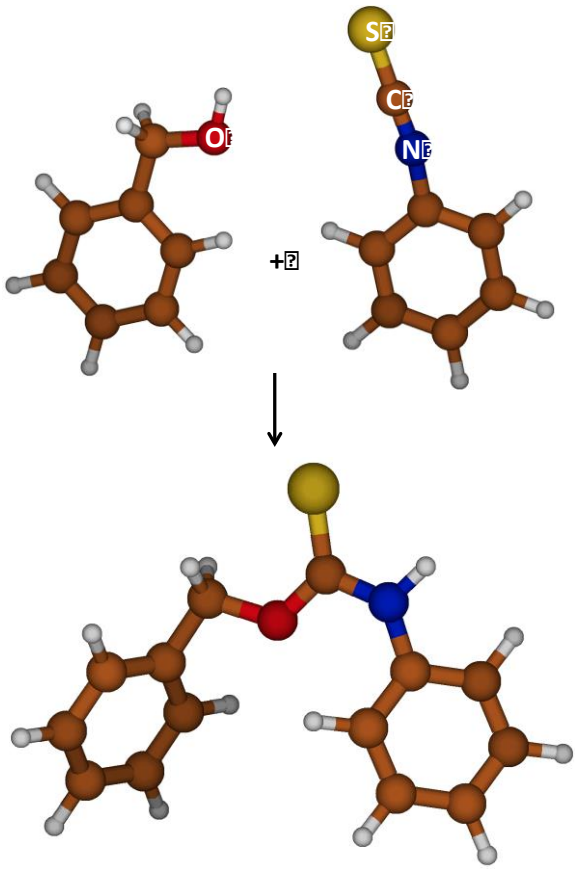

Figure S17. Optimum geometries for the reaction in Scheme S1.

	Benzyl alcohol (a.u.)	Phenyl isothiocyanate (a.u.)	Benzyl thiocarbamate product (a.u.)	ΔG (kcal/mol)
Free energy (60°C)	-346.587719	-722.529357	-1069.120716	-2.28

Table S1. Theoretical 60 °C Gibbs energies for the reaction between benzyl alcohol and phenyl isothiocyanate.

XYZ coordinates (Angstrom)

Benzyl Alcohol

C,0,0.0068573336,0.0017655845,0.
C,0,0.4779658105,1.4351491076,0.
C,0,-0.4137581393,2.508740476,0.
C,0,0.0646894539,3.8226236502,0.
C,0,1.4355500262,4.0737265573,0.
C,0,2.3319845399,3.0010175157,0.
C,0,1.8546426322,1.6927567862,0.
H,0,2.5582171277,0.8587650676,0.
H,0,3.4055268554,3.1862257331,0.
H,0,1.8066954609,5.0976822054,0.
H,0,-0.640738733,4.6529750578,0.
H,0,-1.484161035,2.3156707696,0.
O,0,-1.4111691256,-0.0425087137,0.
H,0,-1.6816942586,-0.9663575888,0.
H,0,0.4094375256,-0.5083416042,-0.8885787758
H,0,0.4094375256,-0.5083416042,0.8885787758

Phenyl isothiocyanate

C,0,-0.0563844529,0.0753527376,0.
C,0,0.5876926816,1.3143868743,0.
C,0,1.9824779203,1.3768742552,0.
C,0,2.7399436923,0.2085493131,0.
C,0,2.081345314,-1.0253825481,0.
C,0,0.6841138717,-1.1035030958,0.
H,0,0.19948116,-2.077482543,0.
N,0,2.8252109528,-2.1924498321,0.
C,0,3.3827094772,-3.2277759013,0.
S,0,4.1617414047,-4.634675564,0.
H,0,3.8274146891,0.2375282866,0.
H,0,2.4871094791,2.3413232458,0.
H,0,0.0019856606,2.2319131091,0.
H,0,-1.1436818508,0.0238056625,0.

=Benzyl thiocarbamate

C,0,0.0390143447,0.0051711038,0.1984358323
O,0,1.3882131716,-0.5054451515,0.1895148316
C,0,2.4055055147,0.3351094303,0.2688022158
N,0,3.6029197401,-0.2816299712,0.2136227216
C,0,3.944261816,-1.6457131406,0.0326280333
C,0,5.2471388284,-1.8912002327,-0.4235588244
C,0,5.6950079335,-3.1952813879,-0.6051217118
C,0,4.8488554872,-4.2725994086,-0.3369090323
C,0,3.5571186827,-4.0246903104,0.1242052207
C,0,3.0951098549,-2.7222264728,0.3181569099
H,0,2.0909863158,-2.5596579827,0.6911047174
H,0,2.8898909233,-4.8560202492,0.3469776775
H,0,5.1955878328,-5.2940610334,-0.4819299366
H,0,6.7093433639,-3.3675736562,-0.9612638688
H,0,5.9082989999,-1.0518057317,-0.6379665849
H,0,4.3817613888,0.3651788988,0.2220613883
S,0,2.2754433388,2.005748908,0.4187770677
C,0,-0.8760710256,-1.1851251824,0.1064144645
C,0,-1.8844684972,-1.3733233876,1.052282322
C,0,-2.749439988,-2.4660056021,0.9531107466
C,0,-2.5997035196,-3.381308533,-0.0874030516
C,0,-1.5857510115,-3.2009044639,-1.0327430828
C,0,-0.7316136988,-2.1047405874,-0.9391745084
H,0,0.0579211807,-1.9627592092,-1.6771020396
H,0,-1.4656585206,-3.9148047058,-1.846296431
H,0,-3.2698055485,-4.2364536868,-0.163295851
H,0,-3.5355523973,-2.6038140125,1.6939817309
H,0,-1.9964860318,-0.6636268603,1.8717734505
H,0,-0.1226679469,0.5694954111,1.1220638084
H,0,-0.073666532,0.6807962082,-0.6573772157

Experimental References.

1. H. Munch, J. S.; Hansen, M. Pittelkow, J. B.; Christensen J.B.; Boas, U., A New Efficient Synthesis of Isothiocyanates from Amines using Di-tert-butyl Dicarbonate *Tetrahedron Lett.*, **2008**, *49*, 3117-3119.

2. Grimes, K.D.; Gupte, A.; Aldrich, C.C., Copper(II)-Catalyzed Conversion of Aryl/Heteroaryl Boronic Acids, Boronates, and Trifluoroborates into the Corresponding Azides: Substrate Scope and Limitations. *Synthesis*, **2010**, *2010*, 1441-1448.

3. Sagi, A.; Weinstain, R.; Karton, N.; Shabat, D., Self-Immolative Polymers. *J. Am. Chem. Soc.*, 2008, **130**, 5434-5435.

4. Meyer, B.; Ward, K.; Koshlap, K.; Peter, L., Second Dissociation Constant of Hydrogen Sulfide. *Inorg. Chem.* 1983, **22**, 2345-2346.

5. Gaussian 09, Revision E.01, M. J. Frisch, G. W. Trucks, H. B. Schlegel, G. E. Scuseria, M. A. Robb, J. R. Cheeseman, G. Scalmani, V. Barone, B. Mennucci,G. A. Petersson, H. Nakatsuji, M. Caricato, X. Li, H. P. Hratchian, A. F. Izmaylov, J. Bloino, G. Zheng, J. L. Sonnenberg, M. Hada, M. Ehara, K. Toyota, R. Fukuda, J. Hasegawa, M. Ishida, T. Nakajima, Y. Honda, O. Kitao, H. Nakai, T. Vreven, J. A. Montgomery, Jr., J. E. Peralta, F. Ogliaro, M. Bearpark, J. J. Heyd, E. Brothers, K. N. Kudin, V. N. Staroverov, T. Keith, R. Kobayashi, J. Normand, K. Raghavachari, A. Rendell, J. C. Burant, S. S. Iyengar, J. Tomasi, M. Cossi, N. Rega, J. M. Millam, M. Klene, J. E. Knox, J. B. Cross, V. Bakken, C. Adamo, J. Jaramillo, R. Gomperts, R. E. Stratmann, O. Yazyev, A. J. Austin, R. Cammi, C. Pomelli, J. W. Ochterski, R. L. Martin, K. Morokuma, V. G. Zakrzewski, G. A. Voth, P. Salvador, J. J. Dannenberg, S. Dapprich, A. D. Daniels, O. Farkas, J. B. Foresman, J. V. Ortiz, J. Cioslowski, and D. J. Fox, Gaussian, Inc., Wallingford CT, 2013.

Chapter 7: Conclusions and Future Outlook

Chapter 2

In this chapter we introduce *N*-thiocarboxyanhydrides (**NTA**s) as a novel class of carbonyl sulfide (COS) / hydrogen sulfide (H_2S) donors. By modifying a previously reported synthetic route we are able to efficiently access the NTA of sarcosine (**NTA1**) in three steps with fair yields. COS release from **NTA1** is confirmed by GCMS and the expected peptidic byproduct of the nucleophilic ring-opening reaction by glycine is confirmed by LCMS. H_2S release experiments demonstrate that the ubiquitous enzyme carbonic anhydrase (CA) is required for the rapid generation of H_2S from the released COS, and that in the absence CA the rate of H_2S generation from COS hydrolysis matches literature precedent. Furthermore, a polymeric NTA (**polyNTA1**) was prepared by copolymerization via ring-opening metathesis polymerization (ROMP) of an NTA bearing a pendant norbornene with a poly(ethylene glycol) (PEG)-norbornene comonomer. **PolyNTA1** was water soluble and demonstrated a H_2S release half-life that was nearly four times greater than that for **NTA1**, indicating that a polymeric donor provides a platform from which COS/H_2S may be extended to greater periods of time.

Future work for this project was undertaken in chapters 3 and 4 in which NTAs with reactive functionalities were synthesized and used to prepare a variety of COS/H_2S donors from a convergent synthetic approach. Looking beyond the scope of this document, NTAs provide a platform from which biologists may study COS as a potential gasotransmitter, independent of H_2S. Additionally, many contemporary synthetic H_2S donors in the literature are limited by toxicity of their byproducts upon H_2S delivery. As NTAs generate peptidic byproducts we are hopeful that in many instances the issue of byproduct toxicity can be circumvented by the use of NTAs.

Chapter 3

This chapter built upon the work in Chapter 2. The major limitation of the first iteration of NTAs (i.e. **NTA1**) as COS/H_2S donors (i.e. the NTA of sarcosine) is the lack of functional handles from which further modification may be performed once the **NTA1** was synthesized. Ideally, a convergent synthetic approach would be taken to prepare H_2S donor conjugates that would not require modification of the entire synthetic route for each donor prepared. To facilitate a convergent synthesis of H_2S donors we built off of the synthetic route used to synthesize **PolyNTA1** to include a variety of a functional handles substituted from the NTA nitrogen, including alkynes, azides, norbornenes, and phenyl substituents (**NTA2-6**).

Once the functional N-substituted NTAs were successfully prepared, each NTA was conjugated to a small molecule, amino acid, or polymeric substrate to demonstrate the substrate scope. The H_2S release profiles of each N-substituted NTA were quite similar, with no change in the shape of the release profile for each NTA and peaking times ranging between 20-30 min. Conjugation of the NTAs to small molecules did not drastically affect the H_2S release profile or peaking time. However, conjugation of the NTAs to water-soluble macromolecules (i.e. PEG) appears to have a drastic effect on the release profile, extending the H_2S peaking time out to ~200 min, similar to the H_2S release profile seen for **PolyNTA1** (Chapter 2). Taken altogether, the work in this chapter demonstrates that a variety of functional N-substituted NTAs can be readily synthesized without alteration of the synthetic route and conjugated to a variety of substrates with the appropriate functionality.

Future work in this area will likely include the synthesis of specific NTA drug, peptide, or polymer conjugates tailored to the needs of a specific research area. For example, an NTA-cardiovascular drug conjugate that may facilitate the investigation of the efficacy of these

compounds in ischemia-reperfusion events. Initial efforts are ongoing with collaborators outside of Virginia Tech to synthesize NTA-drug or polymer conjugates for specific interests of the collaborators.

Along an entirely different vein of research, initial dynamic light scattering (DLS) results for various molecular weight PEG-NTA conjugates synthesized via the Huisgen [3+2] cycloaddition (CuAAC) reaction indicate that these compounds form aggregates on the order of ~200 nm in aqueous media, with the aggregate size roughly scaling with PEG molecular weight. Aggregates of this size were unexpected, but appear to be consistent for the PEG-NTA conjugates. This is an intriguing result that warrants further investigation into the driving force for the formation of aggregates of this size. It would be interesting to investigate whether PEG functionalized with any relatively hydrophobic small molecule via CuAAC would form aggregates of this size in aqueous media.

Chapter 4

This chapter employed the use of the alkyne N-substituted NTA (**NTA2**) to synthesize a biodegradable, water-soluble, NTA-polycarbonate (PC) conjugate. To this end, a cyclic carbonate monomer bearing an alkyl azide (**CM-N_3**) was prepared and subsequently polymerized via ring-opening polymerization (ROP). The resulting polycarbonate (**PC-N_3)** has an azide on each repeat unit to accommodate the CuAAC reaction with **NTA2**.

The polymerization of **CM-N_3** was conducted using a dual thiourea/amine organic cocatalyst system to eliminate the need for heavy transition metal catalysts, which may complicate any *in vivo* or *in vitro* studies in the future. Under the conditions tested the polymerization of **CM-N_3** demonstrated living behavior, reaching > 90 % monomer conversion with low dispersity. **PC-**

N_3 was not water soluble, so an alkyne-functionalized PEG was appended via the CuAAC reaction to generate a water-soluble **PC-*graft*-PEG** as evidenced by ^{1}H NMR and SEC analysis.

Unfortunately, the CuAAC reaction between **PC-*graft*-PEG**, as well as **PC-N_3**, and **NTA2** has shown limited success thus far, reaching a modest 40 % conversion before an insoluble precipitate forms. Unfortunately, this level of conversion does not appear reproducible. The formation of this precipitate occurs across a variety of CuAAC reaction conditions involving **NTA2** and appears to prevent the reaction of progressing. Despite the modest success, preliminary H_2S release data indicate that the **PC-*graft*-PEG-NTA** demonstrates a slow release profile with a peaking time > 300 min, the greatest peaking time seen for NTA-based H_2S donor systems.

Future work will entail optimization of the CuAAC reaction between **NTA2** and **PC-*graft*-PEG**. Attempts at the CuAAC reaction with **NTA2** prior to appending the PEG grafts appear to give even less success than the 40 % conversion achieved, even under the same reaction conditions. Reaction optimization will require proper choice of solvent, copper catalyst, base, and potential addition of a ligand to aid in copper solubility and to help prevent catalyst oxidation. The literature on the CuAAC reaction is vast, and surely there are a set of conditions that will give the desired result. Once reaction conditions are settled upon, further H_2S release data will be gathered. The system can be tuned by varying the molar equivalence of NTA and PEG per polymer chain, as well the molecular weight of the PEG grafts to investigate if these parameters have an effect on H_2S release or solution morphology. Additionally, degradation studies in aqueous media will need to be undertaken as well as *in vitro* cytotoxicity. Hopefully, these studies will lead to success and further analysis *in vitro* and potentially *in vivo*.

Chapter 5

This chapter introduces the 1,6-elimination, or self-immolative, prodrug motif to mediate the release of a discrete persulfide (R–SSH) of *N*-acetyl-L-cysteine (NAC). This is one of the first discrete persulfide donor molecules reported in the literature, and the first to employ the self-immolative motif. Due to the highly reductive nature of persulfides (relative to the analogous thiol and H_2S) we hypothesized that a persulfide donor might show efficacy as an antioxidant *in vitro*. To this end, a pinacol boronic ester (Bpin) moiety was chosen as the chemical trigger, which is responsive to reactive oxygen species (ROS), specifically hydrogen peroxide (H_2O_2). The persulfide donor, termed **BDP-NAC** (Bpin-disulfide prodrug-*N*-acetyl cysteine), was shown to undergo the desired self-immolative reaction in the presence of H_2O_2 via ^{1}H NMR and LCMS analyses, with LCMS providing a high-resolution mass spectrum of the released NAC-persulfide.

A coumarin-based profluorophore analog to **BDP-NAC**, termed **BDP-Fluor**, was synthesized and utilized to demonstrate the trigger specificity of the Bpin moiety for a variety of oxidants and nucleophiles. H_2O_2 gave a 90-fold increase in fluorescence response over all other triggers tested. *In vitro* cytotoxicity studies conducted using H9C2 cardiomyocytes demonstrated that in the absence of exogenous ROS **BDP-NAC** is noncytotoxic up to 200 μM. When the cardiomyocytes were treated with H_2O_2 **BDP-NAC** was shown to entirely mitigate the deleterious effects. Furthermore, **BDP-NAC** was shown to be more effective at rescuing the cardiomyocytes in the presence of exogenous H_2O_2 than a variety of controls, including a non-persulfide releasing Bpin compound delivered simultaneously with common H_2S donors and thiols.

Work in this area has been ongoing in the Matson lab, with three new self-immolative persulfide prodrugs having been synthesized. These new prodrugs are designed to respond to various enzymes to facilitate persulfide generation under a variety of conditions where H_2S has

shown some efficacy. Current efforts are focused on developing a reproducible persulfide trapping assay to ensure that the desired persulfide species is being released in each system. Collaborations with a group in the Virginia-Maryland College of Veterinary Medicine are ongoing, studying the effects of a specific persulfide donor *in vitro*.

Chapter 6

In this chapter the self-immolative motif was applied to an oligomeric poly(thiourethane) (PTU) system, termed **SADP1** for the release of COS/H_2S. **SADP1** is designed to depolymerize in the presence of reducing agents, including H_2S, to generate one molar equivalent of COS upon depolymerization of each monomer unit. **SADP1** is synthesized via a step-growth polymerization mechanism from an AB-type monomer bearing a benzyl alcohol and isothiocyanate (**M1**). **M1** is polymerized in the presence of dibutyltin dilaurate (DBTDL), and reaches a maximum monomer conversion of ~ 85 %, giving a degree of polymerization (DP) of approximately 7 (M_n = 1.6 kg/mol). The low degree of polymerization is supported theoretically via density functional theory calculations for a reaction between an aryl isothiocyanate and a benzyl alcohol species under the reaction conditions.

Depolymerization of **SADP1** in the presence of (tris(2-carboxyethyl)phosphine) (TCEP), as an organo-soluble reducing agent, was monitored by ^{1}H NMR. Over the course of the experiment new peaks grew in that exhibited the characteristic chemical shifts and substitution pattern of the expected byproduct 4-aminobenzyl alcohol. The ^{1}H NMR data was supported by monitoring the depolymerization of **SADP1** via UV-Vis spectroscopy, which demonstrated a gradual blue-shift in the λ_{max} of **SADP1** towards the λ_{max} of 4-aminobenzl alcohol in the presence of TCEP as well as H_2S. Lastly, H_2S release experiments via an H_2S selective electrochemical

probe demonstrate that **SADP1** generates H_2S in the presence of added Na_2S over the course of hours in a manner consistent with signal amplification.

Future work in the self-immolative polymer/oligomer arena will likely require a polymerization method or monomer that will facilitate a greater degree of polymerization. The system, in its current state, may benefit from the addition of a comonomer. There is literature precedence for a self-immolative poly(urethane) system that has been demonstrated to achieve nearly quantitative conversion under the same polymerization conditions as those performed for the synthesis of **SADP1**. Addition of a more reactive comonomer, higher molecular weights may be achieved, but at the expense of COS/H_2S payload. Once the SIP system is optimized synthetically a variety of triggers for depolymerization and COS/H_2S release may be explored. Should it prove feasible, exploration of the polymer's thermal and mechanical properties would likely inform the utility of these polymers as H_2S releasing cell-culture scaffolds, and potentially as H_2S-releasing coatings.